

**ADVANCES IN  
CLAY MINERALS**

# ADVANCES IN CLAY MINERALS

Proceedings of the Spanish-Italian Meeting on Clay Minerals held in Granada,  
Spain, 19-21 September 1996

Edited by *M Ortega-Huertas, A López-Galindo and I Palomo-Delgado*

Sociedad Española de Arcillas  
Gruppo Italiano dell'AIPEA

Universidad de Granada

Copyright © 1996 by Sociedad Española de Arcillas. All rights reserved. No part of this publication may be reproduced, stored in a retrieval system or transmitted in any form or by any means without written permission from the copyright holder.

Spanish-Italian Meeting on Clay Minerals  
(1996, Granada, Spain)

---

Editors: M Ortega-Huertas, A López-Galindo and I Palomo-Delgado

ISBN: 84-8499-482-1

Depósito Legal: GR-752-1996

Imprime: Imprenta Artística, Granada

Printed in Spain

Impreso en España

## **ORGANIZED BY**

Sociedad Española de Arcillas (SEA)  
Gruppo Italiano dell'AIPEA

## **UNDER THE AUSPICES OF**

Universidad de Granada  
Junta de Andalucía  
D.G.E.S. del Ministerio de Educación y Cultura  
Consejo Social. Universidad de Granada  
Facultad de Ciencias. Universidad de Granada  
Minas de Gádor, S.A. Almería  
Caja de Ahorros "La General". Granada  
Tolsa, S.A. Madrid

## **ORGANIZING COMMITTEE**

### **Chairman:**

*M. Ortega Huertas.* Dpto. Mineralogía y Petrología. Universidad de Granada

### **Secretary:**

*I. Palomo Delgado.* Dpto. Mineralogía y Petrología. Universidad de Granada

### **Members:**

*P. Fenoll Hach-Alí.* Dpto. Mineralogía y Petrología. Universidad de Granada

*I. González Díez.* Dpto. Cristalografía y Mineralogía. Universidad de Sevilla

*F. López Aguayo.* Dpto. Geología. Universidad de Cádiz

*E. Sebastián Pardo.* Dpto. Mineralogía y Petrología. Universidad de Granada

With the technical advice of *Manuela Suárez Pinilla.* Head of Protocol. Universidad de Granada



## SCIENTIFIC COMMITTEE

### Chairman:

*E. Galán Huertos.* President of the ECGA. Universidad de Sevilla

### Secretary:

*A. López Galindo.* C.S.I.C.-Universidad de Granada

### Members:

*A. Alvarez Berenguer.* Tolsa, S.A. Madrid

*B. Fabbri.* CNR-IRTEC. Faenza

*S. Fiore.* CNR-IRA. Potenza

*A. Grisoni.* Minerali Industriali. Novara

*J. Linares González.* C.S.I.C. Granada

*J.L. Pérez Rodríguez.* C.S.I.C. Sevilla

*M. Rodas González.* Universidad Complutense. Madrid

*A. Violante.* Università di Napoli

## HONORARY COMMITTEE

### President:

*Excmo. Sr. D. Manuel Pezzi Ceretto*

Consejero de Educación y Ciencia de la Junta de Andalucía

### Members:

*Excmo. Sr. D. Lorenzo Morillas Cueva*

Rector de la Universidad de Granada

*Excmo. Sr. D. José María Quintana González*

Presidente del Consejo Social de la Universidad de Granada

*Ilmo. Sr. D. José Luis Rosúa Campos*

Decano de la Facultad de Ciencias de la Universidad de Granada

*Prof. Dr. D. José María Serratosa Márquez*

Consejo Superior de Investigaciones Científicas. Madrid

*Prof. Dr. D. Emilio Galán Huertos*

Universidad de Sevilla

*Prof. Dr. Fernando Veniale*

Università di Pavia

*Prof. Dr. Antonio Pozzuoli*

Università di Napoli



This volume entitled "Advances in Clay Minerals" contains the proceedings of the "Spanish-Italian Meeting on Clay Minerals", held in Granada, Spain, from 19th to 21st September, 1996. The meeting was organized by the "Sociedad Española de Arcillas" and "Gruppo Italiano dell'AIPEA" with the special collaboration of the University of Granada, among other institutions.

This meeting represents the continuation of the excellent relations between researchers from Italy and Spain as already manifested, for example, in the "First Italian-Spanish Congress" in Seiano de Vico Equense and Amalfi (Italy), September 1984. It is, moreover, an example of present contacts between national Clay Groups, whose continuity and encouragement have been requested by the President of the "European Clay Groups Association" (ECGA). Although this is a meeting between researchers from the two nations, it has also been attended by scientists from Portugal, France, Switzerland, Norway, the United Kingdom and USA.

Three lectures, seventy two posters and thirty one oral communications were all presented within a Scientific Programme including the following topics: Surface Chemistry, Crystal Chemistry and Structures; Geology, Genesis and Geochemistry; Soil Mineralogy; Applications; Ancient Ceramics and Archeometry.

Extended abstracts received for the meeting were studied by the Scientific Committee, to whose members I wish to express my deepest thanks for their efforts and collaboration in the more important scientific aspects of the Meeting.

The "Spanish-Italian Meeting on Clay Minerals" would not have been possible without the enormous enthusiasm and hard work of many people and the support of the institutions involved. Thus, on behalf of the Organizing Committee, I wish to express our appreciation to all these people, but especially to the participants whose contributions have made this Meeting a success.

M. Ortega Huertas  
Chairman



## INDEX

### INVITED LECTURES

- Influence of the Granada school on the Spanish clay research  
*Galán E* 3
- Clay minerals as natural tracers in sediments and atmospheric dust of the Mediterranean Basin  
*Tomadin L* 5
- Application of fractal geometry to the textural study of colloidal associations  
*Cornejo J* 9

### SURFACE CHEMISTRY

- Fenuron adsorption on homoionic smectites  
*Auger J P, Hermosin M C and Cornejo J* 21
- Textural and sorptive properties of iron-coated clays  
*Celis R, Hermosin M C and Cornejo J* 24
- Nature and crystallization of mixed iron and aluminium gels: effect of Fe/Al molar ratio, pH and citric acid  
*Colombo C, Cinquegrani G, Adamo P, Violante P and Violante A* 27
- Sorption of anionic organic pollutants on hydrotalcites with different layer charge  
*Gaitán M, Barriga C, Pavlovic I, Ulibarri M A, Hermosin M C and Cornejo J* 30
- Dinitrophenol and 2,4-dichlorophenoxyacetic acid sorption by organoclays  
*Hermosin M C and Cornejo J* 33
- Thermodynamics of the potassium adsorption process by smectites at high temperatures  
*Linares J, Huertas F, Caballero E and Jiménez de Cisneros C* 36
- Adsorption of the pesticide glyphosate on montmorillonite in presence of copper  
*Morillo E, Maqueda C and Undabeytia T* 39
- Pesticide adsorption on organo-hydrotalcites  
*Pavlovic I, Ulibarri M A, Hermosin M C and Cornejo J* 42
- Effect of dry grinding on ordered (Kga-1) and disordered (Kga-2) kaolinite  
*Pérez Rodríguez J L, Sánchez Soto P J, Pérez Maqueda L A, Jiménez de Haro M C and Justo A* 45
- Adsorption of prometryne from water by organic clays  
*Socias-Viciano M M, Hermosin M C and Cornejo J* 48
- Intercalation compounds between nicotine and saponite  
*Suárez Barrios M, Vicente-Rodríguez M A and Martín Pozas J M* 51

Surface and catalytic properties of the solids obtained by pillaring of a high iron content saponite with Al-polycations  
*Vicente M A, Suárez M, Bañares M A, López González J D, Santamaría J and Jiménez López A* 54

FT-IR study of the acid treatment of different clay minerals (sepiolite, palygorskite and saponite)  
*Vicente M A, Suárez M, Bañares M A and López González J D* 57

Formation and stability of mixed hydroxy Fe-Al complexes in montmorillonite  
*Violante A, Colombo C and Krishnamurti G S R* 60

## CRYSTAL CHEMISTRY AND STRUCTURES

Eventual solid solution in K-NH<sub>4</sub> illite/smectite ordered mixed layer  
*Bobos I and Gomes C* 65

Crystal-chemical features of bentonitic illite/smectite  
*Cuadros J and Altaner S P* 68

Crystal structure and particle orientation in relation to behaviour of clays during drying  
*Iñigo Iñigo A C and Tessier D* 70

Effect of particle size on the dehydration-rehydration processes in magnesium vermiculite  
*Ruiz Conde A, Ruiz Amil A, Sánchez Soto P J and Pérez Rodríguez J L* 73

The use of oblique texture electron diffraction patterns as a tool for structure determination of clay minerals  
*De Santiago Buey C and Nicolopoulos S* 76

## GEOLOGY, GENESIS AND GEOCHEMISTRY

Controlling factors on the compositional variations of diagenetic and low-grade metamorphic chlorites  
*Barrenechea J F, Rodas M and Alonso Azcárate J* 81

The composition of micas in Precambrian and Paleozoic clastic rocks from the Iberian range (Spain)  
*Bauluz B, Mayayo M J, Fernández Nieto C and González López J M* 84

The presence, genesis and significance of palygorskite in some Moroccan Tertiary sequences  
*Ben Aboud A, López Galindo A, Fençll Hach-Ali P, Chellai E H and Daoudi L* 87

Deuterium activity in the kaolin deposit of Sao Vicente de Pereira (Portugal): a discussion based on reaction rates among minerals and H<sup>+</sup> metasomatism  
*Bobos I and Gomes C* 90

Greisenisation indices in the kaolin deposit of Sao Vicente de Pereira (Portugal)  
*Bobos I, Gomes C, Velho J and Miranda A* 93

Mineralogical study of the Silurian black shales of the Ossa Morena zone and of the Iberian massif <i>Bombín Espino M, Suárez Barrios M, Saavedra Alonso J and Martín Pozas JM</i>	94
Clay mineralogy and trace element content of Upper Jurassic sediments from the Corvina 1 well (Algarve platform, south Portugal) <i>Caetano P S, Rocha F J and Gomes C</i>	97
Chemical and mineralogical variability of glaucony facies from superficial sediments on the northern sector of the Alborán continental margin <i>Dominguez Díaz M C, García Romero E, La Iglesia A, Navarro Gascón J V, Santos A and Viedma Molero C</i>	100
Geophysical survey of a kaolin deposit (Alvarães, Portugal) <i>Ferraz E, Matias M, Rocha F and Gomes C</i>	103
Mineralogy and geochemistry of argillites from flysch rosso formation (southern Apennines, Italy) <i>Fiore S, Santaloia F, Santarcangelo R and Tateo F</i>	106
Organic matter migration and halloysite formation in pyroclastic deposits from Mt. Vulture (southern Italy) <i>Fiore S, Genovese G and Miano T M</i>	108
Kinetic approach to the mineral reaction processes in a saponitic clay <i>Garralón A, Cuevas J, Ramírez S and Leguey S</i>	110
Alteration process on Tertiary calc-alkaline pyroclastic flow from Sardinia <i>Ghiara M R, Franco E, Petti C, Lonis R, Luxoro S and Gnazzo L</i>	113
Origin of intergrown phyllosilicate stacks from Verrucano metasediments (northern Apennines, Italy): a transmission and analytical electron microscopy study <i>Giorgetti G, Nieto F and Memmi I</i>	116
Clay minerals in the rambla Salada basin (Murcia province, SE Spain) <i>Guillén F, Arana R and Fernández Tapia M T</i>	119
Clay minerals in recent sediments of the Cádiz bay and their relationships with the adjacent emerged lands and the continental shelf <i>Gutiérrez Más J M, Achab M, Sánchez Bellón A, Moral Cardona J P and López Aguayo F</i>	121
Pelitic levels in the Apulian carbonate platform (Cretaceous): mineralogy and geochemistry as indicators of provenance <i>Laviano R and Mongelli G</i>	124
Magnetostratigraphy of an evaporitic deposit overlying the upper Cretaceous "Argilas de Aveiro" formation (Bustos-Aveiro, Portugal) <i>Leite S, Montenegro J, Rocha F and Gomes C</i>	125
Physicochemical study of the first steps of the transformation of smectite into illite <i>Linares J, Huertas F, Caballero E and Jiménez de Cisneros C</i>	128

Clay mineralogy, geochemistry and paleoenvironmental evolution of Quaternary sediments from the Ovar region (Aveiro, Portugal) <i>Machado A, Rocha F and Gomes C</i>	131
Evidences of stevensite formation from kerolite/stevensite mixed layers. Influence of alkalinity and silica activities <i>Martin de Vidales JL, Pozo M and Casas J</i>	134
Changes vs. similarities in the clay-mineral composition across the Cretaceous-Tertiary boundary <i>Martinez Ruiz F, Ortega Huertas M and Palomo I</i>	137
Clay deposits from oriental sector of Calatayud basin (Spain): mineralogy and geochemistry <i>Mayayo M J, Bauluz B and González López JM</i>	140
The deposit of sepiolite-smectite at Mara (Calatayud basin) <i>Mayayo M J, Torres Ruiz J, González López JM, López Galindo A and Bauluz B</i>	143
Ce-anomalies in the textural components of upper Cretaceous karst bauxites from the Apulian carbonate platform <i>Mongelli G</i>	146
The fractionation of REE, Th and transition elements in weathered biotites from granitoids: a mass balance approach and the role of accessory and secondary phases <i>Mongelli G, Dinelli E, Tateo F, Acquafredda P and Rottura A</i>	149
Mineralogy of clays in sediments from Neogene deposits in the Guadalquivir depression (Spain) <i>Montealegre L and Barrios-Neira J</i>	150
Textural and compositional variations in the Esquivias kerolite/stevensite deposit (Madrid basin, Spain) <i>Pozo M, Casas J and Moreno A</i>	153
Geochemical trends in alluvial-lacustrine Mg clay deposits from Madrid basin (Spain) <i>Pozo M, Moreno A, Casas J and Martin Rubi J A</i>	156
Evidences on diagenetical evolution of lacustrine sediments in the Vicalvaro sepiolite deposit <i>Ramirez S, Cuevas J, Garralón A, Martín Rubi J A, Casas J, Alvarez A and Leguey S</i>	159
Oxygen isotope geochemistry of kaolin minerals from the Campo de Gibraltar area (southern Spain) <i>Reyes E and Ruiz Cruz M D</i>	162
Mineralogy and geochemistry of the "Areias de Esgueira" formation (Aveiro, Portugal): arguments for lithostratigraphic and paleoenvironmental interpretations <i>Rocha F and Gomes C</i>	165

Study of the bentonites from the "Cerro del Aguila" (Toledo, Spain) <i>Santiago Buey de C, Suárez Barrios M, García Romero E, Doval Montoya M and Domínguez Díaz M C</i>	168
Lateritic-bauxitic clays of Andorinha (Cantanhede, Portugal): further mineralogical and geochemical data <i>Santos A, Rocha F and Gomes C</i>	171
Clay mineralogy and geochemistry of Miocene sediments from Setúbal peninsula (Portugal) <i>Silva A P, Rocha F and Gomes C</i>	174
Particle morphology evolution (flake-to-lath) as initial diagenetic transformation of a smectite-illite interstratification within a "dry" geochemical confined environment <i>Veniale F and Setti M</i>	177
A comparative study of the chemical micromorphological and technical characteristics of pure spanish sepiolites <i>Yebra A, López Galindo A and Santarén J</i>	178
Clay mineralogy and the organic matter maturity grade of the Gordexola formation (Basque-Cantabrian basin, northern Spain) <i>Zuluaga M C, Aróstegui J, García Garmilla F and Suárez Ruíz I</i>	181
<b>SOIL MINERALOGY</b>	
Kaolinite formation and soil color in Mediterranean red soils <i>Delgado G, Sánchez Marañón M, Martín García JM, Melgosa M, Pérez MM and Delgado R</i>	187
A lithological discontinuity in a volcanic soil derived from latite (Mt. Cimini complex, Italy) <i>Fiore S, Lorenzoni P and Mirabella A</i>	190
Mineralogical composition and ultramicrofabric of entisols from Sierra Nevada (Granada, Spain) <i>Martín García JM, Delgado G, Párraga J F, Sánchez Marañón M and Delgado R</i>	193
Hydroxy interlayered minerals in soils of Huelva (Spain) <i>Rodríguez Rubio P, Maqueda C and Pérez Rodríguez J L</i>	196
<b>APPLICATIONS</b>	
Sr isotope ratio in relationship to hydraulic permeability of clayey lacustrine from the Tiber Valley (Central Italy) <i>Barbieri Maurizio</i>	201
"Argilas de Aveiro" (Portugal): appraisal of their ceramic properties <i>Coroado J, Rocha F, Correia Marques J and Gomes C</i>	204

Fine-grained weathering products in a waste disposal from the sulfide mine of Vigonzano (Parma province, Italy) <i>Dinelli E, Morandi N and Tateo F</i>	207
Chemistry of pyroxene and melilite formed during the firing of ceramic clay bodies <i>Dondi M, Ercolani G, Fabbri B and Marsigli M</i>	210
Composition and ceramic properties of Tertiary clays from southern Sardinia (Italy) <i>Dondi M, Marsigli M and Strazzera B</i>	212
Grain size distribution of the Italian raw materials for structural clay products: a reappraisal of Winkler's diagram <i>Dondi M, Fabbri B and Guarini G</i>	214
The dynamics of firing process in clays: from "bulk" to "point" investigations <i>Duminuco P, Messiga B, Riccardi M P and Setti M</i>	217
Clay mineralogy and heavy metal content of suspended sediments in an extremely polluted fluvial environment: the Tinto river (SW Spain). Preliminary report <i>Fernández Caliani J C, Requena A and Galán E</i>	218
Clay-based cleaning methods. Adsorption/adsorption of magnesium-sulphate <i>Franquelo M, Maqueda C and Pérez Rodríguez J L</i>	221
Influence of the clay mineralogy and geochemistry on the geotechnical behaviour of the "Argilas de Aveiro" formation (Portugal) <i>Galhano C, Rocha F and Gomes C</i>	224
Adsorption of phenyl salicylate on sepiolite and its use as UV radiation protectors <i>Hoyo del C, Rives V and Vicente M A</i>	227
Mineralogical and sedimentological characterization of clay raw materials and firing transformations in the brick-making industry from the Bailén area (southern Spain) <i>Jiménez Millán J, Molina J M and Ruiz Ortiz P</i>	230
Clay materials from Cameros basin (NE Spain) and their possible ceramic uses <i>Parras J, Sánchez C, Barrenechea J F, Luque F J, Rodas M and Mas J R</i>	233
Processing and properties of mullite-based composites from kaolinite <i>Pascual J, Zapatero J, Ramos J R, Ramiro A, Sánchez Soto P J, Justo A and Pérez Rodríguez J L</i>	236
Mechanochemical effects on kaolinite-pyrophyllite-illite natural mixtures <i>Sánchez Soto P J, Justo A, Avilés M A, Ruiz Conde A, Jiménez de Haro M C and Pérez Rodríguez J L</i>	239
Sintering of a clay containing pyrophyllite and industrial evaluation of its ceramic properties <i>Sánchez Soto P J, Raigón M, Jiménez de Haro M C, Justo A, Pascual J, Pérez Rodríguez J L and Béjar M</i>	242

Clays for waste disposal liners: comparative appraisal of the relevant properties of smectitic clays from Aveiro and Taveiro (Portugal) <i>Santos H, Rocha F and Gomes C</i>	245
Role of clay components in soil stability. Case-histories in the Italian territory <i>Veniale F, Setti M and Soggetti F</i>	248
Swelling-shrinking behaviour of clay levels in marly rocks and its influence on planar sliding events <i>Veniale F, Rodríguez Navarro C and Setti M</i>	249
Emission and fixation of F and S in clay based ceramics <i>Vieira A I, Gomes C, Rocha F and Bobos I</i>	250
Effect of mixing conditions on the rheological properties of some clay suspensions <i>Viseras C, Meeten G H, López Galindo A, Cerézo A and Rodríguez I C</i>	252
Technical properties of a magnesium smectite from Yuncillos <i>Santarén J, Alvarez A, Gutiérrez E and Casas J</i>	255
Swelling behaviour or compacted clayey soils <i>Esposito L and Guadagno F M</i>	258
New applications for the brickmaking materials from the Bailén area, Spain <i>González Díez I, Galán E, Miras A and Aparicio P</i>	261
Sepiolite based materials for ecological control of pesticides <i>Merino J, Casal B, Ruiz Hitzky E and Serratos J M</i>	264
 <b>ANCIENT CERAMIC AND ARCHEOMETRY</b> 	
Proposal of a non destructive analytical method by SEM-EDS to discriminate Mediterranean obsidian sources <i>Acquafredda P, Andriani T, Lorenzoni S and Zanettin E</i>	269
Magnetometric investigation of the archaeological site of Arva (Seville, Spain) <i>Burragato F, Di Filippo M, Grubessi O, Remesal J and Toro B</i>	272
The "Cotto Variiegato": a case-study of XVII century tiles. Some archeometric implications <i>Cairo A, Duminuco P, Riccardi M P, Setti M, Soggetti F and Messiga B</i>	274
Mineralogical and geochemical characterization of clay deposits (Pavia area, northern Italy): inferences of provenance on restoring ancient artifacts <i>Cairo A, Genova N, Meloni S, Oddone M and Setti M</i>	277
Archeometric investigations of the "ceramiche a figure rosse" of Dario's painter (IV cent. b.C) coming from Timmari <i>Canosa M, Lacarbonara F, Laviano R, Lorenzoni S and Acquafredda P</i>	278
Influence of the medium of deposit in the alteration of ceramic materials <i>Capel J, Linares J, Huertas F, Nájera T and Molina F</i>	281

Application of SEM/EDS analysis for studying ceramic materials of archaeological interest <i>Fabbri B</i>	284
Study of ceramic materials from the settlement of Italica (Seville) <i>Flores V, Barrios Sevilla J and Guiraúm Pérez A</i>	287
Elimination of the temperature effect in the variation of the quantitative mineralogical composition of prehistoric pottery: a new method <i>Gallart Martí M D, Mata Campo M P and López Aguayo F</i>	289
Ceramics from the etruscan city of Marzabotto: geochemical-mineralogical approach for identification of the origin and treatment techniques of the raw material <i>Morandi N, Nannetti M C, Minguzzi V, Monti S, Marchesi M, Mattioli C and Desalvo F</i>	292
Hydrolysis of ceramic materials: neoformation or rehydroxylation of clay minerals. Stable isotope analysis <i>Núñez R, Capel J, Reyes E and Delgado A</i>	295
Replicate of archaeological ceramics from Carmona (Seville, Spain) <i>Polvorinos del Río A and Gómez Morón A</i>	298
ESEM analysis of the swelling process in sepiolite-bearing Egyptian limestone sculptures <i>Rodríguez Navarro C, Sebastián Pardo E and Ginell W S</i>	301
Decorated terracotta from the province of Pavia, Italy: a mineralogical and petrographic study <i>Torre López de la M J, Sebastián Pardo E and Zezza U</i>	304
Provenance and technology of Galloroman terra Sigillata imitations from western Switzerland: preliminary results <i>Zanco A</i>	307
 <b>LAST ABSTRACTS</b>	
Clay minerals of the fracture fillings from the "El Berrocal" site: characterization and genesis <i>Pelayo M, Pérez del Villar L, Cózar J S, Reyes E, Caballero E, Delgado A and Núñez R</i>	311
Smectite to illite transformation. Experimental simulation and natural observations <i>Wei H, Roaldset E and Grimstad S</i>	314
 <b>AUTHOR INDEX</b>	 315

# INVITED LECTURES



Dpto. Cristalografía,  
Mineralogía y Química  
Agrícola. Fac. Química,  
Univ. de Sevilla, España

## Influence of the Granada school on the Spanish clay research

*Galán E*

---

Clay research began in Granada with the arrival of Prof. Enrique Gutierrez Rios from Madrid to the Chair of Inorganic Chemistry of the University of Granada in 1946. He was a pupil of Prof. José M. Albareda, the pioneer of clay studies in Spain. In Granada Gutierrez Rios met Juan L. Martín Vivaldi and Francisco González García who were his first pupils to work on clays. Martín Vivaldi worked on the system montmorillonite-water and exchange cations, and González García on thermal effects on smectites. Later, between 1947 and 1949, other chemists from the Faculty of Sciences of Granada started working with Gutierrez Rios: José M. Serratos, Antonia Medina, Juan de Dios López González. All of them (except Serratos who moved to Madrid in 1949) carried out their Ph. D. with Gutierrez Rios on clay topics.

At the same time, Prof. Angel Hoyos de Castro, also a Prof. Albareda's pupil, started a research on soil clays at the Faculty of Pharmacy where he was Chair of Applied Geology. His first pupils were Profs. Miguel Delgado, Julio Rodríguez and Luis Alias.

But clay was not only investigated at the University, because in 1954 the Experimental Station of Zaidin (CSIC) was founded and Gutierrez Rios was also the first director.

In 1952 Francisco González García went to the University of Sevilla to the Chair of Inorganic Chemistry where he began also the clay research on physico-chemistry properties, surface activities, ceramics, and soils.

As in 1957 Gutierrez Rios moved from the University of Granada to the University of Madrid he left in Granada a consolidated group of researchers on clay minerals, who were the leaders of teams at the University (Faculty of Sciences) and at the Experimental Station of Zaidin. Others accompanied Gutierrez Rios to Madrid and the influence of the Granada Clay School began to spread out.

During the Sixties important facts for the dispersion of the Granada Clay School were the incorporation of Martín Vivaldi to the Chair of Crystallography and Mineralogy at the Faculty of Geology in Madrid, the arrival of Salvador González García to the Chair of the Inorganic Chemistry of the University of Salamanca (where he found that Maria Sánchez Camazano was working on soil mineralogy) and the arrival of Julio Rodríguez to the University Autónoma of Madrid. There they had pupils and some of them moved to other Universities (Valladolid, Zaragoza, Cadiz, Sevilla, Salamanca) and others continued developing the clay research not only concerning physico-chemistry properties and crystalchemistry but also in geology, minerals deposits, industrial applications, etc.

In the meantime new generations of chemists and geologists were formed in Granada and clay research was growing interesting all the most important field of research: soils, surface properties, diagenesis, basin analysis, synthesis, interstratified clay minerals, quantitative analysis, etc. And also during the Seventies and Eighties some of them moved to Malaga, Cordoba, Murcia, Madrid, Badajoz, Zaragoza, Ciudad Real, transmitting knowledges and interest for clays.

Nowadays, most of researchers in Clay Minerals in Spain come from the Granada School or have been formed by people trained directly by investigators from Granada. It can be said that Granada School in Clay Research means the top on this field as from Granada comes the most important School of Teachers in Clay.

## Clay minerals as natural tracers in sediments and atmospheric dust of the Mediterranean Basin

*Tomadin L*

Investigations performed during the last 20 years on sediments and eolian dust of the Mediterranean Basin pointed out significant trends in the distribution of the clay minerals, testifying their ability to behave as tracers both in aqueous and in atmospheric environments.

The very small sizes of the clay particles are favouring their transport in suspension over wide distances. The role played by the clay minerals depends, therefore, on their variable "grain size" (up to two orders of magnitude between the largest kaolinite and the smallest smectite particles). Characteristic "clay mineral assemblages" are recognizable in different environments and represent useful tools to investigate their provenance.

A sedimentological approach to the question of clay minerals provenance is related to the different transport ways, to the sedimentary environments, and to the location of the source areas.

Different transport processes, as marine currents in the seawater body, turbidity currents along the sea floor, and eolian currents in the atmosphere, are responsible for the dispersion of clay sediments.

Very peculiar situations occur when the source area is directly connected and closely located to the sedimentation basin or, by contrast, when it is far located and separated from the basin. The influence of the source areas on marine sediments and atmospheric particulate is therefore variable and dependent on the prevalence of local and/or distal supplies.

Besides geological, morphological, oceanological and meteorological factors affecting the composition and the transport of clay sediments, another basic element cannot be disregarded: the location of the Mediterranean. The Basin extends, in fact, between two different climatic zones: a humid temperate to the N, and a dry desertic one to the S. Many evidences show the remarkable influence of the climatic conditions on the weathering processes and on the consequent characteristics of the clay minerals supplied from different source areas.

In the present sediments, usual sampling procedures allow to appreciate the record of clay minerals, representing a dynamic balance among the different transport processes acting in the basin, and among the different supplies. In the atmosphere, a much higher dynamics characterize the movements of the air masses, so that continuous samplings along prefixed tracks are necessary to appreciate the quick transport of atmospheric bodies and the connected mineral evolution of the wind-blown particulate.

Some examples are presented here to illustrate how informations obtained from the distribution patterns of the clay minerals emphasize, on meso-scale, the provenance of the marine sediments and of the atmospheric dust.

The Adriatic is an elongated shelf basin with a peculiar longitudinal dispersion of the sediments. The main source of clay sediments are the fluvial supplies from the western slope. A cyclonic gyre of marine currents distributes these materials in two belts parallel to the Italian coast and corresponding to two sedimentary provinces. A shallow-water belt is composed by clay sediments supplied by the rivers draining the central-southern Apennine (< 50% of poorly-crystallized illite and > 25% of moderately organized smectite). The clay sediments in the off-shore belt are transported by the Po River and show a provenance from the northern Apennine (>50% of moderately-crystallized illite and <25% of well-organized smectite).

Increasing amounts of smectite towards the S observed in the sediments, are the result of the prevailing transport by the marine currents. Evidences of the transport of clay sediments by turbidity currents were observed only in the bathyal basin of the southern Adriatic. The input of eolian dust is generally masked by the overwhelming fluvial supply. A distal source area is in fact recognizable from the trend of the Ch/K ratio, showing an increasing contribution to the S of kaolinite from the Saharan source.

The Tyrrhenian is a deep-sea basin with a reduced or lacking continental shelf. The fluvial supply is relatively scarce, and in the southern part of the basin only ephemeral creeks contribute to the marine sedimentation. The distribution patterns of the present sediments emphasize the variable provenance of the clay minerals. Marine currents are favouring a moderate dispersion of the clay sediments, whereas turbidity currents play a primary role and are responsible of the prevailing transversal dispersion of the sediments. Well-crystallized mica-illite and chlorite clearly show a provenance from the crystalline rocks cropping out in source areas close to the basin (Sardinia and Corsica to the NW and the Calabrian-Peloritan Arch to the SE). Smectite mainly concentrates in the famous volcanic

districts of the Tyrrhenian Basin: the Phlegrean-Neapolitan Area and the Aeolian Islands. The source of smectite is mainly connected with transformation of pyroclastic and hyaloclastitic materials. Low percentages of kaolinite are supplied from all continental areas surrounding the basin. However, important amounts of kaolinite were recognized over a large bottom-area extending to the N as far as 250-300 km from Sicily, and moreover on the top of the sea-mounts.

As a matter of fact, the comparison among the different sources of clay minerals in the Central Mediterranean, points out that significant kaolinite, poorly-crystallized illite, and palygorskite are transported from a far source outside of the basin: the Saharan Desert.

Windborne dust was sampled in the lower atmosphere of the Mediterranean by mesh panels and by high-volume filtration, to investigate the transport mechanisms of the dust, and its mineral composition.

The eolian dust reflects the characteristics of the soils in the source area, and is blown either by direct transport of particles from the African deflation areas, or by indirect transport of materials already present in the atmosphere. Occasional episodes of direct transport contrast with the more continuous effect of the "background" indirect transport. Mass concentrations, measured along continuous sampling tracks, pointed out the significant contribution of the indirect eolian supply when compared with the higher values provided by the occasional direct transport by dust-storm.

The mineralogy of the atmospheric particulate points out characteristic "mineral assemblages", whose composition depends on the location (proximal or distal) of the source areas, and on the direction of the blowing wind. All the investigations emphasized the role played by the clay minerals even in the atmospheric environment. Clay mineral assemblages of "northern provenance" (well-crystallized mica-illite, chlorite, serpentine) and of "southern provenance" (poorly-crystallized illite, kaolinite, palygorskite and smectite) were recognized.

When moving along a fixed tracks, both the bulk- and the clay-mineralogy in the particulate of each atmospheric body, reflect a dominant source area. By veering direction of the wind, the composition of the dust changes, because of the incoming supply of new air masses from a different provenance and with a different dust content.

The comparison between the clay mineralogy of the eolian dust over the Mediterranean, and that of the underlying marine sediments, show the following results: mineral components of windborne dust can be recognized in marine sediments of areas where the eolian supply was not masked by turbidity currents, or by long-distance transport of terrigenous supplies by marine currents.

The ability of the clay minerals as tracers in natural environments can be detected from the effects of the different transport processes. Usefull informations can be obtained not only with large amounts of clay minerals, as in the marine sediments, but also when scarce quantities are present, as in the atmospheric dust.

Tomadin L. (1974). *Bull. Groupe franç. Argiles*, 219-228

Tomadin L. (1975). *Rapp. CIESM*, 23, 4a, 283-285

Tomadin L. (1981). In: F.C.Wezel (ed.). *Sedimentary basins of Mediterranean margins*, 313-324

Tomadin L. et al. (1984). *Oceanologica Acta*, 7, 13-23

Curzi P.V. & Tomadin L. (1987). *Giorn. Geol.*, 49, 101-111

Lenaz R., Landuzzi V., Tomadin L. (1988) , *Mem. Soc. Geol. It.*, 36, 189-200

Tomadin L; & Lenaz R. (1989) In: M. Leinen and M. Sarnthein (eds.). *Paleoclimatology and Paleometeorology: Modern and Past Patterns of Global Atmospheric Transport*. Kluwer Acad. Publ. , 267-282

Tomadin L., Lenaz R., Sartori R. (1990). *Miner. Petrogr. Acta*, 33, 81-91

Tomadin L., Wagenbach D., Landuzzi V. (1996). In: S.Guerzoni & R. Chester (Eds.). *The Impact of African Dusts on the Mediterranean Sea*. Kluwer Acad. Publ., Dordrecht (In press)

## Application of fractal geometry to the textural study of colloidal associations

*Cornejo J*

### 1. Introduction

The behaviour and evolution of many components of the nature is no so regular as to be studied by classical mathematical approaches. The functions governing processes are not generally continuous and/or differentiable and the objects have not perfect geometrical shapes (lines, planes, spheres, etc.)

Mandelbrot's fractal geometry (1975) provides both a description and a mathematical model for many of the seemingly complex forms found in nature. Shapes such as coastlines, mountains and clouds are not easily described by traditional Euclidean geometry. The fractal geometry is associated to measurement problems. The estimated length of a coastline is dependent on the relationship between the linear size of the object to be measured and the linear size of the yardsticks which are used to measure it. In this case the length can increase when the measurement yardstick decreases.

In a much more reduced scale the knowledge of surface and morphological characteristics of solid particles (natural or synthetic) and their associations is one of the main parameters influencing its behaviour in many physicochemical processes (dissolution, crystallization, precipitation, flocculation, etc.) (Van Damme, 1992; Celis et al, 1996). On the other hand, the majority of natural chemical processes occur in heterogeneous environments: geochemical and biochemical reactions take place at the border area of interfaces, in membranes, in pores and in other confined zones. The main difference between homogeneous and heterogeneous reactions is the geometry of the environment in which the reaction takes place being most of the parameters governing a reaction affected by the geometry of the surroundings (Farin and Avnir, 1989).

Most of the geometries one encounters in natural and synthetic materials are so disordered and complex that it becomes a complicated task to take into account

quantitatively the effects of these geometries. Furthermore, the geometry problem appears not only in the evaluation of the degree of irregularity but also in the evaluation of the degree of heterogeneity it exerts in the surroundings. For instance, on the same surface one can find both concave and convex features of irregularity, and the two may affect differently a chemical reaction.

The fractal approach appears to be a potentially useful tool for understanding the mechanisms of formation or destruction of natural or synthetic systems .

## 2. Theoretical considerations

Fractals are mainly used to describe the structures of highly disordered systems being invariable at any characterization scale used to examine them. The dimension of a fractal object is not an integer as it is in euclidean geometry, but always a non integer or fraction. The euclidean dimensions 0, 1, 2 and 3 corresponding to a point, line, smooth plane and a three-dimensional object ( cube, sphere, etc.), respectively, can't describe a coastline, a mountain surface or a cloud shape.

A second and complementary property of a fractal object is to be characterized by the self-similarity indicating that any part of the system under examination looks the same as the whole regardless of the resolution. Increasing the magnification merely reveals an increasing number of smaller irregularities that are morphologically similar to those observed at the larger scale. Self-similarity is a feature which may be a characteristic of a curve, a surface or a three-dimensional system. Mandelbrot (1982) has shown that the geometry of self-similar shapes can be described by a single number, the fractal dimension  $D$ . In fractal geometry it is possible to describe irregular lines (linecoast), no smooth planes (mountain surface) and hazardous volumes (clouds) existing in the nature by single non-euclidean dimension  $D$  different from the integer 1, 2, 3 values.

The length, surface area or volume of an object can be given by  $M_d$  ( $d=1,2,3$ ) (Friesen & Mikula, 1987), and defined as

$$M_d = N_d(r) \cdot m_d$$

where  $N_d$  is the number of yardsticks used of size  $r$  and mass  $m_d \propto r^d$  needed to fill

the object. In euclidean geometry  $N_d(r) \propto r^{-d}$ , being  $M_d$ , in this case, independent of the size of the yardstick used. On the contrary, when  $N_d(r) \propto r^{-D}$  in which  $D \neq d$ , a fractal object is considered whose  $M_d$  is dependent on the yardstick size used. In this way the shapes of the examples given above can easily be explained by the non-integral fractal dimension  $D$ , at least between a number of distinct size ranges  $r_{\min}$  and  $r_{\max}$ . In this way the increase of surface area  $M_2(r)$ , obtained when a smaller yardstick  $r$  is used could indicate a greater degree of roughness in this range.

### 3. Fractal geometry and pore structure of solids

Many of the physical and chemical properties of solids are under the influence of the morphological characteristics and surface geometry. Solid surfaces have complex structural heterogeneities, and it is difficult to express these quantitatively. The fractal geometry has been successfully applied to describe such structural heterogeneities of solid surfaces (IUPAC, 1994), the increase in the specific surface area when decreasing the yardstick used to measure it being an indication of fractal structure. Several complementary methods, such as mercury porosimetry, gas adsorption, thin-section technique and image analysis have been used to characterize the structural heterogeneity of natural and synthetic particles (Ross et al., 1988; Bartoli et al., 1991; 1992; Lefebvre et al., 1992). The application of this theory seems very useful because of the possibility to describe the pore structure of a solid by means of a single parameter such as its surface fractal dimension,  $D_s$ . The relation of this parameter with solids surface properties appears to be a promising and simple tool for understanding complex processes involving solid surfaces.

The methodologies relevant to the determination of the surface fractal dimension,  $D_s$ , have been thoroughly summarized in a recent review article by Farin and Avnir (1989). Each of the several techniques gives us information about the surface irregularities in a determined size range. The range of the yardstick,  $r$ , over which the surface of a particle can be characterized by a fractal dimension lies between the values  $r_{\min}$  and  $r_{\max}$ . Obviously, the lower and upper bounds on  $r_{\min}$  and  $r_{\max}$  are atomic spacing and the particle size, respectively. The physical mechanism(s) responsible for the creation of the self-similar surface may have been such as to further limit  $r_{\min}$  and  $r_{\max}$ .

Moreover, the possibility exists for a number of distinct size ranges to exhibit different types of self-similarity. In fact, in practice, two ranges of self-similarity are usually observed, one of them reflecting the textural fractal dimension, whereas the other one corresponds to the structural fractal dimension (Kindratenko et al., 1994).

#### 4. Surface fractal dimension from gas adsorption and mercury porosimetry

Gas adsorption isotherms and mercury porosimetry have been used for a long time as complementary methods to characterize the porous structure of solids in the micro-, meso-, and macropore range. Mercury porosimetry is generally regarded as the best method available for the routine determination of pore size in the macropore and upper mesopore range whereas nitrogen is the most suitable adsorptive for evaluation of both the surface area and the porosity of micro- and mesoporous materials from a single adsorption isotherm (Gregg and Sing, 1982).

Solids analyzed by nitrogen adsorption and mercury porosimetry techniques exhibit commonly a wide and continuous range of pore sizes from macropores through mesopores to micropores. The analogy with the continuum of electromagnetic wave lengths in the spectrum would seem particularly apt (Gregg and Sing, 1982). Thus, the more fine pores are considered the higher is the value of the measured specific surface area. Fractal approach has emerged recently as an analytical tool which is suitable for the description of such wide and complex pore structures which are found in most porous objects.

**Gas adsorption.** Fractal dimensions can be derived from molecular adsorption measurements in which the measuring scale or yardstick is defined by the effective area,  $\alpha$  ( $\propto r^2$ ), of the adsorbed molecule. Depending on the molecule used,  $\alpha$  can vary from 0.1-0.2 nm<sup>2</sup> for standard gases N<sub>2</sub>, Kr, and Ar, to 1800 nm<sup>2</sup> for some polymers (Avnir et al., 1984). Two approaches are possible in performing molecular adsorption experiments for the purpose of determining  $D_s$ . The obvious one is the use of geometrically similar molecules having a range of molecular diameters, while the second method utilizes only a single type of molecule and varies the particle sizes. The two techniques are equivalent if the particles have the same sort of self-similarity (Friesen and Mikula, 1987).

Recently, Avnir and Jaroniec (1989) have combined the surface fractal approach with micropore-filling theory and derived a Frenkel-Halsey-Hill (FHH) type equation for which the exponent is directly associated with the surface fractal dimension of the micropores:

$$\theta = K[\ln(p_0/p)]^{3-D_s}$$

where  $\theta$  is the relative adsorption,  $K$  is a characteristic constant,  $p_0$  and  $p$  are the saturation and equilibrium pressures, and  $D_s$  is the fractal dimension of the surface accessible to adsorption. By this equation, the surface fractal dimension can be determined by a single adsorption isotherm of many measuring points near completion of the monolayer adsorption on the micropore walls (AJ method). In a more recent paper, Yin (1991) presented an alternate derivation of the AJ equation from Kelvin's capillary condensation equation and a fractal pore size distribution; in this approach, multilayer coverage is viewed instead as the progressive filling of pores of increasing size. The AJ method has been applied by several authors in the sorption of nitrogen on a variety of solids and, in general, values of  $D_s$  obtained have been found to be a good indicator of the surface irregularity at the micropore level (Kaneko et al., 1991; Lefebvre et al., 1992; Celis et al., 1996).

**Mercury porosimetry.** Mercury intrusion porosimetry (MIP) is being used to study the surface fractality in the macro- and upper mesopore range. Based on the description of porous media in fractal terms of Pfeifer and Avnir (1983), Friesen and Mikula (1987) have suggested a fractal model of porous media applied to determine the fractal dimension of coal particles using the MIP technique. This model has also been applied to show the fractal structure of natural soils surfaces (Bartoli et al., 1991) as well as those altered soils after the addition of several compounds (Bartoli et al., 1992). Very recently, Celis et al. (1996) have used the power law:

$$S_{cum} \propto r_p^{2-D_s}$$

to describe the macropore fractal structure of synthetic clay-hydrous iron oxide associations from MIP measurements. In the above expression,  $r_p$  is the pore radius, and  $S_{cum}$  is the cumulative specific surface area calculated from the cumulative pore volumes

assuming cylindrical pore shape.

### 5. Fractal dimension of soil aggregates

The association of soil constituents in heterogeneous aggregates renders disordered state that, in many cases, can be explained by the fractal approach. Fractal geometry has been found to be a very useful tool to describe the complex pore structure of both natural and synthetic soil colloidal aggregates. Some studies use the MIP technique in order to test the fractality of these systems, being the obtained  $D_s$  values a measure of the degree of pore-volume filling of the pore system. One sandy soil and two silty soils were found to be surface fractals by Bartoli et al. (1991) using mercury porosimetry data. These authors attributed high  $D_s$  values to filling of large textural pores, thus decreasing the total pore volume.  $D_s$  values of artificial sand-clay mixtures and silt-clay mixtures, studied by Fies (1984), have been shown to increase as a function of the amount of clay in the mixture (Table I), and this has been attributed to the progressive filling of the large textural pores of the sand or silt by the small clay particles. The same type of results were obtained by Bartoli et al. (1992) after the addition of either Fe(III) polycations or Fe(III) polycation-humic macromolecule associations to a original silty soil. Fe(III) polycations associated with model humic macromolecules were less aggregative agents than were Fe(III) polycations alone, which gave rise to a progressive increase of the  $D_s$  values as a function of the adsorbed iron.

**Table I. Amounts of clay and surface fractal dimensions,  $D_s$ (Hg), calculated from mercury porosimetry for silt- and sand-clay mixtures (data from Fies, 1984).**

Sample	Clay (%)	$D_s$ (Hg)
Silt-clay mixtures	20	3.05
	30	3.10
	40	3.28
Sand-clay mixtures	10	2.66
	30	2.76
	40	2.81

In Table II are shown the surface fractal dimensions, total pore volume and bulk density obtained from mercury porosimetry data for some synthetic associations between calcium Wyoming montmorillonite (CaSWy), iron species, and commercial humic acid (Fluka HA). In agreement with the results obtained by Bartoli et al. (1992), the association of iron with the clay particles gives rise to a increase of the surface fractal dimension of the clay obtained by MIP,  $D_s(\text{Hg})$ . The decrease in both the total pore volume and the bulk density of the samples upon iron association supports the progressive filling of large pores of the clay particles by the small iron species. Similar results are obtained when humic acid, instead of iron species, were associated with the clay (Table II). However, the increase of the  $D_s(\text{Hg})$  value of the CaSWy-precipitated Fe complex after humic acid association (Table II) does not seem to be due to macropore filling by the humic material, but due to the creation of small pores as a result of the dispersant effect of the humic acid, since total porosity of the sample increased after humic acid association.

**Table II. Surface fractal dimensions,  $D_s(\text{Hg})$ , total pore volume,  $V_p$ , and bulk density of synthetic clay-iron-humic acid associations obtained from mercury porosimetry data.**

Association	Fe (%)	C (%)	$D_s(\text{Hg})$	$V_p$ ( $\text{mm}^3/\text{g}$ )	Bulk density* (g/cc)
CaSWy-precipitated iron hydroxide	0	-	$2.28 \pm 0.02$	1368	0.56
	0.67	-	$2.31 \pm 0.01$	1082	0.68
	1.88	-	$2.37 \pm 0.01$	849	0.82
	3.43	-	$2.40 \pm 0.01$	786	0.85
CaSWy-Fluka HA	-	0	$2.35 \pm 0.02$	1590	0.51
	-	2.8	$2.46 \pm 0.03$	1340	0.57
	-	6.8	$2.55 \pm 0.03$	1237	0.58
CaSWy-precipitated iron-Fluka HA	3.40	0	$2.26 \pm 0.01$	1232	0.57
	3.10	4.3	$2.48 \pm 0.04$	2221	0.37

\* Bulk density obtained from the volume of mercury displaced by the sample at atmospheric pressure.

The application of nitrogen adsorption isotherms to the study of natural and synthetic aggregates has received little attention, despite most of the specific surface area available for soil-water interface reactions is due to small pores which are not possible to study by the mercury intrusion porosimetry technique. The reason may be that results obtained from nitrogen adsorption experiments are difficult to interpret because much of the surface of clays and organic materials is not accessible for the nitrogen molecule. However, as reported by Murray et al. (1985), this information appears quite fundamental to the study of such systems because it relates to the thickness and arrangement of particles and, in consequence, the swelling behaviour resulting from the interaction of water with the particles surfaces.

Results of the application of the AJ method to the obtention of the surface fractal dimension of clay-iron-humic acid associations from nitrogen adsorption data are shown in Table III, together with the specific surface areas obtained for the different samples. As mentioned above, surface fractal dimensions obtained by the AJ method,  $D_s(N_2)$ , have been found to be related with the surface irregularity in the micropore range.

**Table III. Surface fractal dimensions,  $D_s(N_2)$  and specific surface areas of synthetic clay-iron-humic acid associations obtained from nitrogen adsorption data.**

Association	Fe (%)	C (%)	$D_s(N_2)$	Surface area (m <sup>2</sup> /g)
CaSWy-precipitated iron hydroxide	0	-	2.54 ±0.01	28
	0.67	-	2.57 ±0.01	30
	1.88	-	2.65 ±0.01	45
	3.43	-	2.62 ±0.01	56
CaSWy-Fluka HA	-	0	2.51 ±0.02	25
	-	2.8	2.13 ±0.04	3
	-	6.8	2.06 ±0.03	2
CaSWy-precipitated iron-Fluka HA	3.40	0	2.62 ±0.01	55
	3.10	4.3	2.36 ±0.03	10

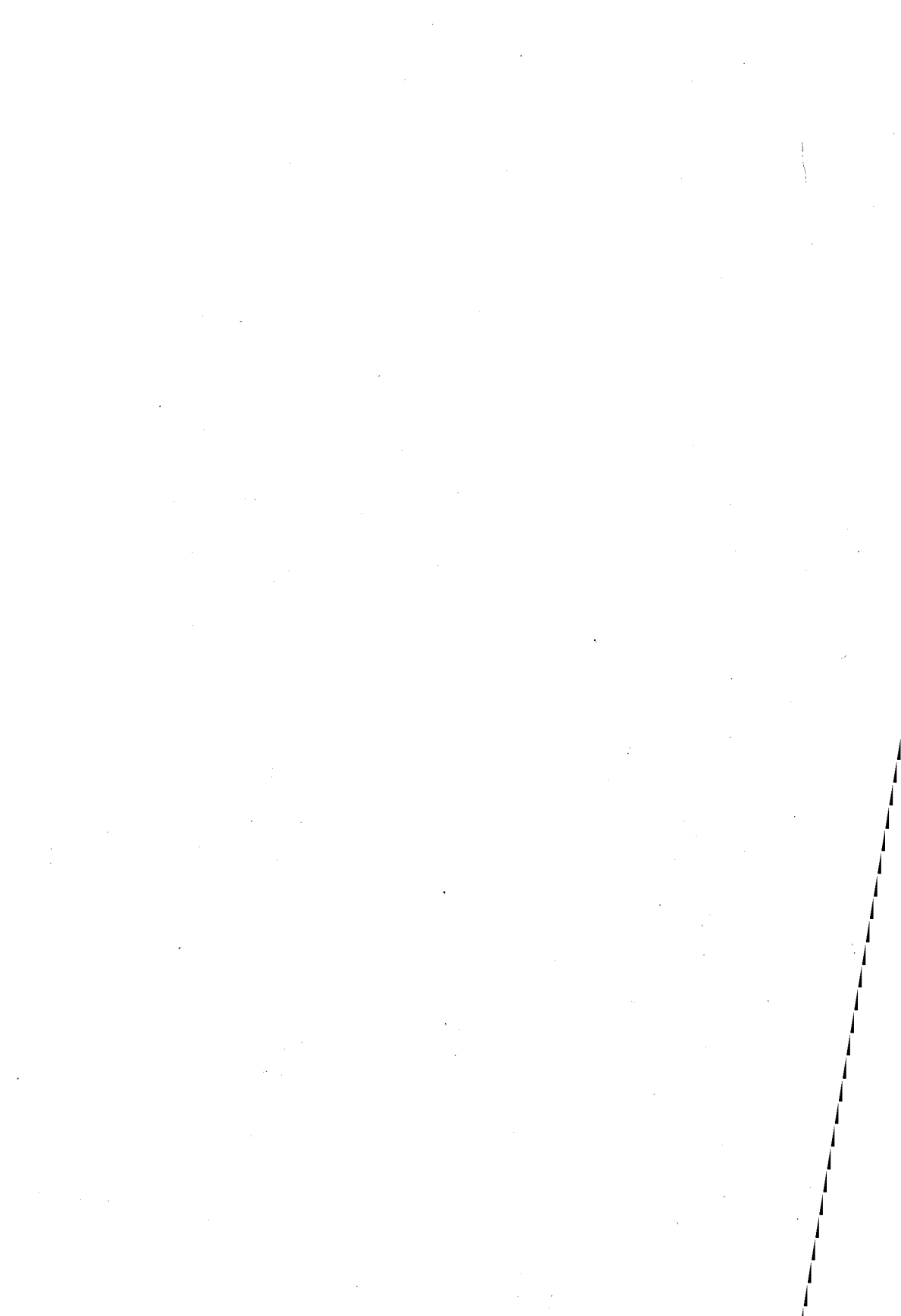
Iron precipitation on the clay surface increase the irregularities at molecular level as indicated by the increase in the surface fractal dimension obtained by nitrogen

adsorption. This increase should give rise to a progressive enhancement of the specific surface area of the clay, as found in Table III. The association of humic acid with mineral surfaces dramatically decreases the surface area accessible to nitrogen, and surface fractal dimensions reported in Table III, suggest that much of the surface due to micropores in the mineral samples is blocked by the organic matter.

**Acknowledgments.** This work has been partially financed by the EU project EV5V-CT94-0470 and Junta de Andalucía (Res.Group 4092). Thanks are due to R. Celis providing some experimental results.

## REFERENCES

- Avnir D, Farin D & Pfeifer P (1984). *Nature*, **308**, 261-263.
- Avnir D & Jaroniec M (1989). *Langmuir*, **5**, 1431-1433.
- Bartoli F, Philipp R & Burtin G (1992). *J. Soil Sci.*, **43**, 59-75.
- Bartoli F, Philipp R, Doirisse M, Niquet S & Dubuit M (1991). *J. Soil Sci.*, **42**, 167-185.
- Celis R, Cornejo J & Hermosin M C (1996). *Clay Miner.*, **31**, 355-363.
- Farin D & Avnir D (1989). *The Fractal Approach to Heterogeneous Chemistry*. (D. Avnir, ed.) J. Wiley & Sons Ltd.
- Fies J C (1984). *Agronomie*, **4**, 891-899.
- Friesen W I & Mikula R J (1987). *J. Colloid Interface Sci.*, **120**, 263-271.
- Gregg S J & Sing K S W (1982) *Adsorption, Surface Area and Porosity*, pp. 89-90. Academic Press Inc., London.
- IUPAC (1994). *Pure & Appl. Chem.*, **66**, 1739-1758.
- Kaneko K, Sato M, Suzuki T, Fujiwara Y, Nishikawa K & Jaroniec M (1991). *J. Chem. Soc. Faraday Trans.*, **87**, 179-184.
- Kindratenko V V, Van Espen P J M, Treiger B A & Van Grieken R E (1994). *Environ. Sci. Technol.*, **28**, 2197-2202.
- Lefebvre Y, Lacelle S & Jolicoeur C (1992). *J. Mat. Res.*, **7**, 1888-1891.
- Mandelbrot B (1975). *Proc. Nat. Acad. Sci. USA*, **72**: 3825-3828.
- Mandelbrot B (1982). *The Fractal Geometry of the Nature*. Freeman. S. Francisco. 468pp.
- Murray R S, Coughlan K J & Quirk J P (1985). *Aust. J. Soil Res.*, **23**, 137-149.
- Pfeifer P & Avnir D (1983). *J. Chem. Phys.*, **79**, 3558-3565.
- Ross S B, Smith D M, Hurd A J & Schaefer D W (1988). *Langmuir*, **4**, 977-982.
- Van Damme H (1992). *Proc. XI Reunión Científica-SEA*, Madrid, 45-88.
- Yin Y (1991). *Langmuir*, **7**, 216-217.



# SURFACE CHEMISTRY



## Fenuron adsorption on homoionic smectites

*Auger J P, Hermosín M C and Cornejo J*

Fenuron is an ureic (1,1-dimethyl-3-phenylurea) herbicide of polar character and high water solubility, having also a protonable amino group. Polar organic molecules can adsorb in smectitic clays by substituting the interlamellar water associated to the inorganic exchangeable cations (Mortland 1970, Sanchez-Martin and Sanchez-Camazano 1987, Hermosin et al. 1993, Cox et al. 1995) and protonable organic molecules can adsorb as molecule and after be protonated by the interlamellar water of clays displacing the original cations (Mortland, 1970, Feldkamp and White 1978, Cox et al. 1994, 1995). On another hand natural hydrophylic clays can be changed to hydrophobic by exchanging their natural inorganic exchangeable cations by large organic ones (James & Boyd 1991); these organo-clays sorbents can interact with polar organic molecules through hydrophobic bonding besides the polar ones (Hermosin and Cornejo 1993, Stapleton et al. 1995, Vimond-Laboudigue et al. 1996). The objective of the present work was to ascertain which of these three mechanisms contribute to the sorption of fenuron by smectites by using smectites with different layer charge and different exchangeable cations.

The mineral used in this study were two montmorillonites (SAz and SWy) and one hectorite (SH) from the CMS. Samples of SWy montmorillonite and SH hectorite were saturated with  $K^+$ ,  $Na^+$ ,  $Ca^{2+}$ ,  $Mg^{2+}$  and  $Fe^{3+}$  by treating the  $<2\mu m$  fraction with a solution of the respective chloride salts. An organic clay was also used by treating SWy with octodecylammonium (SWyC18). The adsorption isotherms of fenuron on clays were determined by batch equilibration technique using 0.1g of sorbent with 10 ml of fenuron solution of concentration ( $C_i$ ) ranging from 1 to 20  $\mu mol/L$ . Equilibrium concentration ( $C_e$ ) was determined by high performance liquid chromatography (HPLC). Difference between  $C_i$  and  $C_e$  was assumed to be due to adsorption.

Fenuron isotherms obtained on the three smectites (Figure 1) are of L-type indicating specific adsorption as given for polar or ionisable molecules (Giles et al. 1960, Cox et al. 1994, 1995). The lower sorption found in the highest layer charge SAz suggests interlamellar fenuron adsorption which is favored in low layer charge SWy and SH.

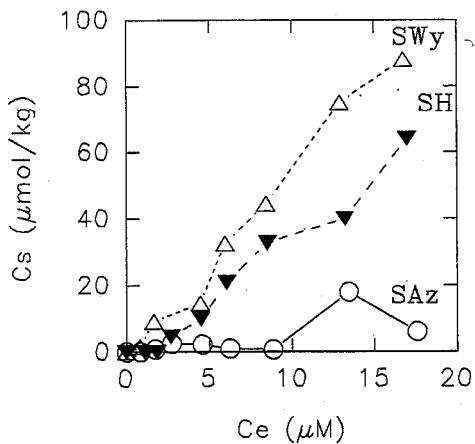


Fig 1. Fenuron isotherms on smectites of different layer charge

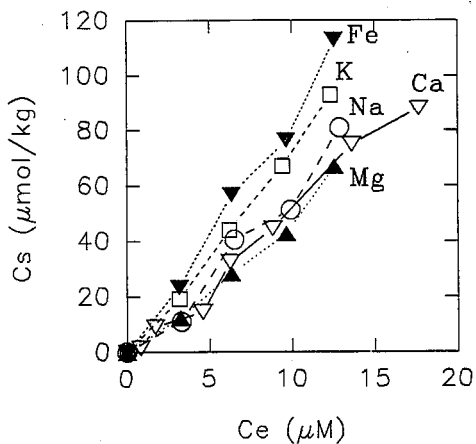


Fig 2. Fenuron adsorption isotherms on homoionic samples of SWy-montmorillonite

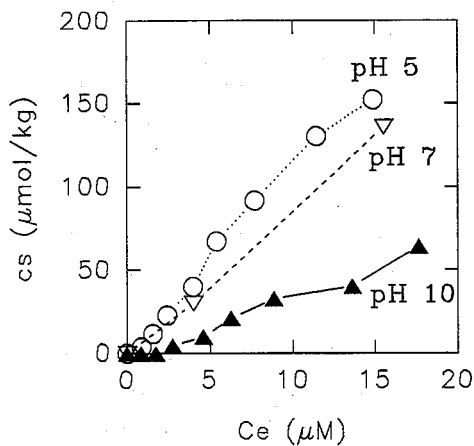


Fig 3. Fenuron adsorption isotherms on SH-Ca at different pH

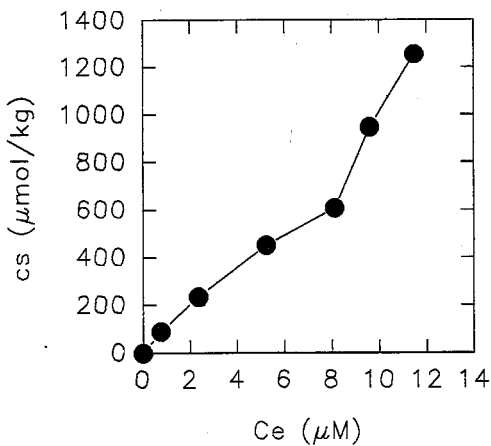


Fig 4. Fenuron adsorption isotherms on an organo-clay (SWyC18)

The effect of the saturating cation in smectites is shown in Figure 2. Differences were developed at fenuron concentration above 5  $\mu\text{M}$ . The lowest sorption was measured for the high ionic potential ions  $\text{Ca}^{2+}$  and  $\text{Mg}^{2+}$  and the highest for the low ionic potential  $\text{K}^{+}$  and  $\text{Na}^{+}$  and the highest ionic potential  $\text{Fe}^{3+}$ . This fact would indicate that fenuron could be bound to the exchangeable cation by polar bond through C=O groups substituting water molecules. The substitution of water should be facilitated in low polarizing cation. The iron cation is a special case, because the acid character of the water associated to the cation depends of its ionic potential (Mortland 1970), and for  $\text{Fe}^{3+}$  this water is highly polarized showing a strong acidic character (Mortland 1970). The low pH of Fe-SWy suspension confirms the acid character of this sample. This acidic water promotes protonation of the aminogroup of the fenuron molecule which adsorbs by displacing some interlamellar inorganic ions. The contribution of this cationic exchange renders the highest sorption for Fe-SWy sample.

The effect of the pH is shown in Figure 3 and suggests that the protonation of the molecule make easier its sorption in the smectites probably by partially displacing the inorganic interlamellar ions. For SH-K no pH influence was observed because in this case only polar sorption through C=O occurs, since  $\text{K}^{+}$  ion is difficult to displace from the interlamellar spaces.

The sorption isotherm on organic montmorillonite SWyC18, shown in Figure 4, indicates that hydrophobic bonding highly promotes the sorption of fenuron in this clay, despite its high water solubility, although the contribution of polar bonds should be possible (Hermosin and Cornejo 1993, Dentel et al. 1995).

**Acknowledgements:** J.P. Aguer on leave from the Universite Blaise Pascal-Clermont-Ferrand acknowledges a fellowship from the Conseil Regional d'Auvergne. This work has been partially financed by CICYT (AGF96-0514) and Junta de Andalucia (R.G. 4092).

## REFERENCES

- Cox, L. et al. 1994 *Clay Minerals* 29, 767-774  
Cox, L. et al. 1995 *European Journal of Soil Science* 46, 431-438  
Dentel, S.K. et al. 1995 *Wat. Res.* 29, 1273-1280  
Feldkamp, J. and White, J.L. 1978 *Developments in Sedimentology* 27, 187-196  
Giles, C.H. 1960 *J. Chem. Soc.*, 3373-3380  
Hermosin, M.C. et al. 1993 *Environmental Science & Technology* 27, 2606-2611  
Hermosin, M.C. and Cornejo, J. 1993 *Journal of Environmental Quality* 22, 325-331  
Hermosin, M.C. and Cornejo, J. 1992 *Chemosphere* 24, 1493-1503  
Jaymes, S.A. & Boyd, S.B. 1991 *Soil. Sci. Soc. Am. J.* 55, 43-48  
Mortland, M.M. 1970 *Advances in Agronomy* 22, 75-117  
Sanchez-Martin, M.J. and Sanchez-Camazano, M. 1987 *Chemosphere* 16, 937-944  
Stapleton, M.G. et al. 1994 *Environmental Science & Technology* 28, 2330-2335  
Vimond-Laboudigue, A. et al. 1996 *Clay Minerals* 31, 95-111

## Textural and sorptive properties of iron-coated clays

*Cellis R, Hermosín M C and Cornejo J*

Clays, metal oxides or oxyhydroxides and organic matter are rarely present in soils, sediments and particulate matter as independent particles, but they are normally associated in stable organomineral aggregates whose structure is the porous media in and through which all soil processes take place. Soil structure is closely related with its porosity geometry which, in turn, depends on the way as the different soil constituents are assembled with each other. Reactions occurring at the soil-water interface are also influenced by interparticle association since this determines the properties of the surfaces exposed by the soil aggregates.

A normally used procedure to study the formation of soil aggregates is their synthesis by association of inorganic and organic soil colloids under several physical and chemical conditions. Perhaps, the simplest example is the association of clays with poorly ordered hydrous iron oxides. The study of this system could be a first step to understand a more complex system like natural soil aggregates.

In the present work several techniques have been used to study the changes in porosity of kaolinite and montmorillonite after ferrihydrite association. A fractal pore size distribution was assumed to describe the textural properties of the clay-iron complexes. The changes in the surface reactivity of kaolinite and montmorillonite upon ferrihydrite association was tested by studying the sorption of the herbicide 2,4-dichlorophenoxyacetic acid (2,4-D) on the clays before and after coating the clay particles with the iron oxyhydroxide.

**MATERIALS AND METHODS**. The clay used for the syntheses were Wyoming montmorillonite, SWy-1, and Georgia kaolinite, KGa-2. Montmorillonite-ferrihydrite and kaolinite-ferrihydrite associations were prepared following a procedure based on the Russell (1979) method for the synthesis of ferrihydrite: suspensions containing 1.4

g of clay and 50 mL of solutions with 0 (control), 7.5, 30, 60 and 120 mg Fe/g clay were boiled for 8 minutes while constantly stirring.  $\text{Fe}(\text{NO}_3)_3$  was used as source of  $\text{Fe}^{3+}$ . The clay-ferrihydrite associations were washed with deionized water, lyophilized, and stored at room temperature until used.

Textural properties, specific surface area and porosity, of the iron-coated clays and control samples were determined by using the adsorption nitrogen isotherm and mercury intrusion porosimetry techniques. Fractal dimensions,  $D_s$ , of surface accessible to nitrogen were obtained from nitrogen adsorption data using the Avnir and Jaroniec (1989) equation.

Distribution coefficients,  $K_d$  ( $\text{L kg}^{-1}$ ), for 2,4-D sorption on the clays and iron-coated clays were obtained using a batch equilibration procedure. Fifty mg of solid were treated with 10 mL of herbicide initial solution ( $C_i = 1 \text{ mM}$ ) using  $\text{CaCl}_2$  as background electrolyte. Suspensions were shaken at  $20 \pm 2^\circ\text{C}$  for 24 h, centrifuged and the equilibrium concentration ( $C_e$ ) determined in the supernatant solutions by HPLC. Differences between initial and equilibrium concentrations were assumed to be sorbed ( $C_s$ ). From sorption data, distribution coefficients ( $C_s/C_e$ ) for the different iron-coated clays and control samples were calculated.

**RESULTS AND DISCUSSION.** Surface properties of kaolinite show little change by ferrihydrite association. Specific surface areas of kaolinite-ferrihydrite complexes were in agreement with values which correspond to a mixture of both components. Surface fractal dimensions obtained from nitrogen adsorption data,  $D_s(\text{N}_2)$ , indicated only a little increase in microporosity in the case of the associations with the highest amounts of iron. Macropore volumes obtained by mercury intrusion porosimetry also showed small insignificant differences in kaolinite macroporosity by iron association, and the original basal spacing of  $7.2 \text{ \AA}$  was also unaffected by the presence of ferrihydrite.

Association of ferrihydrite with montmorillonite led to important changes in the surface properties of the clay. Montmorillonite-ferrihydrite associations have high specific surface areas and pore structures which depend on the amount of iron in the association. Small amounts of iron increase the microporosity of montmorillonite (high  $D_s$  values); however, associations prepared from concentrated  $\text{Fe}^{3+}$  solutions

have a high surface area due basically to the presence of larger pores (low  $D_s$  values).

Sorptive properties of kaolinite and montmorillonite were also affected by the iron coatings. Whereas no sorption (kaolinite) or negative sorption (montmorillonite) of 2,4-D was measured on the pure clays, significantly higher positive sorption was found for increasing amounts of ferrihydrite on the clays surface (Fig. 1). The higher sorption measured for 2,4-D on the montmorillonite complexes compared to that on the kaolinite complexes, even for similar amounts of iron in the samples, agrees with the high specific surface area and porosity found for the montmorillonite-ferrihydrite associations.

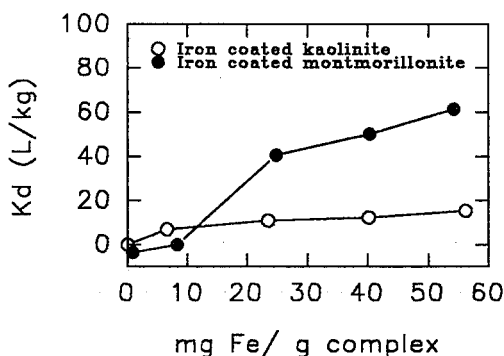


Figure 1. Distribution coefficients for the sorption of 2,4-D on iron-coated clays.

**CONCLUSIONS.** Results of this work show the importance of the association processes between the different soil constituents on the structure and reactivity of the resultant aggregates. Understanding the interaction mechanisms which lead to the formation of natural aggregates seems to be of primary importance to subsequently predict the behaviour of natural particles in physical and chemical processes.

**Acknowledgment.** This work was partially financed by EU project EV5V-CT94-0470 and Junta de Andalucía (Res.Group.4092)

#### **REFERENCES**

- Avnir D & Jaroniec M (1989). *Langmuir* 5, 1431-1433  
Russell D (1979). *Clay Miner.* 14, 109-114

Dip. Scienze Chimico  
Agrarie. Univ. degli Studi di  
Napoli Federico II. Portici  
(NA), Italia

## Nature and crystallization of mixed iron and aluminium gels : effect of Fe/Al molar ratio, pH and citric acid

Colombo C, Cinquegrani G, Adamo P, Violante P and Violante A

The effect of ageing on the mineralogical and chemical composition of hydrolytic species of Al or Fe formed at different pH values, both in the absence or presence of organic ligands has been extensively studied (1, 3). The influence of time, initial pH and presence of inorganic and organic ligands on the nature, chemical composition, mineralogy of mixed Fe(III) and Al precipitates has not been studied in detail (2, 4).

Citrate, produced by bacteria in the rhizosphere and identified in root exudates, is one of the most abundant low molecular weight carboxylic acid present in soil environment. Citrate strongly interacts with both Al and Fe (1,4).

Aim of this work was to study the nature and mineralogy of mixed Al and Fe(III) gels (initial Fe/Al molar ratio (R) ranging from 0.1 to 10) formed at pH values ranging from 4.0 to 10.0 both in the absence or presence of citric acid (Fe + Al/citrate molar ratio (R<sub>cit</sub>) of 0.01 and 0.1) and aged for long ageing period at high temperatures (50-95 °C).

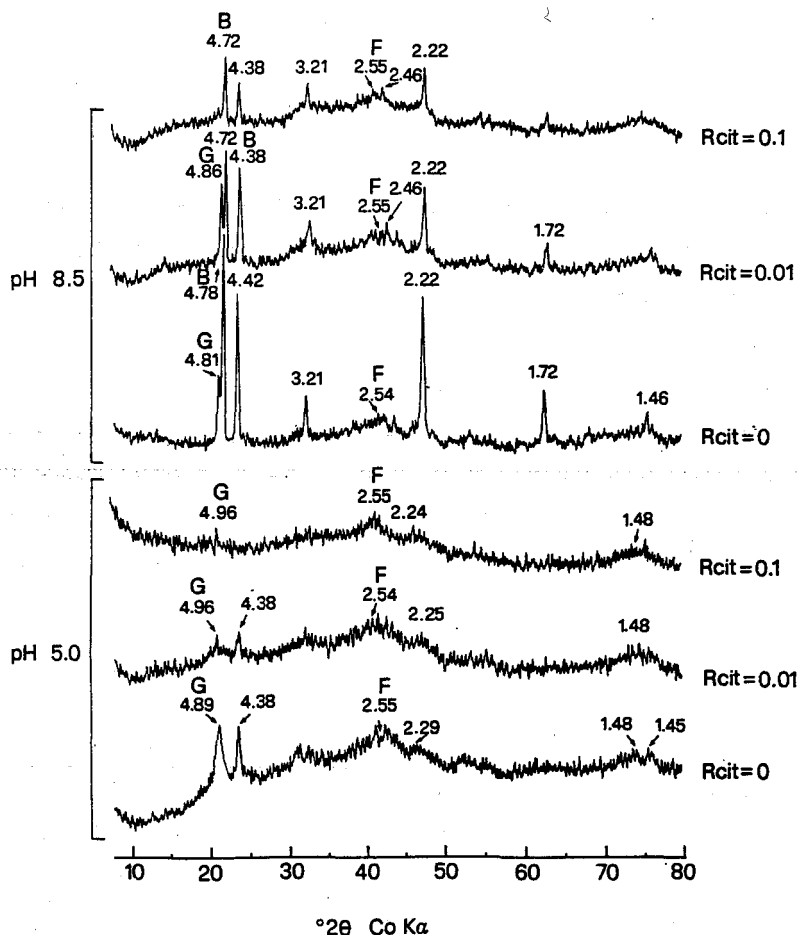
### Materials and methods

Stock solutions of 0.01 M Al(NO<sub>3</sub>)<sub>3</sub> and 0.01 M Fe(NO<sub>3</sub>)<sub>3</sub> were mixed in different proportions to have samples at initial Fe/Al molar ratio (R) of 0, 0.1, 0.5, 1.0, 4.0, 10.0 and ∞. The solutions were titrated to pHs 4.0, 5.0, 6.0, 7.0, 8.0, 8.5, 9.0 and 10.0 by 0.25 M NaOH. After 24 h of ageing of samples prepared at R=1 and titrated to pH 5.0 or 8.5, suitable amounts of citrate were added to the latter samples in order to have (Fe+Al)/citrate molar ratio (R<sub>cit</sub>) of 0.01 or 0.1. The final Fe + Al concentration was 0.005 M in all the samples. During the ageing at high temperatures (50 or 95 °C) subsamples were collected and ultrafiltered (0.2 or 0.01 μm). The filtrates were analyzed for Al and Fe by atomic absorption spectrophotometry. Other subsamples were dialyzed, freeze-dried and analyzed by X-ray diffraction (XRD) differential thermal (DTA)

analyses. Fe and Al were also determined by atomic absorption for the dialyzed samples after dissolution with pH 3.0  $\text{NH}_4$  oxalate.

### Results

The initially formed mixed hydroxy Fe-Al precipitation products were metastable and slowly converted, depending on the R values, ageing time, initial pH and citrate concentration toward more stable  $\text{Al}(\text{OH})_3$  polymorphs and hematite.



X-ray powder diffractograms of the samples aged 30 d at room temperature obtained at pH 5.0 and 8.5 at  $(\text{Fe}+\text{Al})/\text{Citrate}$  molar ratio 0.01 and 0.1. G stands for gibbsite, F for ferrihydrite and B for bayerite.

It was ascertained that at a given pH the higher the initial Fe/Al molar ratio the higher the amount of Fe + Al present in soluble or very fine solids ( $< 0.2$  or  $0.01 \mu\text{m}$ ). Gibbsite without the presence of well crystallized Fe-oxides was formed at pH 5.0 in the samples at  $R \leq 1$ . On the contrary, only after prolonged ageing at 50-90 °C gibbsite or hematite was identified in the samples at  $R > 1$ . Low-crystalline ferrihydrite was still present in samples formed at R of 1 or 4 even after 120 days of ageing at 50 °C and subsequently for 30 days at 95 °C.

Complexes prepared at initial Fe/Al molar ratios of 1 and 2.5 and at pH values of 4.0-10.0 showed strong differences in the mineralogy of the final precipitation products. Large amounts of Fe + Al (25-82 % of Fe + Al) were solubilized from the samples aged 60 days at 50 °C by ammonium oxalate. The samples formed at  $R = 10$  showed ferrihydrite, ferrihydrite + gibbsite, and hematite +  $\text{Al}(\text{OH})_3$  polymorphs + ferrihydrite respectively at pH 4.0, 5.0-7.0 and 9.0-10.0. The samples formed at  $R = 2.5$  showed greater quantities of low-crystalline ferrihydrite, being  $\text{Al}(\text{OH})_3$  polymorphs and hematites formed only at  $\text{pH} > 7$ .

Finally it was observed that increasing concentrations of citrate in samples containing equimolar amounts of Fe and Al strongly inhibited the formation of  $\text{Al}(\text{OH})_3$  polymorphs by promoting the formation of short-range ordered materials at pH 5.0 (Figure). The presence of well crystallized gibbsite and poorly ordered ferrihydrite was observed in the sample formed at pH 5.0 in absence of citric acid ( $R_{\text{cit}}=0$ ), a strong reduction of gibbsite appeared evident in presence of increasing amount of citric acid ( $R_{\text{cit}} = 0.01$  and  $0.1$ ). At pH 8.5 the proportions of gibbsite and bayerite with poorly ordered ferrihydrite decreased with increasing amounts of citrate. The addition of the organic acid in the samples at  $R_{\text{cit}} 0.1$  determines a almost completely inhibition of crystallization of gibbsite.

### References

- (1) Cornell R. M. & Schwertmann U (1979). *Clays & Clay Minerals*. 27, 402-410.
- (2) Huang, P M & Violante A (1986). In: *Interaction of Soil Minerals with Natural Organics and Microbs*. P. M. Huang and M. Schnitzer, editors. Soil Sci. Soc. Amer. Spec. Publ. 17, 549-592.
- (3) Lewis D G & Schwertmann U (1979). *Clays & Clay Minerals* 27, 195-200.
- (4) Rengasamy P & Oades J M (1979). *Aust. J. Soil Res.* 17, 141-153

(1) Dpto. Química  
Inorgánica. Univ. de  
Córdoba, España

(2) Instituto de Recursos  
Naturales y Agrobiología.  
CSIC. Sevilla, España

## Sorption of anionic organic pollutants on hydrotalcites with different layer charge

Gaitán M (1), Barriga C (1), Pavlovic I (1), Ulibarri M A (1),  
Hermosín M C (2) and Cornejo J (2)

Over the last few years, an increasing number of organic pollutants (OP) has been discharged into the environment with increasing human activities, which has caused various problems in water and wastewater treatment systems. The two actual approaches to remediate contaminated waters are physico-chemical and biological process. The physico-chemical process more widely used is the remove of OP by sorption on activated carbon, but the increased sorbent demand needs new competitive sorbents.

Hydrotalcite-like compounds of general formula  $[M_{1-x}^{II} M_x^{III}(\text{OH})_2]A_{x/n}^{n-} \cdot m\text{H}_2\text{O}$  have positively charged brucite layers neutralized with interlayer anions, and water molecules occupying interlayer spaces. These anions and water molecules can be interchanged with other organic anion and polar molecules (1). Recently we have reported the ability of LDH compounds and its calcined products to adsorb phenols from waters (2). The aim of present work is to evaluate the influence of the layer charge of the hydrotalcite in the sorption of the anionic organic pollutant TNP, using three hydrotalcites prepared to give different Al/Mg substitution in their brucite layer and hence with different layer charge.

Hydrotalcite-like compounds  $[M_{1-x} \text{Al}_x(\text{OH})_2](\text{CO}_3)_{x/2} \cdot m\text{H}_2\text{O}$  were prepared with several molar Mg/Al ratio (2,3 and 4) by coprecipitation method at pH = 10, as previously described (3). TNP adsorption was measured by batch equilibration technique at different phenol concentrations (adsorption isotherms) at pH=2. TNP was quantified in solution by spectrophotometric measurements at 360 nm.

The results of the elemental analysis of the three synthesized hydrotalcites are given in Table 1 showing that actual Al/Mg substitution were found slightly lower than those theoretical one. According to these analyses the actual formula and anion exchange capacity were calculated.

The X-ray diffraction patterns of the three samples are typical of a material with the hydrotalcite structure showing very well defined integral basal spacing up to the third order ( $d_{003}=7.8-7.5 \text{ \AA}$ ,  $d_{006}= 3.9-3.8 \text{ \AA}$  and  $d_{009}= 2.6-2.5 \text{ \AA}$  ).

Table 1. Chemical analyses results and lattice parameters of the samples studied

Samples	%Mg	%Al	Mg/Al	$a/\text{\AA}$	$c/\text{\AA}$
Mg2Al-HT	14.4	10.8	1.48	3.04	22.8
Mg3Al-HT	19.3	8.1	2.65	3.06	23.24
Mg4Al-HT	21.3	6.2	3.82	3.07	23.49

The adsorption isotherms of TNP on the three hydrotalcite samples, obtained by plotting the amount adsorbed on the solid  $C_s$  versus equilibrium solution concentration  $C_e$ , are given in Figure 1. These isotherms were of L-type (4) indicating specific and strong interaction mechanism, ionic attraction sorbate-sorbent, as it has been shown earlier (2). No significant differences were developed for the three samples studied, only the lowest charge sample 4:1 shows slightly lower sorption in Fig. 1.

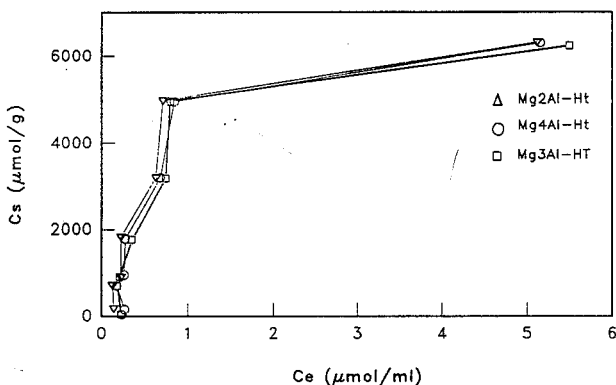


Figure 1. Adsorption isotherms of TNP on MgAl-HT samples

The sorption isotherm data were fit to the Langmuir equation ( $C_1/C_s = C_1/C_m + 1/C_m L$ ) where  $C_1$  is the solute concentration at equilibrium solution,  $C_s$  is the amount of solute adsorbed in the sorbent at equilibrium. The values of  $C_m$  are used as a relative measure of the sorption capacity and were similar to those reached in the plateau of the isotherms and all were higher than those corresponding to the AEC and higher than that reported earlier for similar 3:1 sample (2). The sorption of TNP above AEC would indicate that additional sorption mechanisms, besides the anionic interlamellar exchange, would be contribute to overall adsorption. This has been found in clay minerals for organic cation sorption (5-7) and it has been interpreted as due to sorption of the corresponding neutral molecules (organic cation with a solution counter ion) lipophilically attracted by the organic moiety of the organic cations, forming cluster at the edge

of the interlayers. Similarly, neutral TNP molecules could be adsorbed associated to the initially TNP anions sorbed. However, unlike in clay minerals (6,7) the amount of layer charge seems to have no effect on the TCP sorption by Al/Mg hydrotalcsites.

It is worth to note the higher sorption measured in these samples (Cm - 7500  $\mu\text{mol/g}$ ) compared to those obtained earlier (Cm - 750  $\mu\text{mol/g}$ ) by anionic exchange on similar samples. The reason may lay on the different preparation methods (the slurry was submitted at longer aged time ) which render different crystallinity. It seems that the higher crystallinity of these samples probably implies higher order in the distribution of layer charge which would facilitate the anionic exchange.

XRD patterns and IR spectra of the original HT 3:1 sample, its product corresponding to the highest point in the isotherm and the TNP-HT product obtained by the complete ion exchange with a TNP concentrate solution (40mM) lead that the exchange reaction occurred, the product obtained in the isotherm shows a developing TNP-HT phase at 13.0 Å with their higher order reflections at 6.6 Å and 4.4 Å, and in the IR spectrum appears also the corresponding picrate bands at 3600-3400  $\text{cm}^{-1}$   $\nu_{\text{C-H}}$  aromatic and  $\nu_{\text{O-H}}$  phenolic, 1640, 1617, 1343 and 1285  $\text{cm}^{-1}$  of  $\nu_{\text{N-O}}$ , 1531, 1500 and 1480  $\text{cm}^{-1}$  of ring breathing and at 1378  $\text{cm}^{-1}$  of  $\nu_{\text{C-O}}$  phenolate. The wide 1640  $\text{cm}^{-1}$  band in the product of the isotherm reveals the  $\nu_{\text{C-O}}$  of the carbonate anions still present in this sample as shown in the X-ray diffractogram. These picrate X-ray patterns and IR bands appears very well defined in the product obtained by complete anionic exchange.

Therefore, we can conclude that the amount of substitution in the brucite layer of HT does not influence the sorption of TNP although it is adsorbed by anionic exchange in the interlayer of the structure. In addition TNP molecules seems to be adsorbed in different amount above the AEC of the hydrotalcsites.

*Acknowledgements.* This project has been partially financed by the CICYT proyect no. AMB 93-0097 and the Research Groups 4092 and 6113 of Junta de Andalucia

## References

1. Kopka H. Beneke K. & Lagaly G., (1988) *J. Colloid Interface Sci.* 123,427-436.
2. Hermosin, M.C., Pavlovic, I., Ulibarri, M.A. & Cornejo, J. (1996) *Water Res.* 30,171-177.
3. Reichle, W.T., (1985) *J. Catal.* 94, 547
4. Giles, G.M., MacEwan, T.H., Nakhwa, S.N. & Smith D., (1960) *J. Chem. Soc.* 3973-3993.
5. Narine, D.A. & Guy, R.D. (1981). *Clays & Clay Minerals* 29, 205.212.
6. Jaynes, W.F. & Boyd, S.A. (1991). *Soil Sci. Soc. Am. J.* 58,1382-1391.
7. Hermosin, M.C., Martin, P. & Cornejo, J. (1993). *Environ. Sci. Technol.* 27,2606-2011.

## Dinitrophenol and 2,4-dichlorophenoxyacetic acid sorption by organoclays

*Hermosín M C and Cornejo J*

Organoclays have been earlier studied as sorbent for OP (Cowan 1963, Faust & Miller 1972) but recently there has been an increasing interest for organoclays as sorbent for non-polar organic pollutants (NPOPs) (Mortland et al. 1986; Jaynes & Boyd 1991;), and in less extension for polar or ionizable organic pollutants (PIOPs) (Hermosin et al. 1992, 1993, 1995; Sanchez-Camazano & Sanchez-Martin 1994, Dentel et al. 1995, Stapleton et al. 1995, Vimond-Laboudigue et al. 1996). The objective of this work was to assess the sorption capacity and mechanisms of the PIOP dinitrophenol and 2,4-dichlorophenoxyacetic acid on different organoclays as a function of the type of clay charge and saturating alkylammonium cation. The knowledge of the interaction mechanism sorbent-pollutant at a molecular level as shown in this communication can contribute to establish the basis for sorbent design. 2,4-Dinitrophenol is highly produced for the synthesis of dyes, explosives, wood preservatives, photochemicals and pesticides and thus can reach waters from different sources and 2,4-D is a widely used herbicide which is increasingly found in surface and ground waters.

The organoclays were prepared from the standard of CMR (CMS) smectites, SWy and SAz and hectorite SH-Ca and a vermiculite from Santa Olalla (Spain) deposit by treatment with ethanolic/water solution of the following alkylammonium: hexadecyltrimethylammonium (HDTM) and octadecylammonium (C18). The 2,4-D was purchased from Aldrich and dinitrophenol from Merck as analytical grade and alkylammonium from Sigma. The sorption isotherms were measured by batch techniques using different 2,4-D and DNP concentrations and duplicate samples (with blank controls) and the PIOPs concentration was determined by UV-VIS spectroscopy (280 nm 2,4-D and 360nm, DNP). X-ray diffractograms and FT-IR spectra were obtained on organoclays saturated with 2,4-D and DNP by successive treatment.

Table 1 summarizes the characteristics of the organoclays, the total Freundlich ( $C_s = K_f C_e^{n_f}$ ) sorption capacity  $K_f$  from the isotherms and the same parameter, in the organic carbon basis, named  $K_{oc}$  or organic sorption efficiency (organic sorption capacity by organic carbon unit =  $K_f / oc \times 100$ ). The higher sorption was found for organoclays showing the higher basal spacing (SWC18, SAC18<sub>1</sub>, and SAC18<sub>2</sub>), this is thicker organic interlayer with paraffinic

structure ( $d_{001} > 20$ , Lagaly, 1987), even having high layer charge (SAC18<sub>3</sub> and SAHDTM). The importance of the hydrophobic interaction in this case is developed by the high  $K_{oc}$  of the SWHDTM having even low  $d_{001}$  value. The highest  $K_{oc}$  values for the paraffinic clays (SWC18, SAC18<sub>1</sub>, SAC18<sub>2</sub> and SAHDTM) is due to the interlamellar adsorption as indicated by the expansion of their basal spacing after phenol interaction (Table 2).

**Table 1. Organo clay and DNP-organo clay complexes properties and parameters.**

Org-clay <sup>a</sup>	%OC <sup>b</sup>	CEC meq/100g	LC <sup>c</sup> molc/u.cell	$d_{001,oc}$ nm	Kf umol/g	$K_{oc}$ umol/g	$d_{001,DNP-OC}$ nm
HC18	19	44	0.31	1.7	117	609	1.7
SWC18	17	76	0.69	2.7(b)	676	3840	2.9(b)
SWHDTM	13	"	"	1.7	420	3230	1.7
SAC18 <sub>1</sub>	12	120	1.13	3.0-2.3(b)	376	3159	3.0-2.3(b)
SAC18 <sub>3</sub>	40	"	"	3.3	957	2330	3.6
SAHDTM	24	"	"	2.3	840	3500	3.2
VC18	17	140	1.20	1.7	96	568	1.7

<sup>a</sup>C18=octadecylammonium, HDTM=hexadecyltrimethylammonium; <sup>b</sup>OC=organic carbon content; <sup>c</sup>LC=layer charge, OC=organo clay; OC-DNP=organo clay-DNP complex.

The FT-IR spectrum of DNP-OC complex showed differences with respect to that of DNP indicating strong polar interactions sorbate-sorbent: a) the decrease in the  $\nu_{N=O}$  DNP bands from 1540 and 1334  $cm^{-1}$  to 1524 and 1324  $cm^{-1}$  indicated H-bonds of the nitro groups with the amino groups of the interlayer alkylammonium and b) the increase in frequency of  $\delta_{O-H}$  band from 1348 to 1373  $cm^{-1}$  would suggest phenolic group be H-bond to the basal oxygen of the silicate layers which would interact also with  $\pi$  electrons of the aromatic ring changing also the frequency of the ring breathing modes ( $\nu_{C=C}$  from 1627 and 1598 to 1609, 1568 and 1560  $cm^{-1}$ ).

The 2,4-D sorption capacity, Kf, from Freundlich equation and efficiency  $K_{oc}$  are summarized on Table 2. The highest sorption capacities correspond to OC with paraffinic distribution ( $d_{001} > 2.1$  nm) in the organic interlayer, which firstly determined 2,4-D sorption. The organic sorption efficiency,  $K_{oc}$ , increased with the thick of the organic interlayer, but also with decreasing layer charge, as shown by the highest  $K_{oc}$  value of the SWC18<sub>2</sub> sample. The similar efficiency showed by SWAC18<sub>1</sub> and VC18<sub>2</sub>, having the first sample more hydrophobic alkyl group, suggested additional forces in the interaction of 2,4-D and OC. The interlayer 2,4-D adsorption in the paraffinic OCs (SWC18<sub>2</sub>, SAC18<sub>1</sub>, SAC18<sub>2</sub>, VC10<sub>1</sub>, VC10<sub>2</sub>) is shown by the increase of  $d_{001}$  of the complexes (Table 2).

**Table 1. Organoclay and 2,4-D-organoclay complexes properties and parameters.**

Org-clay <sup>a</sup>	%OC <sup>b</sup>	CEC meq/100g	LC <sup>c</sup> molc/u.cell	d <sub>001,OC</sub> nm	Kf umol/g	Koc umol/g	d <sub>001,2,4D-OC</sub> nm
HC18	19	44	0.31	1.7	110	579	1.7
SWC10	10	76	0.68	1.4	20	200	1.4
SWC18 <sub>1</sub>	11	"	"	1.7	60	545	1.6
SWC18 <sub>2</sub>	18	"	"	2.7(b)	590	3470	3.0-2.7(b)
SWHDT	13	"	"	1.7	30	250	1.7
SAC18 <sub>1</sub>	12	120	1.13	3.0-2.3(b)	230	1916	3.2-2.6(b)
SAC18 <sub>3</sub>	40	"	"	3.3	650	1625	3.6
VC10 <sub>1</sub>	17	140	1.20	2.2	260	1470	2.7
VC18 <sub>2</sub>	18	"	"	2.4	320	1944	3.3
SpC18	2	12	--	--	15	750	--

C10=decylammonium, C18=octadecylammonium, HDTM=hexadecyltrimethylammonium;  
<sup>a</sup>OC=organic carbon content; <sup>c</sup>LC=layer charge; (b)=broad, no well defined.

The features appearing in the FT-IR spectrum of the 2,4-D complexes showed that in the paraffinic OC the herbicide was associated to the interlayer alkylammonium by three binding mechanisms: a) neutral 2,4-D molecules by organophilic "tail-tail" bonds, b) neutral 2,4-D species by polar bonds between C=O of the carboxylic group and N-H of alkylammonium and c) anionic 2,4-D species bonded by ionic forces to R-NH<sub>3</sub><sup>+</sup>. These interactions occurs in that order, this is firstly molecular species were adsorbed by the organic layer which is thick enough after let the interlayer polar and ionic 2,4-D sorption.

**Acknowledgments:** This work was partially financed by CICYT project AGF96-0514 and Junta de Andalucia (Res.Group No.4092).

#### REFERENCES

- Cowan, C.T. 1963. *Clay & Clay Minerals* 10:225-234.  
 Dentel, S.K., Bottero, J.Y., Khatib, K., Demougeot, H., Diquet, J.P. & Anselme, C. 1995. *Wat. Res.* 29: 1273-1280.  
 Hermosin, M.C., Ulibarri, M.A., Mansour, M.M. & Cornejo, J. 1992. *Fresenius Environ. Bull.* 1:472-481  
 Hermosin, M.C. & Cornejo, J. 1992. *Chemosphere* 24: 1493-1503.  
 Hermosin, M.C. & Cornejo, J. 1993. *J. Environ. Qual.* 24: 1493-1503.  
 Hermosin, M.C., Crabb, A. & Cornejo, J. 1995. *Fresenius Environ. Bull.* 4: 514-519.  
 Miller R.W. & Faust F.D. 1972. *Environ. Letter* 4: 211-223.  
 Mortland, M.M., Shaobai, S. & Boyd, S.A. 1986. *Clays and Clay Minerals* 34: 581-585.  
 Jaynes, S.A. & Boyd, S.B. 1991. *Soil Sci. Soc. Am. J.* 55: 43-48.  
 Sanchez-Camazano, M. & Sanchez-Martin, M.J. 1994. *Water, Air and Soil Poll.* 74:19-28.  
 Stapleton, M.G., Sparks, D.R. & Dentel, S.K. 1994. *Environ. Sci. Technol.*: 2330-2335.  
 Vimond-Laboudigue, A., Baron, M.H., Merlin, J.C. & Prost, R. *Clay Minerals* 31:113-126

## Thermodynamics of the potassium adsorption process by smectites at high temperatures

*Linares J, Huertas F, Caballero E and Jiménez de Cisneros C*

### 1. Introduction.

The calculations of some thermodynamic parameters, Gibbs Free Energy, Enthalpy and Entropy, need to know the exact value of the equilibrium constant of the species in reaction. Only in genuine equilibrium states, when reversibility conditions are present, the inference of the equilibrium constant can be easily carried out. In the case of heterogeneous reactions with solid and liquid phases, the reaching of thermodynamic equilibrium depends essentially on several processes affected by the kinetic of the reaction. So, it is necessary to carry out kinetic studies to prove the actuality of the equilibrium conditions.

In hydrothermal kinetic experiences, smectite was submitted to a potassium exchange process. The natural smectites used in this study have the exchangeable sites occupied by Ca, Mg, Na and K, in this order of concentration. When a such smectite is submitted to exchange with KCl solutions of variable ionic strengths, the substitution of those ions is performed by steps and the reaching of equilibrium depend on the potassium concentration and time; temperature has a minimum effect. As Huertas et al. (1995) have studied, the exchange process begins with partial removal of sodium from the interlayer space, only when this ion is practically removed, calcium and magnesium begin to go to the solution. The equilibrium is finally reached when potassium occupies the exchange positions.

Once known the equilibrium constant of the exchange reaction, the calculation of the thermodynamic parameters of the process can be carried out. In this paper the values of Gibbs Free Energy, Enthalpy and Entropy were calculated.

### 2. Material and methods.

The smectite comes from the volcanic region of Cabo de Gata, Almería, Spain. It is of hydrothermal origin, produced by alteration of volcanic tuffs at temperatures not higher than 100°C. The mineralogical composition is smectite (97%) and minor quantities of quartz, plagioclase, calcite and disordered cristobalite. The smectite was treated with KCl solutions from 0.025 to 1 M, at temperatures from 60 to 200°C, during 1 to 360 days in Teflon reactors. The bentonite/solution ratio was 1/5. Solutions and solid phases were separated and analysed.

### 3.- Experimental results and Discussion.

As it is indicated by Cuadros and Linares (1996) and in other paper of this Congress (Linares et al., 1996), after the hydrothermal treatment no evidences of illite transformation

were shown, only slight chemical changes due to the dissolution of accessories and the beginning of the transformation into illite. As was indicated in these papers, the main process taking place was the exchange of all interlayer actions by potassium. The kinetic data show that there is a true equilibrium between the present species.

3.1. The equilibrium constant. The main difficulty to calculate this parameter is the exact knowledge of the activity coefficients of the participant species. The equilibrium constant for an adsorption process can be defined by:

$K = (\gamma_s \cdot C_s) / (\gamma_e \cdot C_e)$ , where  $\gamma_s$  and  $\gamma_e$  are the activity coefficients of adsorbed cation and water, respectively;  $C_s$  is the  $\mu\text{g}$  of adsorbed cation per millilitre of solution in contact with the adsorbent phase, and  $C_e$  are the  $\mu\text{g}$  of cation per millilitre of equilibrium solution.

The value of  $C_s$  it is not the mere concentration of the adsorbed cation. Fu et al. (1948) have deduced an expression permitting a more strict calculation:

$$C_s = [(\rho_1/M_1) A_1] / [(S/N \cdot X_m) - (A_2/M_2 \cdot 10^6)]$$

where,  $\rho_1$  is de specific gravity of the water (g/ml);  $M_1$  and  $M_2$  are the molecular and atomic weight of water and potassium (g/mole);  $A_1$  and  $A_2$  are the area of the water molecule and the cation (cm<sup>2</sup>/molecule);  $N$  is the Avogadro number,  $S$  is the surface area of the adsorbent (m<sup>2</sup>/g) and  $X_m$  the amount of adsorbed cation ( $\mu\text{g}/\text{g}$ ).

The activity coefficients changes with the ionic strength of the solution and temperature and its calculation is very difficult. But, as these coefficients lead to one when the ionic concentration is close to zero, that is to say, at infinite dilution, it is possible to calculate the equilibrium constant of the adsorption process according to the following expression:

$$K_0 = (\gamma_s \cdot C_s) / (\gamma_e \cdot C_e) = \lim_{C_s \rightarrow 0} (C_s/C_e) C_s \rightarrow 0$$

The value of  $K_0$  it can be obtained more precisely plotting  $\ln (C_s/C_e)$  versus  $C_s$  and by extrapolation to  $C_s = 0$ , for each isotherm.

The obtained values were:

For 60°C,  $K_0 = 2.489$ ;                      For 120°C,  $K_0 = 2.657$

For 175°C,  $K_0 = 2.988$ ;                      For 200°C,  $K_0 = 3.013$

3.2. Gibbs Free Energy. Once deduced the value of the equilibrium constant, the Gibbs Free Energy can be calculated by the expression:

$$\Delta G_0 = - RT \ln K_0$$

where  $R$  is the gas constant and  $T$  the absolute temperature.

The calculations have shown the following results for  $\Delta G_0$  (KJ/mol):

For 60°C,  $\Delta G_0 = - 2.525$ ;                      For 120°C,  $\Delta G_0 = - 3.192$

For 175°C,  $\Delta G_0 = - 4.077$ ;                      For 200°C,  $\Delta G_0 = - 4.337$

These negative values show that the adsorption process is spontaneous, but not highly energetic. The obtained values are in accordance with other deduced by similar systems (Garrels and Tardy, 1982; Sposito, 1981, 1984; Sparks, 1987, among others).

3.3. Enthalpy. It can be deduced from the Van't Hoff equation:

$$d \ln K / d \ln T = \Delta H / RT^2$$

assuming that the Enthalpy is constant (independent of temperature) and by integration of this expression, the following equation is obtained:

$$\ln K = (\Delta H / RT) + C, \text{ where } C \text{ is an integration constant.}$$

By plotting  $\ln K$  versus  $1/T$ ,  $\Delta H$  can be obtained from the slope value.

The graphic show that the value at 120°C is slightly anomalous. In any case, the value of  $\Delta H$  can be considered as constant for the range of studied temperatures.

This value is - 1.8 KJ/mole and correspond to an weak exothermic reaction, normal for an exchange process.

3.4. Entropy. This parameter can be obtained applying the classical  $\Delta G = \Delta H - T\Delta S$  for two temperatures, i.e. the maximum and minimum ones.

The obtained value is - 13 J / °mole.

This negative result indicates that the process changes to a more ordered state. The gradual occupation of the exchange sites by potassium (practically dehydrated) in the interlayer space produce a rearrangement of the smectite layers. The water of hydration of the previous cations (Ca, Mg and Na) is removed from the interlayer and this space is transformed in something more "solid" with a layer of "rigid" potassium ions. The previous random distribution of hydrated cations in the original smectite is changed to a new situation in which the order of dehydrated potassium prevails.

#### 4. References.

- Cuadros J. and Linares J. 1996. Experimental kinetic study of the smectite-to-illite transformation. *Geochim.Cosmochim.Acta*, 60, 439-453.
  - Fu Y, Hansen R.L.S. and Bartell F.E. 1948. Thermodynamics of adsorption from solutions .I. *J.Phys.Chem.* 52, 374-386.
  - Garrels R.M. and Tardy Y. 1982. Born-Haber cycles for interlayer cations of micas. *Int.Clay Conf.*1981, 423-440.
  - Huertas F.J., Cuadros J. and Linares J. 1995. Modelling of potassium exchange in a natural, polyionic montmorillonite under hydrothermal conditions. *Appl.Geochem.* 347-355.
  - Linares J, Huertas F, Caballero E. and Jimenez de Cisneros C. 1996. This Congress.
  - Sparks D.L. 1987. Kinetics of soil chemical process. *Soil Sci.Amer.Inc. S.Pub.*61-73.
  - Sposito D.L. 1981. The thermodynamics of soil solutions. Oxford-Clarendon Press, N.Y.
  - Sposito G. 1984. The surface chemistry of soil. Oxford U.Press. New York.
- Note. This work has been carried out into the project 70220501 of ENRESA.

## Adsorption of the pesticide glyphosate on montmorillonite in presence of copper

*Morillo E, Maqueda C and Undabeytia T*

Glyphosate (N-[phosphonomethyl]glycine) is a non-selective, post-emergence herbicide with a very broad spectrum which comes from its excellent herbicidal activity on a diverse group of herbaceous annual and perennial weeds.

When applied to soils, its low herbicidal activity is usually explained by its moderate adsorption by the soil constituents, and its low intrinsic toxicity due to its rapid degradation by microorganisms to non-phytotoxic products. On the other hand, glyphosate is able to coordinate strongly to heavy metals as a tridentate or even tetradentate ligand. This is important from the point of view of the higher or lower availability of the complexes formed with heavy metals from the soil solutions, affecting GPS distribution in soils and sediments.

In relation to clay minerals, GPS adsorption is more related to the cation saturating the interlayer space than to the cationic exchange capacity of the clay. However, there are discrepancies about the possibility to form interlamellar complexes from aqueous solutions when the cation saturating the interlayer space is not trivalent [1-2].

The objectives of this paper is to study GPS adsorption on montmorillonite and the influence that a heavy metal as copper can exert on its adsorption.

### **EXPERIMENTAL**

The montmorillonite used was a standard clay from Arizona (SAZ-1) supplied by the Clay Minerals Repository.

Adsorption experiments on the clay mineral were carried out in triplicate by mixing 0.1 g of sample with 20 ml of glyphosate solutions in 0.01 N NaCl medium. Adsorption was studied also in the presence of different copper concentrations (0, 5, 20 and 30ppm) in order to know the effect of the complexation with glyphosate on its sorption. After reaching equilibrium, the supernatant solutions were centrifuged and the pesticide determined. The pHs of the initial and final solutions were measured.

The copper in the equilibrium solutions was determined by atomic absorption spectroscopy (AAS) with nitrous oxide-acetylene flame. Ca and Mg released from the clay were

determined by AAS with acetylene-air flame.

The pesticide was determined by HPLC by using two post-column reactions. The column used was a Fast Fruice Juice. The first post-column reaction was carried out for oxidizing glyphosate to glycine. The second one was to form the isoindole derivative, which was monitored by a fluorescence detector. The excitation and emission wavelengths were 325 and 450 nm, respectively.

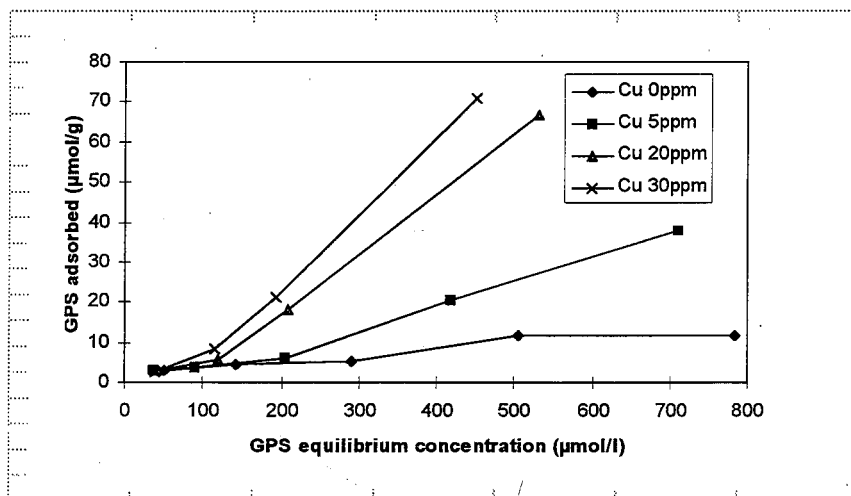
## RESULTS AND DISCUSSION

The adsorption isotherm of GPS when no copper is added can be observed in the figure. The low amount adsorbed ( $12 \mu\text{eq/g}$ ) at the highest concentration used seems to confirm that the pesticide adsorption only occurs on edge positions, since no correlation was found between GPS adsorbed and the amount of interlayer cations released. The competence exerted by phosphates on GPS adsorption [3] is attributed to GPS being adsorbed by the phosphonic moiety on the same adsorption sites on the soil. In the case of clay minerals, glyphosate will be bound through exchangeable iron and aluminum as well as through aluminol sites on the broken edges by exchange ligand, being this latter the main mechanism in our system (no exchangeable iron and aluminium were present). However, when copper is present in solution, the shape of the isotherm changes to a S-type and glyphosate adsorption increases with the initial copper concentration, in an opposite way to copper sorption in presence of glyphosate [4].

In order to go insight into the mechanisms driving GPS adsorption on the clay in presence of the heavy metal, the Cu-GPS species in equilibrium solution have been calculated. The stability constants for these chelates were taken from Motekaitis and Martell [5].

The CuG concentration is practically constant independently of the glyphosate initial concentration what suggests that this species is not controlling both copper and glyphosate adsorption but originating the opposite effect, to decrease Cu adsorption due to the formation of the complex. The CuHG adsorption should not be very important since the copper adsorption decrease with increasing initial glyphosate concentration is due to a free-copper concentration decrease, that is the main species in solution controlling copper adsorption [5]. The increase in glyphosate adsorption when increasing initial copper concentration suggests that glyphosate adsorption is enhanced when the copper adsorbed increases, since from the

Cu-GPS complexes are not inferred to have a marked effect on GPS adsorption as commented above. The montmorillonite treated previously with increasing copper concentrations showed a glyphosate increasing adsorption when increasing the heavy metal loading.



Adsorption isotherms of GPS on montmorillonite in absence and presence of different copper concentrations

#### ACKNOWLEDGMENTS

This work was supported by DGICYT through research project AMB95-0904.

#### REFERENCES

1. McConnell, J.S and L.R. Hossner. *J. Agric. Food Chem.* **37** (1989) 555-560.
2. Shoval, S and S. Yariv. *Clays & Clay Miner.* **27** (1979) 19-28.
3. Sprankle, P; W.F. Meggitt and D. Penner. *Weed Sci.* **23** (1975) 229-234.
4. Morillo, E.; C. Maqueda; M. Bejarano; L. Madrid and T. Undabeytia. *Chemosphere* **28** (1994) 2185-2196.
5. Motekaitis, R.J. and A.E. Martell. *J. Coord. Chem.* **14** (1985) 139-149.

(1) Dpto. Química Inorgánica. Univ. de Córdoba, España

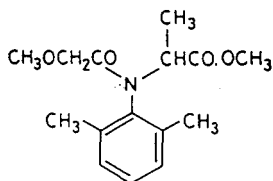
(2) Instituto de Recursos Naturales y Agrobiología. CSIC. Sevilla, España

## Pesticide adsorption on organo-hydrotalcites

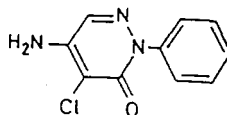
Pavlovic I (1), Ulibarri M A (1), Hermosin M C (2) and Cornejo J (2)

Recent studies showed the utility of organoclays (OC) and hydrotalcite (HT)<sup>1-5</sup> to remove the organic pollutants from waters. Hydrotalcites are antitypes of clay minerals: they consist of brucite layers with Al-for-Mg substitution imparting positive layer charge. This positive layer charge is compensated by inorganic anions which can be easily exchanged, and thus the HT are potential sorbent for anionic organic pollutants<sup>1-3</sup>. Moreover the inorganic exchangeable anions in the interlayer can be substituted by large organic ones giving a lipophilic character to hydrotalcite (organo hydrotalcite, OHT) which may behave similarly to organo clays sorbing pesticides or other organic pollutants<sup>4,5</sup>. The aim of this work is to explore the potential sorption capacity of OHT (with dodecyl sulphate as an interlayer anion) for two pesticide compounds: metalaxyl and chloridazon.

The HT  $[Mg_3Al(OH)_2CO_3 \cdot 4H_2O]$ , and its calcined product (500°C, 24h)  $Mg_3AlO_4(OH)$ , (HT500), were prepared as described previously<sup>6</sup>. The OHT was prepared by the reconstruction method, suspending 1g of HT500 in dodecylsulphate (DDC) 17mM. The herbicides used were metalaxyl and chloridazone, whose structural formulae are shown below:



**Metalaxyl**



**Chloridazone**

The pesticide adsorption on HT-DDC was measured by batch equilibration technique at diverse pH, contact time and DDC concentrations (0.05g of OHT with 10ml of solution). The pH was previously adjusted in the DDC solutions. The suspensions were shaken at  $22 \pm 2^\circ C$  and after 24h the supernatants were filtered to determine pH and pesticide concentration by UV-absorbance at 268nm and 285nm for metalaxyl and chloridazone, respectively.

## Metalaxyl

Table 1. Amounts of metalaxyl removed by OHT at diverse pH

Sample	Metalaxyl removed (%)	Cs ( $\mu\text{mol/g}$ )
pH3	36,9	160
pH6	39,2	152
pH11	11,6	52

0.05g of OHT, 20ml of Metalaxyl 1mM, 24 h

The results summarized in Table 1 show that the amount of pesticide removed by the OHT does not change appreciably in the pH range of pH 3- 6, and decreased drastically at higher pHs. This high adsorption in acidic conditions suggest that the protonated and neutral form of metalaxyl would be favoured to be adsorbed by OHT. It is possible that the attractive effect between the negative charge of sulphate and protonated herbicide facilitates the penetrance of the contaminant into the interlayer.

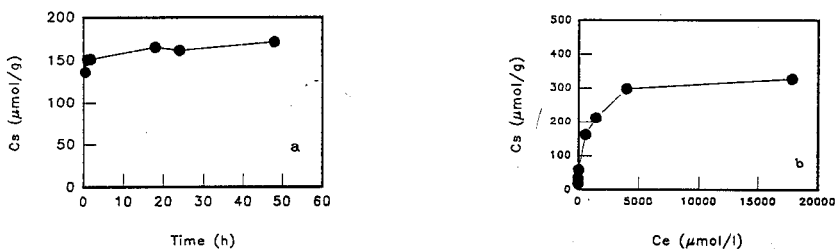


Figure1: a) Evolution of metalaxyl adsorption on OHT; b) Adsorption isotherm of metalaxyl on OHT

Figure 1a indicates the instantaneous sorption of metalaxyl on OHT, by the constant partition of solute between solution and substrate. In half an hour the amount adsorbed corresponds to 80% of amount of pesticide adsorbed in 48h. After that, the slow adsorption step is due to the slow diffusion of the pesticide in the interlayer of OHT.

The adsorption isotherm (figure 1b) was found to be of L-type, according to the classification of Giles et al.<sup>7</sup> suggesting that would be a specific and strong adsorption between sorbent and sorbate. The lipophylic attraction<sup>4,5</sup> between the alkyl chains of metalaxyl and DDC<sup>-</sup>, and by the ionic interaction between the protonated form of Metalaxyl and  $\text{SO}_4^{2-}$  from DDC<sup>-</sup>.

## Chloridazone

The results in Table 2 show that there is no variation of pesticide adsorption on OHT with the pH, which indicates that in this case the degree of protonation of solute does not influence on the adsorption process. Thus, we chosed the pH of 6 for our experimental work.

**Table 2.** Chloridazone adsorption on HT-DDC at different pHs.

Sample	Chloridazone removed (%)	Cs ( $\mu\text{mol/g}$ )
pH3	80,5	7,8
pH6	81	7,6
pH11	80	8,0

\*Amount of Chloridazone removed by 1g of OHT

The kinetic of chloridazone adsorption on HT-DDC is represented on Figure 3, and shows a low pesticide adsorption on OHT. The lower lipophilic attraction comparing with those of metalaxyl is probably because of the absence of the alkylic chains in the structure of chloridazone.

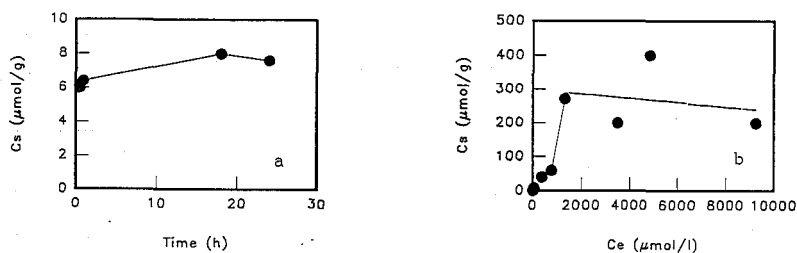


Figure 2: (a) Evolution of Chloridazone adsorption on OHT; (b) Adsorption isotherm of Chloridazone on OHT

The adsorption isotherm represented in Figure 2b is of L type<sup>7</sup> but above the point of concentration value of 1mM there is a great data dispersion, due to their low reproducibility. This is because of very weak and non-specific chloridazone-OHT interaction. In spite of expected Chloridazone affinity for alkylic interlayer because of its low solubility in water, the chloridazone adsorption in this case is not favoured.

**Acknowledgments:** Financially supported by CICYT Project AMB93-0097, and PAI Research groups No 4092 and 6113.

## REFERENCES

- 1.Hermosín, M.C., Pavlovic, I., Ulibarri, M.C. and Cornejo, J. (1993) *Envir. Sci. Health* A28,1875-1888
- 2.Hermosín, M.C., Pavlovic, I., Ulibarri, M.C. and Cornejo, J. (1996) *Wat. Res.* 30, 1 pp:171-177
3. Jaynes, W.F. and Boyd, B.B. 1991. *Soil Sci. Soc. Am. J.* 55: 43-48
- 4.Hermosín, M.C. and Cornejo, J. 1991. *Chemosphere* 24:634-641
- 5.Hermosín M.C. and Cornejo, J. (1993) *J. Environ. Qual.* 22:325-331
- 6.Reichle, W.T. 1986. *Solid State Ionics* 22, 135-141
- 7.Giles G.H., MacEwan T.H., Nakhwa,S.N. and SmithD. 1960. *Studies in adsorption. Part XI. J. Chem Soc.* 3973-3993.

(1) Instituto de Ciencia de  
Materiales. CSIC-  
Universidad. Sevilla, España

(2) Center for Advanced  
Materials Processing.  
Clarkson University.  
Potsdam, NY, USA

## Effect of dry grinding on ordered (Kga-1) and disordered (Kga-2) kaolinite

*Pérez Rodríguez J L (1), Sánchez Soto P J (1), Pérez Maqueda L A (2),  
Jiménez de Haro M C (1) and Justo A (1)*

Grinding of clay minerals produces several changes in their structure and properties, having been studied mainly for kaolinite [1-3] and montmorillonite [4] due to their importance as ceramic raw materials. However, the effects of dry grinding on ordered and disordered kaolinite have been scarcely studied, in particular in connection with the thermal behaviour [5]. The presence of impurities incorporated with kaolinite and its crystallinity influence the formation of high-temperature phases [6,7]. The X-ray diffraction patterns, the endothermic change and the temperature of dehydroxylation decrease with the grinding time and finally disappear [1-3]. The thermal exothermic effect detected at 980°C is practically not modified by this treatment, although some authors reported strong modifications after grinding, as well as when impurities are present [2,7]. The cause of the 980°C effect is controversial in the literature, being attributed to the formation of either mullite nuclei or spinel (gamma-alumina) or both, because at determined heating rates mullite and spinel have the possibility of forming concurrently [8]. New evidences by solid-state nuclear magnetic resonance spectroscopy have indicated that the formation of such exothermic effect is most probably due to the release of energy associated with the Al ions transforming to a more stable six-fold coordination, facilitating the formation of mullite [8].

The aim of the present investigation is to study the effects of dry grinding on a kaolinite from Georgia (USA). Both ordered (KGa-1) and disordered (KGa-2) kaolinite samples have been used, being standard samples by the Clay Minerals Society and supplied by Source Clays Repository (Missouri, USA). The crystallinity, impurity content and other characteristic features are perfectly known and thus useful to control the starting materials before the grinding experiments.

## EXPERIMENTAL METHODS

Dry grinding was conducted in a ball mill (S-1 Retsch) at a rate of 250 rpm. Other grinding experiments were carried out using an agate mill and a vibratory mill. A parallel study on the effects of grinding contamination was also performed. X-ray powder diffraction diagrams (XRD) were obtained using a Siemens D-501 diffractometer. The surface area obtained by nitrogen adsorption were measured using a Micromeritics equipment (model 2200 A). The thermal analysis (DTA-TGA) were carried out using two thermal analyzers (Rigaku, and for high-temperature a Netzsch equipment). Original and ground samples were also examined by electron microscopy (SEM ISI SS-40).

## RESULTS AND DISCUSSION

Grinding of both kaolinite samples produces a strong structural alteration in the 1:1 layer, producing an intense broadening of diffraction peaks and decreasing of X-ray intensities, originated mainly by domain size reduction, with total degradation of the crystal structure of KGa-1 kaolinite after 120 minutes of grinding and rupture of the octahedral and tetrahedral layers. There is a loss of periodicity perpendicular to the layer plane, and the dimensions of the crystallites along the *c*-direction resulted too small to produce coherent scattering. A detailed structural examination has shown that there are random translations along *b*-axis induced at the first stages of grinding in ordered kaolinite (KGa-1), i.e., short grinding times induced only limited layer translations, changing regular stacking modes of the silicate layer into more random, and the structure becomes more disordered, as KGa-2. At higher grinding times, only weak reflections corresponding to anatase in an amorphous matrix are detected. A slight increase in surface area with grinding time is also observed, associated to particle size reduction and weight loss at lower temperatures than in the original (unground) samples. The particles become more agglomerated, and the surface area slightly decrease after 30 minutes. The gradual size reduction and associated morphological changes with occur during grinding the standard kaolinite samples were also revealed by SEM.

The endothermic DTA effects in the original kaolinite samples, associated to dehydroxylation are shifted to lower temperatures as increasing grinding time, and decrease in intensity, disappearing after 120 minutes of grinding. The temperature of the first exothermic effect changes from 992°C to 982°C in KGa-1, and from 985°C to

962°C in KGa-2. At higher grinding times, the transformations of amorphous mechanically- activated phase to mullite and Si-Al spinel occur at relatively lower temperatures than that for original kaolinites, in particular when the starting material is a disordered kaolinite crystal (KGa-2). The area of the exothermic peak becomes almost constant or slightly smaller as increasing grinding time, in contrast with other silicates after grinding, and independently of kaolinite sample KGa-1 or KGa-2. The high-temperature DTA peaks corresponding to mullite (1280°C in KGa-1 and 1253°C in KGa-2) and cristobalite (1460°C in KGa-1 and 1400°C in KGa-2) crystallization are shifted at lower temperatures as increasing grinding time, but they are influenced by the device used for the grinding treatment. This experimental observation is in connection with the formation of a liquid phase associated to the presence of original impurities or provided by the mill, and thus only indirectly to the state of order or disorder in the kaolinite sample used for grinding experiments under laboratory conditions.

#### ACKNOWLEDGMENTS

Financial support of DGICYT through research projects PB92-0014 and MAT96-0507 is gratefully acknowledged.

#### REFERENCES

1. J.G. Miller and T.D. Oulton, *Clays Clay Miner.* **18** (1970) 313.
2. T.A. Korneva and T.S. Yusupov, *Proc. 1st Europ. Sympos. on Thermal Analysis*, Heyden 1976, p. 336.
3. H. Kodama, L.S. Kotliar and J.A. Ripmeester, *Clays Clay Miner.* **37** (1989) 364.
4. B. Cicel and G. Kranz, *Clay Miner.* **16** (1981) 151; C. Volzone, E.F. Aglietti, A.N. Scian and J.M. Porto, *Appl. Clay Sci.* **2** (1987) 97.
5. L.A. Pérez-Maqueda, J.L. Pérez-Rodríguez, G.W. Scheiffle, A. Justo and P.J. Sánchez-Soto, *J. Thermal Anal.* **39** (1993) 1055.
6. S.M. Johnson, J.A. Pask and J.S. Moya, *J. Am. Ceram. Soc.* **65** (1982) 31.
7. G.W. Brindley and J. Lemaitre, pp. 319-370 in: *Chemistry of Clays and Clay Minerals*, Ed. A.C.D. Newman, Longman, Essex, 1987.
8. J. Sanz, A. Madani, J.M. Serratos, J.S. Moya and S. de Aza, *J. Am. Ceram. Soc.* **71** (1988) C418; J.A. Pask and A.P. Tomsia, *J. Am. Ceram. Soc.* **74** (1991) 2367.

(1) Dpto. Química-Física,  
Bioquímica y Química  
Inorgánica, Fac. Ciencias  
Experimentales, Univ. de  
Almería, España

(2) Instituto de Recursos  
Naturales y Agrobiología.  
CSIC. Sevilla, España

## Adsorption of prometryne from water by organic clays

Socias-Viciana M M (1), Hermosin M C (2) and Cornejo J (2)

The use of organo clays (OC) as sorbent for organic pollutants (OP) has been shown effective for diverse non-polar OP which adsorb by partitioning in the organic phase of the organo-clays (Boyd et al. 1988, Jaynes & Boyd, 1991, Nzengung et al 1996). Additional polar or ionic bonds has been shown in sorption by organo-clays of polar OP, such as 2,4-dichlorophenoxyacetic acid (Hermosin et al. 1992, Hermosin & Cornejo, 1993, Hermosin et al. 1995), and it has been suggested in other (PIOPs) polar or ionizable organic contaminants (Hermosin et al. 1995, Dentel et al. 1995). Triazine herbicides, widely found in surface and ground waters, are basic organic molecules which has been shown to adsorb by natural inorganic clays upon protonation and cationic exchange (Mortland 1970, Feldkamp and White 1978). The objective of this work was to evaluate the adsorbent power of some organo-clays for the herbicide prometryne as a function of their surface properties as well as to establish the adsorption mechanism.

The clays used were two standards smectites with different layer charge (CEC) from the Clay Minerals Repository from the CMS, which were exchanged at different rates with a primary (octadecylammonium, C18) and a quaternary (hexadecyltrimethylammonium, HDTM) alkylammonium cation rendering the samples whose organic carbon, organic cation saturation and basal X-ray spacings are summarized in Table 1.

**Table 1. Properties of natural and organic clays used: saturating cation, cation exchange capacity (CEC), organic carbon content (%OC), %organic cation saturation (OCS) and basal spacing value.**

SAMPLE	SATURATING CATION	CEC meq/100g	% OC	% OCS	d <sub>001</sub> nm
SWy	Na	76	---	---	1.5
SWC18 <sub>1</sub>	Octadecylammonium	76	11	67	1.7
SWC18 <sub>2</sub>	Octadecylammonium	76	18	109	2.7
SWHDTM	Hexadecyltrimethylammonium	76	14	76	1.7
SAz	Ca	120	---	---	1.4
SAC18 <sub>1</sub>	Octadecylammonium	120	12	46	2.5
SAC18 <sub>2</sub>	Octadecylammnoium	120	24	92	2.6
SAHDTM	Hexadecyltrimethylammonium	120	24	83	2.3

Sorption isotherms were determined by batch equilibration of 0.02g of clays with 10 ml of prometrone solutions of low concentration ranging from 0.05 to 0.8 mM for 24h. Prometrone concentration was measured by UV absorbance at 230 nm.

The prometrone adsorption isotherms develop different shapes for the natural inorganic clays, SWy displaying a S-type isotherm and SAz showing a L-type isotherms. This shape find explanation in the basic character of the prometrone which adsorbs in the interlayer of clays after protonation promoted by the acid dissociation of the water associated to the interlayer inorganic cations according to the following reaction (Mortland 1966, Feldkamp & White 1978):



where C is the anionic clay layered structure,  $\text{M}^+$  is the inorganic interlayer cation with their hydration water molecules, and P is the prometrone in solution. The organic-SWy clays gives initial convexe curvature in the isotherm being almost L-type although for the SWC18<sub>2</sub>, with the highest alkylammonium content, changes after to C-type. The isotherms of organic-SAz samples were less defined between L and C-type. The L-type isotherms suggest specific interaction prometrone-sorbents, besides the lipophyllic partition as given by the C-character (Giles et al. 1960, Hermosin & Cornejo, 1993, Dentel et al. 1995).

Applying the Freundlich equation ( $X = \text{Kf} \cdot \text{Ce}^{\text{nf}}$ ) to the sorption data the parameters Kf (sorption capacity) and nf (sorption intensity) were obtained and from those, the distribution coefficient,  $\text{Kd}_{0.3}$  ( $\text{Kd} = X/\text{Ce}$ ) and the normalized organic carbon distribution coefficient Koc (organic carbon efficiency), according to the expressions:

$$\text{Kd}_{0.3} = \text{X}_{0.3}/0.30 \quad \text{and} \quad \text{Koc} = \text{Kd}_{0.3}/\text{OC} \times 100$$

which are summarized in Table 2. The highest sorption parameters were found for those OC having the highest basal spacings

The isotherm shapes and sorption parameters suggest a combination of lipophyllic and specific interactions contributing to prometrone sorption by the OC according to the following reactions:



The initial sorbed species are the prometrone molecule attracted by lipophilic interaction (reaction 1) between the triazinic ring and the alkylchains of the alkylammonium interlayer cation (Hermosin & Cornejo, 1992, 1993), but in these organic clays there are not interlayer water to protonate the herbicide molecule, instead once adsorbed a polar interactions is

established between these two species sharing the proton (reaction 2) by an hemisalt formation (Mortland , 1970).

**Table 2. Sorption parameter of prometryne on natural and organic clays.**

SAMPLE	Kf mmol/kg	nf	X <sub>0,3</sub> mmol/kg	Kd <sub>0,3</sub> mmol/kg	K <sub>oc</sub> ·10 <sup>3</sup> mmol/kg
SWy	138.39	1.60	21.11	70.35	---
SWC18 <sub>1</sub>	96.03	0.52	51.30	170,97	1.55
SWC18 <sub>2</sub>	210,52	1.10	56.62	188,72	1.05
SWHDTM	61.34	0.88	21.24	70,80	0.51
SAz	29,04	0.18	23,52	78,40	---
SAC18 <sub>1</sub>	289,07	1.28	61,61	205,38	1.71
SAC18 <sub>2</sub>	389,22	1.12	101,30	337,68	1.41
SAHDTM	1031,33	1.18	251,56	838,53	3.49

The contribution of the polar interaction through reaction 2 would be more important in the case of SWy samples because highest sorption was found in primary alkylammonium sample SWC18<sub>2</sub> which can share easier the proton than the quaternary one SWHDTM. The SAHDTM sample renders the maximum sorption capacity (Kf and Kd<sub>0,3</sub>) and efficiency (Koc) suggesting predominance of the lipophilic interaction in this bulky ion through reaction 1. Results of this work show the possible use of organic clays as sorbent for removal of prometryne and similar herbicides from waters, even as carriers for herbicides in slow release formulation. Work is in progress in this aspect.

**Acknowledgment:** This work has been financed by CICYT project AGF96-0514 and Junta de Andalucía research group No.4092

#### References

- Boyd, S.A., Mortland, M.M. & Chiou, C.T. 1988. *Soil Sci. Soc. Am. J.* 52: 652-656.  
 Dentel, S.K., Bottero, J.Y., Khatib, K., Demougeot, H., Diguët, J.P. & Anselme, C. 1995. *Water Res.* 29:1273-1280.  
 Feldkamp, J. & White, J.L. 1978. *Developments in Sedimentology* 27:187-196.  
 Giles, C.H., MacEwan, T.H., Nakhwa, S.N. & Smith, D. 1960. *J. Chem. Soc.*:3373-3380.  
 Hermosín, M.C. & Cornejo, J. 1992. *Chemosphere* 24: 1492-1497.  
 Hermosín, M.C. & Cornejo, J. 1993. *J. Environ. Qual.* 22:325-331.  
 Hermosín, M.C., Cornejo, J., Ulibarri, M.A. & Mansour, M.M. 1992. *Fresenius Environ. Bull.* 1:472-481.  
 Hermosín, M.C.; Crabb, A. & Cornejo, J. 1995. *Fresenius Environ. Bull.* 4:514-519.  
 Jaynes, W.F. & Boyd, S.A. 1991. *Soil Sci. Soc. Am. J.* 55: 43-48.  
 Mortland, M.M. 1970. *Adv. Agron.* 22: 75-117  
 Nzungu, V.A., Voudrias, E.A., Nkedi-Kizza, Wampler, J.M. & Weaver, C.E. 1996. *Environ. Sci. Technol.* 30, 89-96.  
 Worthing, C.R. & Hance, R.J. 1991. *The Pesticide Manual*, BCPC, Surrey, UK.

(1) Dpto. Geología. Area de  
Cristalografía y Mineralogía.  
Fac. Ciencias. Univ. de  
Salamanca, España

(2) Dpto. Química  
Inorgánica. Fac. Química.  
Univ. de Salamanca, España

## Intercalation compounds between nicotine and saponite

*Suárez Barrios M (1), Vicente-Rodríguez M A (2) and Martín Pozas J M (1)*

### 1. Introduction.

Laminar silicates are able to form interlayer compounds with organic molecules by intercalation of these molecules in the interlayer region of the clay. The size of the organic molecule, the presence on it of groups able to interact by H-bonding or by formation of a coordination compound with the compensating cations of the clay and the nature of the clay condition the formation of the interlayer compounds.

Nicotine, 3-(1-methyl-2-pyrrolidinyl) pyridine, is a polar compound in which the N atom of the pyrrolidine ring is the most active part, the N of pyridine being also active. Nicotine is toxic by inhalation or contact. Combinations with bentonite have been used as insecticide in agriculture. In veterinary, nicotine has been used as ectoparasiticide and anthelmintic.

Although montmorillonite has been widely used for preparing interlayer compounds with a large variety of organic substances, very little has been reported from the study of these compounds with saponite. Thus, the aim of the present work is to study the formation of interlayer compounds between nicotine and saponite.

### Experimental.

Saponite from Yuncillos, Toledo, was intercalated with nicotine for 2, 5 and 8 days, and under different conditions: 1) In repose at room temperature and 2) Heating at 70°C with continuous stirring and under reflux. 1.5 grams of saponite and 5 mL of nicotine were used in each experiment. The solids obtained were studied by chemical analyses, XRD, FT-IR spectroscopy and thermal analyses.

### Intercalation compounds.

Saponite from Yuncillos, Toledo, Spain, supplied by TOLSA, S.A. was employed for the present study. The  $<2\mu\text{m}$  fraction obtained after aqueous decantation of raw saponite was used for the retention experiments. Some of the data about this  $<2\mu\text{m}$  fraction are:

Chemical composition:  $\text{SiO}_2$ : 49.45;  $\text{Al}_2\text{O}_3$ : 4.72;  $\text{Fe}_2\text{O}_3$ : 1.29;  $\text{MgO}$ : 24.34;  $\text{TiO}_2$ : 0.20;

$\text{MnO}$ : 0.03;  $\text{CaO}$ : 0.78;  $\text{Na}_2\text{O}$ : 0.07;  $\text{K}_2\text{O}$ : 0.44;  $\text{H}_2\text{O}$ : 18.31%.

Structural formula:  $[\text{Si}_{3.71} \text{Al}_{0.29}] \text{O}_{10} (\text{OH})_2 [\text{Al}_{0.13} \text{Mg}_{2.58} \text{Fe}_{0.07} \text{Ti}_{0.009} \text{Mn}_{0.02}]$

$[\text{Ca}_{0.062} \text{Mg}_{0.12} \text{Na}_{0.010} \text{K}_{0.042}]$ .

Cation exchange capacity (CEC): 115 mEq / 100 g.

The interlayer compounds between saponite and nicotine were first studied by X-ray diffraction. The  $<2\mu\text{m}$  saponite has a basal spacing of  $14.53\text{\AA}$ . In the compounds obtained after saponite-nicotine interaction, the basal spacing increases to values of  $15.51$ - $16.51\text{\AA}$ . No significant differences are observed between the basal spacing of samples obtained by repose or reflux heating method. The time of contact for the series prepared for each of the methods considered does not have a great influence on the basal spacing. If the basal spacing of totally dehydrated saponite ( $9.77\text{\AA}$ ) is considered, the molecules in the interlayer occupy  $5.73$ - $6.73\text{\AA}$ . This thickness does not permit the formation of multilayer compounds, but only monolayer. The different basal spacings indicate that  $\alpha$ -type complexes are formed, that is, that nicotine molecules are situated coplanarly to the clay layers, parallel to them. The differences in the thickness of the interlayer region in the different samples must be due to the different orientation of nicotine molecules in this region depending on the treatment conditions and, perhaps, to the different elimination of water molecules in each sample.

The bands of saponite are the most intense in the FT-IR spectra of intercalation compounds and only some small bands of nicotine are clearly observed. Bands corresponding to nicotine are observed in the regions  $3000$ - $2700$ ,  $1600$ - $1300$ ,  $810$  and  $715\text{ cm}^{-1}$ . At high wavenumbers, bands corresponding to OH, NH and CH bonds are found. The position of these bands does not vary significantly from nicotine to the interlayer complexes. The most significant variation in this region is the great increase in the intensity of the  $\text{Mg}_3\text{OH}$  mode at  $3682\text{ cm}^{-1}$ , what may be due to the exclusion of water molecules from the interlayer during intercalation, preventing H-bonding of the  $\text{Mg}_3\text{O-H}$  hydroxyl and making this mode more intense.

Between 1650-1300  $\text{cm}^{-1}$ , a large number of bands is observed, the first corresponding to the water deformation mode and all the other corresponding to nicotine molecules. The presence of water bands indicates that interlayer water is not completely substituted by nicotine molecules. The maximum adsorption of Si-O-Si bonds in saponite is centered at 1011  $\text{cm}^{-1}$ , while in the intercalation complexes the maximum in this region is at 1006  $\text{cm}^{-1}$ , perhaps due to the influence of nicotine. A band at 658  $\text{cm}^{-1}$ , due to Si-O-Si bonds, appears at the same wavenumber in the interlayer compound, encompassing the band of nicotine in this region, observed at 615  $\text{cm}^{-1}$  in the free molecule. Also the band of the silicate at 460-450  $\text{cm}^{-1}$ , due to Si-O-Mg bonds, clearly appears in the intercalated solids.

Saponite shows the usual thermal behaviour of this clay, with weight losses from 30 to 200°C, due to the loss of adsorbed water, a very gentle slope from 200 to 800°C and, in excess of this temperature, the loss of constitution hydroxyl groups, these losses adding up to 18% of the weight of the clay. The endothermal effects due to the loss of water molecules and hydroxyl groups are observed in the DTA curve, together with a final exothermic effect at 845°C due to the final phase change from saponite to enstatite.

The interlayer compounds have a first weight loss between 30 and 300°C, with a very broad associated endothermal effect. Most of the nicotine will be eliminated in this step, together with the small amounts of water that can remain in the solids. In the middle region, two endothermal effects are observed, centered at 425 and 540°C, which must correspond to the loss of the last fragments of nicotine and/or to the loss of more intensely retained nicotine, perhaps strongly chemisorbed. At higher temperature, the final phase change to form enstatite is observed.

The amount of nicotine retained, calculated from TG analyses, varies irregularly in the different intercalation compounds, between 26 and 37% of the weight of the solids. The different amount retained by each solid indicates that nicotine is retained not only in the interlayer space, but variable amounts are also retained at the edges of the clay particles. When washing carefully with cyclohexane or benzene, nicotine retained out of the interlayer space is removed, while that retained in the interlayer space remains in the solids, as confirmed by CHN analyses. The thermal analyses of these washed samples permit us to calculate the amount of nicotine retained in the interlayer, finding values between 178 and 189 mg of nicotine per gram of saponite.

(1) Dpto. Química Inorgánica.  
Fac. Química, Univ. de  
Salamanca, España

(2) Dpto. Geología. Área de  
Cristalografía y Mineralogía. Fac.  
Ciencias. Univ. de Salamanca,  
España

(3) Dpto. Química Inorgánica.  
Fac. Ciencias. UNED. Madrid,  
España

(4) Dpto. Química Inorgánica.  
Fac. Ciencias. Univ. de Málaga,  
España

## Surface and catalytic properties of the solids obtained by pillaring of a high iron content saponite with Al-polycations

*Vicente M A (1), Suárez M (2), Bañares M A (1), López González  
J D (3), Santamaría J (4) and Jiménez López A (4)*

### Introduction.

Pillared clays are obtained after calcination of the intercalated compounds prepared by insertion of metallic bulk polycations into the interlayer region of the clays. Polycations of Al, Zr, Ga, Cr or Ti have been used. Pillared clays have good thermal stability and high porosity, which give them important catalytic applications, especially for cracking of heavy oil fractions.

Montmorillonite is the laminar clay more used for pillaring studies. Saponite has been less used, but it has been intensely studied in the recent years, finding that it has an excellent pillaring ability. Saponite is a tetrahedrally charged trioctahedral smectite, originated as a product of the hydrothermal alteration and weathering of basalts and ultramafic rocks. Its octahedral sites are usually occupied by Mg(II) cations, but in its ferrous variety a quantity of Fe(II, III) substitutes Mg(II) octahedral cations; this substitution being important when the ratio Mg/Fe is lower than 5:1. In the present paper, a high iron content saponite is pillared with aluminium polycations, and the surface properties of the solids thus obtained are studied by using ammonia TPD, adsorption of pyridine and decomposition of isopropanol as test reaction.

## Experimental.

The <2 $\mu$ m fraction of griffithite was obtained by aqueous decantation of the basaltic rock from Griffith Park deposit (California, USA). The structural formula of this fraction is:  $[\text{Si}_{6.92} \text{Al}_{1.08}] \text{O}_{20} (\text{OH})_4 [\text{Mg}_{2.92} \text{Fe}^{3+}_{1.58} \text{Al}_{0.28} \text{Ti}_{0.04} \text{Mn}_{0.06}] [\text{Ca}_{0.62} \text{Na}_{0.20} \text{K}_{0.04}]$  and its CEC is 86 mequiv/100g.

Griffithite was intercalated with aluminium polycation solutions, prepared by addition of aqueous NaOH to solutions of  $\text{AlCl}_3 \cdot 6\text{H}_2\text{O}$ , using a relation  $\text{OH}^-/\text{Al}^{3+}=2.2$ . In these conditions, most of aluminium polymerizes as  $[\text{Al}_{13}\text{O}_4(\text{OH})_{24}(\text{H}_2\text{O})_{12}]^{7+}$ , usually designated as Keggin  $\text{Al}_{13}$  polycation. For the intercalation of griffithite with this polycation, ratios of 2.5; 5.0 and 7.5 mmol Al per gram of clay were used. Then, the samples were centrifuged, washed by dialysis, dried at 60°C (intercalated compounds), and calcinated at 500°C for four hours (pillared compounds).

## Results and discussion.

X-ray diffractograms show that the intercalation process begins during the addition of  $\text{Al}_{13}$  solutions and it is completed during the dialysis process. Intercalated solids have basal spacings of about 18.9Å, indicating that  $\text{Al}_{13}$  oligomers are intercalated with their major axis perpendicular to the layers. In pillared solids, the basal spacing decreases to about 17.6Å. The patterns of all the solids show high crystallinity with several reflection orders.

Griffithite fixes about 7% of  $\text{Al}_2\text{O}_3$  during the intercalation process, that is, about 1.6mmol Al per gram of clay. The amount fixed is similar in the three series considered.

The intercalated solids have surface areas closed to 300  $\text{m}^2 \text{g}^{-1}$ , slightly decreasing when calcining. In pillared solids, the sample prepared with a relation Al/clay of 7.5 mmol per gram of clay has the maximum surface area, 293  $\text{m}^2 \text{g}^{-1}$ .

The total acidity of the samples has been analysed by ammonia TPD, between 100 and 400°C. The total amount of NH<sub>3</sub> desorbed is high for the pillared materials, with values ranged between 474 and 685 μmol g<sup>-1</sup>, while natural saponite has a total acidity of 110 μmol g<sup>-1</sup>. In consequence, the formation of nanostructures of alumina between layers enhances considerably the total acidity. The acidity between 200 and 400°C is very high, corresponding to 73-82% of the total adsorbed ammonia. It is noticeable that adsorbed NH<sub>3</sub> remains at temperatures higher than 400°C, indicating that there is a fraction of strong acid sites.

The Brönsted and Lewis acid centres of the pillared sample prepared with a relation Al/clay of 2.5 mmol per gram was investigated by pyridine adsorption. Values of 8 and 176 μmol g<sup>-1</sup> were obtained for Brönsted and Lewis centres, respectively. The formation of cross-linkages of pillars with the saponite layers, where aluminium adopts unsaturated coordination, may be the responsible of Lewis acidity, together with that corresponding to the own nanostructures of alumina which prop apart the layers.

Decomposition of isopropanol is regarded as a test reaction in determining the catalytic activity of these solids. Pillared saponite materials are active in this reaction at 220°C, with high selectivity to propene. Lewis acid sites present in these materials must be responsible for decomposition of isopropanol to propene. The activity is very high, between 29 and 34 μmol g<sup>-1</sup> s<sup>-1</sup>.

The pristine saponite exhibits low activity, close to 3 μmol s<sup>-1</sup> g<sup>-1</sup>, in the same reaction. That clearly indicates that the pillaring process gives rise to materials which develops a high Lewis acid sites concentration being active in the dehydration of isopropanol reaction.

**Acknowledgement.** Financial support of CICYT (MAT96-0643 Project) is gratefully acknowledged.

(1) Dpto. Química  
Inorgánica. Fac. Química.  
Univ. de Salamanca, España

(2) Dpto. Geología. Area de  
Cristalografía y Mineralogía.  
Fac. Ciencias. Univ. de  
Salamanca, España

(3) Dpto. Química  
Inorgánica. Fac. Ciencias.  
UNED. Madrid, España

## FT-IR study of the acid treatment of different clay minerals (sepiolite, palygorskite and saponite)

*Vicente M A (1), Suárez M (2), Bañares M A (1) and López  
González J D (3)*

### Introduction.

Acid activation is an usual method for improving the surface properties of clay minerals. It consists, essentially, in the treatment of the clay with acid solutions;  $H_2SO_4$ ,  $HNO_3$  and, especially, HCl being used. The intensity of the treatments is given by the nature and concentration of the acid used, time of treatment, temperature, etc. The acid activation increases the surface area of clay minerals by disaggregation of clay particles, elimination of several mineral impurities, removal of metal-exchange cations and proton exchange. The solids obtained are used in decolourization, adsorption and catalysis.

IR spectroscopy is usually used as a routine technique in the characterization of these solids, the spectra of the parent clay and of the solids obtained after acid activation being compared. A lot of discrepancies between the different authors are found when comparing the interpretation of the spectra. Sometimes, bands that correspond to other clay minerals, to feldspars, calcite, dolomite or free-silica are assigned to the clay mineral studied. In the present paper, a comparative study of the IR spectra of the solids obtained by acid activation of sepiolite, palygorskite and saponite is carried out.

### Experimental.

The solids obtained by acid activation of the following clay minerals have been studied by IR spectroscopy: Sepiolite from Vallecas, Madrid; Palygorskite from Bercimuel, Segovia; Saponite from Yuncillos, Toledo; and Iron saponite variety griffithite from Griffith Park, California. These samples were submitted to treatment with HCl, using weak conditions for magnesian silicates and more drastic conditions for the aluminic clays. The solids obtained were studied by chemical analyses, XRD, FT-IR, thermal analyses and surface area measurements.

## Results and discussion.

### 1. *Sepiolite.*

Changes in hydroxyl groups and in water molecules bonded to the different metallic cations are observed at high wavenumbers when comparing the FT-IR spectra of natural and acid activated sepiolite. The bands observed in sepiolite at 3689, 3635 (shoulder), 3566, 3420 and 3250 (shoulder)  $\text{cm}^{-1}$ , due to water molecules and OH groups, decrease in intensity during the acid leaching and finally disappear when the octahedric cations are completely removed. Only a wide band centered at about 3430  $\text{cm}^{-1}$  is observed in the activated solids, corresponding to the water adsorbed by the resulting amorphous silica gel.

Between 1200-400  $\text{cm}^{-1}$ , bands corresponding to the Si-O bonds in the tetrahedral sheet and to Mg-O stretching vibration bonds can be observed. The wide band centered in natural sepiolite at 1024  $\text{cm}^{-1}$  is very sensible to acid attack and, changing progressively its form, clearly shows the textural changes in the solids. When the acid attack progresses, the minimum of this band shifts to higher wavenumbers, from 1024 to 1093  $\text{cm}^{-1}$ , indicating that the Si-O-Si structure of the silicate is being removed and a more rigid structure, amorphous silica gel, is being obtained. The progressive broadening of this band with the acid treatment indicates that the structure of the solids becomes more and more amorphous. Bands at 790 and 470  $\text{cm}^{-1}$ , characteristic of free silica, appear in activated samples.

### 2. *Palygorskite.*

Bands at 3619, 3549, 3414 and 3276 (shoulder)  $\text{cm}^{-1}$ , assigned to bonded and zeolitic water and to the OH groups, are observed in the high wavenumbers region in the FT-IR spectrum of natural palygorskite. In activated solids, a wide band at 3430  $\text{cm}^{-1}$ , assigned to water adsorbed by the silica gels generated, is the most important band in this region. A small band at 3621  $\text{cm}^{-1}$ , due to OH groups bonded to Al(III) cations, appears even in the most intensely treated samples, indicating that Al(III) cations have not been completely removed by the acid treatment.

The characteristic band of palygorskite between 1200-1000  $\text{cm}^{-1}$  has the maximum absorbance at 986  $\text{cm}^{-1}$  and shifts to higher wavenumbers with the acid attack. The sample treated with 7N HCl has its maximum absorbance at 1088  $\text{cm}^{-1}$ , showing the destruction of the silicate structure with formation of amorphous silica gel. This band is also considerably wide in the activated samples, confirming the amorphous environment of Si-O-Si bonds.

Bands of free silica at 798 and 477  $\text{cm}^{-1}$  appear in the activated solids. A new band at 535  $\text{cm}^{-1}$ , corresponding to Si-O-Al vibration, is clearly observed in activated solids, confirming that Al(III) remain in the activated solids.

### 3. Saponite.

At high wavenumbers, the band observed at 3426  $\text{cm}^{-1}$  in natural saponite, corresponding to water molecules, decreases in intensity when the octahedral cations are removed by the acid leaching. The band at 3676  $\text{cm}^{-1}$ , assigned to the hydroxyl groups, disappear with the acid treatment and only a wide band centered at about 3420  $\text{cm}^{-1}$ , assigned to water adsorbed by the silica gel generated, is observed in this region in the activated solids.

The band characteristic of the tetrahedral sheet of the silicates at 1200-1000  $\text{cm}^{-1}$  is more simple in layered than in fibrous clays. In saponite, this band appears at 1011  $\text{cm}^{-1}$ . During the treatment, it shifts to higher wavenumbers and takes the form characteristic of amorphous silica gel in activated samples, being centered at 1083  $\text{cm}^{-1}$ . The formation of silica is corroborated by the increase in the intensity of the bands characteristic of this compound at 795 and 466  $\text{cm}^{-1}$ . The band at 448  $\text{cm}^{-1}$  corresponds to the Si-O bending vibrations bonds and the shoulder that appears at 527  $\text{cm}^{-1}$  is assigned to Si-O-Al bonds.

### 4. Griffithite (Iron Saponite).

Griffithite is an iron saponite in which the ratio Mg/Fe is 1.85; that is, about one of each three octahedral positions is occupied by iron. The FT-IR spectra of the solids obtained after acid activation of griffithite are, in the high wavenumber region, very similar to that of Yuncillos saponite. The band of bonded and zeolitic water in original griffithite is substituted in the activated solids by a band corresponding to water adsorbed in the silica generated.

The band situated between 1200-1000  $\text{cm}^{-1}$ , corresponding to Si-O-Si bonds, changes in form as the acid treatment is in progress, showing a broadening of the band and a shift of the wavenumber of maximum absorbance from 1018  $\text{cm}^{-1}$  in the original sample to 1088  $\text{cm}^{-1}$  in activated samples.

Fe(III) is more resistant than Mg(II) to acid attack. Thus, the bands due to the stretching vibration mode of Mg-OH at 680  $\text{cm}^{-1}$  and Mg-O at 443  $\text{cm}^{-1}$  disappear during the treatment. However, the band situated at 584  $\text{cm}^{-1}$ , assigned to Fe-O bonds, is maintained, although with a very low intensity, even in the samples treated the most. The Al-Fe-OH bending vibration, reported at 880  $\text{cm}^{-1}$ , appears only as a weak shoulder at this wavenumber.

Dip. Scienze Chimico  
Agrarie, Univ. degli Studi di  
Napoli Federico II, Portici  
(NA), Italia

## Formation and stability of mixed hydroxy Fe-Al complexes in montmorillonite

*Violante A, Colombo C and Krishnamurti G S R*

The formation and stability of hydroxy Al interlayers in montmorillonite has been studied in great detail (review by Barnhisel & Bertsch, 1989) and also it was shown that Fe systems exhibited a lower degree of interlayering than Al systems (Carstea et al., 1970). Formation and stability of mixed hydroxy Fe-Al complexes in montmorillonite has not received much attention so far, even though it is well known that the hydroxy-material occupying the interlayers of 2:1 expandible layer silicates of soils consisted of Fe as well as Al and Mg (Singleton & Harvard, 1971). Further, the influence of Al on the transformation and crystallization processes of Fe oxides was studied in great detail (review by Schwertmann, & Taylor, 1989) and, on the contrary, substitution of Fe for Al in crystalline Al hydroxides was discounted (Gastuche et al., 1964; Goh et al., 1987). However, only a few reports are available on the formation of mixed Fe-Al complexes in montmorillonite (Tulloch & Roth, 1975; Fey & Dixon, 1981; Bergaya et al., 1993; Zhao et al., 1993). Results of investigations carried out recently on the formation and stability of mixed hydroxy Fe-Al complexes in montmorillonite are presented and discussed.

Aliquots of montmorillonite (Wyoming SWy-1, Bentonite) suspension were mixed with suitable amounts of Al (as Al nitrate) and Fe either as Fe(III) (as ferric nitrate) or as Fe(II) (as ferrous perchlorate) to have samples at different initial Fe/Al (R) molar ratios. The suspensions were immediately titrated with freshly prepared NaOH to either pH 5.0 or pH 6.0 or pH 8.0 and maintained at the respective pH value for at least 4 h. Samples were also prepared in the absence of montmorillonite as described before. All the samples were aged for prolonged periods of time at 25°C and/or 50°C or 70°C or 95°C. During the aging process, aliquots of each suspension at different time periods were centrifuge-washed free of salts and the precipitation products were examined by x-ray powder diffraction (XRD) on a Rigaku Rotaflex 2000 x-ray diffractometer fitted with graphite monochromator (Rigaku Corporation, Tokyo, Japan) using Cu-K $\alpha$  radiation at 50 kV and 150 mA. The chemical composition of the noncrystalline components of the precipitation products was determined using acid-ammonium oxalate selective dissolution analysis.

### Mixed hydroxy Fe(II)-Al complexes

Lepidocrocite, goethite and ferrihydrite were the Fe oxyhydroxides/oxides observed in the system with an initial Fe(II)/Al molar ratio ( $R$ ) =  $\infty$  in the absence of montmorillonite. No crystalline Fe-oxides were detected in the presence of montmorillonite at 5 mmol Fe(II)/g of clay and  $R = \infty$ , even after aging the samples for 30 d at 70°C or 100 d at 25°C.

The XRD patterns of the mixed hydroxy Al-Fe(II)-Mt complexes (formed at  $R = 0.1$ -1.0), aged for 30d at 70°C showed d-spacings ranging from 15.47 to 17.42 Å which on pre-heating at 550°C collapsed to around 14.70 to 13.36Å, indicating formation of stable interlayers. In spite of the large amounts of Al crystallized as gibbsite during the aging process, the complexes still had 36.6-68.9% distribution of Al co-precipitated with Fe indicating that the short-range ordered materials present in the interlayers of montmorillonite even after long aging periods were highly Al-substituted noncrystalline Fe-oxides.

### Mixed hydroxy Fe(III)-Al complexes

In the absence of montmorillonite, Al-substituted poorly crystalline Fe oxides (ferrihydrite) and gibbsite formed in complexes with  $R \leq 4.0$  where as hematite crystallized in the complexes at  $R = 10.0$  after prolonged aging (Colombo & Violante, 1996).

In the presence of montmorillonite, inspite of large amounts of Al crystallized during the aging, the interlayers were highly Al-substituted noncrystalline Fe oxides. The XRD patterns of the mixed hydroxy Fe-Al montmorillonite complexes formed at pH 6.0 had d-spacing of 17.84 Å ( $R=0.5$ ) and 17.27 Å ( $R=1.0$ ) in the samples aged for 30 d at 70°C, which on pre-heating at 550°C for 2 h collapsed to around 12.90 Å [control (9.60Å),  $R=0$  (5 mmol of Al per g of clay) (9.75 Å),  $R=\infty$  (5 mmol Fe per g of clay) (10.13Å)]. This clearly indicated that Fe stabilized the hydroxy-Al interlayers in montmorillonite as mixed hydroxy Fe-Al complexes (Krishnamurti et al., 1995).

The influence of citrate on the stability of mixed hydroxy Fe-Al interlayers was studied both at citrate/(Fe+Al) molar ratio (Ct) of 0.01 to 0.1 at a fixed Fe/Al molar ratio of 1.0 (Fe+Al = 5, and 30 mmoles per g of clay), and at pHs of 5.0 and 8.5. Increasing amounts of citrate increased the proportion of mixed hydroxy Fe-Al complexes formed as stable interlayers in montmorillonite, particularly at pH 5.0; e.g., the XRD pattern of the complexes formed at pH 5.0 with Fe+Al = 30 mmol g<sup>-1</sup> of clay and with citrate/(Fe+Al) molar ratio = 0.1 and aged for 32 d at 50°C had a d-spacing of 22.0 Å which on pre-heating the sample at 500°C collapsed to around 18.5 Å (Table 1).

The importance of organic ligands, such as citrate, in the formation and stability of mixed hydroxy Fe-Al interlayers in montmorillonite, as observed in natural terrestrial environments, needs critical evaluation.

Table 1. Data on the acid ammonium oxalate-extractable Fe and Al contents and the d (001)-spacing of the mixed hydroxy Fe(III)-Al-Ct-Mt complexes, aged for 32 d at 50°C

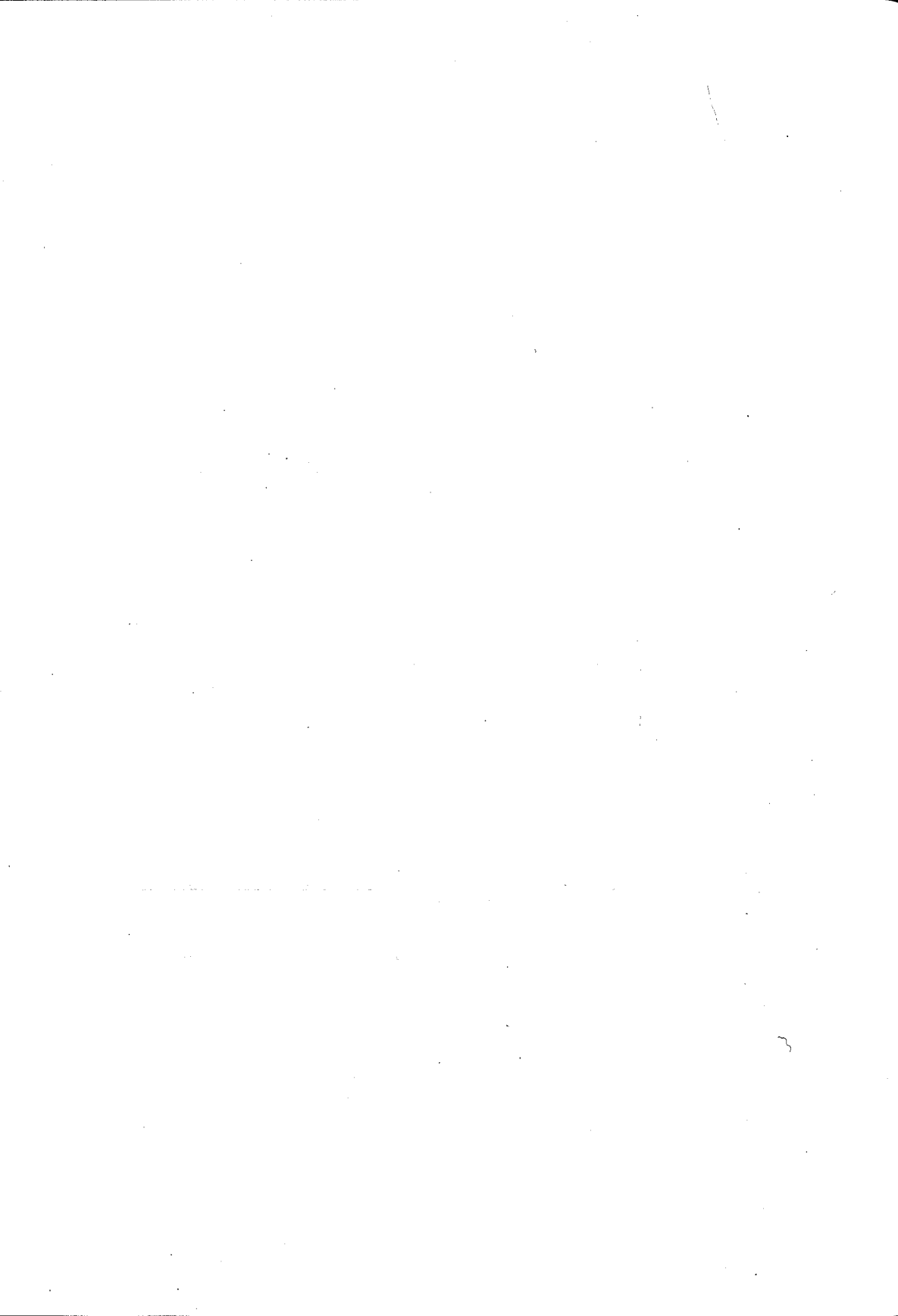
Nature of complex	Fe+Al	Fe <sub>ox</sub>	Al <sub>ox</sub>	d (001)-spacing (Å)		
				25°C	300°C	550°C
pH of formation: 5.0						
Ct <sup>#</sup> = 0	5.0	1.26	0.73	12.4	10.7	10.1
	30.0	3.21	1.01	19.4	11.2	10.1
Ct = 0.01	5.0	1.44	0.97	12.0	11.2	9.8
	30.0	3.35	1.49	19.5	12.5	10.8
Ct = 0.1	5.0	1.38	1.09	19.5	11.2	10.1
	30.0	3.06	1.55	22.0	19.0	18.5
pH of formation: 8.5						
Ct = 0	5.0	1.36	0.51	12.5	12.4	10.1
	30.0	2.95	1.11	17.8	10.8	10.3
Ct = 0.01	5.0	1.22	0.85	12.5	12.2	10.5
	30.0	3.18	1.05	18.0	13.0	12.3
Ct = 0.1	5.0	1.16	0.77	13.0	12.6	10.5
	30.0	2.88	1.08	21.6	20.3	12.5

# Ct = Ct/(Fe+Al) molar ratio

#### References:

- Barnhisel, R.I. & Bertsch, P.M. 1989. pp 729-788. In: *Minerals in Soil Environments*. (J.B. Dixon & S.B. Weed, Eds), SSSA, Madison, WI.
- Bergaya, F., Hassoun, N., Barroult, J. & Galtineau, L. 1993. *Clay Minerals* **28**, 109-122.
- Carstea, D. D., Harward, M. E. & Knox, E. G. (1970) *Soil Sci. Soc. Am. Proc.* **34**, 517-521 and 522-526.
- Colombo, C. & Violante, A. (1996) *Clays & Clay Minerals*. **44**, 113-120.
- Fey, M. V. & Dixon, J. B. 1981. *Clays & Clay Minerals* **29**: 91-100.
- Gastuche, M. C., Bruggenwert, T. & Mortland, M. M. (1964) *Soil Sci.* **98**, 281-289.
- Goh, Tee Boon, Huang, P. M., Dudas, M. J. & Pawluk, S. (1987) *Can. J. Soil Sci.* **67**, 135-145.
- Krishnamurti, G.S.R., Violante, A. & Huang, P.M. (1995) In: *Clays Controlling the Environments*. (Curchman, G.J, Fitzpatrick, R.W., & Eggleton, R.A, Eds) Proc. 10th Int Clay Conf., Adelaide, Australia, Melbourne: CSIRO publishing. 183-186.
- Schwertmann, U; & Taylor, R.M. (1989). pp 379-438. In: *Minerals in Soil Environments*. (J.B. Dixon & S.B. Weed, Eds), SSSA, Madison, WI
- Singleton, P. C. & Harward, M. E. (1971) *Soil Sci. Soc. Amer. Proc.* **35**, 838-842.
- Tullock, R. J. & Roth, C. B. (1975) *Clays & Clay Minerals* **23**, 27-32
- Zhao, D.Y., Wang, G., Yang, Y., Guo, X., Wang, Q. & Ren, J. (1993). *Clays & Clay Minerals* **41**, 317-327.

**CRYSTAL CHEMISTRY AND  
STRUCTURES**



## Eventual solid solution in K-NH<sub>4</sub> illite/smectite ordered mixed layer

*Bobos I and Gomes C*

### 1. Introduction

A new occurrence of random and ordered mixed layer illite/smectite (I/S) containing ammonium as fixed interlayer cation has been reported in the fossil hydrothermal system Harghita Bai, -East Carpathian - (Bobos, 1994). Other hydrothermal occurrences are known in the literature in Japan (tobellite, after Tobe mine) Slovak Carpathian (ammonium hydromica) and in USA. The origin of NH<sub>4</sub> - bearing phyllosilicates is poorly known.

The samples we had studied are related with the porphyry copper alteration which developed in a first phase a zonal alteration centred on the generating intrusions and the following zones of alteration could be distinguished: biotitic, amphibolic, chloritic and argillic. A second phase of alteration did occur with changing the fluid regime from lithostatic to hydrostatic yielding hydraulic fracturing expressed by a breccia pipe structure with irregular polygonal or elliptic blocks of piroxene andesite argillized enriched in ammonium illite or ordered mixed layer NH<sub>4</sub>-I/S (R3). In general, phase relationship between the two components of I/S mixed layers is very deficiently studied and they have been considered as end members of a solid solution or as independent phases.

### 2. Methodology

Samples have been studied by X-ray diffraction (XRD), Infra-red spectroscopy (IR) and chemical analyses. All samples studied had purified in order to separate any impurities.

### 3. Results

XRD analyses evidenced a small expandability corresponding to 5..10% smectite layers. XRD trace for ammonium bearing illite showed for 001 reflection a strong diffraction line, very large in a width at half - height of the illite 001 peak and the weak 002 and 003 diffraction lines. The most specific feature the 005 diffraction line. This peak is very sensitive and therefore, it shows well the passage on NH<sub>4</sub>-I/S to K-I/S. Peak position variable in the range 2,05Å and 2,00Å. The second structural aspect observed in the studied samples was the lack of periodicity between (001) and (002) peaks. In air dried the position of (001) peak shows shift on the interval 10,20..10,70Å and after treatment with ethylene glycol the same peak collapses 0,20..0,50Å. Ratio between d(001) and d(002) is more great than 2. Comments to the XRD results are shown in the Fig. 1. IR spectra are characterized by the

typical absorptions due to N-H bending at  $1430\text{ cm}^{-1}$  with increase in intensity with ammonium content. Nitrogen determination on these samples gave values in the range 1,12..1,83 wt.& where as  $\text{K}^+$  values were situated in the range 0,08..0,45/ $\text{O}_{10}\text{OH}_{12}$ .

#### 4. Concluding remarks

A schematic representation for this eventual type of solid solution of ordered mixed layer I/S is shown in Fig.2, for a single 2:1 mineral phase with different ions ( $\text{K}^+$  and  $\text{NH}_4^+$ ) fixed in interlayer positions.

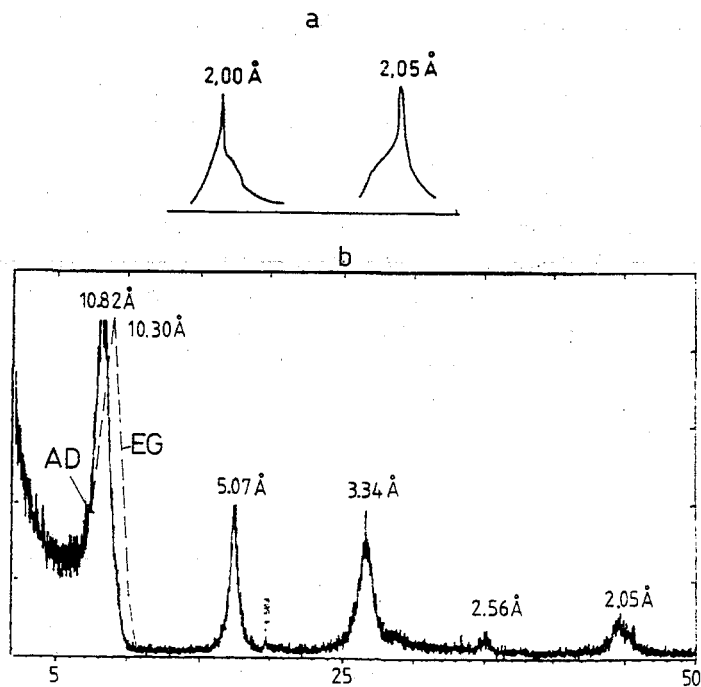


Fig. 1: a) The variable position of (005) diffraction line in the range  $2,05\text{ \AA}$  (high contents of ammonium interlayer cation) and  $2,00\text{ \AA}$  (high contents of potassium interlayer cation): b) XRD pattern of ammonium bearing illite (AD - air dried; EG: ethylene glycol vapour).

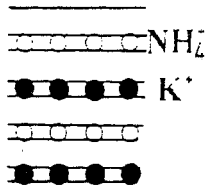


Fig. 2 - A possible representation of ordered mixed layer illite/smectite (R=3) with  $\text{NH}_4$  and K fixed interlayer cation.

Dept. of Geology, Univ. of  
Illinois, Urbana, Illinois,  
USA

## Crystal-chemical features of bentonitic illite/smectite

*Cuadros J and Altaner S P*

### 1. Introduction.

One of the problems with more abundant geological and geochemical literature is the transformation of smectite into illite. However, some aspects of this reaction such as its mechanism, rate and some characteristics of mixed-layer (I/S) minerals are not well known. In this paper, new insight on the crystal-chemical composition of interstratified phases have been made mainly related with the cis-trans octahedral occupancy

### 2. Samples and Techniques.

We studied 30 bentonites with the following age and locations: two Miocene bentonites from Oregon, USA; nine Cretaceous bentonites from Montana, USA; one Carboniferous bentonite from Silesia, Poland; eight Devonian bentonites from the US Appalachians in West Virginia and New York; two Silurian bentonites from Northern Ireland and Newtown, UK; and six Ordovician bentonites from Northern Ireland, Sweden, Wales, and Quebec, Canada. Illite in all these samples had a diagenetic origin. Finally, we also studied a Pliocene bentonite from Almeria, Spain. Illite in this latter sample was originated by a hydrothermal event.

The samples were disaggregated and the fraction less than one micrometer was separated for this study. We did not use dispersant agents in this process. The selected fraction was studied by means of XRD on both oriented aggregates and randomly oriented specimens. They were chemically analyzed with microprobe. They were thermally analyzed (thermogravimetry) to study their dehydroxylation behavior. Finally, they were also analyzed by means of FTIR in order to investigate possible variations of cation ordering in the octahedral sheet.

### 3. Experimental Results and Discussion.

XRD of our oriented samples, treated with ethylene glycol, permitted the determination of the percentage of illite present in the I/S. The samples covered the whole range from pure smectite to pure illite. The analysis of the randomly oriented specimens allowed us to determine their polytype characteristics. Only samples with more than 45 % illite presented reflections which permitted such determination. We found that the amount of illite in I/S is related to the cis-trans site occupancy in the octahedral sheet. As the number of illite layers increases, the I/S becomes increasingly trans-vacant.

The chemical analyses showed a number of features. Si content seems to influence the amount of Mg in the octahedral sheet. For high values of Si (smectite-rich I/S) Mg has a wide

range of abundance. When Si decreases (movement towards illite-rich I/S) the amount of Mg in the octahedral sheet seems to become fixed around a value of 0.5 per full unit cell.

Another feature found is that Al and Fe in the octahedral sheet are linearly correlated, indicating that they exchange for each other. Finally, we observed that Fe also has a certain control on Mg content. For high Fe values the amount of Mg present in the octahedral sheet is variable. A decreasing amount of Fe is associated with Mg values close to 0.5, and Al values close to 3.5 per full unit cell. Interestingly, an octahedral sheet with the composition 3.5 Al and 0.5 Mg allows for a perfect Al-Mg ordering in which Mg atoms are uniformly distributed in the lattice.

Thermal analysis of our I/S samples showed the presence of two dehydroxylation events (at 550 and 650 degrees C). Both of them were present in all samples, but the relative amount of hydroxyls lost in each event varies from sample to sample. The weight losses for these events were quantified. We found that there is a correlation between cis-trans occupancy of the I/S and dehydroxylation behaviour. As the clays become more cis-vacant the dehydroxylation event at higher temperatures becomes more important with respect to the one at lower temperature. This result confirms the interpretation of Drits et al. (1995) of the existence of two dehydroxylation events in smectites.

We analyzed our IR spectra by decomposing and quantifying the region of OH bending (930-750 cm<sup>-1</sup>). The frequencies of OH bending of hydroxyls united to different cation pairs are different, so by quantifying the areas of these bands it is possible to analyze short-range ordering in the octahedral sheet. We found, that, in short-range distances, Fe tends to segregate from both Al and Mg. Also, we found that such segregation is related to cis-trans occupancy. Fe clustering becomes more important as the clay becomes more trans-vacant.

#### 4. References.

Drits, V., Besson, G. and Muller, F. (1995) An improved model for structural transformation of heat-treated aluminous dioctahedral 2:1 layer silicates. *Clays Clay Min.* 43, 718-731.

(1) IRNA-CSIC, Salamanca,  
España

(2) INRA, Science du Sol,  
Versailles, France

## Crystal structure and particle orientation in relation to behaviour of clays during drying

*Iñigo Iñigo A C (1) and Tessier D (2)*

### INTRODUCTION

Clays have several major effects on the properties and performance of soils, one of these being associated with their effects on the water holding capacity of the soil. In soils with appreciable contents of clays, the uptake and release of water give rise to changes in bulk volume (swelling and shrinking), which alters the clay microstructure at different levels of organisation. The nature and amount of clay in any soil are of fundamental importance to the soil behaviour. This behaviour is also strongly affected by climatic conditions, the length of time for soil genesis, as well as soil organisms.

Although the structural units of clays (layers and stacks of layers) are relatively well defined, the arrangements of these units at a macroscopic scale are not well understood. Further studies are necessary to gain a better insight in to the crystal structure and macroscopic properties in order to better understand the continuum of clay water systems relevant to soils.

This abstract deals with the evolution of the microstructure during drying, with special emphasis on the clay particle size and orientation during drying.

### MATERIALS AND METHODS

Three homoionic Ca-clays were prepared, namely Wyoming montmorillonite, Salins Illite and La Bouzule interstratified (I-S) clays. They were homogenized by mechanical stirring to give the consistency of a paste. Drying curves were obtained by first applying increasing suction pressures ( $P < 1.0$  MPa), and then equilibrating at a range of vapour pressures. Classical X-ray diagrams were made by adjusting the diagrams to a model developed by Lanson [1990]. A transmission device was also used in order to study the particle orientation. For this purpose, the clay was placed in a cell specially designed to obtain the diagrams corresponding to different sample orientations. The samples prepared at various levels of drying were also embedded in an epoxy resin according to the method developed by Tessier [1984] for TEM observations.

## RESULTS

At 50% R.H. the layer spacing of Wyoming Montmorillonite was 15.6Å. In Salins 10 Å layer spacings were identified. The La Bouzule sample was an interstratified clay with ~15 and 10 Å. Salins and La Bouzule also contained a small amount of kaolinite.

The TEM studies showed the main clay particle types. In Wyoming montmorillonite the clay particles were made of a various number of layers depending on the level of drying (~20 to ~200). The clay layers were generally curved and their degree of curvature depended on the level of drying. The higher the desiccation, the smaller the curvature radius. In Salins the particles were mainly flat individual crystals, about 100 nm large and 10 nm thick. In La Bouzule, the particles were very large (~2000nm) and their thickness reached about 100 nm. The particles were mainly aggregates of illitic and smectitic crystals.

The examination of clay particle orientation showed that the clay fabric was randomly oriented for the clay pastes. The particle orientation was the main feature appearing during drying and the particle orientation increased progressively with the suction pressure. Nevertheless there were considerable differences between the clays. The La Bouzule clay became strongly oriented at low pressures and the maximum orientation was obtained at 1.0 MPa. Wyoming montmorillonite exhibited weak particle orientations compared to those of La Bouzule and its orientation constantly increased with the level of drying up to 100 MPa (Fig. 1a). The behaviour of Salins illite was intermediate. The range in which the particles were oriented was also different. In Wyoming all orientations were present even in the dry state (Fig. 1a), while in Salin and La Bouzule the range of particle orientation was limited (+/- 40 to 50° relative to the horizontal plane) (Fig. 1b).

## DISCUSSION AND CONCLUSION

Particle orientation and thus changes in the microstructure appeared as one of the main factors characterizing the modification of clay during drying. This result is confirmed for non swelling clays such as Illite as well as for swelling clays such as Wyoming montmorillonite. For the clays studied, the range of particle orientation appeared to depend on two main factors: (1) the particle extension in the ab plane and (2) the crystal structure.

Because the Salin clay was characterized by very fine crystals (~ 100 nm), with layer spacing at 10 Å, strong cohesion forces gave very rigid and flat particles. The packing of these small crystal units gave a poorly oriented clay matrix. By contrast, for the La Bouzule clay, the large particles (~2000 nm) gave a strongly oriented system. It appears however that the amount of smectitic layers was not sufficient to allow the particle to be curved during desiccation. The resulting effect is that the porosity of the La Bouzule clay remains high even in a dry state. In the case of Wyoming montmorillonite, the particles were also large, but the clay layers inside the particles were separated by water

molecules. As a result, the layers can slide one on another and the particles can be curved due to weak cohesion forces in comparison to Salin and La Bouzule. In a dry state, the bulk volume is smaller even if the contribution of the layer spacing in porosity is significant.

In summary, the apparent volume of clays with a high water content is related to the disorientation of particles while for the dry states the pore size, volume and continuity are associated with the geometry of the clay matrix and particularly to the ability of the particles to be curved. In smectite the parallel arrangement of the clay layers gives very compact materials.

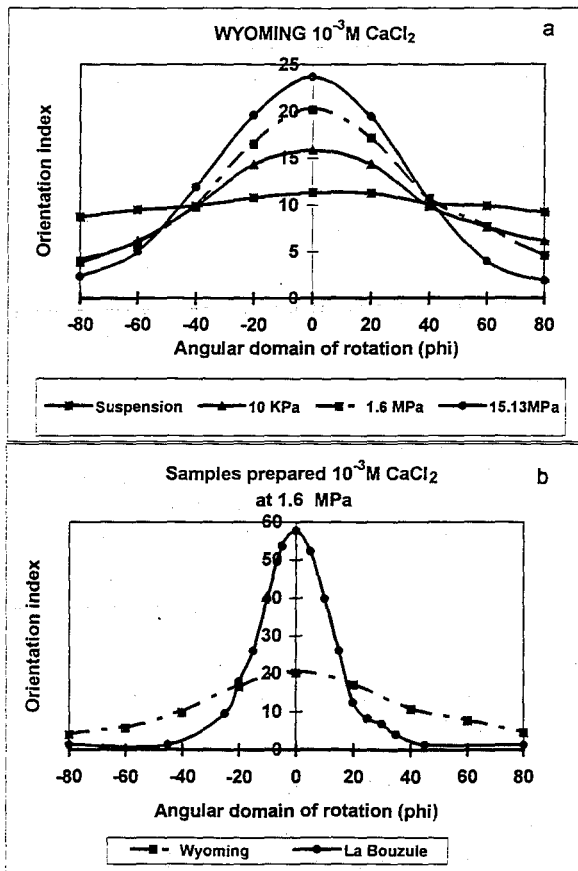


Fig. 1

## Effect of particle size on the dehydration-rehydration processes in magnesium vermiculite

*Ruíz Conde A, Ruíz Amil A, Sánchez Soto P J and Pérez Rodríguez J L*

The dehydration-rehydration in Mg-vermiculite is a complex phenomenon. The mechanism can be considered as comprising intermediate stages, in which the transition takes place apparently through interstratified phases. There is evidence for this in the literature [1-5], but the existence and/or the formation of interstratified phases have not been checked and confirmed by a suitable calculation method. The formation of interstratified or mixed-layer structures in vermiculites was reported many years ago [1]. Different aspects were studied, such as identification in crystal structures, natural and laboratory weathering products, exchange reactions with inorganic cations and formation of complexes or interaction with organic substances [6-9]. Mixed-layer Mg-vermiculites are interesting to understand the structural and crystallochemical features, the interaction with inorganic and organic cations in clays, the formation and study of advanced clay materials, and the study of various geological problems [10]. It is recognized that the hydration state of Mg-vermiculite depends on the water vapor pressure, temperature, and cation species. It has been defined by the number of water layers [ $n(\text{H}_2\text{O})$ ] in the interlamellar space, with a development corresponding to different phases, such as zero-, one-, and two-water-layer hydration states, with basal spacings at 9.02 Å, 11.50 Å and 14.40 Å, respectively [2,3]. In the present work, the dehydration-rehydration of Mg-vermiculite, as large flakes (7x5x0.1 mm) and powder ( $\leq 80 \mu\text{m}$ ), has been studied.

### EXPERIMENTAL

The vermiculite sample used in this study was mined from Santa Olalla deposit (Huelva, SW Spain). Vermiculite powder (particle size  $\leq 80 \mu\text{m}$ ), was obtained using a Retsch Ultra-Centrifugal Mill. Samples of vermiculite (flakes and powder) were made previously homoionic by successive treatment with 1N  $\text{MgCl}_2$  solution. The dehydration

experiments were performed at 100° and 140°C for several days using a Teflon bottle in a PTFE-lined Perkin-Elmer bomb, and air-dry rehydration treatments under laboratory conditions. The vermiculite samples were heated at fixed temperatures and several times, and examined immediately by X-ray diffraction (XRD). Each one of the samples treated were rehydrated at room temperature, and also examined by XRD. Air brought to a relative humidity of 50 % at 20°-25°C was passed continuously over the specimen during examination. The samples were examined by XRD, and the results analyzed by the direct Fourier transform method using the INTER program [11]. The program allows to calculate diffraction effects from given mixtures (XRD Intensity Function) and compared with experimentally recorded diffraction curves. This program was also used to calculate the distribution function of interlayer distances  $W(R)$  by the Direct Fourier transform method, being defined as the probability of finding a layer at a distance,  $R(\text{Å})$ .

## RESULTS AND DISCUSSION

The results indicated the formation of two-water-layer hydration states (14.4 Å, 14.2 Å, and 13.8 Å phases), and one-layer Mg-vermiculite (11.5 Å phase), segregated phases, besides binary interstratified one-two-water-layer hydration states of Mg-vermiculite phases. It was confirmed in Mg-vermiculite flakes the existence of interstratified phases in the conversion from two-one and one-two-water-layer hydration states in Mg-vermiculite flakes by dehydration-rehydration treatments. The dehydration takes place through interstratified phases consisting of alternations of 13.8 Å and 11.5 Å components (25.3 Å, regular interstratified phase). The transformation toward 11.5 Å phase at 140°C is more rapid than at 100°C. The rehydration produces mixed-layers consisting of alternations of 11.5 Å and 14.2 Å components (random interstratified phases). Using powdered Mg-vermiculite, the changes occur faster than in flakes, being produced only at 140°C. Under these conditions, no interstratification can be detected, and the dehydration-rehydration take place spontaneously.

The presence of the interstratified phase in the conversion of two-one- and one-two-water layer hydration states takes place by the mobility of the water molecules in the crystals. The results suggest that the large particles permit a low mobility of water

molecules and the thermodynamic equilibrium between the original and final segregated phases gives rise to a regular phase, characterized by a loss of an equal number of water molecules in the interlayer space. In the case of rehydration, the process must be inverse. It is concluded that the transformation from two- to one-water-layer Mg-vermiculite throughout interstratified phases depends on the particle size, temperature and time of treatment.

#### ACKNOWLEDGMENT

This work was supported by DGICYT through research project PB92-0014.

#### REFERENCES

1. A.M. Mathieson and G.F. Walker, *Amer. Miner.* **39** (1954) 231.
2. G.F. Walker, *Clays Clay Miner.* **4** (1956) 101.
3. M. Suzuki, N. Wada, D.R. Hines and M.S. Whittingham, *Phys. Rev. B* **36** (1987) 2844.
4. C. de la Calle, H. Suquet and C.H. Pons, *Clays Clay Miner.* **36** (1988) 481.
5. H.G. Reichenbach and J. Beyer, *Clay Miner.* **27** (1994) 327.
6. M.M. Mortland, *Adv. Agron.* **22** (1970) 75.
7. P. Olivera Pastor, E. Rodríguez-Castellón and A. Rodríguez-García, *Clay Miner.* **22** (1987) 479.
8. J.L. Pérez-Rodríguez, Morillo E. and C. Maqueda, *Clay Miner.* **23** (1988) 379.
9. A. Ruiz-Amil, F. Aragón de la Cruz, E. Vila and A. Ruiz-Conde, *Clay Miner.* **27** (1992) 257.
10. A. Ruiz-Conde, A. Ruiz-Amil, P.J. Sánchez-Soto and J.L. Pérez-Rodríguez, *J. Mater. Chem.* (in press, 1996).
11. E. Vila and A. Ruiz-Amil, *Powder Diffraction* **3** (1988) 7.

(1) Dpto. Cristalografía y Mineralogía. Fac. Geológicas. Univ. Complutense de Madrid, España

(2) Dpto. Química Inorgánica, y Dpto. Química Inorgánica y Bioinorgánica. Fac. Química y Fac. Farmacia. Univ. Complutense de Madrid, España

## The use of oblique texture electron diffraction patterns as a tool for structure determination of clay minerals

*De Santiago Buey C (1) and Nicolopoulos S (2)*

### INTRODUCTION

Crystal structure determination in poor crystalized minerals (e.g. smectites) has been traditionally carried out by means of X-Ray powder diffraction; although by this technique is possible to distinguish between different structural types of minerals, it is not possible to resolve in detail the crystal structure.

The aim of this work is to put in evidence the effectiveness of the oblique texture electron diffraction patterns (OTEDP's) technique which is specially adequate for the structural study of layer minerals. Moreover, this technique is particularly useful for beam sensitive and low crystallinity minerals, where high resolution TEM images give poor crystallographic information.

The use of OTED patterns has been firstly developed in USSR in the groups of Zvyagin (1) and Vainshtein (2). With the help of electron diffraction cameras and using OTEDP's, crystal structures of several compounds have been studied (semiconductors, metals, silicates...). A recent review of all this work appears in the International Tables for X-Ray Crystallography (3). More recent investigations by Drits (4) on clay minerals show that crystal structure problems like polytypism or the presence (or not) of different cations in different crystallographic positions can be solved with the use of OTEDP's. Again, Dorset (5) using direct method procedures has confirmed the validity of crystal structure determination of several clay minerals previously solved by Zvyagin using this method.

The previous investigations (1-5), put in evidence the power of oblique texture electron diffraction patterns to resolve several structure problems of layer silicates like polytypism and cation location in different crystallographic positions.

### EXPERIMENTAL METHOD

Aggregations of thin plate-like particle are usual objects in OTED studies. If a drop of a suspension containing thin layer mineral crystallites is put on a thin colloid film, a textured preparation is

obtained after drying. The crystallites are arranged with their best-developed faces parallel to the support surface and are rotated at random about the texture axis which is normal to the support plane. The reciprocal lattice of an oriental polycrystalline sample may be treated as the result of rotation of a single-crystal reciprocal lattice about the texture axis. In layer silicates silicates the  $ab$  plane is the best developed one, so that the texture axis is parallel to  $c^*$ .

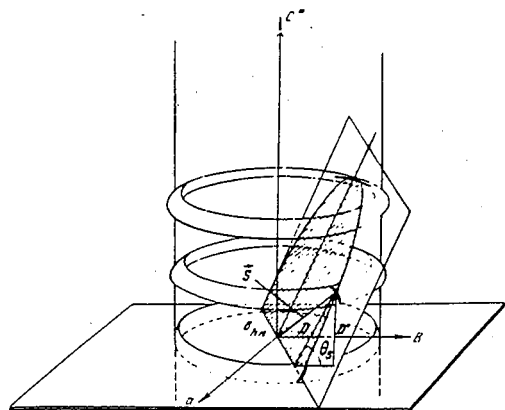


Figura 1 (Vainshtein, 1956)

Oblique section of the reciprocal lattice.

When the lattice is rotated about the texture axis, lattice points with like  $hk$  indices, lying on lines parallel to  $c^*$ , form nodes having the shape of sets of rings arranged on coaxial cylinders. If the specimen is perpendicular to the electron beam the pattern represents a normal section of the reciprocal lattice (perpendicular to the  $c^*$  axis) and the reflections appear as continuous circles. At a given tilt angle, the diffraction pattern shows an oblique section of the reciprocal lattice containing a set of ellipses.

Analysis of the arrangement of reflections on the different set of ellipses provides information on the dimensions and the shape of the unit cell, much more readily than in the case of X-Ray powder diffraction. On the other hand, the distribution of relative intensities of reflections along the ellipses provide a valuable information about octahedral sites occupation, the type of interlamellar cations and layer stacking order. Furthermore, for phyllosilicates, the problem of unit-cell parameters determination and indexing is facilitated by the fact that each ellipse contains reflections with a known set of  $hk$  indices, and  $h+k$  is always even, as the corresponding crystal lattices are C centered (1-3).

Transmission electron microscopy observations were performed on a JEOL 2000 FX microscope operated at 200 Kv and equipped with a side entry specimen holder.

## RESULTS AND DISCUSSION

In the present work we study the crystal structure of trioctahedral smectite found in the "Formación Arcillas Verdes" from the Tajo Basin (1) and collected at the basis of the "Cerro del Aguila". The previous X-Ray diffraction and TEM study, confirmed that the mineral is a saponite. A more detail crystal structure investigation by OTEDP's showed according to the geometry and special arrangement of reflections along the ellipses that the sample is monoclinic, with a monoclinic angle:  $\beta = 100^\circ$ . In fact, it is demonstrated that there is a relation between structural perfection in the layers and the

crystallographic system of the mineral (1). Generally, the Monoclinic system presents much more structural disorder than the triclinic one. Furthermore, the diffuseness of reflections in the ellipses is consequence of the poor crystallinity of this smectite.

After indexing of reflections arranged on different ellipses (fig. 2), unit cell parameters have been determined:  $a = 5,2 \text{ \AA}$  ;  $b = 9,2 \text{ \AA}$  and  $c = 9,6 \text{ \AA}$ . The value of  $b$  parameter confirms the trioctahedral

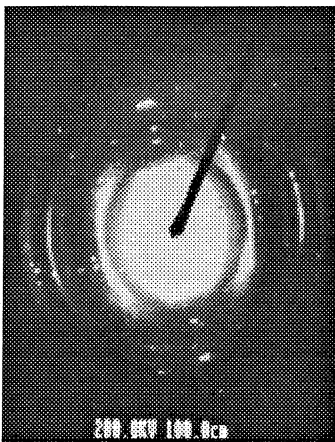


Figura 2

Oblique Texture from the smectite

Tilt angle  $\varphi = 48^\circ$

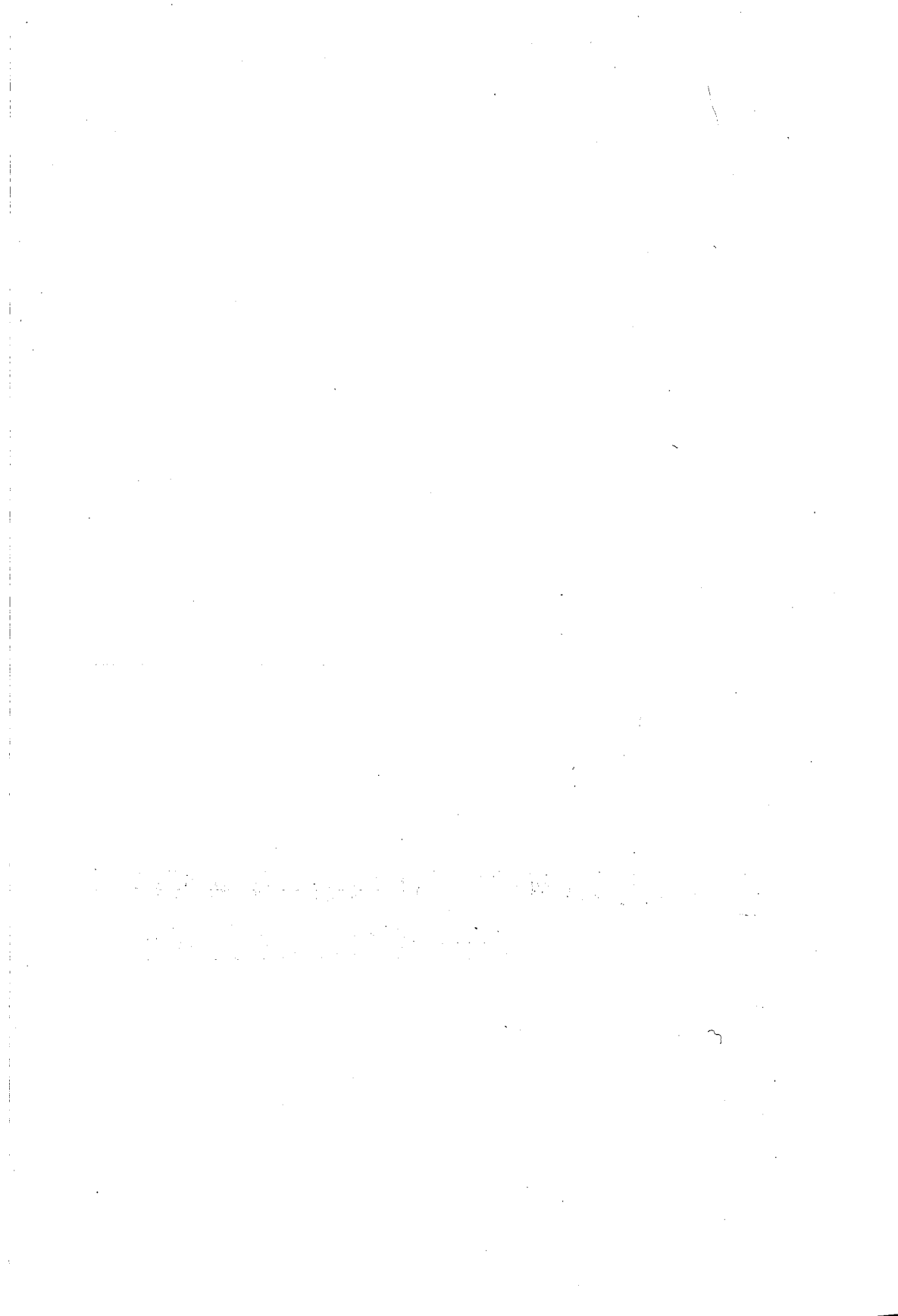
variety of the smectite. On the other hand, the small value of  $c$  axis indicates loss of interlayer water molecules during the study of the sample in the microscope.

The above data show that the examined sample is a trioctahedral smectite without strict  $c$  repeat unit.. The nonrigorous  $c$  repeat unit is the result of disordered displacements of network in layers along  $b$  axis direction (1). In fact, as long as it doesn't exist any well defined layer stacking in the smectite, polytype description cannot be applied in this case. Alternatively, the stacking sequence of this mineral can be described as 1M, with possible space groups  $Cm$  or  $C2/m$  (1,4).

## BIBLIOGRAFIA

1. Zvyagin, B.B. (1967): "Electron diffraction analysis of clay mineral structures" Plenum Press. New York. pp 364 .
2. Vainshtein, B.K. (1964): "Structure analysis by electron diffraction" Pergamon Press Oxford... pp 288 .
3. Zvyagin, B.B. (1992): "Oriented texture patterns". International Tables for X-Ray Crystallography; Volume C. pp 359 - 360.
4. Drits, V.A. (1981): " Electron diffraction and High-Resolution Electron Microscopy of mineral structures" Springer Verlag, pp 303 .
5. Dorset, D.L. (1995): "Structural Electron Crystallography" Plenum Press, New York and London, pp 457 .
6. Brell et al. (1985): "Clay mineral distribution in the Evaporitic Miocene Sediments of the Tajo Basin, Spain" Miner. Petrogr. Acta Vol. 29 pp 267-276.

**GEOLOGY, GENESIS AND  
GEOCHEMISTRY**



(1) Dpto. Cristalografía y  
Mineralogía. Fac.  
Geológicas. Univ.  
Complutense de Madrid,  
España

(2) Dpto. Geología. Fac.  
Ciencias Experimentales.  
Univ. de Huelva, España

## Controlling factors on the compositional variations of diagenetic and low-grade metamorphic chlorites

*Barrenechea J F (1), Rodas M (1) and Alonso Azcárate J (2)*

### Introduction

Chlorite is one of the most common rock forming minerals in sedimentary materials affected by diagenetic to low-grade metamorphic conditions. During the last decade, different authors have focused their efforts in an attempt to correlate the compositional variations of chlorites (specially the Al<sup>IV</sup> content) with their temperature of formation (De Caritat et al., 1993). However, up to date, chlorite geothermometry cannot be regarded as a reliable tool because on one side, the observed compositional trends might be explained in terms of varying amounts of mixed-layered components like corrensite (Shau et al., 1990) and on the other, it is not based on equilibrium reactions (Essene and Peacor, 1995). Moreover, additional factors like lithology, mineral assemblage and sedimentological characteristics may produce important variations on the chlorite compositions. The aim of this work is to study the influence of such parameters on the chlorite compositions in a series of siliciclastic and carbonate materials of late Barremian-Aptian age, affected by diagenetic to low-grade metamorphic conditions, in the Eastern part of the Cameros basin (NE Spain).

### Materials and Methods

The studied samples correspond to different stratigraphic cross sections performed through the Urbión and Enciso Groups, which consist respectively of siliciclastic and carbonate dominated sediments. A detailed description of the sedimentological features, mineral assemblages and distribution of P-T conditions along the basin can be found in Barrenechea et al. (1995) and Alonso-Azcárate et al. (1995). The crystallochemical parameters of the chlorites have been determined from X-ray diffractograms and Transmission Electron Microscopy (TEM/EDX) analyses have been performed in selected chlorite samples in order to achieve their chemical composition.

### Characterization of the chlorites

In the diagenetic lutites of the western border of the basin, berthierine (7 Å chlorite) and to a minor extent irregular mixed-layer chlorite/vermiculite are common phases of the  $< 2\mu\text{m}$  fraction. Diagenetic chlorites recognized in carbonate samples present the highest values of  $\text{Si}^{+4}$ ,  $\text{Al}^{\text{VI}}$  and octahedral vacancies, together with low  $\text{Al}^{\text{IV}}$  and  $\text{Mg}^{2+}$  contents (Table 1). Following the classification of Wiewiora and Weiss (1990), these chlorites correspond to Mg-chamosites.

The chlorites found in the siliciclastic and carbonate samples affected by very low-grade metamorphic (anchizonal) conditions correspond respectively to Mg-chamosites and Fe-clinoclores. The chlorites of the carbonate samples are richer in  $\text{Si}^{+4}$  (and consequently poorer in  $\text{Al}^{\text{IV}}$ ) and  $\text{Mg}^{2+}$  than those included in the siliciclastic ones. A significative decrease in the  $\text{Si}^{+4}$  content of the chlorites from the carbonate materials is observed as conditions close to the anchizone/epizone boundary are approached.

	GR	AM	SP	MN	EN	YA
Si	6.13	6.03	5.37	5.70	5.14	4.63
$\text{Al}^{\text{IV}}$	1.87	1.97	2.63	2.30	2.86	3.37
$\text{Al}^{\text{VI}}$	3.89	3.45	3.27	3.29	3.35	3.65
Fe	4.83	4.17	4.93	3.13	5.88	6.06
Mg	2.06	3.47	3.47	4.92	2.24	2.18
□	1.21	0.89	0.33	0.77	0.52	0.11

Table 1.- Representative chlorite compositions determined by TEM/EDX analyses and calculated on the basis of 28 oxygen atoms. Samples SP and YA correspond to siliciclastic materials while samples GR, AM, MN and EN represent carbonate rocks. Analyses have been ordered from left to right according to the increasing metamorphic conditions. (□ → octahedral vacancies).

The compositions of the chlorites included within the siliciclastic materials in the low-grade metamorphic (epizonal) areas are rather uniform, with high values of  $\text{Al}^{\text{IV}}$  contents, Fe/Mg ratios and octahedral occupancy and the lowest values of contamination with K. Chlorites in these samples may appear as polycrystalline micronodules (up to 4 mm wide), or as platy crystals included in the clay matrix.

Most of the chlorite analyses present variable amounts of contamination with  $K_2O$ . A remarkable feature within each stratigraphic cross section is the good positive correlation found between the octahedral vacancies and the  $K_2O$  content, with regression coefficients ranging from 0.75 to 0.96. These correlations indicate that different proportions of illite interstratified with the chlorite layers would be responsible for the presence of octahedral vacancies in these samples (Jiang et al., 1994). The  $K_2O$  contents determined in the chlorite analyses increase with the decreasing metamorphic grade.

A significant increase in the  $Al^{IV}/Al^{VI}$  ratio is observed for both the carbonate and siliciclastic materials with increasing metamorphic conditions, the highest values corresponding to the previously mentioned polycrystalline micronodules included in the siliciclastic rocks of the low-grade metamorphic areas.

### Concluding remarks

The composition of the chlorites in the studied samples is influenced by different factors. On one side, as a general trend, there is an important increase in the  $Al^{IV}/Al^{VI}$  ratio with the increasing metamorphic conditions. However, it is necessary to consider the influence of other factors like lithology, since within any specific range of metamorphic conditions, the chlorites from carbonate materials tend to be richer in  $Si^{4+}$  and  $Mg^{2+}$  than those included in the siliciclastic rocks.

The apparent proportion of octahedral vacancies in the chlorites is related with the presence of variable amounts of other phyllosilicates (mainly illite) interstratified within the chloritic layers, more than with actual vacancies in their structures.

### References

- Alonso-Azcárate, J.; Barrenechea, J.F.; Rodas, M.; Mas, J.R. (1995). *Clay Miner.*, **30**, 407-419.
- Barrenechea, J.F.; Rodas, M.; Mas, J.R. (1995). *Clay Miner.* **30**, 119-133.
- Caritat, P.; Hutcheon, I.; Walshe, J.L. (1993). *Clays and Clay Min.* **41**, 219-239.
- Essene, E.J.; Peacor, D.R. (1995). *Clays and Clay Min.*, **5**, 540-553.
- Jiang, W.T.; Peacor, D.R.; Buseck, P.R. (1994). *Clays and Clay Min.*, **42**, 5, 593-605.
- Shau, Y.H.; Peacor, D.R.; Essene, E.J. (1990). *Contrib. Mineral. Petrol.*, **105**, 123-142.
- Wiewióra, A.; Weiss, Z. (1990). *Clay Miner.*, **25**, 83-92.

Dpto. Ciencias de la Tierra.  
Área de Cristalografía y  
Mineralogía. Fac. Ciencias.  
Univ. de Zaragoza, España

## The composition of micas in Precambrian and Paleozoic clastic rocks from the Iberian range (Spain)

*Bauluz B, Mayayo M J, Fernández Nieto C and González López J M*

### Geological setting

The Iberian Range is a mountain chain, trending NW-SE in direction, located in the NE of Spain. It is formed of Precambrian and Paleozoic sediments which are discordantly overlain by Permian, Triassic and Tertiary sediments. Precambrian and Paleozoic materials are mainly detrital rocks; two source areas located in the SW (Centro-Iberian Zone) and in the NE (Cantabro-Ebroian Massif) (Carls, 1988) are supposed to exist. Different tectonic stages divided the basin and producing variations in thickness of the sediments: the Hercynian orogeny caused its structure, producing folds with axial-planar cleavage, and reverse faults, both following the NW-SE orientation. During the Permian the evolution of the basin fits to an aulacogen model, that was later strained in the Alpine orogeny.

### Materials and Methods

Samples (pelites and greywackes), 295 as a whole, belong to a group of profiles chosen because of their stratigraphic continuity; their age ranges from Precambrian (upper Vendian) to Permian. They are mainly formed of quartz and micas (muscovite, phengite, illite) and occasionally chlorite, kaolinite, feldspars and carbonates. Micaceous phases and clay mineral associations have been studied in detail in order to ascertain diagenetic or metamorphic reached conditions.

Micas have been characterized by XRD (whole sample and silt and clay fractions), studying their crystallochemical parameters: crystallinity (IC),  $b_0$ ,  $d_{001}$ , crystallite size (N), polytypes, as well as their expandability (S). Determination of IC values were carried out as recommended by IGCP 294 IC (Kisch, 1991), and these data together with N values were transformed to CIS data (Warr & Rice, 1994). Thereby, it was possible to use as anchizone limits those given by these authors ( $0.25-0.42^\circ 2\theta$  in relation to I.C., and 52-23 nm in relation to N for illites from the clay fraction of pelites). Textural study was carried out by petrographic microscope and SEM (back-scattered images) and the chemical composition was studied using EPMA and TEM (AEM).

### Results

An important variation in the mica features through the stratigraphic profile has been noted from the obtained results. Three groups have been defined: micas included in Precambrian

and Cambrian rocks (Pc&Cb), those forming part of Ordovician and Permian ones (O&P) and, finally, those belonging to Silurian, Devonian and Carboniferous rocks (Sl, D & Cr). IC,  $b_0$  and N values are reported in the next table; ranges and modes (in brackets) are listed.

		silt fraction			clay fraction		
		$b_0$ (Å)	IC ( $^{\circ}2\theta$ )	N (nm)	$b_0$ (Å)	IC ( $^{\circ}2\theta$ )	N (nm)
Pc&Cb	pelites	8.994-9.062 (9.014)	0.21-0.29 (0.26)	45-122 (59)	8.995-9.051 (9.030)	0.22-0.43 (0.26)	23-92 (45)
	greywackes	8.975-9.028 (8.997)	0.23-0.58 (0.39)	15-77 (41)	8.986-9.036 (9.016)	0.26-0.76 (0.39)	11-59 (18)
O&P	pelites	8.999-9.027 (9.002)	0.22-0.56 (0.28)	16-92 (41)	8.990-9.035 (9.018)	0.26-0.57 (0.32)	15-59 (38)
	greywackes	8.970-9.053 (8.978)	0.25-0.95 (0.50)	7-65 (9)	8.970-9.060 (8.999)	0.32-0.97 (0.95)	6-38 (7)
Sl,D&Cr	pelites	8.975-9.050 (8.980)	0.30-0.85 (0.46)	9-41 (18)	8.973-9.060 (8.986)	0.42-0.96 (0.85)	7-15 (14)
	greywackes						

Micas from Pc and Cb rocks exhibit the most homogeneous and lowest IC values, showing slight differences between their silt and clay fractions. They display null expandability and belong mainly to the 2M1 polytype in both fractions. Along with micas, chlorite is detected in the finer fractions, and in the Precambrian rocks there also are corrensites, together with small quantities of quartz and albite possibly neophormed.

Micaceous phases from O and P rocks display IC values different in pelites than in greywackes, both in clay and in silt fractions. 2M1 is the major polytype, but 1M increases in the clay fraction. Micas are the main phyllosilicates in the fine fractions, being sometimes the only ones, although chlorite or kaolinite have been occasionally detected.

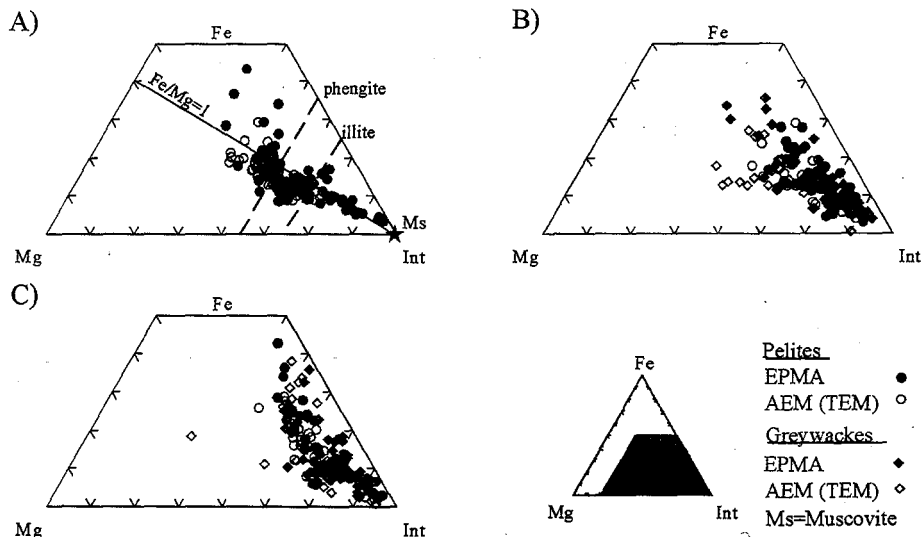
Micaceous phases from Sl, D, and Cr rocks exhibit the most important variation in IC. The illitic material, concentrated in the clay fraction, is characterized by its expandability (Ir parameters until 1.90), and is formed of mixtures of illite and ISII, with S being approximately 15%. They belong to the 2M1 and 1M polytypes, the latter increasing in the clay fraction. Along with mica the presence of kaolinite is common, being in several cases the major phyllosilicate. Both phases have been observed to form intergrowths (SEM).

According to chemical analyses, micas display different degrees of phengite substitution. Interlayer cations (mainly  $K^+$ ) range from 0.60 to 1.00 atoms (by half cell). Micas from Pc and Cb rocks show the highest interlayer charge and phengite substitution, although there are also muscovites (Fig. A); in P and O rocks they are mainly muscovites and illites (Fig. B), and in Sl, D & Cr rocks are illites with muscovites (Fig. C). In these figures the phengite substitution and the Fe/Mg ratio are shown.

## Conclusions

Mineral and chemical features indicate that post-depositional evolution ranges from upper anchizone for the first group of samples (PC & Cb) to diagenesis for the last one (Sl, D & Cr), whereas the O & P rocks show characteristics of the transition from anchizone to diagenesis. Improvement of IC, N and stabilization of 2M1 polytype through the profile reflects recrystallization and removal of expandable layers. This fact has been ascribed mainly to the effects of temperature. However, other factors such as stress, lithology and mineral chemistry have been reported to have some influence on illite features. Porosity and size grain have influenced in the IC values in diagenetic conditions (from Ordovician to Permian rocks) while in Pc rocks, which show cleavage due to the Hercynian orogeny, tectonic strain has probably affected the IC. It has been already argued (Kisch, 1987) that strain of the phyllosilicate lattice lowers the temperature of the activation threshold for the recrystallization of illite.

The presence of kaolinite in S, D and Cr rocks supports the low degree of evolution reached by these materials, since kaolinite is highly unstable with the increase of temperature, specially with the availability of K, Mg and Fe ions, since they favour its illitization in the last stages of the diagenesis. Recrystallization of P micas probably is in relation to the new tectonic situation that takes place.



Carls P (1988). *Canad. Soc. Petrol. Geol. Mem.* 14, 421-466.

Kisch H J (1987). *Low temperature metamorphism.* Blackie & Son, Glasgow, 227-300.

Kisch H J (1991). *J. Met. Geol.* 8, 31-46.

Warr L W & Rice A H N (1994). *J. Met. Geol.* 12, 141-152.

(1) Instituto Andaluz de Ciencias de la Tierra, CSIC-Universidad, Granada, España

(2) Dep. Géologie, Fac. Sciences-Semlalia, Université Cadi Ayyad, Marrakech, Maroc

(3) Dep. Géologie, Fac. Sciences et Techniques, Université Cadi Ayyad, Marrakech, Maroc

## The presence, genesis and significance of palygorskite in some Moroccan Tertiary sequences

Ben Aboud A (1), López Galindo A (1), Fenoll Hach-Alí P (1), Chellai E H (2) and Daoudi L (3)

In Spain, clays with palygorskite and/or sepiolite have accumulated mainly in continental or perimarine Tertiary basins, where sedimentation occurs in a lacustrine environment under certain very restricted conditions, in the presence of silica and magnesium, with an arid to semi-arid climate and an alkaline pH (Galán and Castillo, 1984). This paper describes a preliminary study of the mineralogy of both the total sample and the clay fraction of some Moroccan Tertiary sequences. These have been accumulated in basins with similar paleo-environmental conditions to those described for Spain. The aim of the study was to verify the presence of fibrous clays in these sequences and to suggest their origin.

### Location and lithology

Samples were obtained from four outcrops (their geographic location is illustrated in Fig. 1). The first of these corresponds to the Erguita basin, to the NE of Taroudannt. This sequence, with fluvio-lacustrine sediments of Upper Eocene-Oligocene age, is located in the Ida Ou Gaïlal valley. The stratigraphic column, with a thickness of 110 metres, is made up of alternating siltstones, sandstones and conglomerates with diffused salt. At the top white marls and marly limestones were found. The sequence ended with a level of limestone.

The second outcrop is located in the basin at the southern edge of the Upper Atlas (Tiniguert synclinal). This sequence is located to the NE of Ouarzazate, and includes Mio-Pliocene materials that have accumulated in a sebkha continental-lacustrine type environment. It has a thickness of 167 metres, and begins with levels of laminar gypsum and siltstones, which are followed by alternating levels of limestones, marls and siltstones.

Within the latter, the gypsum reappears in fibrous and nodular forms.

Samples were obtained from a third outcrop, in the Ouarzazate basin and to the NW

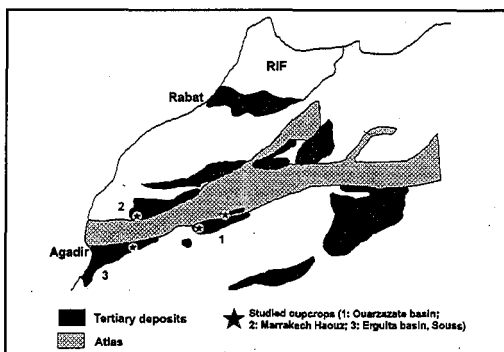


Figure 1. Location of studied outcrops

of the town. Here, the materials are similar in age and environment of deposition to the above-described case. These materials correspond to a repetition of red, greenish-yellow, greenish and grey-green clayey levels, with a thickness of some 50 metres. Gypsum is ubiquitous but is only so in diffused form through the clays.

The final outcrop forms part of the northern flank of the Western Upper Atlas. The materials (with a thickness of up to 100 metres) are of Paleogene age and have been deposited in a restricted, basically lagunar, area. The sequence begins with levels of phosphates, sandstones with silex nodules and a small alternation of sandstones and marls with silex, followed by a thick group of marls and sandstones with conglomerates and a limestone set. After this, there is a second red group of sandstones and red clays, in which two levels of sandstones with micro-conglomerates are intercalated.

### **Methodology**

The mineralogical study of the samples was carried out by DRX in a Philips PW1710 equipment. The clay fraction was studied in oriented aggregates treated with EG, DMS and thermic heating to 550°C. The quantitative analysis was carried out by computer, using diffractometric and chemical data (López-Galindo *et al.*, 1996a).

The chemical analyses of the principal elements were carried out by FRX using a Philips PW 1404 equipment. The trace elements and rare earths were determined by ICP-MS with a Perkin-Elmer SCIEX Elan-5000 apparatus. The morphology and the microcomposition of the clay particles were studied, respectively, with SEM (Zeiss DSM 950) and TEM (Philips CM20) equipment.

### **Results and discussion**

**Mineralogy** .- The samples contained mainly phyllosilicates, carbonates and quartz. The former were present in greatly varying quantities, with concentrations of between 10% and 80%. The phases detected in the clay fraction were palygorskite, illite, interstratified illite-smectite, smectite (both Al and Mg), kaolinite and chlorite. Palygorskite was constantly present in the clay fraction, in quantities varying from 10% to 70%. The greatest concentrations appeared in the Ouarzazate basin, where it represented up to 50% of the total sample.

**Geochemistry** .- The results obtained from correlating the mineralogical and geochemical variables make it evident that the clearly detrital phyllosilicates (illite, interstratified I/S, kaolinite, chlorite and Al-smectite) accumulate most of the trace elements. The content of rare earths and elements from the first transition series observed in palygorskite falls between the low values measured in neofomed phyllosilicates (sepiolite and stevensite) in Spanish deposits and the high values found for the detrital phyllosilicates (*cf.* Torres-Ruiz *et al.*, 1994). The content here is of the same order as that present in other Spanish deposits of palygorskite (López-Galindo *et al.*, 1996b). These geochemical data, together with the micro-composition of the individual particles of palygorskite and the morphology observed by SEM, seem to indicate that this mineral may have been formed by the structural transformation of a detrital aluminium-silicate precursor, of illite and/or Al-smectite

type.

In conclusion, the paleogeographic conditions of the basins where the studied materials accumulated indicate that these were deposited in lacustrine environments during periods of arid to semi-arid climate that, on occasion, became evaporitic (bearing in mind the presence of gypsum and/or halite), where there existed a high concentration of Si and Mg. The detrital phyllosilicates then underwent a process of post-sedimentary alteration that led to the formation of palygorskite.

*This research was financed by project AMB93-0794 (CICYT) and by Group 4065 of the Junta de Andalucía.*

### References

- Galán E and Castillo A (1984). Sepiolite-palygorskite in Spanish Tertiary basins: genetical patterns in continental environments. In A Singer and E Galán (Eds): *Palygorskite-sepiolite. Occurrences, genesis and uses*. Development in Sedimentology 37, Elsevier, 87-124.
- López-Galindo A, Torres-Ruiz J and González-López JM (1996a). Mineral quantification in sepiolite-palygorskite deposits using X-ray diffraction and chemical data. *Clay Minerals*, 31, 217-224.
- López-Galindo A, Ben Aboud A, Fenoll-Hach Alí P and Casas J (1996b). Mineralogical and geochemical characterization of palygorskite from Gabasa (NE Spain). Evidence of a detrital precursor. *Clay Minerals*, 31, 33-44.
- Torres-Ruiz J, López-Galindo A, González-López JM and Delgado A (1994). Geochemistry of Spanish sepiolite-palygorskite deposits: genetic considerations based on trace elements and isotopes. *Chem. Geol.*, 112, 221-245.

Dpto. Geociências, Univ.  
de Aveiro, Portugal

## Deuterium activity in the kaolin deposit of Sao Vicente de Pereira (Portugal): a discussion based on reaction rates among minerals and $H^+$ metasomatism

*Bobos I and Gomes C*

---

### 1. Introduction

Advanced argilic alteration from São Vicente de Pereira is located in a metasedimentary complex (migmatites, gneisses) - Medium Proterozoic - belonging to the Ossa Morena zone. The most important mineralogical features of the hydrothermal alteration are characterized by the development of kaolinite  $\pm$  halloysite - 7Å and kaolinite + illite assemblages on an intense foliation (constituting a pathway for the migration of fluids) in migmatite rocks and/or gneiss veins with pegmatite facies. Metasediments advanced argillized are crosscutted by tourmaline+quartz veins or only quartz veins. Veins of pure halloysite - 7Å can be found with a attitude perpendicular to the relict foliation of migmatite rocks. Quartz-muscovite assemblages (enriched in fluor) and mica-bearing fluor showing incipient or advanced stages of kaolinization accompanied the tourmaline veins. Hydrothermal activity is connected with progressive increase of  $H^+$  metasomatism and with additional input of meteoric waters. Hydrothermal area (possibly a hydrothermal system) is spatially associated with ductile shear zones, the most important pathway for the hydrothermal fluids.

### 2. Methodology

Two minerals: K-feldspar and muscovite (mica-bearing fluor provided or greisen alteration) deserved particular attention and study. Thermodynamical activity has been expressed by the ratio of the  $H^+$  metasomatism activity and  $SiO_2$  (aqueous solution) activity.

### 3. Discussion

This study involve thermodynamical aspects about the discussion of silicates and the incongruent reaction of silicates hydrolysis expressed by the mineral assemblages identified

in the kaolin deposit. Initial stage of feldspar dissolution consists of exchange of  $H^+$  for  $K^+$  and  $Na^+$  on the feldspar surface. Decomposition of the silicate minerals is a rate-limiting step activating complex during hydrolyses of feldspar in aqueous solutions (neutral or alkaline pH) with additional of  $H_2O$  dipoles (according to Helgenson et al., 1984). It is a prediction of mass transfer among minerals and aqueous solutions. Three types of reaction involved equilibrium among K-feldspar and  $H^+$  metasomatism with successively higher pH values, namely:

- (1)  $KAlSi_3O_8 + 4H^+ \rightleftharpoons 3SiO_2 + K^+ + Al^{3+} + 2H_2O$
- (2)  $KAlSi_3O_8 + H^+ + H_2O \rightleftharpoons 3SiO_2 + K^+ + Al(OH)_3^0$
- (3)  $2KAlSi_3O_8 + 3H_2O \rightleftharpoons Al_2Si_2O_5(OH)_4 + 4SiO_2 + 2K(OH)$

Two types of chemical reaction can be written down for the alteration of muscovite to kaolinite:

- (4)  $2K_2Al_4(Si_6Al_2)O_{20}(OH)_4 + 6H_2O + 4H^+ \rightleftharpoons 3Al_4Si_4O_{10}(OH)_8 + 4K^+$
- (5)  $3K_2Al_4(Si_6Al_2)O_{20}(OH)_4 + 20H^+ \rightleftharpoons 4Al_4Si_4O_{10}(OH)_4 + 2Si^{+4} + 2Al^{3+} + 6K^+$

Calculation of the activities of thermodynamic components (respectively K-feldspar and kaolinite sites and aqueous solutions) was carried out using equation (a).

$$(a) \quad a_i = K_i \prod_s \prod_j X_{j,s}^{v_j \cdot i}$$

An additional prediction put forward in this paper take into account the amounts of  $Al^{total}$  content in low temperature silicates (quartz form veins) and the ability to incorporate  $Al^{total}$  in quartz and halloysite-7Å. A possible dissolution of quartz from veins and precipitation of Al bearing waters have been also taken account. Our results have been plotted in the activity diagrams of  $\log(K^+/H^+)$  versus  $\log Si$  (for differen pH and temperatures) and in phase diagram applicable to the weathering of granite. They are compared with experimental data and with natural phyllosilicates formed in different weathering, hydrothermal and sedimentary occurrences,

#### 4. Concluding remarks

All silicates discussed in this paper are interpreted by the mass action law for aqueous solutions which tend to precipitate and then to crystallize. Three possibilities have been taken into account according to a real geologic system and the thermodynamical calculations of phase relationships have contributed to our understanding of the mineral solubilities and differentiation manifested in the nature by minerals assemblages observed in hydrothermal and weathering altered rocks. Two distinctly fields are separated of kaolinite found in São Vicente de Pereira kaolin deposit: one field which attested a hydrothermal genesis for kaolinite from feldspar and mica as precursor mineral and the second field which attested the weathering conditions of halloysite - 7Å derived from kaolinite formed most probably as the result of an enrichment in Al<sup>IV</sup> in meteoric waters.

#### 5. Reference

Helgeson HP., Murphy WM & Aagard P (1984): *Geochimica et Cosmoch. Acta*, **48**, 12: 2405-2432.

Dpto. Geociencias, Univ. de Aveiro, Portugal

## Greisenisation indices in the kaolin deposit of Sao Vicente de Pereira (Portugal)

*Bobos I, Gomes C, Velho J and Miranda A*

The São Vicente de Pereira region situated in the northwestern border of Ossa Morena zone is spatially associated with a ductile shear zone. Geological background comprise a metasedimentary complex with a migmatites, gneisses and tonalite gneisses assigned to Medium Proterozoic in the upper part belongs to the Ossa Morena zone and granitic gneissic rocks (presyn. deformation  $S_3$ ) in the lower part belongs to the Central Iberic zone. There is a structural control of post-magmatic events following preferently either regional alignements with attitude dominantly N40-50°W or regional faults with attitude dominantly N40-60°E. Two stages of hydrothermal activity did occur in the area producing firstly a sequence of greisenisation events including a exogreisen system and later by a post-greisenisation alteration. The late hydrothermal event is related with an easy and abundant circulation of pneumatolitic - hydrothermal fluids enriched in Si, B, F, Cl and, as results of that, silicification, tourmalinisation and fluoritization took place. Hydrothermal activity is connected with the progressive increase of  $H^+$  metasomatism. Also, a meteoric convective system played a substantial role together with an additional input of meteoric waters. A large amount of  $H^+$  ions are consumed producing mineral assemblages which include clay minerals of kaolinite and illite groups. Supergene alteration is superimposed on the late hydrothermal event.

Two types of greisen alteration have been identified in the kaolin deposit of São Vicente de Pereira, A light-green greisen composed of mica bearing fluor with and incipient stage of kaolinisation and quartz-tourmaline rich greisen. Around the quartz-tourmaline veins advanced argillic is present containing well crystallized kaolinite. Two generations of tourmaline having different morphology have been identified: acicular crystals and poligonal or globular crystals.

(1) Dpto. Geología. Area de  
Cristalografía y Mineralogía.  
Fac. Ciencias. Univ. de  
Salamanca, España

(2) Instituto de Recursos  
Naturales y Agrobiología.  
CSIC. Salamanca, España

(3) Ingeniería 75, S.A.  
Madrid, España

## Mineralogical study of the Silurian black shales of the Ossa Morena zone and of the Iberian massif

*Bombín Espino M (1, 3), Suárez Barrios M (1), Saavedra Alonso J  
(2) and Martín Pozas J M (1)*

### Introduction

The Lower Paleozoic black shales, resulting from transgressive events that occurred during the Ordovician and Silurian, occupy large areas not only on the Iberian Peninsula (Verneuil y Barrande, 1855) but also in the rest of Europe (Jaeger, 1964 in Turingia; Helmke, 1973 in SW Sardinia; Jaeger & Schöulaub, 1980 in the Carnic Alps) and N. Africa (Jaeger y Massa, 1965). During these transgressive events, a pronounced stratification of the masses of oceanic waters occurred, causing the development of euxinic environments in shelf areas and a strong organic production related to upwelling phenomena.

Precise dating of the rocks has been carried out to the abundance of graptolites which permit complete sampling of the Silurian series in terms of biozonas.

In the present work, we study rocks located in the Ossa Morena Zone (OMZ) and in the Iberian Massif (IM) related prospecting for metalliferous black shales. The mineralogical identification technique employed (XRD) being found to be the most suitable for these rocks in which the existence of an important amount of carbonaceous material and the small size of the minerals hinder their recognition by optic microscopy.

### Methodology

Samples were selected with the collaboration of paleontologists in order to ensure the age of each. Since all the samples analyzed contain fossils that allow precise classification, it is known that the minerals forming these rocks are, initially, neither diagenetic or metamorphic transformations from other previous rocks.

Sampling in the IM was carried out at different points of the Castellano Branch or Hesperian Chains. All samples correspond to graptolitic black shales from the Bádernas Formation (Checa Slates) or to small intercalations of shales in the Los Puertos Quartzites (Valentian Quartzite).

In the OZM, the areas of Moura and Barrancos were sampled in the Portuguese sector and the nuclei of the Valle and Cerrón del Hornillo synclines in the Spanish sector. Samples SV-1D and CH-0B correspond to Valle Slates of Ordovician age and the rest to the Lower Slates with Graptolites.

The mineralogical study was conducted by X-ray diffraction of powdered samples using the whole rock and the  $<2\mu\text{m}$  fraction obtained by decantation after organic matter elimination by attack with  $\text{H}_2\text{O}_2$ . The  $<2\mu\text{m}$  is studied as oriented film under ambient conditions, after solvation with ethylene glycol and after heating to  $550^\circ\text{C}$ . A Siemens model D-500 XRD apparatus with a Cu anticathode and graphite monochromator was employed. The different mineral phases were quantified by "Reflecting Power Method" (Martín Pozas, 1975). Each sample was step-scanned at  $1^\circ 2\theta/\text{min}$ ; crystallinity index (Kubler Index) and  $b_0$  measurements, by (060) reflection, of illite were performed.

Chemical analysis were performed by neutron activation analysis at the ACTLABS laboratories of Canada.

## Results

The mineralogical composition of the rocks studied (Tables I and II) reveals certain differences between both zones, although all the samples are mainly composed of quartz and illite. In the samples from OMZ, these minerals may appear with plagioclase and/or chlorite. Quartz is more abundant than in the IM.

Quartz and illite may appear in the samples from the IM, associated with potassium feldspar, plagioclase, chlorite, pyrite, pyrophyllite and a regular interstratified of rectorite-like illite-smectite. The mineralogy of these samples, as may be seen in Table II, is more complex than that of the OMZ, the presence of rectorite and pyrophyllite being important in samples OR-4, Checa(3-2) and CHE-4. In Spain, pyrophyllite has been described in Devonian rocks and soils derived from them as an inherited mineral (Pérez Rodríguez et al., 1990).

Sample	Q	FK	P	I	Cl.	C.I.	b <sub>0</sub>	I'
FXN-1	50	-	1	38	11	0,339	8,9952	46
FXN-2	60	-	1	36	3	0,386	9,0246	37
FXN-2'	89	-	-	11	-	0,371	9,0228	13
FN-O	79	-	1	20	-	0,334	8,9988	25
CH-1E'	80	-	-	20	-	0,434	9,0066	25
CN-1	85	-	1	14	-	0,277	9,0126	17
CH-0B	14	-	1	81	4	0,718	8,9970	79
SV-1D	32	-	6	52	10	0,430	8,9970	63

Table I: Mineralogical composition and parameters of the samples from the OMZ. Q: quartz, P: plagioclase, KF: potassium feldspar, I: illite, Cl: chlorite, C.I.: crystallinity of illite, b<sub>0</sub>: illite cell parameter and I': percentage of illite found from %K<sub>2</sub>O in chemical analysis.

Sample	Q	FK	P	I	Cl.	Others	C.I.	b <sub>0</sub>	I'
TR-1/0	43	-	1	47	9	-	0,382	8,9946	55
OR-2	15	1	1	83	-	-	0,320	8,9982	99
Checa 3	21	-	1	78	-	-	0,418	8,9958	81
CHE-1G	17	t	1	82	-	-	0,477	8,9994	85
CHE-1H	13	-	1	83	3	Py	0,594	8,9982	82
CHE-1I	12	-	1	87	-	-	0,452	8,9976	84
CHE-1I'	16	-	1	80	3	Py	0,589	9,0042	81
CHE-1J	19	2	-	79	-	Py	0,599	9,0000	84
CHE-1K	16	-	-	84	-	Py	0,440	8,9988	84
CHE-1L	17	-	-	83	-	-	0,536	9,0030	63
OR-4	5	2	-	?	-	Pph, It	-	8,9910	49
CHE(3-2)	7	1	-	?	-	Py, Pph., It	-	8,9946	72
CHE-4	3	-	-	?	-	Py, Pph., It	-	8,9718	40

Table II: Mineralogical composition and parameters of the samples from the IM. Q: quartz, P: plagioclase, KF: potassium feldspar, I: illite, Cl: chlorite, Py: pyrite, Pph: pyrophyllite, It: interstratified, t: traces, C.I.: crystallinity of illite, b<sub>0</sub>: illite cell parameter and I': percentage of illite found from %K<sub>2</sub>O in chemical analysis.

Then data obtained from chemical analysis of major elements confirm the mineralogical data deduced from X-ray diffraction. Aluminium is directly related to the illite content, in agreement with the dioctahedral nature of this deduced from the reflection value (060) of this mineral. The highest percentages of Fe oxides are found in the samples having chlorite.

A semiquantitative analysis of the illite content was carried out based on the data from chemical analysis since the K<sub>2</sub>O analyzed is only found in this mineral (and in the small

proportion of feldspars found in some samples studied). Since illite has a mean percentage of  $K_2O$  of 7%, the percentage of this mineral in the rocks studied was calculated, with the finding of a very good correlation with the data obtained from the XRD study (Tables I and II). The occurrence of pyrite (< to 4%) identified in XRD by its reflection at 1.63Å, is confirmed by the data on S contents.

The  $b_0$  parameter of illite is in all cases between 8,9917 and 9,0228, which according to Guidotti (1984) would be indicative of lower conditions of metamorphism, no facies beyond that of green schists being reached.

According to Kisch (1990), the limits between diagenesis-anchizone and anchizone-epizone are situated between illite crystallinity index values of 0,4 and 0,25°2 $\theta$ , respectively. In the samples studied, this crystallinity index ranges between 0,27 and 0,71, allowed them to be situated in the fields of diagenesis and of anchizone.

It may therefore be suggested that both the mineralogical data and the calculated illite crystallinity parameters are coherent with other observed geological characteristics, in all cases pointing to a cold oceanic sedimentary environment (Rateev, 1969) and very low or no metamorphism.

## References

- Guidotti, C.V. (1984). Micas in Metamorphic Rocks. In: Bailey, S.W. (ed.) *Reviews in Mineralogy*, 13, Mineral Society of America: 357-467.
- Helmke, D. (1973). Zur Stratigraphie des Silur und Unterdevon der lagerstätten provinz Sarrabus-Gerrei. *Neues Jb. Geol Paläont. Mh.* 19: 529-544.
- Jaeger, H. (1964). Der gegenwärtige Stand der stratigraphischen Erforschung des Thüringer Silurs. In: Beiträge zur regionalen Geologie Thüringens. *Abhandlungen Deutsche Akademie Wissenschaften (Kl. Bergbau, Hüttenwesen, Montangeologie)*, 2: 27-51.
- Jaeger, H. & Massa, D. (1965). Données stratigraphiques sur le Silurien des confins Algéro - Marocains du Sud. *Bull. Soc. Géol. Fr.* (7), VII: 426-436.
- Jaeger, H. & Schönlaub, H.P. (1980). Silur und Devon nördlich der Gundersheimer Alm in den Karnischen Alpen (Österreich). *Carinthia II*, 170/90: 403-444.
- Kisch, H.J. (1990). Calibration of the anchizone: a critical comparison of illite "crystallinity" scales used for definition. *J. metamorphic Geol.* 8: 31-46.
- Martín Pozas, J.M. (1975). Análisis cuantitativo de fases cristalinas por DRX. En: Difracción de muestras policristalinas. Método de Debye-Scherrer. Instituto de Ciencias de la Educación de la Universidad de Valladolid.
- Pérez Rodríguez, J.L., Maqueda, C. & Justo, A. (1990). Mineralogy of soils containing pyrophyllite from Southern Spain: isolation and identification of the mineral. *Soil Science* 150 (4): 671-679.
- Rateev, M.A., Gorbunova, Z.N., Lisitzyn, A.P. & Nosov, G.L. (1969). The distribution of clay minerals in the oceans. *Sedimentology* 13: 21-43.
- Verneuil, E. & Barrande, J. (1855). Description des fossiles trouvés dans les terrains Silurien et Devonien d'Almaden, d'une partie de la Sierra Morena et des montagnes de Tolède. *Bull. Soc. Géol. Fr.* (2<sup>e</sup> ser.) 12: 964-1025.

(1) CEPUNL. Fac. Cien. Tecnologia. Univ. Nova de Lisboa, Portugal

(2) Dpto. Geociencias. Univ. de Aveiro, Portugal

## Clay mineralogy and trace element content of Upper Jurassic sediments from the Corvina 1 well (Algarve platform, south Portugal)

Caetano P S (1), Rocha F J (2) and Gomes C (2)

### INTRODUCTION

The Algarve Basin (South Portugal) corresponds to an E-W sedimentary basin, 150 Km long and 13 to 30 Km wide on land; offshore, the basin extends throughout the continental platform (Fig. 1). Hydrocarbon exploration on the Portuguese southern continental platform led to the drilling of five offshore wells during the mid 70's and early 80's (Ruivo-1, Imperador-1, Corvina-1, Algarve-1 and Algarve-2). Corvina 1 well was drilled on the continental platform, 10 Km off the coast to the SE of Faro, and reached a maximum depth of 3083 m.

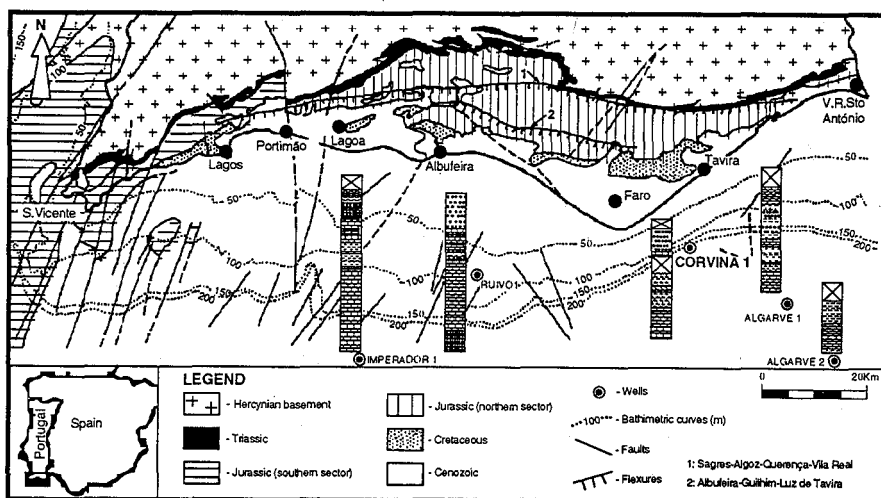


Fig. 1 - Geographical location and geological setting of Corvina 1 well

During the Upper Jurassic two main environments can be recognized based on land outcrop and offshore data: the Southern Sector in the western part of Algarve (includes an area West of Lagoa and the area on the continental platform where the aforementioned wells were drilled) and the Northern Sector in the eastern part (area between Lagoa and Tavira)

(MARQUES & OLÓRIZ, 1989a). Upper Jurassic outcrops in the Southern Sector are represented by sediments characteristic of a carbonate platform system with some important clastic influxes. The Northern Sector is limited to the North by Paleozoic basement rocks and to the South and West by the raised blocks of the Southern Sector. Block structuration of this sector during the Upper Jurassic led to a marly-carbonate sedimentation in deep areas and to reefal and parareefal buildups on bottom highs. Studies carried out on these Upper Jurassic materials have allowed to distinguish two megasequences in relation to which twelve discontinuities were individualized, some caused by interactions between tectonics and eustasy (MARQUES & OLÓRIZ, 1989b, MARQUES *et al.*, 1991). This stratigraphic framework has also been correlated to the eustatic curve of HAQ *et al.* (1987,1988), slightly modified by MARQUES *et al.* (1991).

## MATERIALS AND METHODS

Samples of the Corvina 1 well were gathered as cuttings at every 5 m interval. The most recent available data, based on faunal content (well logs and reports deposited at the Gabinete para a Pesquisa e Exploração de Petróleo, Lisboa), attributes the interval between depths 1838m and 2300m (462m) to the Upper Jurassic. The interval between 1800m and 2350m (550m), embracing the whole Upper Jurassic, was studied (a total of 103 samples were collected within the studied interval). This interval is represented by a succession of carbonates (limestones/dolomites and marls), claystones and, towards the top, some sandstone levels.

The mineralogical studies of the insoluble residues, particularly of their clay components, has been based mainly on X-ray diffraction (XRD) determinations, carried out on non-orientated and orientated specimens. Qualitative and semi-quantitative determination of clay and non-clay minerals has been done in both fractions. For semi-quantitative determinations of clay and non-clay minerals, criteria recommended by SCHULTZ (1964) and THOREZ (1976) has been followed.

The Mn and Sr content of the carbonate fraction was measured in each sample. All samples were washed to eliminate contamination by seawater and crushed to 200 mesh. After this pretreatment, samples were dissolved in 1 N acetic acid. Trace element analyses were carried out by atomic absorption spectrophotometry on a Perkin-Elmer 2380 equipment following the method described by RENARD & BLANC (1971, 1972). To compensate for possible contamination resulting from flushing of the insoluble residue, the results are normalized to a 100% CaCO<sub>3</sub> sediment using the equation of RENARD (1986), as for Mn:

$$\text{Mn}_{100} = [\text{Mn (ppm)} \times \text{CaCO}_3 (\%)] / 100$$

## RESULTS AND DISCUSSION

The mineralogical data allowed the definition of a vertical zoning, which in general terms is very consistent with the previously established stratigraphy. An evolution of clay minerals can be assumed from an illite-kaolinite association at the base of the studied Upper Jurassic section of the borehole (corresponding to the Oxfordian) to, firstly, an illite-smectite-kaolinite association found in the samples corresponding to the Kimeridgian, secondly, to a more smectite association (illite-smectite) related with the Early Tithonian and, finally, at the top (Late Tithonian) to an illite-kaolinite association, closely similar with the first one.

The obtained results for trace element content variations through the studied interval have allowed to distinguish Mn and Sr geochemical zones that reflect the evolution of high/low or increasing/decreasing content trends. Uphole trends in Mn content show an overall increase in values, from about 50-100 ppm to a maximum recorded value of 516 ppm at depth 1995 m. followed by an overall decrease until the top, with minimum recorded values of about 50 ppm. In addition to these general trends, short-term fluctuations distinguish ten Mn geochemical zones (CO<sub>3</sub>Mn 1 to CO<sub>3</sub>Mn 10).

Sr content shows a highly variable evolution with sharp short-term oscillations with amplitudes of 100 ppm or more. However, it is possible to establish a long-term variation curve with: an uphole increase from values about 100 ppm to values about 200 ppm (at depths around 2200 m); followed by a decrease in values to about 50 ppm or less (at depths around 1950 m); a new increase in values to about 150 ppm (at a depth around 1900 m); and finally a decrease in values to less than 10 ppm. The short-term fluctuations distinguish eleven Sr geochemical zones (CO<sub>3</sub>Sr 1 to CO<sub>3</sub>Sr 11) with zones CO Sr 3 and 9 representing the highest recorded values (207 and 249 ppm, respectively).

## REFERENCES

- Haq, B. U., Hardenbol, J. & Vail, P. R. (1987). *Science*, **235**, 1156-1166.
- Haq, B. U., Hardenbol, J. & Vail, P. R. (1988). *SEPM Spec. Pub.*, **42**, 71-108.
- Marques, B. & Olóriz, F. (1989a). *Cuad. Geol. Ibérica*, **13**, 251-263.
- Marques, B. & Olóriz, F. (1989b). *Cuad. Geol. Ibérica*, **13**, 237-249.
- Marques, B., Olóriz, F. & Rodriguez-Tovar, F. J. (1991). *Bull. Soc. Geol. France*, **162/6**, 1109-1124.
- Renard, M. & Blanc, P. (1971). *C. R. Acad. Sc. Paris*, **272**, 2285-2288.
- Renard, M. & Blanc, P. (1972). *C. R. Acad. Sc. Paris*, **274**, 632-635.
- Renard, M. (1986). *Mar. Micropaleontol.*, **10**, 117-164.
- Schultz, L. G. (1964). *U.S. Geol. Surv. Prof. Paper*, **391-C**, 1-31
- Thorez, J. (1976). Ed. G. Lelotte, Belgique.

(1) Dpto. Química Agrícola,  
Geología y Geoquímica. Fac.  
Química. Univ. Autónoma.  
Madrid, España

(2) Dpto. Cristalografía y  
Mineralogía. Fac. Ciencias. Univ.  
Complutense de Madrid, España

(3) Instituto de Geología  
Económica. CSIC. Madrid,  
España

(4) Instituto de Conservación y  
Restauración de Bienes  
Culturales. Madrid, España

(5) Dpto. Cristalografía y  
Mineralogía. Fac. Química. Univ.  
de Cádiz, España

## Chemical and mineralogical variability of glaucouy facies from superficial sediments on the northern sector of the Alborán continental margin

*Domínguez Díaz M C (1), García Romero E (2), La Iglesia A (3),  
Navarro Gascón J V (4), Santos A (5) and Viedma Molero C (2)*

Much progress has been made on the last few years towards the understanding of genetic and environmental processes associated with the formation of green grains (verdine and glaucouy) from marine sediments (Odin et al. 1986; Amorosi, 1995 and Rao et al. 1995). This work presents the first mineralogical study of the glaucouy facies from the northern sector of the Alborán continental margin.

The Alborán Sea is a Neogene basin with a narrow shelf with strong slope and shelf-break at 110 m depth. This zone is characterized by the interaction of the cold highly turbulent incoming atlantic superficial watermass with the warm and saline mediterranean watermass. The lowest holocene sediments were deposited during a transgressive episode that took place about 13,000 and 6,500 years ago, a time-span during which the sea-level reached the high eustatic level. The sediments deposited during this period form a layer of transgressive sands on the shelf. In the past 6,000 years a sedimentary progradation of the mud has taken place, covering the previously deposited sands on the outer shelf during the stabilization of the eustatic trend (Hernandez Molina et al. 1994).

The studied samples were taken with a dredger (shypek drag) and were collected on the continental self and slope off the coast of Benalmadena (Málaga), during a oceanic survey between Málaga and Gibraltar (1973). The samples were taken from the the ship Jafuda Cresqués and the cruise organized by the Instituto Español de Oceanografía. The dredge profiles were traced following a trend perpendicular to the shore.

The study of the sediments was performed on various types of grains. The techniques used to perform the study were: X-ray diffraction (Random Power and Oriented Agregates), Electron Microprobe and Scanning Electron Microscopy.

By means of a binocular magnifying glass three types of morphologies have been distinguished:

- 1.- Dark-green almost black spheroidal and ovoidal grains with a fairly smooth and frequently cracked surface.
- 2.- Olive-green lobulated grains.
- 3.- Bioclasts partially filled with olive-green material.

The samples taken at greater depths (~ 225 m) show very high percentages of type 1 grains. In the finer sizes these grains are associated with the type 2, and a reduction of the total grain percentage is observed.

At lesser depths the total grain percentage decreases and the olive-grain percentage increases which can also be observed when reducing the studied fraction size.

The samples taken at depths less than 100 m mainly consist of bioclasts partially filled with olive-green material, showing a very small quantity of grains, with an increased percentage of type 2. The shallower sediments hardly show any grains.

Type 1 grains (studied in thin sections by optical microscopy) show homogeneous green colour. Their structural formula corresponds to glauconites with a tetrahedral charge comprised between 0.23-0.25, low amounts of Al and tetrahedral  $Fe^{3+}$ , a charge layer between 0.7-0.9, and K as main interlayer cation. A representative formula of these would be:  $(Si_{3.77}Al_{0.12}Fe^{3+}_{0.1})(Fe^{3+}_{1.46}Mg_{0.5})Ca_{0.01}K_{0.81}O_{10}(OH)_2$ . The diffractograms correspond to 1M glauconites.

The SEM morphological study shows that the grains consist of well formed laminar particles with a very homogeneous distribution stepped face to face, and a very low porosity. Brownish yellow cracks can be observed under Optical Microscope in some of the grains. Microprobe analyses of these zones show a charge layer between 0.5-0.6, a reduction of K and Si, an increase of tetrahedral Al, and octahedral Fe.

Type 2 grains show shades of green-yellow under the optical microscope. Their structural formula is  $(Si_{3.65}Al_{0.35})(Fe^{3+}_{1.85}Mg_{0.39})Ca_{0.05}K_{0.48}O_{10}(OH)_2$ . The tetrahedral charge is somewhat higher than that of the dark-green grains (it may reach values of up to 0.35), Fe only rarely occupies tetrahedral positions. The charge layer between 0.5-0.8, K is still the main interlayer cation although its percentage is smaller as expected. X-ray diffractograms correspond to disordered mixed-layered ( $R=0$ ) 1/Sm or Glauconite/Sm.

The SEM study of the internal morphology reveals a tactoid structure (Benett, et. al 1986). The contacts between the laminar particles are always edge to edge with a very high porosity. Some zones have laminar particles forming glomerules, yet without losing edge to edge contacts.

The bioclasts can be partially filled with a cryptocrystalline material showing brown shades, and less frequently dark shades. In most cases it has not been possible to calculate the unit cell formula from the Electron Microprobe Analyses. When it was possible, the formula correspond to a mineral with contents of K lower than 0.5, a

tetrahedral charge between 0.4-0.5, an octahedral charge between 0.1-0.25 and a charge layer between 0.5-0.7, with gradation in K contents.

Consequently, it appears there is a clear evolution of the genetic process of glauconite grains in the Alboran Sea. There is an evolution from a material poorly crystalline, which is agglomerated in the interior of the bioclasts, towards a micaceous material with mixed-layer as intermediate materials. This evolution is accompanied by the incorporation of Fe and K into the structure of these materials.

## REFERENCES

AMOROSI, A. (1995). *J. of Sedimentary Research*, **4**, 419-425.

BENETT, R.H, and HULBERT, M. H. (1986). *Clay Microstructure*. D. Reidel Publishing Gompany.

HERNANDEZ MOLINA, F. J.; SOMOZA, L.; REY, J. and POMAR, L. (1984). *Marine Geology*, **120**. 129-1734.

ODIN, G. S. and FULLAGAR, P. D. (1988). In *Developments in Sedimentology*. Ed. Odin G. S. 295-332.

RAO, V. P.; THAMBAN, m, AND LAMBOY, M. (1995). *Marine Geology*, **127**. 105-113.

## Geophysical survey of a kaolin deposit (Alvaraes, Portugal)

Ferraz E, Matias M, Rocha F and Gomes C

### INTRODUCTION

The present work deals with the application of geophysical methods to the study of a dual kaolin deposit, sedimentary and residual, in terms of stratigraphy and bedrock topography, and the comparison of the data obtained with information achieved from drilling.

The determination of the composition and volume of the materials, the depth of the bedrock and the thickness of different layers, is an important contribution for the appraisal of the potentialities of the deposit, that are unknown so far.

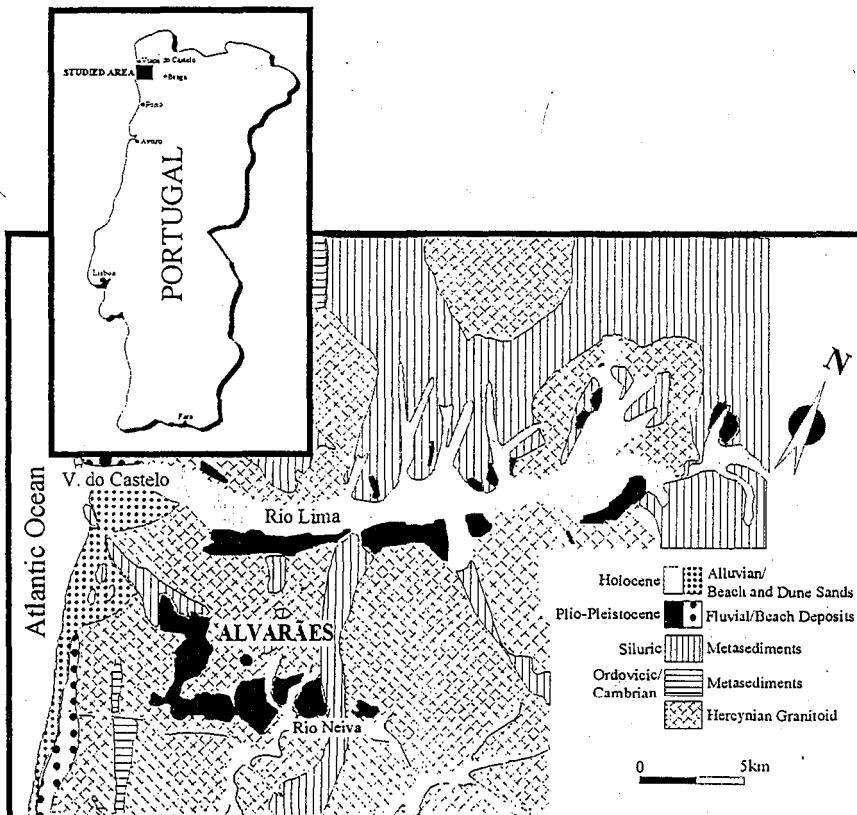


Fig. 1 - Location and geological setting

The working area ("Couto Mineiro de Alvarães") is located near the village of Alvarães, NW Portugal, 65 km north of Porto and 14 km south of Viana do Castelo, and is limited to the north by the Lima River, to the east by the "Serra da Padela" hills and to the south by the Neiva River (Fig. 1).

#### GEOLOGICAL SETTING

The "Couto Mineiro de Alvarães" is geologically located in the Alvarães basin, in the Central Iberian Zone of the Hesperian Massif, west of the Vigo-Régua shear zone (Pereira *et al.*, 1992). Geomorphologically, the area is very steep with high mountains separated by deep valleys.

The Alvarães basin is filled by Tertiary/Quaternary sedimentary deposits covering an area of about 20 km<sup>2</sup> and with thicknesses varying from 30 to 70 m. The sedimentary deposits, located nearby the residual deposits, are mainly composed by two units (Barbosa, 1974):

1. an upper unit, "white kaoliniferous sand", composed by intercalated layers of kaoliniferous sands and refractory white-greyish clays ("Barro D"); the average thickness of this unit is 4 m.
2. a lower unit, "Reddish heavy clay", composed by sands and reddish clays ("Barro vermelho"); the thickness of this unit can attain 15 m, locally.

In places, underneath the sedimentary kaolin lies the residual kaolin which genesis is related to the alteration of the regional two-mica granite.

#### CERAMIC USES

There are important reserves of heavy clay and both sedimentary and residual kaolin that have been exploited by local ceramic plants since 1958.

These industrial raw materials, particularly those related to the sedimentary deposits, are exploited in several quarries.

Very recently, a new horizon of white heavy clay was found underneath the "heavy reddish clay".

Residual kaolin contains 20 ~ 40 % of commercial kaolin with high whiteness. There is a good correlation between whiteness and abundance of pegmatite veins.

Kaolin total reserves are estimated in 2.2 MT; the kaolin reserves for paper industry are about 1.1 MT while those for the ceramic industry are about 0.5 MT.

The "Barro D" is used in a nearby plant producing refractory bricks, whilst the "heavy reddish clay" is used in the production of structural ceramics.

#### GEOPHYSICAL STUDIES

The applied geophysical methods did comprise resistivity techniques, in particular Wenner tripotential soundings. Afterwards alpha, beta and gamma measurements were used so that data quality was assessed.

Electrical soundings were carried out 50 m apart, along the main pathways and with a general E-W orientation. This particular strike might correspond to the sedimentary basin main feeding direction. Two sets of electrical soundings were accomplished, set C1 to C8 and S1 to S15.

#### CONCLUSIONS

From the two sets of electrical soundings, two resistivity pseudo-sections were drawn and give an approximate 2D image of the area.

Electrical soundings were interpreted in a interactive way with appropriate software in a PC environment. Before a final model was achieved, comparison was carried out between the different soundings in order to improve the interpretation. Finally, a coherent interpretation model is proposed, showing the structure of the studied area.

#### REFERENCES

- Barbosa, B. (1974) - Barro vermelho dos depósitos de Alvarães e Vale do Cávado. Relat. Int., Serv. Fom. Min., Porto.
- Pereira, E. *et al.* (1992) - Carta Geológica de Portugal na escala 1/200000. Notícia Explicativa da Folha 1. Serv. Geol. Portugal, 83 pp.

## Mineralogy and geochemistry of argillites from flysch rosso formation (southern Apennines, Italy)

*Fiore S, Santaloia F, Santarcangelo R and Tateo F*

Pre-Pliocene argillites form a large part of thrust units of the Southern Apennines chain. Although many geological investigations have carried out on these sediments, there isn't unanimous opinion among researches. They are referred to a single or to two distinct sedimentation basins. To give a contribution to solve this problem, IRA has planned some mineralogical and geochemical investigations, of which this study is a part, and which regards the Flysch Rosso formation (auct.).

Two sections of Flysch Rosso (Cretaceous - Lower Miocene) have been sampled at Vaglio di Basilicata (hereafter CC) and Campomaggiore (hereafter CM), both in the province of Potenza (Italy). They are constituted by alternance of green and red shales, intercalated by black levels (from some cm up to 50 cm in thickness), radiolarian cherts (section CC) and Mn-rich horizons (section CM).

Mineralogy of samples is dominated by clay minerals (61 - 84%), quartz (15 - 29%), feldspar (< 5%). Appreciable amounts of hematite (CC: 1 - 4%; CM: 3 - 7%) are present in the red shales. Mineralogy of clay fraction (< 2 $\mu$ m) is characterised by high amount of dioctahedral smectite (CC:  $x = 57\%$ ; CM:  $x = 60\%$ ), variable illite (CC:  $x = 12\%$ ; CM:  $x = 8\%$ ), and kaolinite (CC:  $x = 12\%$ ; CM:  $x = 24\%$ ); chlorite is always subordinate with respect to the other minerals. The samples of the two studied sections are also different for the crystal chemistry of smectite: CM is characterised by random interstratified mixed layer I/S (15 - 30%) whereas CC is marked by Al-hydroxide interlayer.

Major and trace (Ni, Cr, V, Rb, Sr, Y Zr, Nb, and Ba) element abundance show overall similarity in the two localities, except for Fe and Mn. As concern REE abundance, they vary within a moderately wide range ( $\Sigma$ REE = 144 - 240 ppm). Some PAAS (Post Archean Australian Shale) normalised REE patterns exhibit an enrichment in intermediate elements; others are parallel to the PAAS pattern. Therefore ratios indicative of fractionation vary within a wide range:  $La_N/Yb_N = 0.845 - 1.349$ ;  $La_N/Sm_N = 0.538 - 0.825$ ;  $Gd_N/Yb_N = 1.210 - 2.017$ . Some samples also show a pronounced positive Ce-anomaly ( $Ce/Ce^* = 0.820 - 1.454$ ) whereas  $Eu/Eu^*$  is almost constant (0.975 - 1.095)

The data obtained permit us to put forward some hypotheses regarding provenance of sediments and the origin of their different colours.

Al/Ti ratio indicates input from acidic rocks, continental in origin as indicated by detrital coefficient  $Al/(Al+Fe+Mn)$  and by rare earth elements ( $\Sigma$ REE,  $Ce/Ce^*$ ). Detrital contribution from ridge and/or ophiolite rocks were negligible, as suggested by contents

and ratios involving MgO, Ni, and Cr. Detrital contribution, however, changed with time as indicated by the occurrence, for instance, of the radiolarian cherts.

U/Th, V/Cr, and  $U_{\text{authigenic}}$  calculated for both red and green samples, indicate oxic conditions; black shale levels, however, record rapid change of conditions at the water-sediment interface.

The bell shape pattern of intermediate REE recorded by many samples seems to be a distinctive character of Flysch Rosso sediments. However, it is unclear if this anomaly is carried out by detrital minerals or is superimposed by diagenesis. This aspect is currently being investigated.

As concerns the shale colour, it appears that it is controlled by the presence of hematite and by its dimension and not by the molar fraction  $Fe^{++}$ .

(1) Istituto di Ricerca sulle Argille, CNR. Area di Ricerca di Potenza, Italia

(2) Istituto di Chimica Agraria. Univ. di Bari, Italia

## Organic matter migration and halloysite formation in pyroclastic deposits from Mt. Vulture (southern Italy)

Fiore S (1), Genovese G (1) and Miano T M (2)

In previous geochemical and mineralogical investigations carried out on pyroclastic deposits outcropping in the Mt. Vulture volcanic area (Italy), it was detected the presence of very little amount of organic matter in buried layers without any trace of meteoric alteration. This occurrence led to hypothesise migration of organic matter from present-day soil to deeper layers, favoured by the very high porosity of these rocks which would allow the passage of a great amount of meteoric water and the compounds dissolved in it.

In the present research the validity of such a hypothesis has been looked into.

The samples studied were collected from a pyroclastic series of Mt. Vulture volcano near Barile (Potenza, Italy), at about 20 m below the soil. The sampling was carried out in an "active" quarry to exclude any possible influence of alteration process and to verify the absence of paleosols neighbouring the layers.

Seven pyroclastic layers were investigated for granulometry (12 grain size classes), mineralogy (< 2  $\mu\text{m}$ , 2-4  $\mu\text{m}$ , 4-8  $\mu\text{m}$ , and 8-16), and content of organic matter (whole rock).

X-ray diffraction analysis showed that the four grain size fractions were composed of the same minerals: halloysite (7 Å), halloysite (10 Å), non expandible 10 Å mineral, quartz, pyroxenes, analcite, as well as a high amount of glass. In accordance with literature, quartz is an exotic mineral and it comes from sedimentary substratum.

The amount of organic matter is little (0.24 - 0.45%) but significant respect to the content measured in the present-day overlying soil (1.17%). No relationships were found between height of sampling and content of organic matter, or with fulvic-like and humic-like acids.

The data obtained clearly indicate that organic matter moves from the soil downward and that halloysite is not pedogenetic in origin. The high statistical relationship between coarser particles (> 4.76 mm) and organic matter suggests that it is "trapped" within the voids of pumice grains. Halloysite might be originated by alteration of glass caused by i) low temperature volcanic fluids and/or by ii) meteoric circulating water. In this latter case, an important role might be played by organic acids, as was the case with kaolinite (Linares & Huertas, 1971; *Science*, **171**, 896-897)

The data obtained in this study give rise to an important inference: buried paleosols developed on volcanic substratum are open systems and so the content and type of organic matter in geochemical studies should be considered very carefully.

Dpto. Química Agrícola,  
Geología y Geoquímica. Fac.  
Ciencias. Univ. Autónoma de  
Madrid, España

## Kinetic approach to the mineral reaction processes in a saponitic clay

*Garraón A, Cuevas J, Ramírez S and Leguey S*

### INTRODUCTION

In the course of hydrothermal reaction experiments with a saponitic clay from the Madrid basin, at temperatures above 120°C, evidence for the dissolution of sepiolite has been detected, which is present as accessory mineral. Formation of smectite was also observed. An evaluation of the apparent time dependence of the process were made, to obtain rate constants of the sepiolite dissolution. With this purpose, hydrothermal reactions with a clay: water relation of 1:3 were realized at the temperatures of 60, 90, 120, 175 and 200°C with reaction intervals of one month to one year. Changes in the chemistry of reaction waters were also monitored.

In the study of the kinetic process of sepiolite dissolution and smectite formation, some assumptions were made. The variation in the chemical composition of the water was not considered, as this parameter remains constant for each temperature.

Due to the semiquantitative character of the mineralogical composition, obtained by X-ray diffraction, a correction of the data were made using physico-chemical parameters, that could be considered dependant on the mineralogical composition of the sample. For %sepiolite, the X-ray data were adjusted with the BET surface values for each sample using a second order polynomial function.

$$(\text{Sep})\% = 91.15 + 4.482\text{BET} - 0.024(\text{BET})^2 \quad r = 0.968$$

With the recalculated values, the rate constants for each temperature were determined. To analyze the experimental data, two different approximations were used. The first approach supposes a trend to equilibrium for all the temperatures, reaching a stationary

mineral composition. This approach has been defined as "Limited Dissolution". The second approach brings with the possibility of the 100% transformation of the starting mineral composition. This assumption approximates to an open system, and has been considered to evaluate the long term evolution of the material.

## RESULTS AND DISCUSSION

If the dissolution process is considered to reach a stationary value for each temperature, the data were adjusted to an equation as follows:

$$\%Sep = Sep_{\infty} + A_1 e^{(-kt)}$$

With this equation,  $Sep_{\infty}$  will be equal to the final value, and  $Sep_{\infty} + A_1$  concern to the zero-time value of sepiolite content in the sample. The rate constants obtained for the sepiolite dissolution were adjusted to the Arrhenius's equation:

	Limited Dissolution		Total Dissolution	
	A(days <sup>-1</sup> )	Ea(Kcal/mol)	A(days <sup>-1</sup> )	Ea(Kcal/mol)
60-90°C	----	----	2.84*10 <sup>-3</sup>	2.28
120-200°C	2209772	18.00	48.73	7.09

Ea: Activation Energy. ; A: pre-exponential factor.

The reactions carried at 60° and 90°C, showed an erratic increase in the BET surface values, that did not allow a good fitting of the results in these temperature range. The Activation Energies ranging between 7 and 18 are similar to those obtained by Abdul-Latif and Weaver (1969) (19.4 Kcal/mol) or Cornejo and Hermosín, (1991) (12.3 Kcal/mol) for sepiolite acid dissolution, applying an apparent first order kinetics.

### Smectite formation

A similar method were used with the data obtained from X-ray diffraction, adjusting to a linear equation as function of the values of CEC from the sample, varying with the apparent smectite content.

$$\%Smectite = -0.28535 + 1.32767 \text{ CEC}$$

$$r = 0.960$$

The rate constant values always show, for all the temperatures, a trend to smectite formation. From these rate constants, the following Activation Energies were obtained:

Limit Formation		Total Formation	
A(days <sup>-1</sup> )	Ea(Kcal/mol)	A(days <sup>-1</sup> )	Ea(Kcal/mol)
9.48±2.75	5.01±0.83	0.97±1.99	4.81±0.56

The Activation Energies obtained are magnitudes lower than the expected for breaking bonds and are typical for reactions controlled by diffusion mechanisms.

With the Activation Energies values obtained for the sepiolite dissolution and for smectite formation processes, it is possible to affirm that the reaction is controlled by the initial sepiolite dissolution. This process evolves to smectite at temperatures higher than 120°C, but at temperatures lower than 90°C, the sepiolite dissolution did not show signs to be produced. At this temperatures (60° and 90°C) the extrapolated values by the BET surface variation, show a trend to increase the sepiolite content. This process agrees with the hypothesis of sepiolite formation from Mg-smectite in the Vicalvaro's deposit (Ramírez et al., 1995). However, stevensites from this deposit are characterized by high BET surface value, so actual data did not allow us to establish global kinetics for sepiolite formation.

Although the sepiolite formation process is possible at low temperatures, the increase of the CEC and the smectite content in the samples, supported by a higher consistence in the kinetic study for the smectite formation, implies as more possible, the process of production of a high surface smectite rather than sepiolite.

## REFERENCES

- Abdul-Latif, N. & Weaver, C.E. (1969). *Clays and Clay Minerals*. 17: 165-178.
- Cornejo, J. & Hermosín, M.C. (1991). *Bol. Soc. Esp. Miner.*, 14: 65-70.
- Ramírez, S., Garralón, A., Cuevas, J., Martín Rubí, J.A., Casas, J., Alvarez, A. & Leguey, S. (1995). *Bol. Soc. Esp. Miner.* 18-2: 47-48.

(1) Dip. di Scienze della Terra. Univ. degli Studi di Napoli Federico II. Napoli, Italia

(2) Progemisa Società Sarda Valorizzazione Georisorse. Cagliari, Italia

## Alteration process on Tertiary calc-alkaline pyroclastic flow from Sardinia

Ghiara M R (1), Franco E (1), Petti C (1), Lonis R (2), Luxoro S (2) and Gnazzo L (1)

A series of representative pyroclastic units from northern Sardinia were sampled. Nearly all units showed advanced alteration processes leading to new formation of mainly clinoptilolite and, to a lesser extent, mordenite both generally coexisting with montmorillonite. The large Sardinian Tertiary Oligo-Miocene pyroclastic flows proved very useful to investigate the alteration processes as these rocks were emplaced in volcano-tectonic depressions in the subaerial, lacustrine and marine environments. Clinoptilolites are, as well as mordenite, indeed the most interesting zeolites occurring in nature and mined worldwide.

According to radiometric ages (K/Ar) the Tertiary calc-alkaline volcanism of Sardinia started at 32 Ma, with a climax of activity between 24 and 18 Ma. In this period most of the ignimbritic products outpoured all over the island. Volcanic sequences interbedded with continental to marine sediments are mainly found within the Sardinian Oligocene - Miocene rift which extends 220 Km across Sardinia on a NS trend. Pyroclastic flows are medium-grained, moderately welded and poorly sorted.

All the investigated rocks show a porphyroclastic texture with porphyritic index ranging from 20 to 35%. The flattening of glass fragments and pumice produced a slightly eutaxitic texture at the base of the pyroclastic unit. Phenoclastic assemblages and glass chemistry indicate that ignimbrites range from rhyodacite to rhyolite.

The methods employed were: X-ray diffraction, electron microprobe analysis, scanning electron microscope, IR spectroscopy and thermal analyses.

Our investigations on pyroclastic flows of northern Sardinia have shown that together with clinoptilolite, mordenite and montmorillonite also analcime and silica minerals (quartz and opale-CT) likewise occur between secondary minerals. Textural features clearly show that zeolites are mainly a devitrification product, while the spherulitic silica minerals aggregates are linked to vapor phase crystallization. Semiquantitative XRD analyses show alteration degrees of glassy components ranging from 30 to 100%. This may be linked to variation or zonation in welding leading to more or less circulation of

minero-genetic agents. X-ray data and microscopic features indicate that the abundance of clinoptilolite is variable. In some thin sections a complete alteration of glassy shards to clinoptilolite is observed while in others the clinoptilolite is essentially confined to the cineritic matrix. Alkaline and alkaline-earth atoms of clinoptilolite range from 1.6 to 3.8 and from 1.0 to 2.2 a.f.u., respectively. Si/Al ratios range from 4.4 to 5.0, whereas the Na/K ratios range from 0.3 to 1.7. Therefore, according to Iijma classification, these clinoptilolite compositions lie between high silica and low-Ca clinoptilolites.

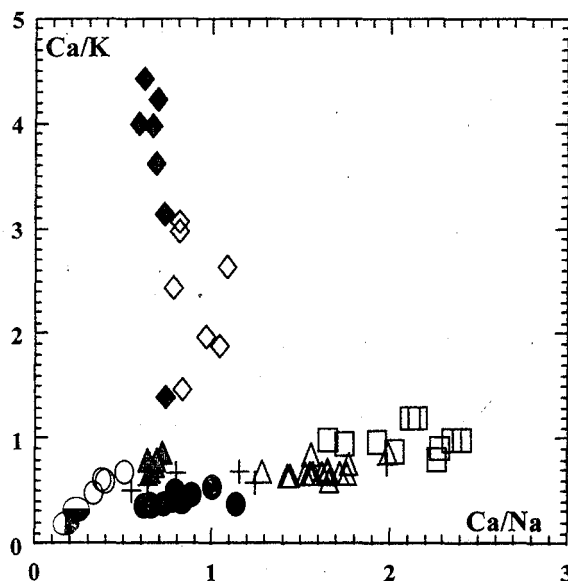
Mordenite is less frequent than clinoptilolite. Like clinoptilolite, some thin sections showed a complete alteration of both glassy shards and cineritic matrix; whereas others showed that mordenite is exclusively contained into the cineritic matrix. The chemical composition of mordenite shows alkaline and alkaline earth atoms ranging from 2.7 to 4.6 a.f.u. and from 1.5 to 2.6 a.f.u., respectively. Si/Al ratios range from 4.4 to 5.3 whereas Na/K ratios range from 1.0 to 7.2. XRD analyses of nearly all samples showed a dioctahedral smectite (15.50-4.53-1.51 Å) in the cineritic mass. X-ray diffraction analyses show that the smectite basal (001) spacing varies from about 12 to 15 Å. This expands to 16.67 Å when treated with glycol ethylene for 1 hour at 60°C.

The comparison between the chemistry of the unaltered glass and secondary minerals suggests that during the zeolitization process a selective alkaline drop and the slight simultaneous increase in Ca and Mg occurs. In particular Barth's cell parameters indicate for clinoptilolite a preferential removal of Na occurred, Na < K occurred in the formation of mordenite (Table 1). This prompts an intriguing question on the mobility alkaline elements. Assuming starting glasses very similar in chemical composition, it is clear Na appears to be most mobile during clinoptilolite formation, whereas the opposite is inferred for mordenite formation. This may be due to several factors namely, interacting fluid speciation (TDS, pH, halogens contents) absolute temperature and thermal history of glass. However, the large variations in Ca/Na and Ca/K ratios of zeolites suggests that fluid composition plays a key role in the alteration process of Tertiary pyroclastics in Sardinia (fig.1). As already experienced by Ghiara et al. (1990; 1996) the interaction fluids must be characterized by very low salinity and medium to high pH values. On the basis of the above results it may be inferred that zeolitization process of pyroclastic flows is largely extended to a regional scale, suggesting that there is no connection between these alterations and the local geological environment.

Table 1. Anhydrous Barth's standard cell contents of unaltered glasses (1: sample 15; 2: sample 5614), clinoptilolite (samples 15, 5615, 6302, 6504, 6500) and mordenite (samples 6331, 6327, 5614).

Element	15 (6)	5615 (11)	6302 (10)	6504 (4)	6500 (15)	Glass 1 (7)	6331 (5)	6327 (8)	5614 (7)	Glass 2 (7)
Si	66.16	65.83	66.23	66.21	65.83	64.44	66.44	65.57	66.78	64.18
Ti	-	0.05	0.02	0.01	0.02	0.07	0.07	0.07	-	-
Al	14.03	14.34	14.04	13.96	14.07	14.86	13.72	14.27	13.08	15.00
Fe <sup>3+</sup>	0.06	0.03	0.04	0.06	0.09	0.04	0.02	0.20	0.33	0.05
Mg	1.22	1.04	1.68	1.05	1.43	0.33	0.05	0.28	0.39	0.25
Ca	2.19	1.97	2.67	1.73	2.48	1.13	2.58	3.51	3.02	1.51
Na	2.37	2.51	1.30	4.42	1.55	6.91	3.84	4.11	4.55	7.37
K	3.63	4.79	2.73	2.93	3.59	7.40	3.35	1.59	0.96	6.81
Ba	0.05	-	-	-	0.07	-	-	-	-	-
Mn	0.01	0.03	0.02	0.06	0.05	0.05	0.10	0.04	0.03	0.03
P	-	-	-	-	0.05	-	-	-	-	-
Cr	0.05	0.06	0.03	-	0.14	0.03	0.08	0.20	0.06	0.03
F	-	-	-	-	0.22	-	-	0.29	-	0.28
Cl	0.08	-	-	-	0.06	0.19	-	0.11	-	0.08
ΣOxigens	160	160	160	160	160	160	160	160	160	160

Fig. 1. The Ca/Na vs Ca/K ratios of analyzed zeolites showing the clinoptilolite and mordenite trends. Averaged micro-analysis of unaltered shards of two pyroclastic flows were also plotted (● sample 15; ● sample 5614). □ sample 6302, ● sample 5615, ○ sample 6504, + sample 15, Δ sample 6500 ▲ sample 6331, ◆ sample 5614, ◇ sample 6327. Note the position of glassy shards with respect to the two trends.



(1) Dip. di Scienze della Terra, Univ. di Siena, Italia

(2) Instituto Andaluz de Ciencias de la Tierra, CSIC-Universidad. Granada, España

## Origin of intergrown phyllosilicate stacks from Verrucano metasediments (northern Apennines, Italy): a transmission and analytical electron microscopy study

*Giorgetti G (1), Nieto F (2) and Memmi I (1)*

### Introduction

Grains of intergrown phyllosilicates (IPG) widely occur in cleaved and low-grade metamorphosed clastic rocks from Verrucano Group (northern Apennines, Italy). These stacks have been re-examined after Franceschelli et al. (1989; 1991) using SEM and HRTEM in order to better characterize them and to clarify their origin.

Different types of IPG have been recognized with high resolution techniques: 1) Chl+Ms±Kln; 2) Chl+Ms+Pg±Kln; 3) Ms+Pr±Pg; 4) Ms+Pr+Su; 5) Ms+Pr+Chl+Su; 6) Su+Ms (mineral abbreviations according to Kretz, 1983). All them can be basically divided in two groups: (i) type (1) and (2) are constituted of Chl with micas and Kln forming thin lamellae parallel intergrown or crosscutting Chl packets; this is also the case of type (6) IPG with sudoite as an optically continuous mineral and minor muscovite packets. (ii) In type (3), (4), (5) IPG, muscovite can be recognized as a continuous mineral whose packets are crossed and splitted by the other phyllosilicates. Sometimes, IPG present a mineralogical association which is different from the phyllosilicate association of the rock matrix: this feature, together with textural evidences, indicates that IPG represent isolated microsystems which have not re-equilibrated with the whole rock.

### TEM results.

In IPG of the former group, Chl is the most abundant phase: it occurs in several hundred angstrom thick packets with undeformed and defect-free 14Å-layers. Micas are always a two-layer polytype and they occur either as isolated layers interstratified with Chl, or in packets of variable thickness. In highly altered samples, Kln is also present as a 1T polytype with different degree of crystallinity; it occurs in packets of 7Å-layers intercalated with mica packets. Textural relations between the various phyllosilicates are as follows:

Chl - Mica: they are generally intergrown with parallel (001), showing coherent grain boundaries; in this case, lateral transformation from one 14Å-layer to one 10Å-layer can

be observed. Analytical electron microscopy permitted to identify as mica the contamination produced by these 10Å-layers. Low- or high-angle grain boundaries can rarely occur.

Ms - Pg: coherent or low-angle grain boundaries are observed; Pg is always a discrete phase and no intermediate sodium-potassium mica is recovered.

Ms - Kln: they have parallel basal planes or slightly different orientation along the  $c^*$  direction. Grain boundaries are not parallel to one layer but they are indented with lateral transitions from two 10Å-layers to three 7Å-layers.

In type (6) IPG, sudoite occur in hundred angstrom thick packets, defect-free and with straight lattice fringes. Ms occur in small packets, highly defective and disoriented along  $c$ . Also in this case Su and Ms may have coherent or low- / high-angle grain boundaries. Lateral transition from 14Å-layer to 10Å-layer can be observed.

IPG of the latter group are mainly constituted of muscovite and pyrophyllite. Muscovite occur as a two-layer polytype; HR images show that Ms is present both in several hundred angstrom thick packets, undeformed and with straight lattice fringes, and in small packets with slightly different orientation along the  $c^*$  direction. Prl is present in thick packets as a 2M or 1T polytype; it is easily recognizable from Ms for its different contrast. Chl and Su occur as minor phases, in thick packets (Chl) or in wedges terminating inside Ms packets (Su). Sometimes, thin packets of Pg are present.

Ms - Prl, Ms - Su, Ms - Chl, Ms - Pg may be perfectly parallel intergrown: SAED show 00l row with two sets of reflections and HR images show packets with contacts parallel to the basal planes. Low-angle grain boundaries can also be observed: the  $c^*$  directions have different orientation and (001) of one phase abut against (001) of the other phase.

As proposed by Franceschelli et al. (1991), morphology and texture of IPG suggest that they originated from pristine grains (chlorites or muscovite) through a combination of metamorphic and tectonic events. The ultimate origin of pristine grains is detritic and they predate the deformation event: they are deformed, and metamorphic phyllosilicates grow at highly strained sites.

TEM data confirm this model and allow to characterize the reaction mechanisms involving phyllosilicates: topotactic growth is facilitated along the basal planes and transformations occur through dissolution-crystallization reactions. Nucleation is favoured by strain. Pristine phyllosilicates were so replaced by newly-formed phyllosilicates originating a mineral association in equilibrium with metamorphic P-T conditions.

## References

- Franceschelli M Mellini M Memmi I Ricci C A (1989). *Contrib. Mineral. Petrol.* **101**, 274-279
- Franceschelli M Memmi I Gianelli G (1991). *Contrib. Mineral. Petrol.* **109**, 151-158
- Kretz R (1983). *Am. Mineral.* **68**, 277-279

## Acknowledgement

TEM analyses were performed at the C.I.C of the Universidad de Granada and at the C.I.A.D.S. of the Università di Siena. This work was financially supported by Italian Ministry of University and Scientific and Technological Research grants (MURST to I.M.) and by Spanish Research Project grants PB92-0961, PB92-0960 and Research Group of the Junta de Andalucía 4065.

Dpto. Química Agrícola,  
Geología y Edafología. Fac.  
Química. Univ. de Murcia,  
España

## Clay minerals in the Rambla Salada basin (Murcia province, SE Spain)

*Guillén F, Arana R and Fernández Tapia M T*

---

The Rambla Salada basin is one of the most representative examples of soil erosion and desertification risk in southern Spain. Soil degradation means a partial or total loss of the productivity capacity as a result of different processes, among these we emphasize on the mediterranean area the soil erosion. In connection with this study (project AGF95-0635 of the Spanish CICYT) we are carried out a complete geological investigation in the Rambla Salada basin with a special interest on clay mineral levels in small areas more affected by different models of soil degradation.

In this basin appear continental or marine materials from Oligocene to Quaternary with different lithologies such as conglomerates, limestones, marls, gypsum, clayey levels, travertines, etc. There are also in this area an important outcrop of ultrapotassic rocks from lamproitic type in proximity of Barqueros, a small village in southern part of the Rambla Salada basin.

In an initial phase we have selected 16 samples distributed in different stratigraphic sequences more affected by the soil degradation processes in order to establish the mineralogy of the total sample and the nature of clay minerals succession. The most representative terms in total sample are calcite, clay minerals, quartz, dolomite and accidentally variable amounts of gypsum and feldspar minerals. Clay fraction in these samples is formed by smectite, illite, palygorskite and traces or minor quantities of kaolinite and chlorite. The semiquantitative mineral compositions obtained by X-ray methods is pointed out in Table I. Mineralogical composition of these materials suggest several geological processes developed in this basin specially all through upper Miocene with an important increase in clay minerals from

limestones and marls. Likewise we can verify that the most developed soil degradation processes occur in small zones with higher contents in smectites due perhaps to alternating episodes of swelling and shrinkage.

Table I. Mineral composition of the argillaceous levels in the Rambla Salada basin.

Sample	Cc	Dol	Q	Sm	Il	Pal	Chl	K	Gy	Fd
SZ1	51	5	5	7	14	16	1	1	-	-
SZ2	49	5	12						4	-
SZ4	35	13	12	2	26	-	1	1	2	4
SZ5	47	5	11	13	14	8	1	1	-	-
SZ6	40	11	11	9	24	-	1	1	-	3
AC1	49	2	20	4	13	17	tr	tr	-	2
AC2	52	-	11	3	14	15	1	1	-	3
AC3	43	6	11	15	20	-	tr	tr	-	4
AC4	42	4	8	19	25	-	tr	tr	-	1
CC1	47	4	8	nd	nd	nd	nd	nd	11	1
CC2	32	13	7	9	10	11	-	-	16	2
CC3	38	6	13	16	15	-	1	1	2	5
PU1	35	11	12	16	21	-	2	-	-	3
PU2	53	4	11	12	16	-	1	1	-	2
CZA1	41	6	15	13	19	-	2	1	-	3
CZA2	62	4	12	9	11	-	1	1	-	-

Cc, calcite; Dol, dolomite; Q, quartz; Sm, smectite group; Il, illite; Pal, palygorskite; Chl, chlorite; K, kaolinite; Gy, gypsum; Fd, feldspars minerals; tr, traces; nd, not determined.

Acknowledgement. To Spanish CICYT for financial support (project AGF95-0635).

Dpto. Cristalografía y  
Mineralogía, Estratigrafía,  
Geodinámica, y Petrología y  
Geoquímica. Fac. Ciencias  
del Mar. Univ. de Cádiz,  
España.

## Clay minerals in recent sediments of the Cádiz bay and their relationships with the adjacent emerged lands and the continental shelf

*Gutiérrez Más J M, Achab M, Sánchez Bellón A, Moral Cardona J P and López Aguayo F*

The clay minerals in recent sediments of Cádiz Bay bottoms have been studied of knowing the sedimentary interchange with the adjacent continental shelf and the mineralogical similarities with the neighbouring emerged areas.

Samples were obtained with van-veen dredge and gravity cores. Granulometric (mechanical and laser procedures) and mineralogical analysis (x-ray diffraction) were developed to establish the different sedimentary facies and factor analysis was used for determination of the mineralogical associations.

In Cádiz Bay two zones have been differentiated: a external zone open seaward, mainly controlled by the waves, and an inner area (lagoon) with an intermediate tidal regime. The sediments in both zones are siliciclastic, but while in the lagoon the mud predominates, the external zone is filled up by quartzitic sands.

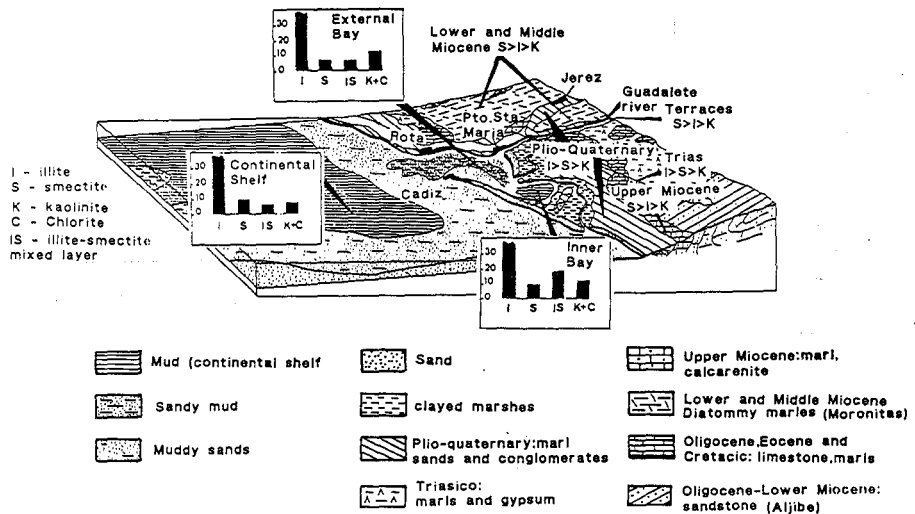
The clay fraction is composed by illite (I), kaolinite (K), smectite (Sm), illite-smectite random mixed-layers (I-S), chlorite (Chl) and palygorskite (Pk) ( $I > K > Sm = I-S = Chl \pm Pk$ ). In the external bay the clay mineral association is dominated by illite with an average content oscillating between 50-70%, especially concentrated near the Guadalete river mouth, followed by K+Cl (15-25%), Sm (10-15%) and illite-smectite random mixed-layers (5%). In the inner bay the main mineral is also illite, although with lower contents (<50%), followed by I-S (15-20%), Sm (<10%) and K+Cl (10-15%).

The sedimentary processes are controlled by the supplies of the Guadalete river, which are distributed as muddy accumulations in front of its mouth and as sandy barrier and beach in the littoral. Southwards the absence of rivers is substituted by the action of tidal currents. Moreover, the bay receives contributions, as much from the erosion of emerged old tidal flat as from the tidal channels. Suspension matter is also provided by currents and flood tide from the deeper waters out of the bay.

In continental shelf the sediments are also siliciclastics with an high quartz content in the sandy areas (85%). Two main sectors can be established: a muddy sector, from the Guadalquivir river mouth to Cádiz, and a sandy sector, from Cádiz to Trafalgar Cape (Fig.1). The most abundant clay mineral is illite, followed by smectites and kaolinite+chlorite. Other clay minerals present are illite-smectite and illite-chlorite (I-Chl) random mixed-layers.

The sedimentary dynamic pattern assumes that the muddy sediments on the continental shelf come from the Guadalquivir river mouth and are transported toward the SE by the Atlantic Surficial Water and the littoral currents (Madelian, 1970; Melieres, 1974; Ojeda, 1989; Gutiérrez Mas et al., 1995).

In the neighbouring continental areas, the geological units present in the Guadalete river basin include clays, marls and sands sequences from the Subbetic Trias, Upper Miocene and Plio-Quaternary, as well as overlying Holocene fluvial terraces, marshy muds, dune and beach sands and gravels (Mabesoone, 1963; Vigier, 1974). The main clay mineral associations are: Subbetic Trias: I>Sm>K (Mabesoone, 1963); Lower and Middle Miocene: Sm>I=K (Vigier, 1974); Upper Miocene: Sm>I>K (Vigier, 1974); Plio-Quaternary: I>K>Sm (Mabesoone, 1963); Guadalete terraces: Sm>I>K (Moral Cardona, 1994).



From the different clay mineralogical associations, a possible interrelationship between different environments should be proposed. Supplies from the Guadalete river basin to the Cádiz external Bay are I, Sm and K+Chl. The adjacent continental shelf provide I>K+Cl>Sm coming from the Guadalquivir river basin. The supplies of illite from these two zones and the relative impoverishment of smectites for its lower settling rate near the coast (Manickan, 1985) permit that the illite will be the most abundant clay mineral in the external bay.

These minerals reach to the lagoon, a confined environment, where the illite is partially transformed in I-S random mixed-layers. The action of the tidal ebb generates an outflow and a part of the I-S mixed-layers is transported seaward, this flow is initiated in the inner of the lagoon and reaches deeper waters of the external bay and even of continental shelf.

**ACKNOWLEDGMENTS.**- This work has been supported by CICYT Spanish project AMB94-0501 and Group 4166 of the Junta de Andalucía.

#### REFERENCES

- GUTIERREZ MAS, J.M.; LOPEZ-GALINDO, A.; GONZALEZ CABALLERO, J.L. & LOPEZ-AGUAYO, F. (1995): *Rev. Soc. Geol. España*, **8** (1-2), 61-71.
- MABESOONE, J.M. (1963): *Geologie in Mijnbouw*. 42:23-43.
- MADELIAN, F. (1970): *Extrait des Cahiers Oceanographiques*, **22** (1), 43-61.
- MANICKAN, S; BARBAROUX, L. & OTTMANN, F. (1985): *Sedimentology*, **32**, 721-741.
- MELIERES, F. (1974): *Thèse Univ. Paris*. 235 pp.
- MORAL CARDONA, J.P. (1994): *Tesis de la Univ. de Cádiz*. 464 pp.
- OJEDA, J. (1989): *AEQUA. monografías*, **1**. 123-132.
- VIGUIER, C. (1974): *Thèse Doct. Univ. Bordeaux*. 449pp.

(1) Dip. Geomineralogico.  
Univ. degli Studi di Bari,  
Italia

(2) DiSGG. Univ. degli Studi  
della Basilicata. Potenza,  
Italia

## **Pelitic levels in the Apulian carbonate platform (Cretaceous): mineralogy and geochemistry as indicators of provenance**

*Laviano R (1) and Mongelli G (2)*

The Apulian Carbonate platform consists of an imposing serie of shallow sea-water limestone, Mesozoic-lower Tertiary in age, forming a part of the Apenninic foreland. In the Murge area (central Apulia) the limestone has been grouped into two stratigraphic successions: "Calcere di Bari" Formation and "Calcere di Altamura" Formation. The "Calcere di Bari" Formation presents in its upper part a break of deposition, marked by a pelitic level and an overlying breccia level. The "Calcere di Altamura" Formation is transgressive on the "Calcere di Bari" and is referred to the Senonian-Maastrichtian. Pelitic levels, referred to a marine depositional environment, have been also recognized within the two stratigraphic succession.

The aim of this study is to verify if eventual differences in provenance and depositional environment involving pelitic levels within a carbonate succession, can be stressed by geochemical and mineralogical markers. With this in mind, we have analyzed a set of ten clay samples and two breccia samples, grouped into four subsets and corresponding to the following stratigraphic positions:

- AC samples, pelites occurring within the "Calcere di Bari" Formation;
- AG samples, pelites occurring between the "Calcere di Bari" Formation and the "Calcere di Altamura" Formation;
- BR samples, breccia with fine, reddish matrix, occurring between a pelitic level (AG samples) and the overlying limestone of the "Calcere di Altamura" Formation;
- AA samples, pelites occurring within the "Calcere di Altamura" Formation.

Preliminary results, based on the chemical composition, suggest that AG and AA samples have some distinct features relative to both AC and BR samples. AC samples, for instance, are higher in the Fe, V, Cr and Ni contents, suggesting differences in provenance.

(1) Dpto. Geociencias. Univ.  
de Aveiro, Portugal

(2) Instituto Geofísico. Univ.  
do Porto, Portugal

## Magnetostratigraphy of an evaporitic deposit overlying the upper Cretaceous "Argilas de Aveiro" formation (Bustos-Aveiro, Portugal)

*Leite S (1), Montenegro J (2), Rocha F (1) and Gomes C (1)*

### INTRODUCTION

The Aveiro region corresponds to the northern sector of the Portuguese Occidental Meso-Cenozoic sedimentary basin. At the Aveiro region a gap in the stratigraphic record do occur beyond upper Cretaceous. In fact, Rocha (1993) on the present continental part of the basin, just on a lithostratigraphic basis, refers the eventual existence of Paleogene and Neogene deposits, which, in front of the present shoreline, have been identified by Mougenot (1989) overlying Maastrichtian deposits and showing an overall thickness estimated at about 550 meters. On the other hand, Pliocene and Pleistocene outcrops do occur corresponding mainly to old beach deposits and to fluvial terraces.

Recently, mineralogical and geochemical studies had been carried out by Rocha & Gomes (1994, 1996) on two interesting outcrops located in Esgueira and Bustos (Fig. 1).

In Esgueira, northern suburb of Aveiro town, the position in the local stratigraphic column of the so-called "Areias de Esgueira" formation is still undefined, being placed in the interval upper Cretaceous - Pliocene. "Areias de Esgueira" formation, which overlies the "Argilas de Aveiro" formation dated upper Cretaceous, is composed of brown sands, medium grained, intercalated by black clayey layers containing marcassite nodules and remains of fossil plants as well as brown to red clayey layers coated at their top by very thin iron rich crusts, and yellow sands, medium to coarse grained becoming gradually finer towards the top, exhibiting cross-bedding. The results achieved by Rocha & Gomes (op. cit.) point out, in global terms, to a gradual and regressive evolution of the environment of deposition of the "Areias de Esgueira" formation and to particular local discontinuities and changes of some physico-chemical parameters.

In Bustos (located about 10 km to the SSE of Aveiro), the upper Cretaceous "Argilas de Aveiro" formation, source of heavy clays of paramount importance for the numerous structural ceramics plants working in the region, is covered, without apparent discontinuity, by thin

layered silty, clayey and evaporitic sediments (rich in salts, sulphates and chlorides), named as "Evaporitos de Bustos".

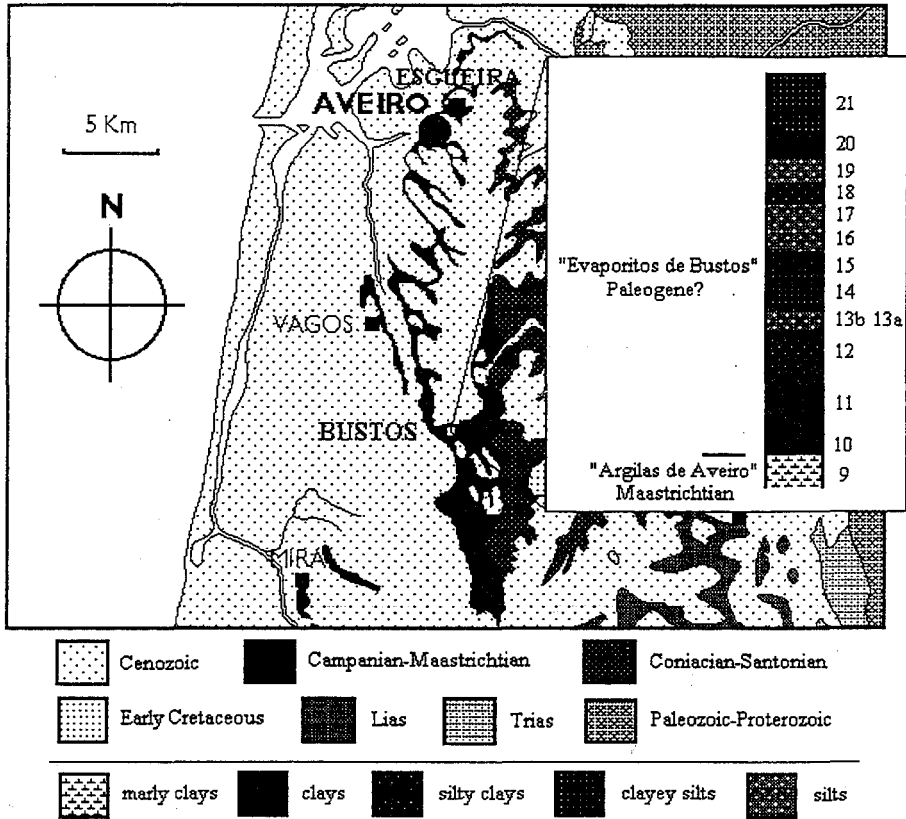


Fig. 1 - Location and geological setting.

The present paper deals with the development of geophysical methods, based mainly on termomagnetic properties of the sediments, for magnetostratigraphic purposes, that is, to discriminate the "Argilas de Aveiro" formation from the overlying "Evaporitos de Bustos" formation.

#### MATERIALS AND METHODS

Magnetic fabric of the sampled sediments is related to the sedimentation prevailing conditions. For its characterization both anisotropy of magnetic susceptibility (AMS) and

anisotropy of remanent magnetization (ARM) were carried out and also, measurements of the initial susceptibility and their temperature dependency.

So far, particular attention was paid to the Bustos outcrop in what concerns the transition between the greenish clays of the "Argilas de Aveiro" formation (Campanian-Maastrichtian) and the overlying black clays corresponding to the basal sediments of the "Evaporitos de Bustos" formation. In order to discriminate both clays the magnetic properties previously referred were determined in samples representing those clays.

## RESULTS AND DISCUSSION

Samples representing the "Argilas de Aveiro" greenish clays, either from Esgueira or Bustos, behave similarly in regards to the magnetic properties being investigated. As a matter of fact, they do not contain ferro or ferrimagnetic minerals and the paramagnetic minerals are much more represented than diamagnetic minerals.

On the other hand, samples representing the "Evaporitos de Bustos" black clays contain ferro and ferrimagnetic minerals and behave consistently, despite a slight variation found along the vertical cross-section.

The available results are consistent with the mineralogical data corresponding to the fine fractions of both clays reported by Rocha & Gomes (1994, 1996). In fact, samples of the greenish clays from "Argilas de Aveiro" collected in both outcrops are characterized by similar composition in regards with both clay minerals (essentially illite+smectite) and the associated non-clay minerals (essentially quartz+K-feldspar). On the other hand, black clays from "Evaporitos de Bustos" are characterized by a distinctive composition in regards with both clay minerals (smectite+illite, smectite being the dominating one) and the the associated non-clay minerals (essentially Fe and Mn oxides/hydroxides, pyrite and iron sulfates).

## REFERENCES

- Mougenot, D. (1989) - Geologia da Margem Portuguesa. *Doc. Técnicos*, 32, Inst. Hidr., Lisboa.
- Rocha, F. (1993) - *Argilas aplicadas a estudos litoestratigráficos e paleoambientais na Bacia Sedimentar de Aveiro*. PhD Thesis, Universidade de Aveiro, 399 p.
- Rocha, F. & Gomes, C. (1994) - *Bol. Soc. Esp. Mineralogia*, 17(1), pp. 12-13
- Rocha, F. & Gomes, C. (1996) - Mineralogical, geochemical and geostatistical analysis of a Cenozoic evaporitic formation eventually from Paleogene in the Aveiro region (Portugal). Subm. to 4th Intern. Symp. Geochem. Earth's Surface, Leeds.

Estación Experimental del  
Zaidín. CSIC. Granada,  
España

## Physicochemical study of the first steps of the transformation of smectite into illite

*Linares J, Huertas F, Caballero E and Jiménez de Cisneros C*

### 1. Introduction.

The transformation of smectite into illite is one of the most important reactions in diagenesis and hydrothermal zones. In spite of the great volume of papers related to these topics, the quantitative aspects of its mechanism and rate are not well known, or at least are controversial. Recently, the use of bentonite as a barrier in radioactive waste disposal has promoted new ways of study, because the smectite around the canister can be transformed into illite due to the action of temperature and the percolation of solutions. To establish the safety of the repositories, the stability or "longevity" of smectite, that is to say, the rate of the transformation reaction of smectite into illite must be known.

During hydrothermal experiences made to determine the suitability of smectite materials as barriers, no detectable signals of physical transformation have been found by routine analytical methods, during reaction times of one year. However, some chemical characteristics related to this reaction underwent measurable changes. This paper is devoted to discuss only this last topic.

### 2. Material and methods.

The original bentonite, from Almeria (Spain), contains 97% of smectite material with quartz, plagioclase and amorphous silica as accessories. A more precise analysis shows that the smectite material is a random smectite-illite mixed-layer with 15% of illite. The bentonite was treated with KCl solutions from 0.025 to 1 M, at temperatures from 60 to 200°C, during 1 to 360 days in Teflon reactors. The bentonite/solution ratio was 1/5. At the end of each experience, solutions and a solid phases were separated and analysed.

### 3. Experimental results.

After hydrothermal reaction, solid phases show no evidences of illite by XRD, ATD-TG and FTIR. Only NMR provide a light possibility of transformation, but variations of pH, silica in solution and potassium content in smectite were observed depending on the temperature, time and potassium in solution.

3.1. Potassium adsorption. It depends essentially on the amount of this cation in the system. The influences of temperature and time are minimal as can be seen in the following equation:

$$K_{ads} = - 0.237 - 0.021T^{\circ}C - 0.010t \text{ (days)} + 1.087 \ln K_{in}$$

where,  $K_{ads}$  is the potassium adsorbed on smectite;  $T^{\circ}C$ , the temperature;  $t$ , the time and  $K_{in}$  the initial potassium concentration in solution.

The maximum amount of  $K_{ads}$  corresponds to the compensation of the total charge of smectite without evidences of irreversible adsorption. This process can be described by Freundlich isotherms:

For 60°C:	$K_{ads} = 0.449(K_{eq})^{0.566}$	For 120°C:	$K_{ads} = 0.462(K_{eq})^{0.518}$
For 175°C:	$K_{ads} = 0.460(K_{eq})^{0.517}$	For 200°C:	$K_{ads} = 0.465(K_{eq})^{0.523}$

$K_{eq}$  is the potassium concentration in the equilibrium solution. These equations show that the process is a typical adsorption one.

Other similar equations in which  $K_{in}$  is substituted by  $K_{eq}$  have been deduced. These last equations permit to calculate the potassium adsorbed from the percolating solution and the time necessarily for the complete substitution of interlayer cations, taking into account the flow rate of groundwaters. The equations obtained are:

For 60°C:	$K_{ads} = 0.376(K_{in})^{0.599}$	For 120°C:	$K_{ads} = 0.394(K_{in})^{0.549}$
For 175°C:	$K_{ads} = 0.398(K_{in})^{0.540}$	For 200°C:	$K_{ads} = 0.395(K_{in})^{0.554}$

As it can be seen, the variations with temperature are minimal. These equations show that the potassium transported by groundwater towards the canister can be adsorbed in smectite promoting its "potassification". Some easy calculations show that, with a slow flow of diluted percolation water, smectite can be converted into K-smectite in relatively short geological times. This is the first step in the conversion of smectite into illite. In an actual case, the percolation solution contains other cations besides potassium. Thus, there will be a competition between all the cations for the interlayer space, and the time for the complete conversion in potassium-smectite will be lengthened.

A semiempiric modellization of the exchange process in which potassium substitutes to Na, Ca and Mg, initially in the interlayer position, has been accomplished. This process takes place in two successive stages. In the first, Na is replaced by K while Ca and Mg are only exchanged, in a second phase, when practically all the Na has been removed (Huertas et al. 1995).

3.2. Silica in solution. The variation of the silica concentration in solution after each hydrothermal experience has two steps. At the beginning, the silica concentration has a fast increase with respect to time, later the variation is attenuated. The first step can be attributed to the dissolution of the minor amounts of non smectitic phases; while the second one will be caused by the transformation of smectite into illite, which is

impoverished in silica. Taking into account the release of silica with time in the second step, it was possible to calculate the kinetic equation of the transformation of smectite into illite. This task has been published elsewhere (Cuadros and Linares, 1996).

The following multiple regression equation is obtained:

$$\ln \text{SiO}_2 = 1.2094 + 0.0208 \text{ T}^\circ\text{C} + 0.0016 t + 0.0060 K_{\text{in}}$$

It shows that the silica content is almost an exclusive function of temperature.

In the repositories, the presence of silica will be a problem because its possible transport from warm to cold zones can promote its precipitation. So, cementation of smectite particles can occur and the swelling of smectite will be impeded.

3.3. pH variations. The variation of the pH values depends essentially on the amounts of silica in solution, coming from the smectite into illite reaction, because the formation of  $\text{SiO}_2\text{H}_2$  polymeric groups impose a strong acid character to the solution. Thus, this parameter can be related also with the first stages of the transformation of smectite into illite. To explore other influences the following equation was obtained:

$$\text{pH} = 7.5749 - 0.0030 \text{ T}^\circ\text{C} - 0.0013 t - 0.0044 K_{\text{in}}$$

This equation shows the minimal importance of each parameter. However, all the parameters have the same negative sign indicating the possibility of environmental acidification when they increase. This acidification can contribute to the canister corrosion; fortunately, as the influence of these parameters is low, the possible acidification near the canister will be small.

3.4. Surface Area. It was measured to obtain some knowledge about the texture of the solid. The following multiple regression equation was calculated:

$$\text{Surface Area} = 532.5937 + 0.0674 \text{ T}^\circ\text{C} + 0.0625 t - 1.8961 K_{\text{in}}$$

The principal parameter affecting the Area is the initial potassium concentration. But the effect of potassium is inverse to those of temperature and time. Thus, surface area increases with both last parameters while decreases with the potassium concentration. Potassium ions are adsorbed into the interlayer space promoting the collapse of the layers. In this way, swelling area, actual crystal size and total surface decrease.

#### 4. References.

-Huertas, F. J., Cuadros, J. and Linares, J. (1995). Modelling of potassium exchange in a natural, polyionic montmorillonite under hydrothermal conditions. *Appl. Geochem.* 347-355.

-Cuadros, J. and Linares, J. (1996). Experimental kinetic study of the smectite-to-illite transformation. *Geochim. Cosmochim. Acta*, 60, 439-453.

Note. This work has been carried out with the financial support of ENRESA (project 70220501).

## Clay mineralogy, geochemistry and paleoenvironmental evolution of Quaternary sediments from the Ovar region (Aveiro, Portugal)

Machado A, Rocha F and Gomes C

### INTRODUCTION

The region under study (Fig. 1) belongs to the Ovar municipality (North of Aveiro) and is part of an extensive littoral region characterized by flat terrains, consisting mainly of old beach deposits of Plio-Pleistocene age and dunar deposits of Holocene age, which cover lower Cretaceous sedimentary formations and the Proterozoic Schist-Grauwacke Complex.

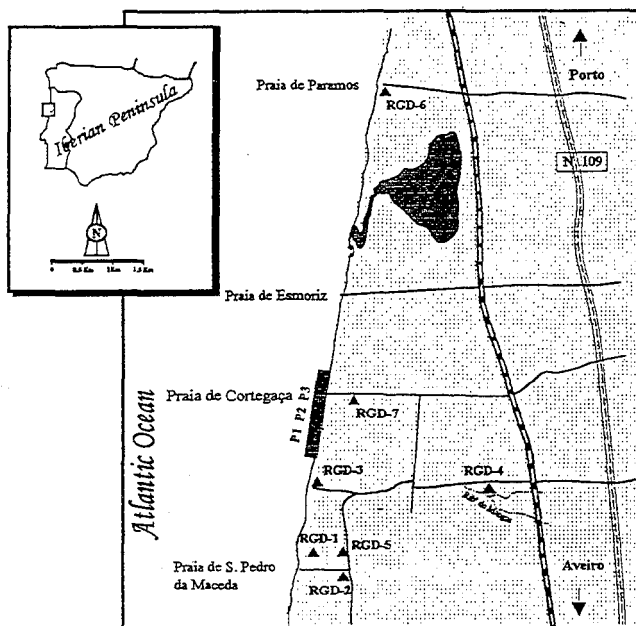


Fig. 1 - Borehole location

Coastal erosion uncovered the so called Cortegaça beach formation. A preliminary study of the mineralogical composition, in particular of the clay fraction, of that formation has been done by Machado et al. (1995). In general terms, the different lithological units are characterized

by the dominance of illite, most probably on dependance of phyllitic rocks dominant in regional terms. Kaolinite is abundant also in some units, whereas smectite, chlorite, vermiculite and irregular 10-14 Å interstratifications are the accessory clay minerals. Iron hidroxides and evaporitic minerals are present in some units. The vertical variation of the illite/kaolinite contents allowed the discrimination of three distinctive sequences, from the basis to the top: 1) greensish sandy clay; 2) greyish sand layers with well marked cross-bedded showing on top a bioturbated podzol; 3) bioturbated beach and dune sand.

Recently, a borehole sampling programme was carried out within the framework of a research project involving teams from the Universities of Aveiro and Minho, aiming at the understanding of the Aveiro lagoon evolution. Seven boreholes reaching in average depths of 40 meters were carried out (Fig. 1).

The main goal of this paper is the use of the fine fractions (silt and clay) mineralogy and geochemistry for the establishment of a fine vertical zonography, able to discriminate and characterize the climatic oscillations that did occur both in the surrounding continental source areas and in the sedimentation environments as well as the morphoclimatic reconstruction.

## MATERIALS AND METHODS

More than three hundred samples from the boreholes and the three beach profiles had been studied. The mineralogical study of these sediments, particularly of the clay components, has been based mainly on X-ray diffraction (XRD) determinations, carried out in both the less than 38 µm and 2 µm fractions. Qualitative and semi-quantitative determination of clay and non-clay minerals has been done in both fractions. For semiquantitative determinations of clay and non-clay minerals, criteria recommended by Schultz (1964) and Thorez (1976) had been followed. Chemical analyses of both major elements (MgO, Al<sub>2</sub>O<sub>3</sub>, SiO<sub>2</sub>, CaO, TiO<sub>2</sub>, Fe<sub>2</sub>O<sub>3</sub>, Na<sub>2</sub>O and K<sub>2</sub>O) and minor elements (Cu, Ni, Co, Zn, Pb, Cd, Mn and Cr), have been carried out using X-ray fluorescence, atomic absorption spectrometry and flame-spectroscopy methods. For the typification and hierarchization of the relationships between mineralogical variables identified and quantified geostatistical analysis was carried out.

## RESULTS AND DISCUSSION

The mineralogical studies make evident a gradual vertical evolution marked by the following main features: 1) dominance of quartz and phyllosilicates in the fine fraction associated to discrete amounts of feldspar and other accessory minerals; evaporite minerals and iron

hydroxides are particularly important in some thin layers; 2) general dominance of illite over kaolinite in the clay fraction with oscillations of either the illite/kaolinite contents or the smectite content. The geochemical data available is consistent with the vertical zonography established on the basis of the mineralogical data, with some particular layers richer in  $Al_2O_3$ ,  $TiO_2$ ,  $Fe_2O_3$ , Cu, Zn, Pb, Mn and Cr.

The illite dominance expresses an environment characterized by low hydrodinamism whereas its gradual enrichment towards the sequence top means that the environment became progressively more confined. The environment changed from a littoral one, supramareal, to a lagunar one and finally to a continental air exposed one.

On the basis of the qualitative and quantitative mineralogy the reconstruction of the climate prevailing at the time of the sedimentary processes responsible for the formation of the different sequences points out to an evolution from a temperate climate, slightly warm, with low contrasting seasons to a more mild temperate climate which in turn changed progressively to a climate characterized by lower temperature and rainfall.

To analyse the virtual climatic oscillations the following parameters had been used: Illite/kaolinite (I/K) and Illite + Chlorite/kaolinite + vermiculite (I + C/K + V). Interpretation of these parameters allowed the definition of several climatic alternating episodes, characterized by more warm and wet climates and more cold and dry climates.

#### REFERENCES

- Machado, A.; Silva, A. P.; Rocha, F. and Gomes, C (1995) - Contribuição da mineralogia das argilas para o estudo paleogeográfico das formações areno-pelíticas da Praia de Cortegaça (Ovar) - *Memória n° 4*, Mus. Lab. Min. Geol. Univ. Porto, 647-652.
- Schultz, L. G. (1964) - Quantitative interpretation of mineralogical composition from X-ray and chemical data for the Pierre Shale. *United States Geological Survey Professional Paper* 391-C, 1-31.
- Thorez, J. (1976) - *Practical identification of clay minerals*. 99pp. (Editions G. Lelotte, Belgique).

(1) Dpto. Química Agrícola,  
Geología y Geoquímica. Fac.  
Ciencias. Univ. Autónoma de  
Madrid, España.

(2) C. Ciencias Medio  
Ambientales. CSIC. Madrid,  
España

## Evidences of stevensite formation from kerolite/stevensite mixed layers. Influence of alkalinity and silica activities

Martín de Vidales J L (1), Pozo M (1) and Casas J (1, 2)

### Introduction

Kerolite (Ke) and kerolite/stevensite (Ke/St) mixed-layers are uncommon Mg clay minerals that are considered to be of low temperature origin. Economic deposits, scarcely distributed in the world, have been recognized in Nevada (USA), Amboseli (Kenya) and Madrid Basin (Spain). Mineralogical research on pink clay lithofacies belonging to the Intermediate Unit of Miocene from Madrid Basin showed that they are composed of nearly pure magnesian 2:1 phyllosilicates of "intermediate character" between end-member kerolite ( $x \sim 0$ ) and stevensite (Martín de Vidales et al 1988). More recently, Martín de Vidales *et al.* (1991) studied the structural features of these materials establishing that consist of random Ke/St mixed layer phases ( $R=0$ ) with 50-80% Ke layers and a very small crystallite size with a mean of three unit-cells stacked in the  $c^*$  direction. Sedimentological research (Pozo & Casas 1995) indicates a shallow lacustrine environment (mud flat) in which Ke/St lithofacies are associated to ponds development where an origin and evolution related both to early diagenetic and pedogenic processes are inferred. The aims of this study were to investigate the crystallochemical and mineralogical variations that show these random mixed-layers and their relation with the sedimentary sequences in the genetic environment. Likewise to establish the chemical conditions for Ke/St mixed layers origin and their evolution.

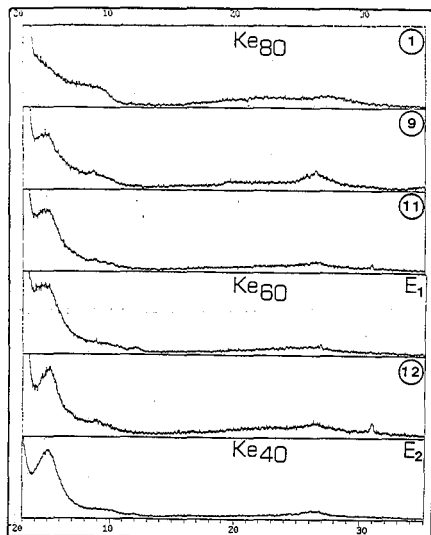
### Materials and methods

Two representative general sections nearby Pinto (P) and Esquivias (E) villages were sampled (Figure 1a). Ke/St deposits can be included in the Magnesian Unit established by Pozo et al (1994) and are made up of pinkish massive lutites and clay clast arenites, alternating with green saponitic mudstones and massive siliciclastic sandy intercalations. In Pinto area is remarkable also the presence of dolocretes affecting mainly the green mudstone lithofacies.

About 50 samples of "pink clays" have been studied. They correspond to nearly pure Ke/St mixed layers with minor (<5%) quantities of dioctahedral illite. In some cases dolomite, calcite, feldspars and quartz were identified as associated minerals. In this work only twelve



On the other hand hydrothermal treatments of sample 1 Ke(80%)/St(20%), lead to nearby similar XRD patterns. Sample 11 (60%Ke/40%St) was obtained from sample 1, treating 0.35-0.50 g of material with 25 ml of 0.2 M NaOH solution at 210°C during 5 days whereas sample 12 (60%Ke/40%St) was obtained from sample 1 following the same treatment adding 0.35



mmole of sodium metasilicate (figure 2. E1 and E2). These results clearly indicate that alkalinity and/or silica increasing in the alteration solutions constrain the solid state transformation of highly kerolitic phases to more stevensitic randomly mixed layers. Experimental data are in agreement with compositional differences observed in the studied areas. The comparison between pink clays from Esquivias and Pinto sedimentary sequences indicate a higher kerolitic character in the former. The increase of stevensite layers observed in samples from Pinto will be explained by a different hydrochemistry in this area, where intensive pedogenic

carbonates formation has been reported (Pozo *et al.* 1995). A correlation between stevensite formation and rise of alkalinity during carbonate precipitation is inferred.

#### References

- MARTIN DE VIDALES, J.L., POZO, M., MEDINA, J.M. & LEGUEY, S. (1988). *Estudios Geol.*, 44, 7-18.
- MARTIN DE VIDALES, J.L., POZO, M., ALIA, J.M., GARCIA NAVARRO, F. & RULL, F. (1991). *Clay Miner.*, 26, 329-342.
- POZO, M. y CASAS, J. (1995). *Boletín Geol. y Min.* 106-3: 265-282.
- POZO, M., CASAS, J. & MORENO, A. (1994) Abstracts of the I.A.S. Meeting Ischia '94
- REYNOLDS, R.C. (1985) NEWMOD, a Computer program for the Calculation of one dimensional Diffraction Patterns of Mixed Layered Clays. R.C. Reynolds, Hanover, U.S.A.
- SUQUET, H. & PEZERAT, H. (1988) *Clays and Clay Miner.* 36, 184-186
- VILA, E. RUIZ-AMIL, A & MARTIN DE VIDALES, J.L. (1994) Computer program for X-ray diffraction analysis, Internal Report, C.S.I.C., Madrid, Spain.

(1) Instituto Andaluz de  
Ciencias de la Tierra. CSIC-  
Universidad. Granada,  
España

(2) Dpto. Mineralogía y  
Petrología. Fac. Ciencias.  
Univ. de Granada, España

## Changes vs. similarities in the clay-mineral composition across the Cretaceous-Tertiary boundary

*Martínez Ruíz F (1), Ortega Huertas M (2) and Palomo I (2)*

### Introduction

The paleoceanographic changes leading to the mass extinction marking the Cretaceous-Tertiary (K/T) boundary are recorded in marine sections by a sharp decrease in carbonate sedimentation as consequence of the decrease in the biological productivity. The nature and composition of the K/T boundary layer and levels above and below this boundary have been used to support extraterrestrial or terrestrial hypothesis. In this paper we present a study of different K/T boundary sections in order to compare their clay mineral associations as well as finding out if they can potentially reflect changes across this boundary. The studied sections belong to the Mediterranean domain (Spain: Agost and Caravaca; Tunisia: El Kef; and Italy: Petriccio) and the Atlantic domain in the Basque-Catabrian Basin (Spain: Sopelana and Zumaya, and France: Hendaye and Biarritz). The K/T boundary is marked by a clayey layer 2-3 mm thick.

### Methods and Results

Representative samples were used for mineralogical analyses (bulk mineralogy and clay minerals) using XRD. TEM-AEM was used for quantitative chemical microanalyses of the clay minerals. The bulk mineralogy is characterized by calcite, phyllosilicates and quartz as main components. The K/T boundary also contain K-feldspar and Fe-oxides spherules, and other trace minerals as celestite, barite, gypsum, ilraenite, rutile or zircon have been detected in the boundary layer and the lowermost danian levels.

The clay mineral associations are different in the two studied domains. In the Mediterranean domain they are characterized by smectites, illite and kaolinite. The micaceous minerals correspond to phengite, illite or mica with a glauconitic trend. The chemical composition of the micaceous minerals and semectites is summarized in Tables 1 and 2. In the Atlantic domain the clay mineral association is characterized by dioctahedral micas (phengite, illite) (Table 1) associated with illite/smectite mixed layers R1, kaolinite and chlorite, there are no smectites. The nature of the clay mineral in the uppermost Maastrichtian and lowermost Danian is also similar.

**Table 1.** Dioctahedral micas formulae (T: Tertiary, K/T: Cretaceous-Tertiary Boundary, C: Cretaceous)

Section	Age	Si	Al <sup>VI</sup>	Al <sup>IV</sup>	Mg	Fe	Ti	∑oct.	K
Agost	K/T	3.44	0.56	0.88	0.25	0.90	-	2.03	0.98
	C	3.26	0.74	1.47	0.05	0.63	-	2.15	0.97
Caravaca	T	3.50	0.50	1.56	0.17	0.17	0.13	1.99	0.98
	K/T	3.47	0.53	1.35	0.10	0.10	-	2.16	0.83
Petriccio	C	3.26	0.74	1.68	0.09	0.18	-	1.95	0.97
	T	3.31	0.69	1.69	0.21	0.21	-	2.11	0.77
	K/T	3.23	0.77	1.21	0.28	0.53	-	2.02	0.98
El Kef	C	3.26	0.74	1.71	0.22	0.090	-	2.02	0.98
	T	3.26	0.74	1.47	0.05	.63	-	2.21	0.99
	K/T	3.26	0.74	1.71	0.22	0.09	-	2.02	0.98
Zumaya	C	3.28	0.72	1.75	0.03	0.20	-	1.98	0.96
	T	3.34	0.66	1.74	0.17	0.30	0.02	2.05	0.96
	K/T	3.19	0.81	1.56	0.04	0.33	0.02	2.05	0.98
Hendaye	C	3.51	0.49	1.66	0.04	0.17	-	1.97	0.79
	T	3.20	0.80	1.76	-	0.22	-	2.01	1.00
	K/T	3.15	0.85	1.79	-	0.20	-	2.02	0.99
	C	3.22	0.78	1.82	-	0.16	-	1.98	0.99

**Table 2.** Smectite formulae

Section	Age	Si	Al <sup>VI</sup>	Al <sup>IV</sup>	Fe	Mg	Ti	∑oct	K	Ca	eint
Agost	T	3.57	0.43	1.30	0.52	0.30	0.05	2.17	0.33	0.01	0.34
	K/T	3.60	0.40	1.40	0.48	0.20	-	2.08	0.35	0.05	0.40
	C	3.65	0.35	1.40	0.50	0.12	0.01	2.03	0.39	0.02	0.41
Caravaca	T	3.69	0.31	1.39	0.50	0.19	0.05	2.13	0.20	0.03	0.23
	K/T	3.66	0.34	1.50	0.38	0.21	0.03	2.12	0.23	-	0.23
	C	3.63	0.37	1.38	0.42	0.22	0.06	2.06	0.27	0.06	0.33
Petriccio	T	3.61	0.39	1.57	0.42	0.21	-	2.02	0.11	0.11	0.22
	K/T	3.64	0.36	1.38	0.54	0.31	0.03	2.26	0.27	0.12	0.39
	C	3.63	0.37	1.59	0.41	0.21	0.03	2.24	0.13	0.11	0.24
El Kef	T	3.66	0.34	1.54	0.44	0.19	-	2.17	0.10	0.09	0.19
	K/T	3.63	0.37	1.57	0.35	0.19	0.03	2.14	0.11	0.13	0.24
	C	3.63	0.37	1.59	0.36	0.21	0.02	2.18	0.11	0.10	0.21

## Discussion and Conclusions

In the Mediterranean domain there are no qualitative changes in the clay minerals associations in the K/T boundary layer, Maastrichtian and Danian levels, being these associations very similar at Agost and Caravaca, which suggests similar sources for the clay minerals and diagenetic processes. The same associations are found at Petriccio and El Kef. This similarity agrees with the same paleogeographical context for those sections, there are no changes across the K/T boundary that can be related to the boundary event. However from a quantitative point of view, in these sections the K/T boundary layer clearly differs from Danian and Maastrichtian levels, with

much higher smectite content, almost a pure smectite at Caravaca. A mixed pedogenetic and volcanogenic origin of the smectite in the Mediterranean domain is likely according to the paleogeography, exposure of local rocks comprising volcanic components and the hydrolyzing climates at that time (Ortega Huertas *et al.*, 1995). But the smectite increase in the boundary layer indicates an additional source. Considering the bulk mineralogy, this layer is characterized by abundant spherules, part of the smectites can derive therefore from the alteration of spherules. The higher percentage of smectites in the boundary layer at Caravaca can be explained by a higher degree of alteration of those spherules. Whereas at Agost we have reported abundant Fe-oxides spherules (Martínez Ruiz *et al.*, 1992) or even glaucony spherules, reported also at Petriccio (Montanari, 1993), at Caravaca we have only reported K-feldspar spherules and just a few very altered Fe-oxides have been observed.

In the Atlantic domain there are no significant changes in mineralogy marking the boundary neither from a qualitative point of view nor quantitative. REE patterns are also similar in the K/T layer than in Maastrichtian and Danian levels (Ortega Huertas *et al.*, 1995). The clay mineral associations can be related to the erosion of the exposed areas and denudation of the paleozoic massifs and mesozoic sediments which supplied clay minerals to the basin, an active uplift and erosion prevented the formation of pedogenetic smectite. Those clay mineral associations also reflect diagenetic processes modifying the original clay mineral supply, the existence of illite/smectite mixed layers R1 is attributed to the degree of burial diagenesis.

As consequence, there is no global trends in the clay mineral associations that reflect a global change, the clay mineral associations are related to regional factors. No chemical differences have been observed in the K/T boundary smectites that could support an extraterrestrial hypothesis. The clay mineral associations can not be used therefore as support of extraterrestrial or terrestrial hypothesis.

### References

- Elliot WC, Aronson JL, Millarad HT Jr and Gierlowoski-Kordech, E. (1989). *Geol. Soc. Am. Bull.*, 101:702-710.
- Martínez Ruiz F, Ortega Huertas M, Palomo I and Barbieri M. (1992). *Chem. Geol.*, 95: 265-281.
- Montanari A. (1991). *J. Sed. Petrol.*, 671: 315-339.
- Ortega Huertas M, Martínez Ruiz F, Palomo I and Chamley H. (1995). *Sed. Geol.*, 94: 209-227.

### Acknowledgements

This paper was support by Spanish Projects PB-92-0960 and PB-92-0961 (DGICYT) and Research Group 4065 of "Junta de Andalucía".

**Table 1.** Dioctahedral micas formulae (T: Tertiary, K/T: Cretaceous-Tertiary Boundary, C: Cretaceous)

Section	Age	Si	Al <sup>VI</sup>	Al <sup>IV</sup>	Mg	Fe	Ti	∑oct.	K
Agost	K/T	3.44	0.56	0.88	0.25	0.90	-	2.03	0.98
	C	3.26	0.74	1.47	0.05	0.63	-	2.15	0.97
Caravaca	T	3.50	0.50	1.56	0.17	0.17	0.13	1.99	0.98
	K/T	3.47	0.53	1.35	0.10	0.10	-	2.16	0.83
Petriccio	C	3.26	0.74	1.68	0.09	0.18	-	1.95	0.97
	T	3.31	0.69	1.69	0.21	0.21	-	2.11	0.77
	K/T	3.23	0.77	1.21	0.28	0.53	-	2.02	0.98
El Kef	C	3.26	0.74	1.71	0.22	0.090	-	2.02	0.98
	T	3.26	0.74	1.47	0.05	.63	-	2.21	0.99
	K/T	3.26	0.74	1.71	0.22	0.09	-	2.02	0.98
Zumaya	C	3.28	0.72	1.75	0.03	0.20	-	1.98	0.96
	T	3.34	0.66	1.74	0.17	0.30	0.02	2.05	0.96
	K/T	3.19	0.81	1.56	0.04	0.33	0.02	2.05	0.98
Hendaye	C	3.51	0.49	1.66	0.04	0.17	-	1.97	0.79
	T	3.20	0.80	1.76	-	0.22	-	2.01	1.00
	K/T	3.15	0.85	1.79	-	0.20	-	2.02	0.99
	C	3.22	0.78	1.82	-	0.16	-	1.98	0.99

**Table 2.** Smectite formulae

Section	Age	Si	Al <sup>VI</sup>	Al <sup>IV</sup>	Fe	Mg	Ti	∑oct	K	Ca	εint
Agost	T	3.57	0.43	1.30	0.52	0.30	0.05	2.17	0.33	0.01	0.34
	K/T	3.60	0.40	1.40	0.48	0.20	-	2.08	0.35	0.05	0.40
	C	3.65	0.35	1.40	0.50	0.12	0.01	2.03	0.39	0.02	0.41
Caravaca	T	3.69	0.31	1.39	0.50	0.19	0.05	2.13	0.20	0.03	0.23
	K/T	3.66	0.34	1.50	0.38	0.21	0.03	2.12	0.23	-	0.23
Petriccio	C	3.63	0.37	1.38	0.42	0.22	0.06	2.06	0.27	0.06	0.33
	T	3.61	0.39	1.57	0.42	0.21	-	2.02	0.11	0.11	0.22
	K/T	3.64	0.36	1.38	0.54	0.31	0.03	2.26	0.27	0.12	0.39
El Kef	C	3.63	0.37	1.59	0.41	0.21	0.03	2.24	0.13	0.11	0.24
	T	3.66	0.34	1.54	0.44	0.19	-	2.17	0.10	0.09	0.19
	K/T	3.63	0.37	1.57	0.35	0.19	0.03	2.14	0.11	0.13	0.24
	C	3.63	0.37	1.59	0.36	0.21	0.02	2.18	0.11	0.10	0.21

## Discussion and Conclusions

In the Mediterranean domain there are no qualitative changes in the clay minerals associations in the K/T boundary layer, Maastrichtian and Danian levels, being these associations very similar at Agost and Caravaca, which suggests similar sources for the clay minerals and diagenetic processes. The same associations are found at Petriccio and El Kef. This similarity agrees with the same paleogeographical context for those sections, there are no changes across the K/T boundary that can be related to the boundary event. However from a quantitative point of view, in these sections the K/T boundary layer clearly differs from Danian and Maastrichtian levels, with

much higher smectite content, almost a pure smectite at Caravaca. A mixed pedogenetic and volcanogenic origin of the smectite in the Mediterranean domain is likely according to the paleogeography, exposure of local rocks comprising volcanic components and the hydrolyzing climates at that time (Ortega Huertas *et al.*, 1995). But the smectite increase in the boundary layer indicates an additional source. Considering the bulk mineralogy, this layer is characterized by abundant spherules, part of the smectites can derive therefore from the alteration of spherules. The higher percentage of smectites in the boundary layer at Caravaca can be explained by a higher degree of alteration of those spherules. Whereas at Agost we have reported abundant Fe-oxides spherules (Martínez Ruiz *et al.*, 1992) or even glaucony spherules, reported also at Petriccio (Montanari, 1993), at Caravaca we have only reported K-feldspar spherules and just a few very altered Fe-oxides have been observed.

In the Atlantic domain there are no significant changes in mineralogy marking the boundary neither from a qualitative point of view nor quantitative. REE patterns are also similar in the K/T layer than in Maastrichtian and Danian levels (Ortega Huertas *et al.*, 1995). The clay mineral associations can be related to the erosion of the exposed areas and denudation of the paleozoic massifs and mesozoic sediments which supplied clay minerals to the basin, an active uplift and erosion prevented the formation of pedogenetic smectite. Those clay mineral associations also reflect diagenetic processes modifying the original clay mineral supply, the existence of illite/smectite mixed layers R1 is attributed to the degree of burial diagenesis.

As consequence, there is no global trends in the clay mineral associations that reflect a global change, the clay mineral associations are related to regional factors. No chemical differences have been observed in the K/T boundary smectites that could support an extraterrestrial hypothesis. The clay mineral associations can not be used therefore as support of extraterrestrial or terrestrial hypothesis.

### References

- Elliot WC, Aronson JL, Millarad HT Jr and Gierlowoski-Kordech, E. (1989). *Geol. Soc. Am. Bull.*, 101:702-710.  
Martínez Ruiz F, Ortega Huertas M, Palomo I and Barbieri M. (1992). *Chem. Geol.*, 95: 265-281.  
Montanari A. (1991). *J. Sed. Petrol.*, 67: 315-339.  
Ortega Huertas M, Martínez Ruiz F, Palomo I and Chamley H. (1995). *Sed. Geol.*, 94: 209-227.

### Acknowledgements

This paper was support by Spanish Projects PB-92-0960 and PB-92-0961 (DGICYT) and Research Group 4065 of "Junta de Andalucía".

Dpto. Ciencias de la Tierra.  
Area de Cristalografía y  
Mineralogía. Fac. Ciencias.  
Univ. de Zaragoza, España

## Clay deposits from oriental sector of Calatayud basin (Spain): mineralogy and geochemistry

*Mayayo M J, Bauluz B and González López J M*

### Geological setting

The analysed rocks belong to Miocene infill of Calatayud Basin, located between the two branches, Castilian and Aragonese of the Iberian Range. The studied samples correspond to several profiles and holes that were collected at, and close to, the sepiolite deposit of Mara (Zaragoza) which is mining nowadays. Miocene sediments were originated from weathering of Paleozoic quartzites, sandstones and shales in Vicort and La Virgen Mountains which constitute the northeastern edge of the basin. These sediments show noteworthy variation of facies both horizontally and vertically. Their sequential distribution consists of coarser detrital facies in marginal zones, clays and marly facies in transitional zones, and evaporitic facies at central sectors of the basin. These are characteristic deposits of playa-lake and/or ephemeral lake environments, at arid to semiarid climatic conditions.

### Mineralogy

On the basis of mineralogical composition (determined by X-ray diffraction), the following lithological groups have been established: Al-clays, Mg-clays, marls, carbonates and sulphates, which are dominated by illite, Mg-smectite and/or sepiolite, mixtures of clay with dolomite, dolomite and gypsum, respectively. Calcite, quartz and feldspars are minor components. Fine fractions of these samples are mainly constituted by clay minerals: illite, beidellite, stevensite-saponite, palygorskite and sepiolite depending on their lithology.

The variation of crystallochemical parameters of illites from silt and clay fractions is not significative and it appears to be within the margins of experimental error. Illites exhibit low to very low degree of phengitization and paragonitization, and therefore muscovitic compositions which, together with their crystallinities, indicate that they are detrital in origin. Crystals of sepiolite, analyzed by AEM-TEM, present a tetrahedral substitution up to 0.46 Al atoms, and/or 0.15 Fe atoms by unit cell, whereas the octahedral content ranges between 0.01 and 0.45 Fe atoms, and 7.3 and 8.0 Mg atoms. The Mg-smectites are intermediate members of stevensite-saponite series on the basis of their charge distribution (Güven, 1988), and their total octahedral content oscillates from 2.32 to 2.66 atoms by unit formula.

## Geochemistry and statistical study

Distribution of major elements in the established lithological groups reveals the inherited versus neophormed character of the phases from analyzed samples. Thus, the immobile elements Al, Ti and K are notably enriched in Al-clays, whereas the more mobile elements, such as Ca and Mg are concentrated in neophormed phases, represented by Mg-clays, carbonates and sulphates. Immobile trace elements, such as rare elements (REE) transition trace elements (TTE), Y, Th, Zr, and Nb are positively correlated with Al, Ti and K. Sulphates and carbonates are relatively enriched in Sr, reflecting the similar behavior of this element with Ca. Marly facies exhibit the highest contents in Li, as it was pointed out by Tardy et al (1972) in other countries. The normalized to PAAS (Post-Archean Australian Shales) REE patterns from facies dominated by inherited and neophormed phases are different too. The relatively immobile behavior of lanthanides is reflected in low REE contents of evaporitic facies, and relatively higher REE contents in detrital facies. In these last facies, the selective depletion in HREE can be attributed to the preferential removal of these elements in the alkaline stages of weathering (Balashov et al, 1964; Cantrell & Byrne, 1987).

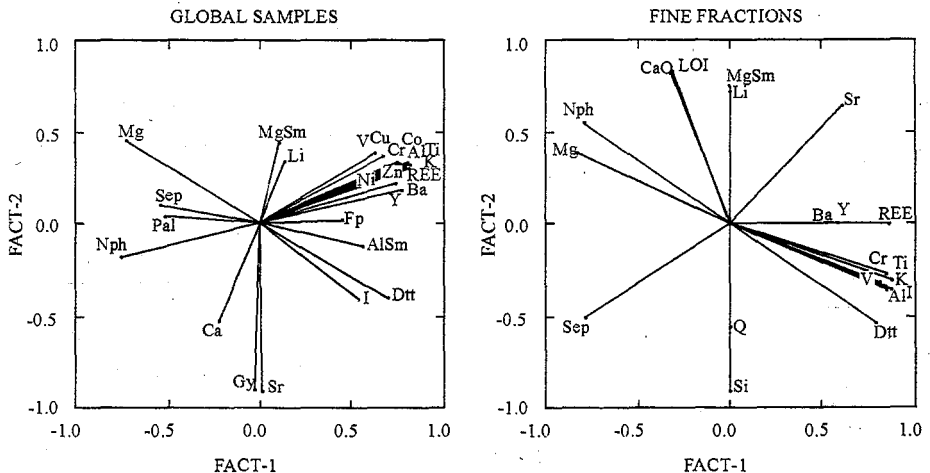
R-mode factor analysis carried out on data obtained from chemical and mineralogical analyses of global samples results in a three factor model that explain about the 68% of total variance. Variables with high positive loadings on the first factor (32% of variance) are  $Al_2O_3$ ,  $K_2O$ ,  $TiO_2$ , REE, TTE, etc., i.e. elements concentrated in detrital phases, whereas those with negative loadings are MgO, sepiolite and palygorskite (fibrous clays). The second factor accounts for the 23% of variance of data set, and exhibits positive loadings for LOI, dolomite and CaO, and negative loadings for sepiolite, palygorskite, illite and associated elements but with less statistical weight than on factor 1. Variables with highest loadings on the third factor are gypsum, Sr and Ca, on the positive side, versus Mg-smectite and Li, on the negative one, but these with relatively lower loadings.

If only samples from transitional zones are considered, the three factor model accounts for about the 71% of total variance. In this case, the difference observed with respect to the above consists in the variables showing high loadings on the third factor. They are only Mg-smectites and Li, but with a greater statistic weight than the above case. This fact seems to reflect the preferential fixation of Li on the neophormed layer silicates.

The geochemistry of fine fractions also reflects the origin of different clay minerals. Thus, detrital Al-clays show enrichments in REE, TTE, Y, Th, Zr, and Nb, whereas neophormed Mg-clays represent the opposite pole. It is noteworthy the clear enrichment in Li that the Mg-smectites present. The preferential fixation of this element more in layered clays than in fibrous ones has been attributed to the ability of Li to balance the negative octahedral charge which is commonly present in the former clays and normally absent in chain lattice clays.

Factor analysis of carbonate-free fine fractions reveals a three factor model that accounts for about the 78% of total variance. Variables associated to detrital clays ( $\text{Al}_2\text{O}_3$ ,  $\text{K}_2\text{O}$ ,  $\text{TiO}_2$ , REE, etc.) have positive loadings on the factor 1 (46%), and those associated with fibrous clays have negative loadings. Mg-smectites and their accompanying elements (Mg, Ca, Sr, Li) show high positive loadings on the factor 2 (22%), whereas the rest of phyllosilicates present negative, lower loadings. On the third factor, TTE are the only variables showing high loadings, suggesting that these elements are possibly associated with other non-phyllosilicate phases such as Fe-Mn oxi-hydroxides and feldspars.

The REE contents of fine fractions that are remarkably enriched in a particular clay mineral seem also to reflect their origin. Thus, among the neophormed phases, sepiolite shows the lowest REE content reflecting their formation by precipitation from  $\text{SiO}_2$ -and-Mg-rich solutions which are depleted in REE. Samples which have as principal components Al-smectite and illite present a higher REE content. These clays show REE patterns slightly above of the PAAS pattern, whereas those of Mg-smectite are slightly beneath it. This last fact could be due to the possible formation of these clay from a "precursor" clay by "transformation" processes, with a concomitant "memory" of chemistry of precursor in the neophormed clay, together with the relatively closed characteristics of their genetic environment.



Balashov Y A, Ronov A V, Migdisov A A & Turanskaya N V (1964). *Geoch. Int.*, **10**, 951-969.

Cantrell K J & Byrne R H (1987). *Geochim. et Cosmochim. Acta*, **51**, 597-605

Güven N (1988). *Reviews in Mineralogy*, **19**, 497-552.

Tardy Y, Krempp G & Trauth N (1972). *Geochim. et Cosmochim. Acta*, **36**, 397-412.

(1) Dpto. Ciencias de la Tierra.  
Área de Cristalografía y  
Mineralogía. Fac. Ciencias. Univ.  
de Zaragoza, España

(2) Dpto. Mineralogía y  
Petrología. Fac. Ciencias. Univ.  
de Granada, España

(3) Instituto Andaluz de Ciencias  
de la Tierra. CSIC-Universidad.  
Granada, España

## The deposit of sepiolite-smectite at Mara (Calatayud basin)

Mayayo M J (1), Torres Ruíz J (2), González López J M (1), López  
Galindo A (3) and Bauluz B (1)

The deposits of sepiolite, palygorskite and Mg-smectite studied are located in the marly-carbonate transitional facies of the Calatayud-Daroca subbasin, a Tertiary basin adjacent to that of the River Ebro, filled with Miocene lacustrine sediments. The sector studied is located between the villages of Mara, Orera and Ruesca. These deposits were formed in continental alkaline lacustrine environments, during periods of tectonic calm, in warm climates with semiarid or seasonally arid conditions. The mineralized intervals are made up of alternating layers of clays, marls and carbonates, with variable thickness ranging from 10 cm to 1 m, the mean values being 50-60 cm. These alternances constitute repetitive sequences of 1-3 metres thick which seem to represent short cycles shallowing upwards made up of clays and/or marls with a layer of palustrine carbonates at the top.

### Mineralogy

The samples studied have a complex mineralogy, within which groups of different origins may be distinguished:

**Detritic minerals:** The main detritic minerals are illite  $\pm$  interstratified illite-smectite and quartz, with proportions of up to 61% and 38%, respectively. Although less common than the above minerals, Al-smectite is also relatively abundant, with contents of up to 15%. The remaining detritic minerals (chlorite, kaolinite, K-feldspar and plagioclase) are found as minor phases or entirely absent from many samples.

**Neoformed silicates:** These are main components of almost all the clayey samples, with contents of up to 88%. The most abundant phases are sepiolite and Mg-smectite, in proportions of up to 80% and 50%, respectively. Palygorskite is a less common phase, with values of up to 17% being recorded. Clinoptinolite has also been observed, though in quantities of less than 5%.

Sepiolite is essentially present in the form of masses of interweaving fibres, 5-10  $\mu\text{m}$  in size. Growths of sepiolite fibres, in fine filaments, are often observed on planar phyllosilicate agglomerates. Fibrous-filamentous groupings, sometimes in a bundle-like form, are also observed, though to a lesser extent. Palygorskite is present as fibrous groupings similar to those of sepiolite and, less frequently, as single fibres in sizes of up to 100  $\mu\text{m}$  in length. Clinoptinolite is found in the form of agglomerates of idiomorphous prismatic crystals, usually sized between 50 and 100  $\mu\text{m}$ , filling small fissures and holes in a clayey matrix.

**Carbonates:** These are basically of dolomitic composition. The predominant textures are micrites, with patchy distributed zones of microsparite which are more prevalent in finer-grained carbonates. They are characteristic of a neomorphic fabric. Chemically, they are non-stoichiometric, with molar  $\text{MgCO}_3$  contents ranging from 44.5% to 47.7% and average values of 42.25 ( $\pm$  1.43) %. They are disordered and present anhedral to subhedral morphologies. All these features are characteristic of primary or very early diagenetic

dolomites, and indicative of formation at low temperature.

*Phosphates:* Some clay levels occasionally present varying quantities of apatite which can represent up to 35% of the total weight. It occurs as small idiomorphous crystals, with maximum dimensions of 2-4  $\mu\text{m}$ . It has values of  $a = 9.3619 \text{ \AA}$  and  $\Delta 2\theta (004)-(410) = 1.52$ , an F content of around 3.7% and little substitution of  $\text{PO}_4^{3-}$  by  $\text{CO}_3^{2-}$  ( $\text{CO}_2 = 0.91 - 1.27$ ).

## Chemistry

Sepiolite shows little substitution of Si by  $\text{Al}^{\text{IV}}$  and a varying amount of  $\text{Fe}^{\text{IV}}$  (up to 0.22 per unit cell). Palygorskite has a wide range of substitution of Si by  $\text{Al}^{\text{IV}}$  (from 0.27 to 0.95 atoms per unit cell), an octahedral occupancy varying between 3.79 and 3.99 atoms of  $\text{Al}+\text{Mg}+\text{Fe}$ , with predominance of the first two, and is rich in potassium compared with other sedimentary palygorskites cited in the literature. Illite presents a notable degree of homogeneity in the tetrahedral and octahedral layers and a great variability in potassium content (from 0.6 to 0.8 atoms).

The compositional study of smectites reveals the existence of three groups: dioctahedral (beidellite-type), di-trioctahedral and trioctahedral (saponite and stevensite type) smectites. The beidellites have an average tetrahedral charge ranging from 0.25 to 0.50 and an octahedral occupancy of 2.1 to 2.2 atoms by half unit cell. The di-trioctahedral smectites exhibit a slight tetrahedral substitution (up to 0.17 atoms of Al for four positions) and an average Mg/Al octahedral ratio of 1.8. These smectites can be considered Al-stevensites. The stevensites have a very low Fe content and an average octahedral Al content of 0.25 atoms. Finally, saponite has a mean tetrahedral Al content of 0.39 atoms and an octahedral occupancy of 2.66 atoms.

The major and trace elements constitute well differentiated groups, depending on the nature and origin of the minerals. Thus, Al, Fe, K, Ti, REE, Sc, V, Cr, Co, Ni, Zr, Nb, Hf, Th, Cs, Rb and B are found as part of the detritic fraction of the samples, Mg is mainly found in the neoformed phyllosilicates and/or in dolomites, while Ca forms a fundamental part of the carbonates (calcites and/or dolomites). F is the only minor element that is found in relation to the neoformed phyllosilicate content, being especially concentrated in sepiolite. Furthermore, analysed calcites present the following molar ratio mean values:  $\text{Sr}/\text{Ca} = 2.1 \times 10^{-4}$ ,  $\text{Na}/\text{Ca} = 1.4 \times 10^{-3}$ , and  $\text{Mg}/\text{Ca} = 0.016$ . The values for their equilibrium solutions were  $1.6 \times 10^{-3}$ , 58 and 0.44, respectively, suggesting that these solutions are similar in composition to Na-enriched meteoric waters. The corresponding values for analysed dolomites were:  $\text{Sr}/\text{Ca} = 4.9 \times 10^{-4}$ ,  $\text{Na}/\text{Ca} = 7.9 \times 10^{-3}$ , and  $\text{Mg}/\text{Ca} = 0.857$ , and the values for solutions were  $8.2 \times 10^{-3}$ , 633 and 7.1, respectively. These values indicate that the dolomitizing brines were similar in composition to Na-enriched seawater (Drever, 1982). The distribution patterns of REE normalised to North American Shale Composite (NASC) for the whole sample show a noticeable progressive depletion of heavy REE (HREE).

## Isotopic analysis

*Carbonates:* The  $\delta^{18}\text{O}$  values of micritic calcites range from -8.6 to -7.0‰ (PDB), that correspond to calcites precipitated in isotopic equilibrium with waters of  $\delta^{18}\text{O}$  values between -5.8 and -4.7‰ (SMOW), respectively (Anderson & Arthur, 1983). These waters are clearly meteoric in origin. Dolomicrites show a wide  $\delta^{18}\text{O}$  range, from +2.9 to -5.4‰ (PDB), which corresponds to solutions that are clearly more evolved than meteoric waters, probably as a consequence of evaporative concentration. The positive correlation ( $r = 0.89$ )

existing between Na-content and  $\delta^{18}\text{O}$  values of dolomicrites seems to confirm this hypothesis.

**Silicates:** The values found are:  $\delta^{18}\text{O}$  (illite) = +18.6 ‰ (SMOW),  $\delta^{18}\text{O}$  (sepiolite) = +14.0 ‰,  $\delta^{18}\text{O}$  (Mg-smectite) = +17.3 ‰ and  $\delta^{18}\text{O}$  (silica) = +27.8 ‰. According to the silica-water fractionation equation of Clayton *et al.* (1972) in an environmental temperature range of 25-30 °C, it can be concluded that this silica precipitated in waters of clearly meteoric origin. The application of the smectite-water isotopic fractionation equation (Savin and Lee, 1988) for the same temperature range produces values that are isotopically very similar to those for silica precipitation.

## Conclusions

REE and transition trace elements of the first series, on the one hand, and F content, on the other, can be used to distinguish between inherited phyllosilicates and those formed by chemical precipitation in the depositional basins.

The textural and geochemical characteristics of neoformed phyllosilicates seem to show that sepiolite and Mg-smectite correspond to primary phases originated by precipitation from basin solutions in a lacustrine environment under arid/semiarid climatic conditions, whereas palygorskite is derived from postdepositional processes from the transformation of detrital aluminosilicates. Clinoptinolite is also formed by diagenetic processes filling the micropores and microfissures of samples.

The apatite concentrations are formed by the diagenetic recrystallization of vertebrate bones, which are relatively frequent in these stratigraphic sequences in neighbouring zones (Andrés *et al.*, 1992) as well as in other deposits of fibrous and Mg-smectite clays (e.g. Tajo basin, Morales *et al.*, 1992).

Carbonates are of edaphic origin, with the C mainly being provided by the decomposition of C<sub>3</sub> plants.

Sepiolite, Mg-smectite and cryptocrystalline silica all formed in equilibrium with surface solutions of similar isotopic fractionation. These are different from the solutions in equilibrium with palygorskite and carbonates, which are isotopically heavier and related to more evaporated solutions.

*This research has been financed by the project AMB93-0794 (CICYT) and by groups 4065 and 4028 of the Autonomous Government of Andalucía.*

## References

- Anderson, T.F. & Arthur, M.A. (1983): Stable isotopes of oxygen and carbon and their application to sedimentologic and paleoenvironmental problems. In: M.A. Arthur, T.F. Anderson, I.R. Kaplan, J. Veizer and L.S. Land (Eds.), *Stable Isotopes in Sedimentary Geology. SEPM Short Course* Nº 10, Soc. Econ. Paleont. Mineral, Tulsa, OK.
- Andrés, J.A., Canudo, J.I., Cuenca, G & Laplana, C. (1992): Los vertebrados del terciario continental de la mina de sepiolita de Mara (Prov. de Zaragoza). VIII Jornadas de Paleontología (resúmenes). Museu de Geologia de Barcelona y Sociedad Española de Paleontología, 3-4.
- Clayton R N, O'Neil J R & Mayeda T K (1972). Oxygen isotope exchange between quartz and water. *J. Geophys. Res.*, **77** (17), 3057-67.
- Drever, J.I. (1982): *The geochemistry of natural waters*: Prentehall, Englewood Cliffs, N.J., 388 pp.
- Morales J, Capitán J, Calvo J P & Sesé C (1992). Nuevo yacimiento de vertebrados del Mioceno Superior al Sur de Madrid (Cerro Batallones, Torrejón de Velasco). *Geogaceta*, **12**, 77-80.
- Savin S M & Lee M (1988). Isotopic studies of phyllosilicates. In "Hydrous phyllosilicates (exclusive of micas)" (Bailey S W, Ed.). *Rev. in Miner.*, **19**. Miner. Soc. Amer. 189-223.

## Ce-anomalies in the textural components of upper Cretaceous karst bauxites from the Apulian carbonate platform

Mongelli G

Bauxitization is a weathering process which is today restricted to a narrow range of wet tropical climatic conditions. During this process occurs a fractionation of major, minor, and trace elements. In southern Italy, in shallow-water carbonate sediments, are interbedded Upper Cretaceous bauxites. Their texture is mostly made by iron-rich ooids embedded in a pelitomorphic matrix. In a preliminary study (Mongelli, 1994) an important chemical fractionation has been recognized between ooids and matrix of karst bauxites from the Apulian carbonate platform. A major feature of this fractionation, which involves the REE, is the occurrence of large positive Ce-anomalies in the matrix.

The samples, red in colour and with ooidic texture, were collected from two sites in the Spinazzola area. Three samples were sampled along a vertical profile in the lowermost part of a deposit filling a canyon-like karst cavity. A fourth sample was sampled in a deposit filling a sinkhole. After mechanical disaggregation of the rock, intact ooids have been hand-picked and the ooids depleted fine matrix ( $<32 \mu\text{m}$ ) has been separated by wet sieving. Mineralogical analyses were performed by XRD ( $\text{NiK}\alpha$  radiation). Elemental concentrations were obtained by XRF and INAA. Microscopic observations were carried out by a SEM equipped with an ED X-ray spectrometer.

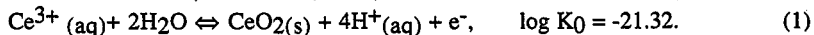
Boehmite, hematite, anatase and kaolinite are the phases detected by XRD in the bulk samples. The ooids, particles of concentric structure formed by irregular shells, consist mainly of hematite with minor boehmite and anatase. In the pelitomorphic matrix boehmite prevails on hematite, kaolinite and anatase. Backscatter electron images and EDX determinations reveal the occurrence of a REE-bearing Ca-fluorocarbonate occurring only in the matrix, as pore filling aggregates, and having a large positive Ce-anomaly ( $\text{Ce}/\text{Ce}^*=5.8$ ). The fluorocarbonates of the bastnäsite group are the most frequent REE minerals in karst bauxites and are concentrated on the alkaline barrier of the footwall limestone (Maksimovic and Pantó, 1996). The  $\text{RE}_2\text{O}_3/\text{CaO}$  ratio ( $\approx 13$ ) of the aggregates suggest affinity for the mineral parisite [ $\text{REE}_2\text{Ca}(\text{CO}_3)_3\text{F}_2$ ].

The bulk samples, normalized to the chondrite, are depleted in Si, Fe, Mn, Mg, Ca, Na, K, Sr, Cr and Ni and enriched in Ti, Al, Rb, Ba, Sc, V, Th, U, Nb, Zr and Y. They show variability in the LREE (La 300-360x chondritic) and a narrower range in HREE contents (Yb 27-38x chondritic). The  $\text{Eu}/\text{Eu}^*$  index varies from 0.70 to 0.80, and the  $\text{Ce}/\text{Ce}^*$  ratio changes within a 0.72-1.26 range. The distribution of the "mobile" trace elements Rb, Sr, Ba, Ni and Cr in the samples collected along the vertical profile display a downward enrichment similar to those observed in deposits bauxitized "in situ" at the expense of matrix-like material collected in the karst zone (Maksimovic et al., 1991). The progressive enrichment

has been attributed to the role played by the carbonate footwall as pH barrier for the downward percolating solutions.

A chemical fractionation occurs between ooids and matrix. Fe is enriched and Si, Ti and Al are depleted in the ooids relative to the matrix. For the trace elements, a preferential concentration of Th, Zr, Y, Sc, V and REE but Ce, and a depletion of Nb and Ni is observed in the ooids. Sr, Rb, Ba, U and Cr show a more erratic behaviour. Ce is mostly concentrated in the matrix which has positive Ce-anomaly. The Ce/Ce\* ratio of the matrix changes within a 1.50-3.02 range. The ooids have higher (La/Yb)<sub>ch</sub> index and show negative Ce-anomaly with a Ce/Ce\* ratio changing within a 0.35-0.97 range. The Eu/Eu\* index is constant among the textural components.

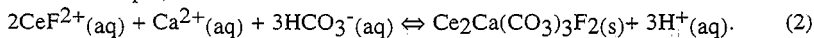
Although the REE have very similar chemical properties, they suffer interelemental fractionation during the weathering processes. The weathered material can be enriched in light-REE (LREE) and depleted in heavy REE (HREE) relative to the parent rock, and it can show positive Ce-anomalies due to the Ce<sup>3+</sup>→Ce<sup>4+</sup> redox change. Braun et al. (1990) demonstrated that positive Ce-anomalies in lateritic profiles are mineralogically related to the precipitation of cerianite (CeO<sub>2</sub>). In the analyzed bauxites, the only Ce-bearing secondary phase detected is the fluorocarbonate. In the lattice of Ca-fluorocarbonates, which consists of (REEF), (CO<sub>3</sub>) and [Ca(CO<sub>3</sub>)] layers, a trivalent RE atom is bonded to three F and six O atoms to form 9-coordinate polyhedron. A major question related to the occurrence of the bauxitic fluorocarbonate is the strong fractionation observed between Ce<sup>3+</sup> and the other REE. In some karst deposits Ce does not exhibit the preferential enrichment "per descensum" observed for the other REE (Maksimovic & Pantó, 1996). This fractionation, which involves a Ce concentration in the uppermost part of the karst deposits, has been attributed to the Ce<sup>3+</sup>→Ce<sup>4+</sup> redox change. Karst bauxites having hematite as prevailing iron phase are generally associated to a vadose, highly oxidizing, environment of formation and the meteoric water, enriched in mobile elements, percolates through the material. The cerium oxidation and the consequent CeO<sub>2</sub> precipitation may occur, in the 5 to 6 pH range and assuming a Ce activity of 10<sup>-9</sup> M, for Eh values ranging between 0.38 V and 0.61 V, via the reaction (Braun et al., 1990):



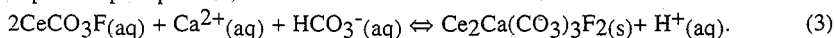
In a vadose environment similar Eh conditions can be easily encountered, and the cerianite precipitation in the uppermost part of a bauxite deposits should consequently originate a Ce-depletion in the percolating solutions. A confirm of the existence of Ce-depleted solutions may be represented by the negative Ce-anomalies observed in the ooids: these anomalies and the REE enrichment of the ooids likely indicate that Ce-depleted solutions has been scavenged by the iron oxide, which can host trivalent cation impurity in lattice positions. Schwertmann & Murad (1983) observed maximum hematite formation in the 7-8 pH range and at near-neutral to basic pH carbonate and phosphate REE-complexes prevail (e.g. Lee & Byrne, 1992). Carbonate and phosphate complexes show an increase in stability with increasing atomic number and this, in turn, can explain the higher (La/Yb)<sub>ch</sub> observed in the ooids relative to the matrix.

A decrease of the pH of the surficial solutions, possibly due to a decrease of the ionic strength, can cause the conversion of Ce<sup>4+</sup> to Ce<sup>3+</sup> in the uppermost part of karst deposit.

Acidic percolating solutions can mobilize  $Ce^{3+}$  as fluoride complex (Wood, 1990) and further cerium can precipitate as parisite in the matrix voids, toward the carbonate footwall barrier at alkaline pH, via the reaction:



Alternatively, the conversion of  $Ce^{4+}$  to  $Ce^{3+}$  can be due to an Eh decrease, possibly related to a rise of the ground water level. Ground waters have generally near-neutral to slightly alkaline pH and in a similar condition cerium is not stable as fluoride complex. The existence of a REE mixed carbonate-fluoride complex, although it has not been proved, has been suggested (e.g. Wood, 1990). A fall of the ground water level in the bauxite deposit may induce a cerium transport as  $CeCO_3F(aq)$  toward the carbonate footwall barrier, and thus the parisite precipitation, via the reaction:



#### REFERENCES

- Braun J J, Pagel M, Muller J P, Bilong P, Michard A & Guillet B (1990). *Geochim. Cosmochim. Acta* **54**, 781-795
- Lee J H & Byrne R H (1992). *Geochim. Cosmochim. Acta* **56**, 1127-1138.
- Mongelli G (1994). *Plinius* **12**, 72-74.
- Maksimovic Z, Mindszenty A & Pantó G (1991). *Acta Geologica Hungarica* **34**, 317-334
- Maksimovic Z & Pantó G (1996). *The Min. Soc. Series* **7**, 257-279. Chapman & Hall, London.
- Schwertmann U & Murad E (1983). *Clays and Clay Miner.* **31**, 277-284.
- Wood S A (1990). *Chem. Geol.* **82**, 159-186.

(1) DiSGG. Univ. della Basilicata. Potenza, Italia

(2) Dip. di Scienze della Terra e Geo-Ambientali. Univ. di Bologna, Italia.

(3) Istituto di Ricerca sulle Argille. CNR. Potenza, Italia

(4) Dip. Geomineralogico. Univ. di Bari, Italia

## The fractionation of REE, Th and transition elements in weathered biotites from granitoids: a mass balance approach and the role of accessory and secondary phases

*Mongelli G (1), Dinelli E (2), Tateo F (3), Acquafredda P (4) and Rottura A (2)*

The distribution of REE, Th, and transition elements in three suites of weathered biotites from tonalite, granite and granodiorite parent rocks, provides information on the fractionation processes affecting these elements during weathering.

LREE and Th are mineralogically controlled by monazite. In the early stage of weathering, dominated by vermiculite, monazite is retained as inclusion in the host weathered biotite, and LREE and Th exhibit an enrichment, up to 75%, relative to the fresh mica. When biotite evolves toward kaolinite, monazite is splitted and less than 50% of the original LREE and Th contents are preserved in the weathered mica. HREE are not controlled by primary accessory phases and, in the early stage of weathering, suffer a depletion, likely related to a stabilization in aqueous solution as carbonate complexes. During kaolinitization, a HREE enrichment relative to LREE is observed, possibly governed by the solubility product of REE-hydroxides. A positive Ce-anomaly is recognized where significant amounts of kaolinite are detected. The fractionation of cerium relative the other REE is due to the  $Ce^{3+} \rightarrow Ce^{4+}$  redox change, yielding to the occurrence of insoluble cerianite. Some REE patterns of weathered biotites show a positive Eu anomaly, possibly related to low  $Eu^{2+} \rightarrow Eu^{3+}$  transformation rates. Generally the  $Eu/Eu^*$  and the  $La/Th$  ratios are slightly affected by weathering. Relevant changes involve other element ratios, such as  $La/Yb$  and  $Th/Sc$ .

Biotite weathering lead to remobilization of transition elements and produce depletion for V, Cr, Cu and Zn, which are expelled, like many six-fold coordinated elements, from octahedral sites. The element Pb is enriched up to 70 % relative to the parent and it is likely controlled by iron oxi-hydroxides and phosphate minerals trapping lead deriving from feldspar dissolution.

(1) Dpto. Ciencias y Recursos Agrícolas y Forestales. ETSIAM. Univ. de Córdoba, España

(2) Dpto. Química Inorgánica. Fac. Ciencias. Univ. de Córdoba, España

## Mineralogy of clays in sediments from Neogene deposits in the Guadalquivir depression (Spain)

Montealegre L (1) and Barrios-Neira J (2)

The Guadalquivir depression is a wide Neogene basin that originated in post-mantle steps. Its northern half lies on the Hercinian Iberian shelf; its southern half, is a large olithostromic mantle with Tortonian fillings (VERA, 1983; PORTERO, 1984; MONTEALEGRE, 1990). This depression exhibits two distinct domains, *viz.* an autochthonous one at the north and an allochthonous one at the south (Fig. 1).

The autochthonous zone (N) consists of unconformable sediments on the Paleozoic shelf of the Iberian massif. The following series from the Upper Miocene (Helvetian-Tortonian) series are present: edge facies (in the bottom), blue marls and Andalusian sandstones. The edge facies consists of transgressive, structurally complex, shallow biocalcarene series resting unconformably on the shelf (Sierra Morena). The blue marls make the deep marine formation that spans most of the central countryside. Its sandy character increases towards the top. The series ends in a yellow sandstone formation that signals the last episode of the basin filling. There are local terms, intercalated between the previous series such as the Teba facies (biocalcarenes) white marls and moronites (siliceous facies), *etc.*

The allochthonous zone is considered a detachment from the front of the outer cover of the Andalusian ranges and makes up an extensive olithostroma. There are materials from the Upper Trias (mixed marl Keuper). Torn materials from the Jurassic and Cretaceous and domain others of the outer platform in the Andalusian ranges. There are mixed Neogene and Paleogene rocks.

In this work, we studied the mineralogy of the clays from stratigraphic sequences, clay and sandstone quarries, isolated efflorescences and probing sites (Fig.1).

TABLE I. Clay mineralogy of the materials studied

Stratigraphic group	Sand	Clay	I	Cl	K	Sep	Sm	V	Int
Andalusian	s	-	(2)	-	(3)	-	(1)	-	(4)
Blue Marl Tortonian	-	c	(3)	-	(1)	-	(2)	-	(4)
Detritic formation	s	-	(3)	(1)	(1)	-	(2)	-	(3)
N edge facies	s	-	(3)	-	(1)	-	(2)	(1)	(3)
Ol-Mioc. white facies	-	c	(2)	-	(2)	(1)	-	-	(5)
Olithostroma	-	c	(3)	-	-	-	(3)	(1)	(3)
Triassic	-	c	(3)	(3)	-	-	(1)	-	(3)

s = sandy c = clays & minerals

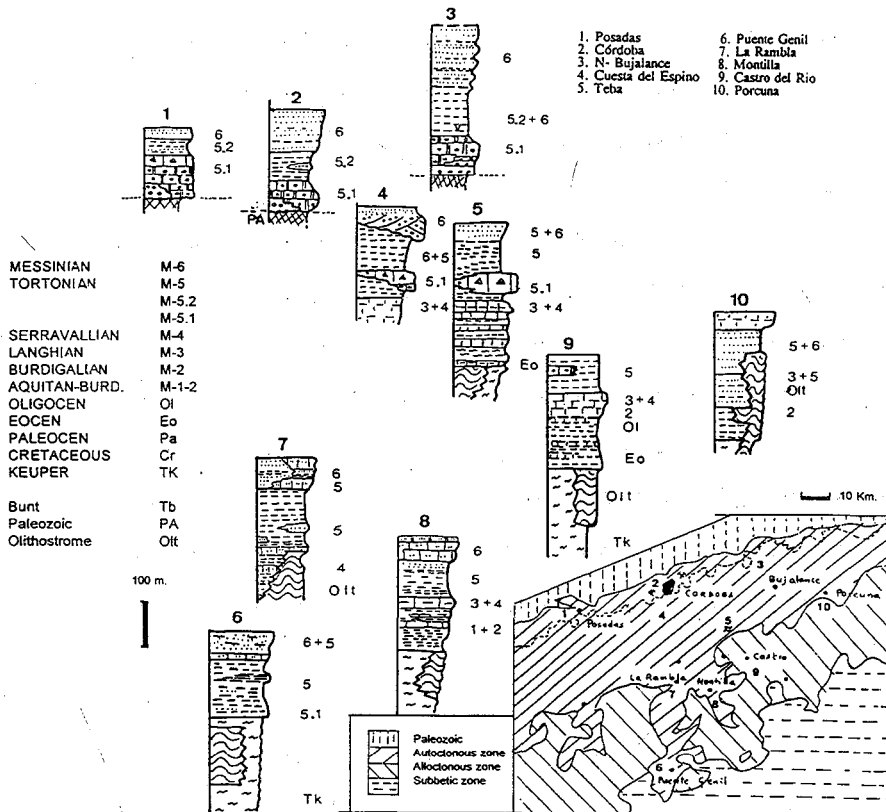


Fig. 1.— Stratigraphic description of the depression: series and correlations in the central sector.

The results obtained allowed us to establish a distribution pattern for the main clay minerals among the different stratigraphic levels. There are in the Trias illites, chlorites and interstratified Clh-V. The olithostroma materials contain a mixture of sediments of variable age, with predominant I and Sm and interstratifieds. The white facies (albarizas), are similar to those in the western sector (GALAN *et al.*, 1989; GARCIA GUERRERO *et al.*, 1989); I, K and interstratifieds of I-Sm, are prevalent. Among detritic materials, those containing I, Sm and interstratified are dominant. Blue marls more often contain the Sm, I and interstratifieds I-Sm. The last detritic materials abound with K and interstratified (Table I).

The presence of some dominant minerals in the Neogene series allows one to establish groups of "mineralogical facies":

- 1.- Association between (V-Chl) interstratified, chlorite and illite from Keuper.
- 2.- Association with I and (Sm-V) interstratifieds in the northern edge facies.
- 3.- Association of Sm, I and (Sm-I) interstratifieds in the blue marl formation.
- 4.- Association of I, I-Sm, Sm-V and Sm in detritic formations in the southern edge.
- 5.- Association of Sm and I in diatomitic marly, similar to those reported by GALAN *et al.* (1989). There are also I-Mo interstratified in addition to other minerals.
- 6.- Association of K, (I-V) interstratified and hydromic: Andalusian.

The previous data and associations can be interpreted in terms of clay genesis. The evolution of the clays minerals can be ascribed to sedimentation processes inherited by I, Sm and even Clh and occasionally I-V, which were degraded to I-Sm, hydromicaceous and I-V, during the erosive stage preceding the deposit, as well as to V-I and I forms through sedimentary aggradation. Were formed by neosynthesis Sm, Clh and occasionally Sep and K.

## REFERENCES

- GALAN, R. & GONZALEZ, I. (1989): 9th Int. Clay Conf., Strasbourg.
- GARCIA-GUERRERO, A and al.: 9th Int. Clay Conf., Strasbourg.
- MONTEALEGRE, L. (1976): PhD Thesis, University of Granada, Spain.
- PORTERO, J.M. & ALVARO, M. (1984): I Cong. Esp. Geol., vol.III: 241-252.
- VERA, J.A. & FONTBOTE, J.M. (1983): *Geología de España*, vol.II, IGME & NCG, Madrid.

(1) Dpto. Química Agrícola,  
Geología y Geoquímica. Fac.  
Ciencias. Univ. Autónoma de  
Madrid, España

(2) C. de Ciencias Medio  
Ambientales. CSIC. Madrid,  
España

## Textural and compositional variations in the Esquivias kerolite/stevensite deposit (Madrid basin, Spain)

Pozo M (1), Casas J (1, 2) and Moreno A (1)

Fine-grained facies belonging to the Lower and Intermediate units from Madrid basin show an excellent sedimentary record containing both ceramic and special clay deposits actively exploited for economic purposes. The existence of large Mg-clay deposits in the Madrid basin is well known, especially those of sepiolite and/or bentonite composition. These materials have been interpreted as marginal lacustrine facies forming a belt to the south and east of Madrid city, and marking a lateral transition from open lacustrine deposits to arkosic alluvial fan materials with source from the Spanish Central Range (Calvo *et al.* 1989).

The Mg-clay deposits under study in this work have a different composition and are located at the lower part of Intermediate Unit whose strata are well exposed between Pinto and Esquivias villages, southwards of Madrid. These clays are characterized by their pinkish to pale brown color and previous mineralogical research showed that they are composed of kerolite/stevensite mixed layers (Ke/St) (Martín de Vidales *et al.*, 1991). Sedimentological interpretation indicates a shallow lacustrine-palustrine environment in which Ke/St facies are related to ponds development where authigenic Mg-clays are formed (Pozo and Casas 1995). The scope of this study was to establish the variability in composition and texture of economic deposits of Ke/St as well as their genetic implications.

The sampling has been done on 9 stratigraphic sections from quarries, outcrops and boreholes located northeast of Esquivias village. (Figure 1). The mineralogical study of 397 samples was performed by means of X Ray Diffraction. The estimation of the percentage of expandable layers for kerolite/stevensite interstratified minerals was carried out with the NEWMOD program (Reynolds, 1985). Chemical analysis were carried out by XRF, ICP and Atomic Absorption Spectrophotometry. Philips SEM-500 with EDS equipment was used for undisturbed samples in SEM. Petrographic studies were made on standard thin sections.

Esquivias deposit is composed of Ke/St bearing pink clays alternating with green mudstones and sporadic sandy levels included in the named "Magnesic Unit" (Pozo *et al.* 1994). This unit has a mean thickness of 15 m where four lens-shaped pink clay beds, up to three

meters thick, have been differentiated. One of the most outstanding feature is the poor development of carbonates often like scattered calcite nodules. From a textural point of view three main pink clay lithofacies have been established: R<sub>1</sub>. Desiccation breccias and conglomerates, R<sub>2</sub>. Clay clast intrarenites, and R<sub>3</sub>. Lutites. Clastic textures are interpreted as a mixture of gel morphologies and reworked intraclasts whilst lutites implies induration by the action of cementing clays.

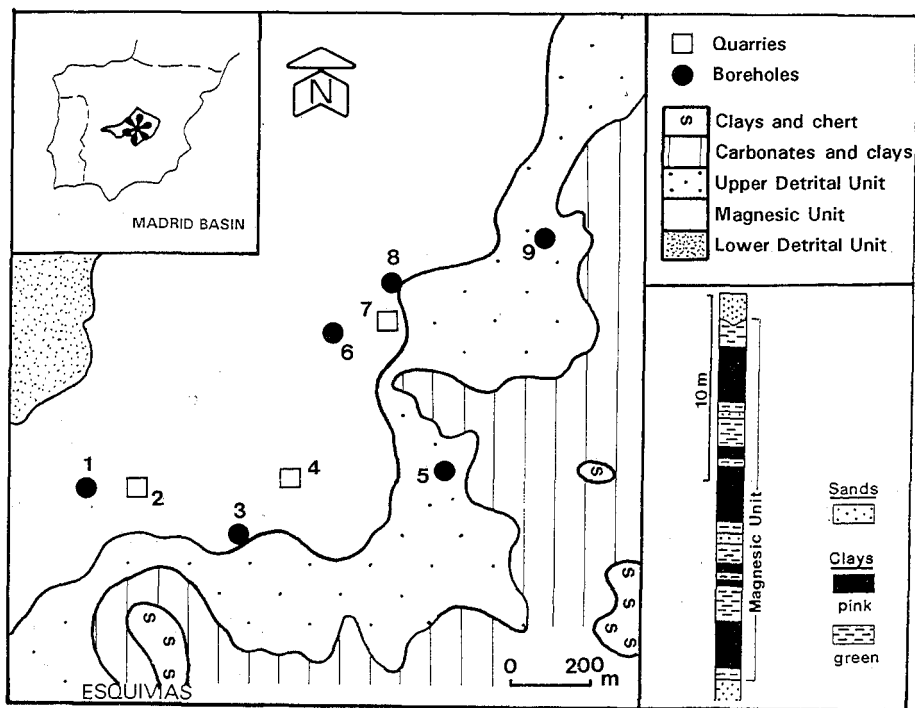
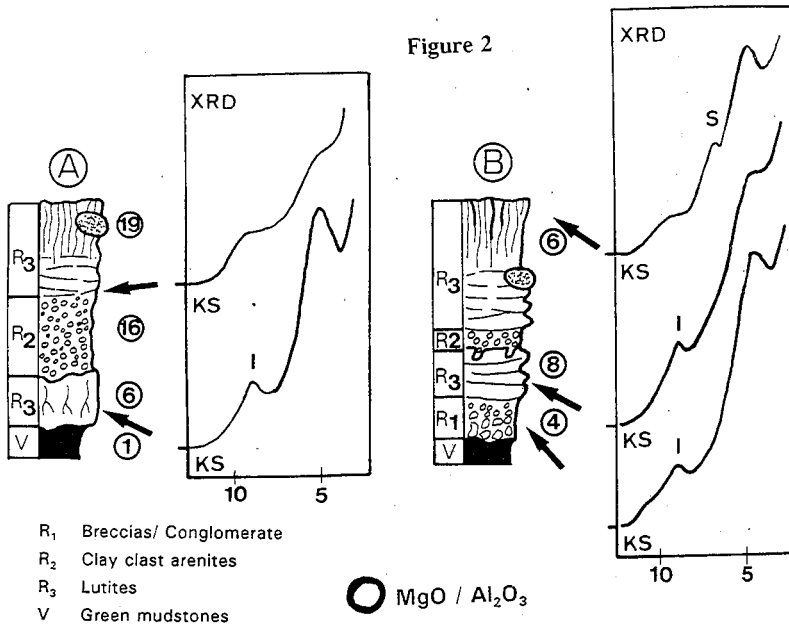


Figure 1

The X ray patterns show slightly different patterns as a function of stevensite proportion in the Ke/St mixed layer. In all the samples studied kerolite is predominant ranging between 60-80%. Minor contents in sepiolite and illite have been detected. Chemical analysis indicates, as does mineralogy, a high MgO content in the samples analyzed but with MgO/Al<sub>2</sub>O<sub>3</sub> ratios ranging from 4,2 to 31,1. This variation is related with detrital contamination (input, reworked), specially illite content in samples. This fact is supported by the good correlation between Al<sub>2</sub>O<sub>3</sub> and K<sub>2</sub>O observed. Lithofacies, mineralogy and MgO/Al<sub>2</sub>O<sub>3</sub> ratio associated to sequences in two representative pink clay beds are shown in figure 2.



Compositional and textural results indicates significant differences both in vertical and lateral sections along the area studied, being interpreted in relation with the sedimentary setting (detrital input) as well as the type and intensity of diagenetic processes (pH, salinity). On the other hand an important role played by pedogenic processes (desiccation, vertisolization, burrowing and root activities) in the final texture has been observed.

Kerolite/stevensite mixed layers are a rare occurrence worldwide because of the scarcity and selectiveness of their deposits but also for the difficulties in their recognition.

### References

- CALVO, J.P., ALONSO, A.M. & GARCIA DEL CURA, M.A. (1989). *Palaeogeog., Palaeoclim., Palaeoecol.*, 70, 199-214.
- MARTIN DE VIDALES, J.L., POZO, M., ALIA, J.M., GARCIA NAVARRO, F. & RULL, F. (1991). *Clay Miner.*, 26, 329-342.
- POZO, M. y CASAS, J. (1995). *Boletín Geol. y Min.* 106-3: 265-282.
- POZO, M., CASAS, J. & MORENO, A. (1994) Abstracts of the I.A.S. Meeting Ischia '94
- REYNOLDS, R.C. (1985). NEWMOD, a Computer program for the Calculation of one dimensional Diffraction Patterns of Mixed Layered Clays. R.C. Reynolds, Hanover, U.S.A.

(1) Dpto. Química Agrícola,  
Geología y Geoquímica. Fac.  
Ciencias, Univ. Autónoma de  
Madrid, España

(2) C. de Ciencias Medio  
Ambientales. CSIC, Madrid,  
España

(3) Instituto Tecnológico y  
Geominero de España. Madrid,  
España

## Geochemical trends in alluvial-lacustrine Mg clay deposits from Madrid basin (Spain)

Pozo M (1), Moreno A (1), Casas J (1, 2), and Martín Rubí J A (3)

### Introduction

The neogene sedimentary record of Madrid Basin contains probably the most important Mg clay deposits in the world. This assumption is based not only on the mineral reserves but also in the several Mg phases reported (bentonite, kerolite, sepiolite). The Miocene Intermediate Unit (Aragonian-Vallesian age), made up of sands, clays, limestones and chert in alternating sequences, has as a characteristic the existence of important deposits of sedimentary magnesium clays, which have been interpreted as marginal lacustrine facies, forming a belt to the south and east of Madrid city, and marking a lateral transition from open lacustrine deposits to arkosic alluvial fan materials prograding NW-SE ward with source from the Spanish Central Range (Calvo *et al.*, 1989). The Mg clays deposits under study in this work are bentonites and kerolites (really kerolite/stevensite mixed layers) located at the lower part of the Intermediate Unit and belonging to alluvial and lacustrine sedimentary environments. This paper deals with the geochemical and mineralogical comparison of lacustrine-palustrine lithofacies of magnesium clays from different locations as well as to establish their geochemical trends.

### Sampling and analytical procedures

The geological map with the location of sampling points are shown in figure 1. About 185 samples were taken out in five general lithological sections from outcrops, boreholes and quarries. Sampling areas are closed to Pinto, Esquivias, Yuncos, Villaluenga and Cabañas de la Sagra villages. The mineralogical study of the samples was carried out by XRD and optical microscopy (thin sections). Chemical analysis were made by XRF and ICP for major, minor and trace elements respectively. Colorimetric methods were used with F and atomic absorption spectrophotometry for Na and Li.

### Results and discussion

Pinto and Esquivias area: Three mineralogical associations have been differentiated.

(1) Green mudstones: Phyllosilicates (saponite-illite/mica-kaolinite)-feldspars-quartz-dolomite-opal C/T-barite-zeolites. (2) Pink lutites and clay clast arenites: Phyllosilicates (kerolite-stevensite-sepiolite-illite)-calcite-quartz. (3) White to grey lutites: Phyllosilicates (sepiolite-Mg

smectite)-calcite.

Villaluenga area: Two mineralogical associations have been differentiated. (1) Green lutites: Phyllosilicates (saponite-illite-sepiolite-Al-smectite-kaolinite)-feldspar-quartz-calcite. (2) Pink lutites: Phyllosilicates (sepiolite-stevensite/saponite-illite)-(quartz + feldspar).

Yuncos area: One mineralogical association has been differentiated.

(1) Brown lutites : Phyllosilicates (saponite-illite-sepiolite-kaolinite)-quartz-feldspars.

Cabañas de la Sagra area: Two mineralogical association have been differentiated.

(1) White nodulized lutites : Phyllosilicates (sepiolite-Mg smectite-illite)-quartz. (2) Yellowish grey lutites : Phyllosilicates (stevensite/saponite-illite-sepiolite)-quartz-feldspar-dolomite.

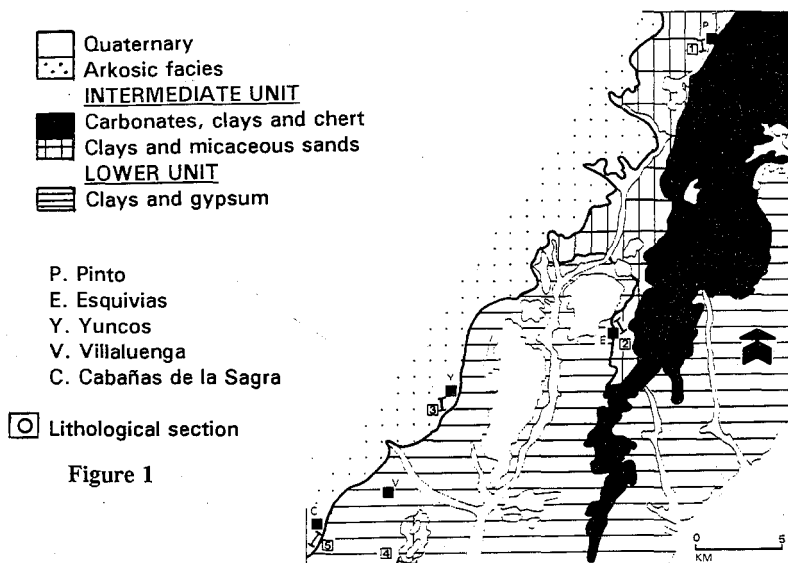


Figure 1

### Geochemistry

The bivariate study of analyzed major elements shows an excellent intercorrelation among  $Al_2O_3$ ,  $Fe_2O_3$ ,  $TiO_2$  and  $K_2O$  with Pearsons lineal correlation coefficients above +0.94. Among trace elements Rb, La, Y, Sc and Nb are also incorporated. All these elements are related with detrital minerals. Magnesium, vinculated to neofornated minerals, shows an excellent negative correlation with all the elements above mentioned. Only F with its higher values in sepiolite samples is positively intercorrelated with  $MgO$ . Lithium is specially incorporated to Villaluenga pinkish lithofacies where stevensite is the main smectitic mineral.

Factorial analysis make up with major and minor elements is plotted in figure 2. Three factors were taken. The principal one ( $F_1$ ) account for as much as 49.4% of total variance, which is measure by the eigenvalues. The second factor ( $F_2$ ) account for 16.3% of total variance. Plot of factorial matrix point out strong negative intercorrelations among  $F_1$  and

elements related to detrital fraction ( $\text{Al}_2\text{O}_3$ ,  $\text{Fe}_2\text{O}_3$ ,  $\text{K}_2\text{O}$  and  $\text{TiO}_2$ ). This factor ( $F_1$ ) shows a good positive correlation with  $\text{MgO}$ . Factor  $F_2$  is positively correlated with  $\text{SiO}_2$  and negatively with  $\text{CaO}$ . Figure 2b shows a plot of scores of individuals as points in the space of first and second factors. Pinkish lithofacies from Pinto, Esquivias and Villaluenga are related to  $\text{MgO}$  showing higher  $\text{SiO}_2$  contents. White lutites (sepiolites) and clay lithofacies from Cabañas de la Sagra are related to  $\text{MgO}$  too. On the other hand brown lutites from Yuncos and green mudstones from Pinto, Esquivias and Villaluenga are binding with inherited components ( $\text{Al}_2\text{O}_3$ ,  $\text{Fe}_2\text{O}_3$ ,  $\text{K}_2\text{O}$  and  $\text{TiO}_2$ ), being outstanding than Green lutites from Magan area show a lesser detrital character than the others. This fact correlates very well with the detrital mineralogy associated to this lithofacies (illite-mica, kaolinite, feldspars and quartz).

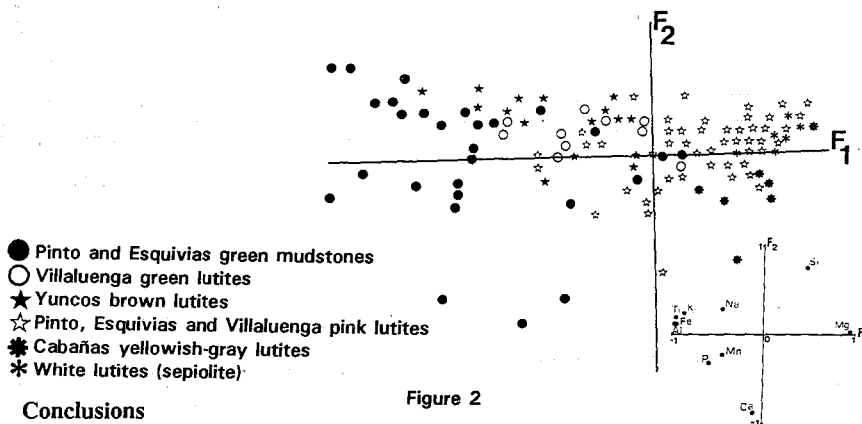


Figure 2

### Conclusions

The alternation of green mudstones with pinkish lutites like those observed in Pinto, Esquivias and Villaluenga areas suggest cyclic shift of the lake shoreline during expansive and retractive episodes in semiarid climatic conditions. Two different geochemical trends have been established. One related to the origin of Mg clays by both transformation of inherited clays and neoformation in mudflat deposits (green clays). On the other hand, Mg clays formation in shallow paludine deposits where neoformation from silica magnesium gels (kerolite, kerolite-stevensite, stevensite) and later dissolution-precipitation processes (sepiolite) are inferred.

Bentonites in Yuncos and Cabañas deposits are related to sedimentation in shallow stagnant waters related to paludine environments originated in the transition zone between a saline-alkaline lacustrine margin (source of Mg) and the input of clastic fine materials (source of Al, Fe, K and Ti) with silica laden waters in an alluvial fan distal complex. Latter postsedimentary processes should be responsible for sepiolite formation.

### References

Calvo, J. P., Alonso, A.M. & García del Cura M.A. (1989). *Palaeogeog., Palaeoclim., Palaeoecol.* 70, 199-214.

(1) Dpto. Química Agrícola,  
Geología y Geoquímica. Fac.  
Ciencias. Univ. Autónoma de  
Madrid, España

(2) Instituto Tecnológico y  
Geominero de España. Madrid,  
España

(3) TOLSA, S.A. Madrid, España

## Evidences on diagenetical evolution of lacustrine sediments in the Vicálvaro sepiolite deposit

*Ramírez S (1), Cuevas J (1), Garralón A (1), Martín Rubí J A (2),  
Casas J (3), Alvarez A (3) and Leguey S (1)*

The Vicálvaro sepiolite deposit is located within the lacustrine sequences in the so-called Intermediate Unit of the Miocene in the Madrid Basin. Sepiolite, trioctahedral Mg-smectites or carbonates, as main components of these sediments, has been interpreted in several ways in relation to their genesis: from direct precipitation in an alkaline evaporitic lacustrine environment to as complex diagenetic post-depositional processes including pedogenic or the interaction with fresh diluted groundwaters (smectite alteration). (Jones, 1986; Khoury, 1982; Hay et al., 1991).

These work focuses to the study of sequences that cut across deepest zones of the primitive lake areas (central zones as divided by Leguey et al., 1995). Our aim was to study diagenetical relations between basal materials (black detrital clays) and the massive sepiolite deposit. Fig. 1 captures the deposit distribution and -I, 0 y I sections analyzed in this manuscript.

The study comprises the complete analysis for 60 samples including mineralogy (XRD), major and trace elements (XRF and ICP-AES). Some smectitic clay samples have been selected. These samples have been submitted to a detailed mineralogical, chemical and physico-chemical analysis (XRD oriented-glycolated aggregates, structural formulae calculations, BET surface and cation exchange properties). C and O isotopic data on carbonates are also determined.

The mineralogical evolution from basal clays to massive sepiolite levels (-I, 0 y I path) is characterized by a decrease in dolomite and by the general presence of recrystallized calcite either filling pores or as cements in the upper levels of the 0 and I sections. Dioctahedral phyllosilicates are largely consumed: kaolinite and montmorillonite are absent with the exception of the upper levels in contact with detrital materials (arkoses). Illite is the aluminosilicate that remains as accessory mineral in the Mg-smectite assemblage. From sections 0 to I (Mg-smectite-sepiolite path), stevensite clays, varying layer charge, seems to evolve towards massive sepiolite, being the

smectite from section I characterized by either of low charge stevensite or higher charge saponite-type smectite, both with fixed compositions (table 1).

Fig. 1. Vicálvaro sepiolite deposit. A: Geological sketch. B: Localization of sections and zonal pattern.

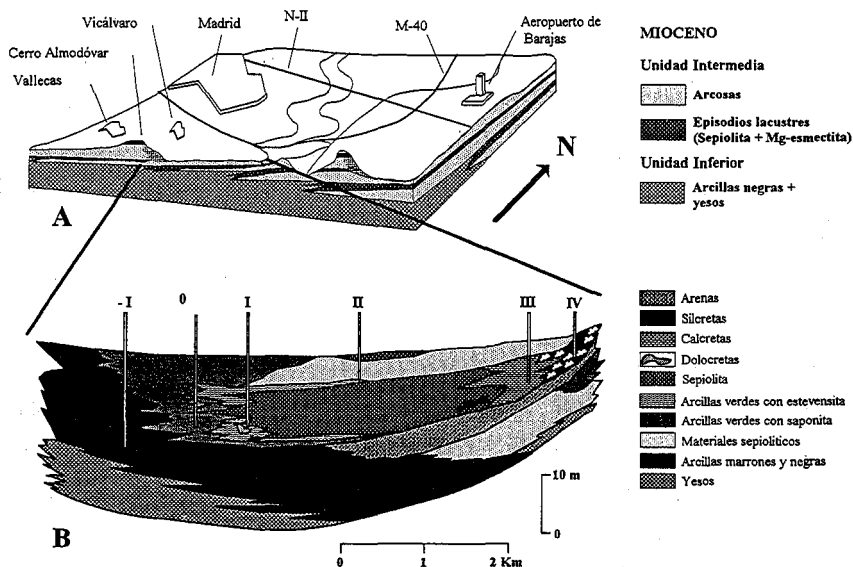


Table 1. Structural formulae of smectites from section I ( $O_{20}(OH)_4$ ).

Sample	tetrahedral sheet			octahedral sheet			interlayer region			crystallochemical type	
	Si	Al	(1) charge	Al	Fe	Mg	charge	X <sup>+</sup>	K		layer charge
55	7.36	0.64	0.49	0.53	0.27	4.69	0.22	0.76	0.15	0.71	SAP-STV
50	7.77	0.23	0.20	0.13	0.08	5.51	0.35	0.56	0.03	0.55	STV
49	7.54	0.46	0.40	0.28	0.15	5.23	0.25	0.66	0.06	0.65	SAP-STV
46	7.51	0.49	0.41	0.43	0.16	4.95	0.33	0.70	0.08	0.74	SAP-STV
35	7.83	0.17	0.14	0.12	0.06	5.55	0.36	0.50	0.03	0.50	STV

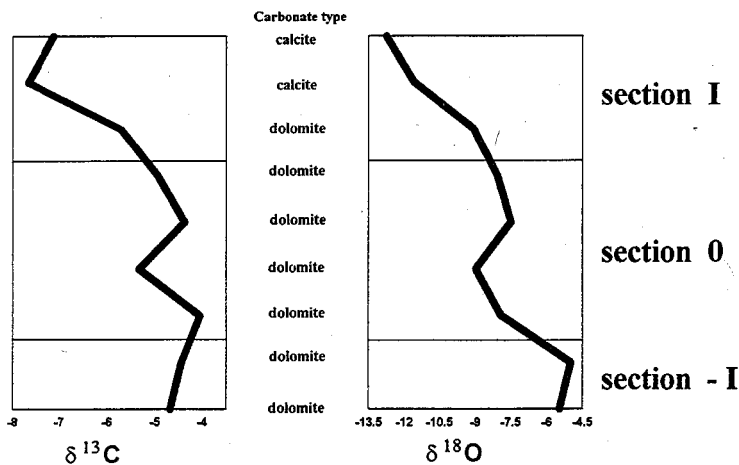
(1) Tetrahedral charge corrected for K assuming illite impurities.

Correlation analysis between trace elements and the mineralogical composition establishes two main groups inversely correlated: first, Be and transition elements as Cr, V, Co, Cu, Zn, Y and Nb are clearly associated with detrital minerals; meanwhile, Li and F are strongly correlated with authigenic Mg-silicates. The evolution representing sections -I (dolomite, detrital

aluminosilicates) → 0 (Mg-smectite) → I (interface with massive sepiolite) is characterized by the diminution of significant correlations between detrital and trace elements. This fact has been interpreted as an evidence for a post-depositional diagenetic alteration.

Isotopic O and C data from carbonates have been represented in Fig. 2. The variations consigned in  $\delta^{18}\text{O}$  and  $\delta^{13}\text{C}$  are typical of continental environments. Dolomites in sections 0 to I yield slight lower values respecting basal clays. Calcite from Mg-clays and sepiolite assemblages are much more lighter than dolomite. Evolution of dolomites implies a change to a moderate saline environment from the high evaporative environment characterizing the initial stage of the lake. The general presence of lighter calcite is an evidence of the extensive circulation of fresh waters in the post-depositional stage related to sepiolite formation.

Fig. 2. Evolution of isotopic data in the studied lacustrine sections.



## References

- Hay, R.L., Guldman, S.G., Matthews, J.C., Lander, R.H., Duffin, M.E., Kyser, T.K. (1991). *Clays Clay Miner.* **39**, 84-96.
- Jones, B.F. (1986). *U.S. Geol. Surv. Bull.* **1578**, 291-300.
- Khoury, H.H., Eberl, D.D., Jones, B.F. (1982). *Clays Clay Miner.* **30**, 327-336.
- Leguey, S., Martín Rubí, J.A., Casas, J., Marta, J., Cuevas, J., Alvarez, A. y Medina, J.A. (1995). *Clays: Controlling the Environment*, G. J. Churchman, R. W. Fitzpatrick y R. A. Eggleton eds. Proc. 10 th Int. Clay Conf., Adelaide, Australia, 1993. CSIRO. Publishing Melbourne, Australia, 383-392.

(1) Estación Experimental del Zaidín. CSIC. Granada, España

(2) Dpto. Química Inorgánica, Cristalografía y Mineralogía. Fac. Ciencias. Univ. de Málaga, España

## Oxygen isotope geochemistry of kaolin minerals from the Campo de Gibraltar area (southern Spain)

*Reyes E (1) and Ruíz Cruz M D (2)*

The origin of kaolinite in shales, as well as its transformation to dickite, have been scarcely investigated. Difficulties mainly derive from both shale textures, which do not permit the accurate identification and quantification of detrital and authigenic kaolinite by optical microscopy, and their homogeneous grain-size, which impedes the obtaining of kaolinite-rich separates for X-ray determinations.

The occurrence of kaolin minerals filling distensive zones of fractures in Cretaceous shales from the Campo de Gibraltar area, permits to have amounts of kaolin minerals enough for their accurate characterization. X-ray diffraction (XRD), scanning electron microscopy (SEM) and oxygen-isotope geochemistry have been used with the aim of investigating the origin of these minerals as well as the possible controls on the kaolinite to dickite transformation.

The studied samples belong to late Cretaceous units (Almarchal and Facinas) from the Campo de Gibraltar flysch formations and have been taken in five wells and cross-sections located across the Gibraltar Strait.

### Results

The XRD study of fracture fillings has permitted the identification of kaolinite and dickite, as well as their quantification, when both minerals appear mixed (Ruiz Cruz et al. (1995). XRD patterns of both kaolinite and dickite belong to very ordered phases, with Hinckley indices in the order of 1.0 for kaolinite and 1.8 for dickite. Ruiz Cruz et al. (1995) also pointed out some morphological differences between kaolinite-rich samples, where typical vermiform stacks dominate, and dickite samples, which showed thin stacks and plates shifted parallelly to basal surfaces. Nevertheless, the mixture of both sizes and morphologies is common in most of the studied samples.

Table 1 summarizes the results of the oxygen isotope analyses of kaolin minerals and calcite.  $\delta^{18}\text{O}$  values of kaolin minerals (kaolinite, dickite or mixtures) show some

variations within each section as well as between the different sections. Average values range from 17.6‰ for samples containing kaolinite and dickite, to 19.1‰ for dickite samples. Variations in  $\delta^{18}\text{O}$  values of kaolin minerals within each section are generally more important than those induced by differences in quartz content and, consequently, no information can be obtained about the  $\delta^{18}\text{O}$  values of quartz.  $\delta^{18}\text{O}$  values for calcite from veins associated to marly or shale beds are very homogeneous (-8.2‰).

Table 1.- Isotopic analysis of veins

Section	Mineral	Average $\delta^{18}\text{O}$ (measured)	$\delta^{18}\text{O}$ (calculated)
1.- Bolonia well	kaolinite + dickite	17.6	
	kaolinite		18.4
	dickite		15.4
2.- Los Pastores	dickite	19.0	
3.- Malabata well	dickite	18.5	
4.- KT well	dickite	19.1	
5.- Puerto del Rayo	dickite	18.5	
1.- Bolonia well	calcite	-8.1	
5.- Puerto del Rayo	calcite	-8.5	

## Discussion and Conclusions

The wide formation of authigenic kaolinite and dickite appears to be directly related to development of thrusting after the Burdigalian time, which resulted in tectonic burial beneath thrust sheets locally >3 km. In this stage an intensive dissolution took place in shales, together with the precipitation of calcite and kaolin minerals in veins. Textural data and mass balance calculations indicate that kaolin minerals formed primarily from smectite dissolution. This process, described by Anh & Peacor (1987) produced, in our case, kaolin minerals and I/S mixed-layers, instead of kaolinite and illite.

The locus of equilibrium  $\delta^{18}\text{O}$  H<sub>2</sub>O and temperature values for kaolin minerals and calcite have been drawn in Fig. 1. If we assume minimum  $\delta^{18}\text{O}$  shale pore-water similar to that of Cretaceous seawater (-1‰, after Sheppard, 1986), temperatures of 62°C and 86°C can be calculated, respectively, for kaolinite and dickite formation in sections where both polytypes coexist (Fig. 1 a). Since initial temperature for dickite formation must have been similar or slightly higher in more deeply buried sections, a shift of the  $\delta^{18}\text{O}$  porewater composition to about 3‰ can be estimated from  $\delta^{18}\text{O}$  values of dickite in these sections, in which a narrow range of temperatures (86°-96°C) can be deduced for dickite formation (Fig. 1b). This evolution in the  $\delta^{18}\text{O}$  pore-fluid values, similar to that determined in shale sequences by Eslinger and Yeh (1986) can be related in our case to the influence of smectite dissolution.

Assuming a mean temperature gradient of 30°C/km, burial depths ranging from 2 to 3 km can be calculated for the studied sequences. These values agree with both composition and ordering of the I/S mixed-layers (Chamley, 1989), and reveal, in spite of the complex tectonic of this area, decreasing tectonic burial from the thrust front toward the more external part of the Gibraltar arc.

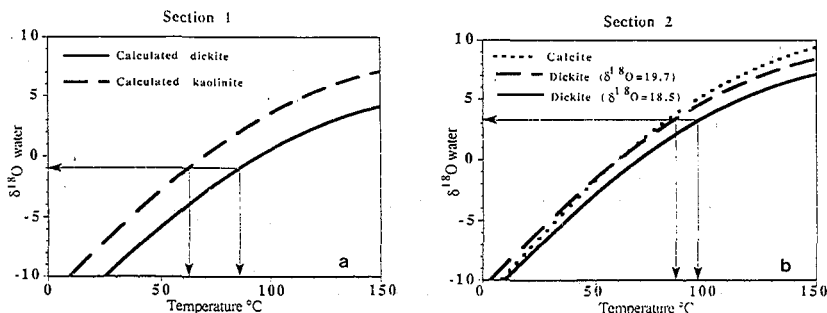


**Figure 9.-** Relationships between pore-water  $\delta^{18}\text{O}$  and precipitation temperature for: a) Calculated oxygen isotope values of kaolinite and dickite in section 1. b) Minimum and maximum oxygen isotope values of dickite and mean value of calcite, in section 2.

The range of  $\delta^{18}\text{O}$  values (in the order of 2‰) observed in some sections indicate that kaolin minerals are not equilibrated with the maximum temperature attained during veins formation. Consequently, if kaolinite was the first phase formed, as indicated by textural relations, their transformation to dickite probably did not involve a generalized dissolution-precipitation process. This probably explains the wide development of dickite in these sequences, were, at the estimated temperatures, the only stable polytype would be kaolinite (Ehrenberg et al., 1993).

## References

- Ahn, J. H. & Peacor, D. R. (1987) *Proc. Int. Conf. Denver (1985)*, p. 151-157.  
 Chamley, H. (1989) *Clay sedimentology*. Springer-Verlag, Berlin, 623 pp.  
 Ehrenberg, J.N., Aagard, P., Wilson, M.J., Fraser, A.R. & Duthie, D.H.L. (1993). *Clay Miner.*, **28**, 325-352.  
 Eslinger, E.V. & Yeh, H.-W. (1986). *Geochim. Cosmoch. Acta*, **50**, 59-68.  
 Ruiz Cruz, M.D., Galán, E. & Moreno Real, L. (1995). *Proc. 8th Euroclay Conf.*, Leuven, 333.  
 Sheppard, S.M.F. (1986) *Reviews in Mineralogy*, **16**, 165-183.

Dpto. Geociencias. Univ. de Aveiro, Portugal

## Mineralogy and geochemistry of the "Areias de Esgueira" formation (Aveiro, Portugal): arguments for lithostratigraphic and paleoenvironmental interpretations

Rocha F and Gomes C

The Aveiro region corresponds to the northern section of the Portuguese Occidental Meso-Cenozoic sedimentary basin. At the Aveiro region a gap in the stratigraphic record do occur beyond upper Cretaceous. In fact, Eocene, Oligocene and Miocene formations have not been identified in the region. Pliocene and Pleistocene outcrops do occur corresponding mainly to old beach deposits and to fluvial terraces. In Esgueira, northern suburb of Aveiro (Fig. 1), the position in the local stratigraphic column of the so-called "Areias de Esgueira" formation is still undefined, being placed in the interval upper Cretaceous - Pliocene.

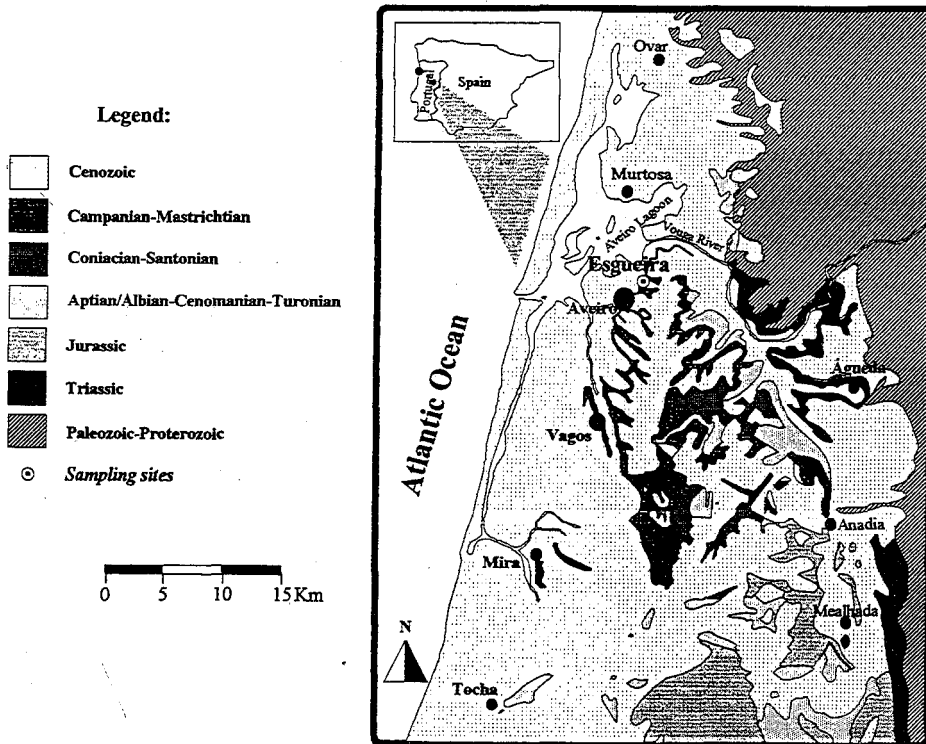


Fig. 1 - Location and geological setting.

At the northern side of the Esgueira valley, in a place known as Olhos de Água, occur the three outcrops under study and reported in this paper. The "Areias de Esgueira" are composed of brown sands, medium grained, intercalated by black clayey layers containing marcassite nodules and remains of fossil plants as well as brown to red clayey layers coated at their top by very thin iron rich crusts, and yellow sands, medium to coarse grained becoming gradually finer towards the top, exhibiting cross-bedding.

These paper deals with the mineralogical and geochemical study of the "Areias de Esgueira" formation, particularly of the clay components, since they had been considered important for a better understanding of that formation in stratigraphic, paleoclimatic and paleogeographic terms.

The mineralogical study of the "Areias de Esgueira" formation has been based mainly on X-ray diffraction determinations, carried out in both  $<38\mu\text{m}$  and  $<2\mu\text{m}$  fractions. Qualitative and semi-quantitative determination of clay and non-clay minerals has been done in both fractions. Chemical analyses of both major elements ( $\text{MgO}$ ,  $\text{Al}_2\text{O}_3$ ,  $\text{SiO}_2$ ,  $\text{CaO}$ ,  $\text{TiO}_2$ ,  $\text{Fe}_2\text{O}_3$ ,  $\text{MnO}$ ,  $\text{Na}_2\text{O}$  and  $\text{K}_2\text{O}$ ) and minor elements (Zn, Cu, Ni, Sr, Rb, Pb, Cr, Ba, Nb, Zr, Y, Th and V), have been carried out using X-ray fluorescence and flame-spectroscopy methods. Cluster analysis and multivariate analysis of both mineralogical and chemical data had been carried out.

Table I - Mineralogical results (mean compositions)

Lithology	$<38\mu\text{m}$ Fraction	$<2\mu\text{m}$ Fraction
Plio-Pleistoc.	Qz(35%), Fs(55%), Fk(10%)	K(95%), I(5%), MI(t)
Yellow sands	Qz(30%), Fs(60%), Fk(7%), P(3%), Gt(t)	K(85%), I(15%), MI(t), Lp(t)
Iron rich crusts	Qz(15%), Fs(15%), Fk(5%), Gt(65%), Lp(t)	K(80%), I(20%), Lp(t), MI(t)
Black clays	Qz(40%), Fs(40%), Fk(20%), P(t), Gy(t)	K(43%), I(50%), S(7%), Lp(t)
Brown clays	Qz(35%), Fs(50%), Fk(10%), P(5%), Gt(t),Lp(t)	K(40%), I(60%), MI(t), Lp(t)
Up. Cretaceous	Qz(50%), Fs(35%), Fk(10%), P(5%), Gt(t)	K(30%), I(60%), S(10%), MI(t)

Qz: Quartz; Fs: Phyllosilicates; Fk: K-Feldspar; P: Plagioclase; Gt: Goethite; Lp: Lepidocrocite;

Gy: Gypsum; K: Kaolinite; I: Illite; S: Smectite; MI : Mixed-layers; (t)- traces.

Table I contains the main results achieved by the mineralogical studies corresponding to a sequence from the Olhos de Água outcrop, starting with the "Argilas de Aveiro" belonging to the upper Cretaceous and positioned at the base of the "Areias de Esgueira" and finishing with the white Plio-Pleistocene sands and gravels occurring at the top of the outcrop.

From the application of R-mode factor analysis to the fine fraction mineralogical data, with redistribution of Phyllosilicates contents by Kaolinite, Illite, Chlorite, Smectite and Mixed-layers, some interesting considerations may be withdrawn:

- Factor 1 explains K-feldspars, Smectite, Dolomite, Zeolites and Siderite.
- Factor 2 explains Kaolinite, Mixed-layers and Sulfates.
- Factor 3 explains Quartz, Illite, Plagioclase and Opal C/CT.

The R-mode factor analysis of the fine fraction chemical data allows the withdrawal of the following considerations:

- Factor 1 shows Nb, Rb, Y, Zr, Th,  $K_2O$ ,  $MgO$ ,  $TiO_2$  and  $SiO_2$  in front of Pb, Ignition Loss and  $Al_2O_3$ .
- Factor 2 shows V, Cr,  $Fe_2O_3$ , CaO and MnO in front of Ba.
- Factor 3 shows Cu e Zn in front of  $Na_2O$ .

The cluster analysis shows that the studied samples could be grouped in three clusters, one comprising the samples corresponding to the three different types of clays found in the outcrop (green clays from the upper Cretaceous "Argilas de Aveiro" formation, brown clays and black clays from the "Areias de Esgueira" formation), other comprising the samples of the iron-rich crusts, and one another comprising the samples corresponding to the two different types of sands (one assumed to belong to the "Areias de Esgueira" formation and the other to Plio-Pleistocene). One sample (OA 42), representing a iron-crust is notoriously segregated.

Both analytical and statistical results were utilized not only for lithostratigraphical analysis but also for paleoenvironmental reconstruction. The analysis of the data available allows the withdrawal of the following conclusions:

- Between the green clays of the "Argilas de Aveiro" formation and the brown and black clays of the "Areias de Esgueira" formation none notorious mineralogical/geochemical discontinuities could be found.
- The clays referred to are well discriminated from the overlying yellow sands.
- The iron-crusts correspond to a post-deposition, supergenic deposit.

The composition of the clay fractions of the studied samples point out to a gradual evolution, in global terms, of the environment of deposition and to particular local discontinuities and changes of some physico-chemical parameters.

As a final remark it appears that the "Areias de Esgueira" deposits could represent terminal deposits of the "Argilas de Aveiro" formation which had been deposited in channels of a deltaic system during a regressive period.

(1) Dpto. Cristalografía y Mineralogía. Fac. Geológicas. Univ. Complutense de Madrid, España

(2) Dpto. Geología. Area de Cristalografía y Mineralogía. Fac. Ciencias. Univ. de Salamanca, España

(3) Dpto. Química Agrícola. Geología y Geoquímica. E.U. Santa María. Univ. Autónoma de Madrid, España

## Study of the bentonites from the "Cerro del Aguila" (Toledo, Spain)

*Santiago Buey de C (1), Suárez Barrios M (2), García Romero E (1), Doval Montoya M (1) and Domínguez Díaz M C (3)*

At present, there are many bentonite exploitations located in the "Arcillas Verdes" Unit from the Tajo Basin (Brell, 1985; García Romero, 1988; Domínguez Díaz, 1994, etc). The high purity of these bentonites makes them very interesting and this is the cause of the study of the geochemical, mineralogical and physical properties of them. Some of these properties have been studied before by different authors: (Galan et al. 1986, Cuevas, 1991). The main property of soil defining its behaviour is, not only its crystallographical and mineralogical nature, but also the type and distribution of clay particles and their tendency to be connected to particle aggregates separated by voids of varying size. This is the reason why a study of the microstructure of the material as well as a more detailed crystal structure investigation of the main mineral can be very useful to explain its physical-chemical and rheological behaviour.

To do this study, samples have been taken in a bentonite quarry located at the base of the "Cerro del Aguila". These samples have been studied by X Ray Diffraction (random powder and oriented aggregate). The microstructural study has been taken by Scanning Electron Microscopy. The Transmission Electron Microscopy (TEM-EDX) allows calculation of the unit cell formula. The investigation of the microstructure has been completed with oriented sections according to the method proposed by Tessier (1984). This technique allows the direct observation of different orientated sections and makes the measurement of interplanar spacing easier. This allows mineral identification as well as the understanding of their textural relationships. To go deeply into the microscopical study of this sample, we turned to the electron diffraction. In this way Oblique Texture Electron Diffraction Patterns have been carried out (Zvyagin, 1967).

The textural characterization has been completed by adsorption-desorption of N<sub>2</sub> and mercury porosimeter. These methods allow recognition of the surface area and pore volume.

Furthermore, basic parameters of geotechnical behaviour have been obtained by hygroscopic wet, retraction limit, Atterberg limits, plasticity index, Proctor, Normalized Proctor and Swelling test of Lambe.

X Ray diffraction has shown that the main composition is a trioctahedral smectite and not more than 10% of illite has been detected.

Data analysis obtained by TEM - EDX have confirmed it is a saponite with a structural formula :  $(\text{Si}_{7,32} \text{Al}_{0,67}) (\text{Al}_{0,98} \text{Mg}_{3,23} \text{Fe}_{0,89}) \text{Ca}_{0,08} \text{K}_{0,39} \text{O}_{10} (\text{OH})_2$

The study of the microstructure shows the differential consolidation of this bentonite, which contains very wide microstructure zones of Cornflake type, which is the characteristic type of smectites. These areas are full of different size pores. On the other hand, there are zones with few pores, which contain dense and large aggregates of particles. In general it can be observed quite opened structures formed by laminar particles which keep edge to edge and edge to face contacts. This means that the collapse potential of this structure is very high. Moreover, fibrous shapes and laminar-fibrous aggregates are relatively abundant. Three different types of morphologies have been recognized depending on their size and textural relationships with the rest of laminar particles they are associated with. Since Sepiolite has not been detected by DRX, we cannot assume that these fibres belong to it.

A crystal structure study by Oblique Texture Electron Diffraction Patterns shows that the crystal is monoclinic with an angle  $\beta = 100^\circ$  and the unit cell parameters are:  $a = 5.2 \text{ \AA}$ ,  $b = 9.2 \text{ \AA}$  and  $c = 9.6 \text{ \AA}$ . The stacking sequence of this mineral can be described as 1M. Textural Patterns show a high structural disorder degree. It is obvious that the crystallographical identification of the sample is very important because the main part of the physical-chemical properties of smectites are directly related to the crystallographical properties.

The specific surface area of the sample (calculated by application of the BET equation) is  $114 \text{ m}^2/\text{g}$ . This value is greater than the usual ones is obtained from smectites ( $40 - 80 \text{ m}^2/\text{g}$ ). The nitrogen adsorption-desorption isotherm at 77K corresponds to type II in the IUPAC classification. The isotherm presents a hysteresis loop to type H3 of the same classification. This hysteresis loop can be related to the existence of flat voids, which agree with the particle laminar shape of smectites. The micropores area, calculated by Pearce method, is  $38 \text{ m}^2/\text{g}$  approximately.

The study of the biggest pores ( $> 300 \text{ \AA}$  of radius) was performed using a mercury porosimeter. A distribution of pores in minor range ( $< 0.1 \mu\text{m}$ ) is obtained in the  $0.02\text{-}0.04 \mu\text{m}$  interval. Bulk and skeletal density, calculated by this method, is 1.8 and 2.5 cc/g, respectively. The structural properties of the sample, together with the great amount of little size porosity accesible to water and other fluids, provide a great natural adsorption capacity.

The high plasticity (62%), the very high absorption and swelling capacity and its considerable high Liquid Limit (104%), shown by the geotechnical tests, are due to the porosity of the microstructure and crystal structure of smectites. When these materials are subjected to compactation stress (Proctor and Modified Proctor), the density obtained is never higher than  $1.23 \text{ gr/cm}^3$  which is very low for the impermeability obtained.

In summary, it can be concluded that the bentonites from the "Cerro del Aguila" have a high mineralogical purity degree as well as a great structural disorder. Furthermore, they show a high porosity and specific surface value. These data can be related to its microstructure, which consists, not only in the usual smectite particle arrangement, but also display a conspicuous fibrous morphology. These characteristics must have an influence on the bentonite properties.

#### BIBLIOGRAFIA

- BRELL et al. (1985): "Clay mineral distribution in the Evaporitic Miocene Sediments of the Tajo Basin, Spain" Miner. Petrogr. Acta Vol. 29 pp 267-276.
- CUEVAS RODRIGUEZ, J. (1991): "Caracterización de las esmectitas magnésicas de la Cuenca de Madrid como material de sellado. Alteración Hidrotermal" ENRESA. Publicación Técnica Num 04/92
- DOMINGUEZ DIAZ, MC. (1994): Tesis Doctoral. U.C.M.
- GALAN, E. et al (1986): Applied Clay Science, 1 pp 295-309.
- GARCIA ROMERO, E. (1988): Tesis Doctoral. U.C.M.
- SUAREZ BARRIOS, M. (1992): Tesis Doctoral. Univ. de Salamanca.
- ZVYAGIN, B.B.(1967): "Electron diffraction analysis of clay mineral structures" Plenum Press. New York. pp 364 .

Dpto. Geociencias, Univ. de Aveiro, Portugal

## Lateritic-bauxitic clays of Andorinha (Cantanhede, Portugal): further mineralogical and geochemical data

Santos A, Rocha F and Gomes C

Several geological, mineralogical and geochemical features as well as genetic considerations related to the karst-type lateritic-bauxitic clays of Andorinha (Cantanhede-Portugal) had been reported by Gomes (1965,1966,1967, 1968, 1979, 1982, 1987, 1991). Those clays which during the sixties and seventies had been exploited to make refractory bricks and in, a smaller scale, taylor's chalk, fill some dissolution sinkholes developed on the local middle Jurassic limestone. These filled sinkholes follow a preferred alignment ( E-W ) as shown in the sketch of the geologic map shown in fig.1 and some of them are covered by an early Cretaceous sandstone rich, in places, of white feldspar and kaolinite whereas in other places contains a red or purple clay matrix.

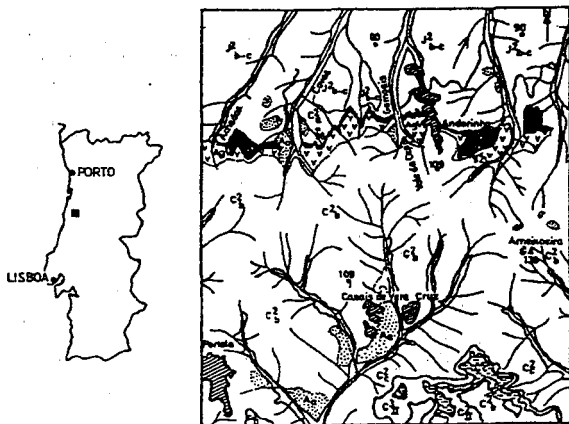


Fig. 1 - Geology of the Andorinha region, 1:50.000, where hyperaluminous clays do occur.

 Middle Jurassic limestone	 Hyperaluminous clays
 Lower Cretaceous sand	 Cretaceous (Senonian) sandstone
 Lower to middle Cretaceous sandstone	 Cretaceous (Turonian) limestone
 Tertiary and Quaternary sands	

However, clay fillings do not contain siliciclastic minerals, such as quartz, feldspar or mica. On the other hand, they exhibit supergenic minerals and textures which indicate the effects of both diagenetic and epigenetic processes that took place inside the sinkholes as consequence of repeated wetting and drying episodes. Kaolinite, hematite, goethite, gibbsite, bohemite, anatase, rutile, pyrolusite and a Sr,Ba, Al phosphate-sulfate (crystallochemically close to svanbergite) are the minerals identified in the lateritic-bauxitic clays. Gomes (1991) reports geochemical data proving both mobilization and enrichment of some chemical species in the clay bodies.

Firstly, the present paper deals with the establishment of a profile representing the vertical discrimination of the various lithological, textural and mineralogical facies recognized in the clay bodies that fill the sinkholes. Individually, clay bodies exhibit differences in regards to lithological, textural and mineralogical facies. The virtual sequence for the identified facies, from bottom to top, is as follows: dark plastic clay facies, massive non-plastic clay facies, breccia-like facies, nodular facies, pisolitic facies, lateritic cuirasse. To the described facies correspond a certain variation in what concerns clay minerals and associated non-clay minerals evolution ( Fig. 2 ).

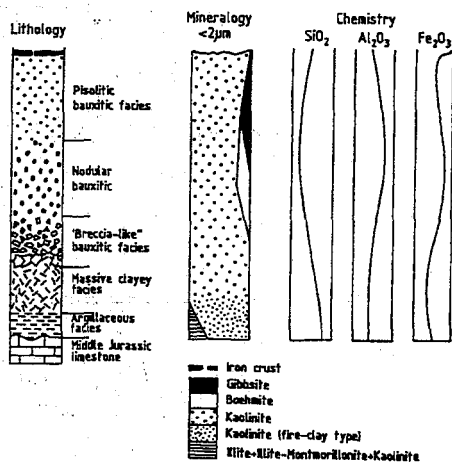


Fig. 2 - Vertical evolution of clay and non-clay minerals.

Secondly, lithological, textural, mineralogical and geochemical studies were carried out on samples collected along transversal N-S profiles, for two of the clay filled sinkholes (Fig.3). On the other hand, variations on crystallinity of kaolinite were measured on those samples.

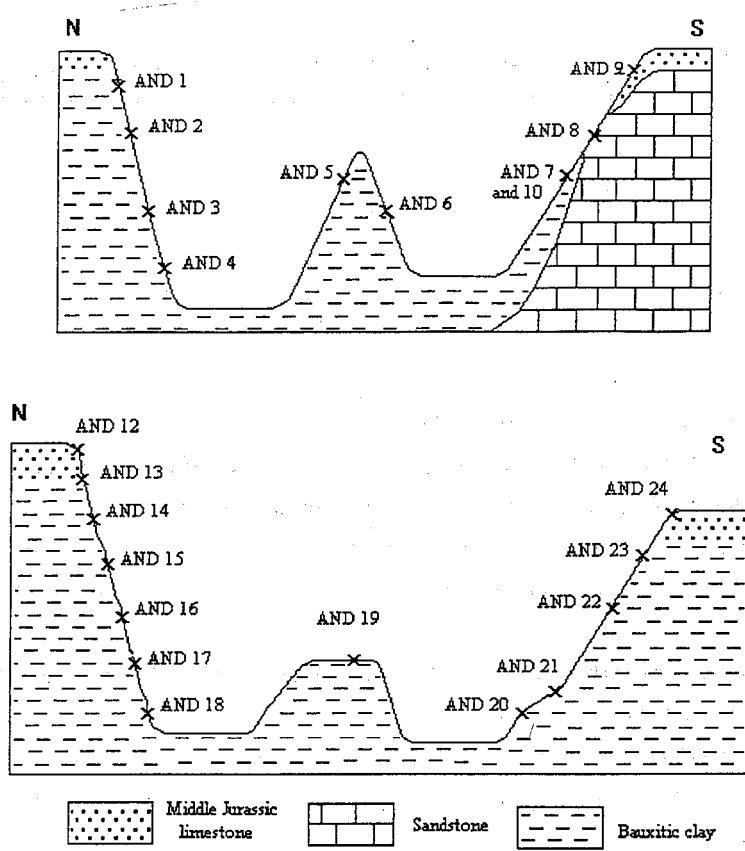


Fig. 3 - Transversal N-S profiles.

For both profiles, it was found a centripetal enrichment in oxides/hydroxides of Fe, Mn, Ti and Al. This enrichment coincides with the occurrence, in the central part of the clayey body, of the Ba, Sr, and Al phosphate-sulfate previously referred to. Both compacity and hardness of the clayey material increases centripetally as well. The central part of the clayey bodies that fill the sinkholes is in fact a disturbed zone characterized by its breccia-like facies, an expression of the effects of repeated wetting and drying cycles, more pronounced in that zone because of the outlet for the infiltrated waters is located underneath.

Finally, some considerations on the genetic evolution of the lateritic-bauxitic clays are put forward.

## Clay mineralogy and geochemistry of Miocene sediments from Setúbal peninsula (Portugal)

*Silva A P, Rocha F and Gomes C*

---

### INTRODUCTION

Setúbal peninsula is located to the South of Lisbon, close to the mouth of the Tagus river. It is part of the Tagus Tertiary basin and is made up of two major morphostructural units: Arrábida hills with steepy relief, formed of limestone, dolostone, marl, conglomerate, sandstone and shale, dated from Mesozoic up to Miocene and the Albufeira synclinal characterized by smooth relief and lower altitudes, formed of sand, clay, calcareous sandstone and eolian sands, dated from Miocene up to Holocene.

The present paper deals with the investigation of three Miocene outcrops located at Foz da Fonte, Penedo and Costa da Caparica (Fig. 1).

At the outcrop of Foz da Fonte, lower Miocene is overlying medium Cretaceous (Cenomanian) limestones. An alternation of limestone and micaceous sand, calcareous sandstone and lumachela characterizes lower Burdigalian.

The outcrop of Penedo is dated as medium Miocene and base of upper Miocene. That outcrop consists of fine marly and micaceous sandstone; medium grained sandstone with glauconia, ferruginous concretions, rolled pebbles and fossiles; sandy limestone rich in glauconia; fossiliferous conglomerate with a marly-glauconiferous matrix; marly limestone. In this outcrop, upper Miocene consists of fine sands with thin layers containing calcareous concretions.

At the outcrop of Costa da Caparica, Langhian (medium Miocene) is poorly represented. On the contrary, Serravalian and Tortonian are well represented. Serravalian is characterized by sequences of silty pyritiferous bluish clays in which grain size decreases upwards, separated by erosian surfaces.

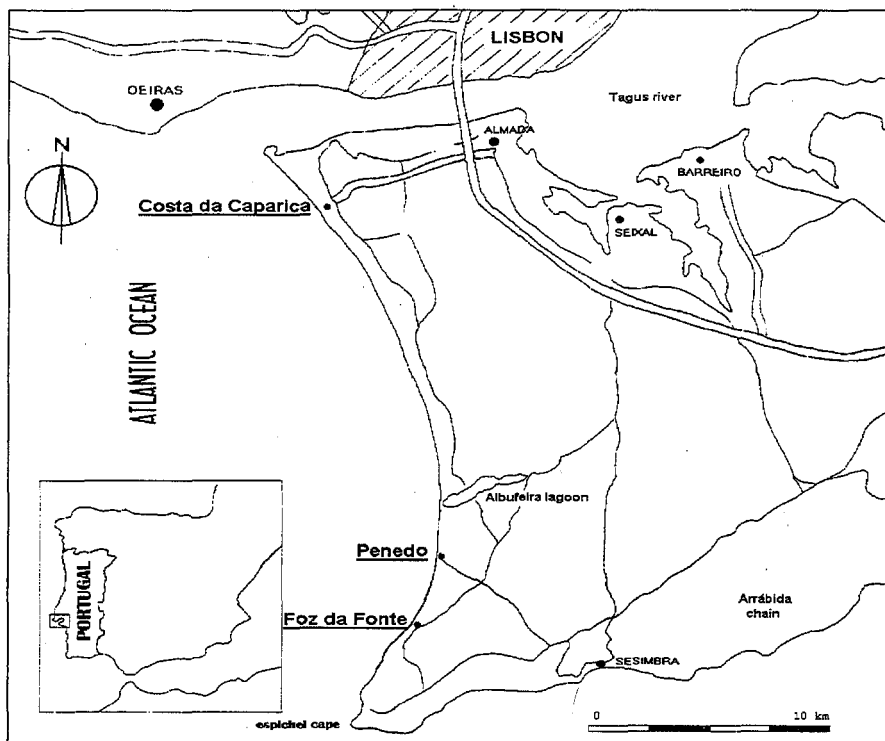


Fig.1 - Geographic setting of the areas under study.

The main goal of the present paper is to utilize both mineralogical and geochemical data of the sediments, in particular relative to their clay fractions, for the establishment of stratigraphic markers and for paleoambiental reconstruction.

#### MATERIALS AND METHODS

Thirty seven samples, collected in the three outcrops: Foz da Fonte, Penedo and Costa da Caparica, has been studied.

The mineralogical study of these sediments, particularly of the clay components, has been based mainly on X-ray diffraction (XRD) determinations, carried out in both the less than 38  $\mu\text{m}$  and 2  $\mu\text{m}$  fractions. Qualitative and semi-quantitative determination of clay and non-clay minerals

has been done in both fractions. The clay mineral composition was determined in oriented specimens. For semiquantitative determinations of clay and non-clay minerals, criteria recommended by Schultz (1964) and Thorez (1976) had been followed. Chemical analyses of both major elements (MgO, Al<sub>2</sub>O<sub>3</sub>, SiO<sub>2</sub>, CaO, TiO<sub>2</sub>, Fe<sub>2</sub>O<sub>3</sub>, Na<sub>2</sub>O and K<sub>2</sub>O) and minor elements (Cu, Ni, Co, Zn, Pb, Cd, Mn and Cr), have been carried out using X-ray fluorescence, atomic absorption spectrometry and flame-spectroscopy methods.

## RESULTS AND DISCUSSION

Lower Miocene in Foz da Fonte outcrop consists of sedimentary units, represented at its base, in what concerns the fine fractions, by quartz, calcite and K feldspar and by illite, kaolinite and rare smectite. Mineral composition becomes upward richer in carbonates (particularly dolomite) and show slight oscillations in illite and kaolinite contents.

Medium Miocene in Penedo outcrop consists, at the base of the profile, in the case of the fine fractions of their sediments of quartz, K feldspar, Na-Ca feldspar and calcite, whereas illite and kaolinite represent the clay minerals. Upwards in the profile sediments become enriched in carbonates (calcite dominates but dolomite occurs in some layers) as well as in smectite. Several greenish layers rich in glauconite, attributed to Tortonian, occur at the top of the profile.

Mineral composition of the uppermost section of medium Miocene in the Costa da Caparica outcrop is similar to mineral composition of equivalent strata from Penedo outcrop. Nevertheless, in the present case is characterized by an upwards increase in carbonates (essentially calcite), in illite and not so remarkably in smectite.

Mineral composition of the lowermost section of the upper Miocene (Tortonian) becomes much more siliciclastic, composed mainly by quartz associated to small contents of K feldspar, as non-clay minerals and illite and layers rich in glauconite. Going up in the section mineral composition becomes richer in calcite and illite is practically the only clay mineral present.

Dip. di Scienze della Terra.  
Univ. di Pavia, Italia

## Particle morphology evolution (flake-to-lath) as initial diagenetic transformation of a smectite-illite interstratification within a "dry" geochemical confined environment

Veniale F and Setti M

Mechanisms of diagenetic smectite-to-illite conversion are still matter of debate. Especially, the formation of lath-shaped illite is questioned: whether authigenic (neoformed), or derived from a smectite precursor via a transition mechanism ("cannibalization" of smectite) in which illite forms from smectite by dissolution, precipitation and growth operated by the action of interstitial solutions. A different illitization mechanism for random and ordered interstratifications was also postulated, by which the conversion of smectite into illite might have proceeded via solid state transformation.

Investigating the diagenetic processes occurred in "varicoloured" shales along the Appennines stripe in central and southern Italy, a facies marked by needles of illite has been encountered. The chemical composition of lath-illite particles includes < 5% of potassium (EDXA microanalysis), quite similar to the amount detected in smectite flakes: this corresponds to 40% of discrete illite within a smectite/illite interstratification.

Detailed SEM observation have evidenced that a direct morphological transition from flakes to laths occurred, via a flattening and thinning of the original wavy flakes; furthermore, the formation of lath-particle proceeded from edge scallops by disaggregation of larger coherent particles in which the laths are already evident. This is probably due to a modification of the order degree (from random to more ordered) within the interstratification, coupled with lowering of expandibility.

There are still some questions to be clarified: i) kinetics (rate) of the transformation reactions; (ii) influence of the thermal history; and (iii) the role of water content, on the intermediate stages of conversion. However, the obtained results show that the early stage of diagenetic smectite-to-illite transformation occurred by disaggregation of flaky particles into lath-like ones. Likely, such diagenetic transformation took place without noticeable chemical change in a geochemically confined environment with small water/rock ratio, as could happen in shales (by drying-wetting cycles due to pulsated squeezing during tectonic events).

(1) Instituto Andaluz de  
Ciencias de la Tierra, CSIC-  
Universidad. Granada,  
España

(2) TOLSA, S.A. Madrid,  
España

## A comparative study of the chemical, micromorphological and technical characteristics of pure spanish sepiolites

*Yebra A (1), López Galindo A (1) and Santarén J (2)*

Sepiolite is an Mg-hydrated fibrous phyllosilicate which is common in some spanish continental tertiary basins (*cf.* Galán and Castillo, 1984; Torres-Ruiz *et al.*, 1994). It possesses certain absorptive and rheologic properties, derived both from its texture and its structure, which make it highly interesting for many industrial applications (Alvarez, 1984). Thus, a correct technical characterization of this mineral must take into account all the chemical and micromorphological variables that may have a bearing on its behaviour.

This paper comprises a microgeochemical and textural study of three samples of virtually pure sepiolite, of similar chemical composition but different behaviours in certain tests for physical characterization. The objective of the study was to establish whether there exists any correlation between the two sets of variables.

### Materials and methods

Samples were obtained from the Tajo basin, from three quarries exploited by the TOLSA SA company, identified as *Vicálvaro* and *Parla* (in the province of Madrid) and *Yunclillos* (in the province of Toledo). X ray diffraction was performed with Philips PW1710 apparatus equipped with an automatic slit and an exploration speed of 1° / minute. Chemical microcomposition analysis was carried out with a Philips CM20 electronic microscope. Textural analysis was carried out on the basis of the microphotographs obtained with a Zeiss DSM 950 SEM, with an enlargement range of 200 to 5000X, using the MIP4 (adv, v.4.3) program (Micron España SA).

Textural study based on image analysis is, a priori, an ideal technique to determine parameters such as fibre size, porosity and the shape of particle bundles. This technique is practically the only one that is valid when the material studied presents a high degree of anisotropy, such as is the case of fibrous clays, because conventional granulometric analysis (sieving, optical microscope, gravity sedimentation, centrifugation, laser analyser) is more useful for equidimensional particles, where size is considered to be the diameter of a sphere of equivalent volume (Svarosky, 1990). Furthermore, sepiolite is frequently present in populations of fibres of distinct shapes and sizes, producing very diverse bundles, even within the same sample. This fact can only be appreciated with the aid of SEM applied to the original sample, combined with image analysis of the results. Thus, on the one hand, additional data are obtained regarding the number of bundles and their porosity (taking this to be the inter-particle space not occupied by the matrix (Frykman, 1992). On the other hand, the image is improved by segmentation using levels of grey to suit it to the requirements of the analysis to be performed (Dilks and Graham, 1985; Evans *et al.*, 1994), as each segmented bidimensional image may be treated in terms of

mathematical parameters (Allard and Sotin, 1988).

## Results

DRX examination showed that the three sepiolites studied were structurally identical, with unit cell values of  $a=13.5253 \text{ \AA}$ ,  $b=26.978 \text{ \AA}$  and  $c=5.2531 \text{ \AA}$  (mean volume of the unit cell  $1916.7646 \text{ \AA}^3$ ).

The microcomposition data calculated from a population of 30 particles per sample also evidenced a high degree of similarity. The average structural formula was  $(\text{Si}_{11.81}\text{Al}_{0.19})\text{O}_{30}(\text{Mg}_{7.96}\text{Al}_{0.04})(\text{OH})_4(\text{OH}_2)_4 \cdot (\text{H}_2\text{O})_6$ . The composition ranges were: Si, 11.57-12; Mg, 7.55-8;  $\text{Al}^{\text{VI}}$ , 0-0.39 atoms per unit cell.

The textural data show there were no great differences in the mean width or length of the sepiolites from Yuncillos or Vicálvaro. However, the former presented a greater dispersion of length values, and the latter, a greater dispersion of width values. In addition, the sepiolite from Yuncillos appeared in bundles of greater size, whilst the bundles from Vicálvaro were more numerous. Finally, the sepiolite bundles from Parla were the most uniform in dimension and also those that occupied the greatest percentage of the total surface. The porosity resulting from the aggregation state was greatest in the sample from Parla, which is attributed to the greater percentage of fibres forming bundles. The lower porosity observed in the Yuncillos and Vicálvaro samples may be due to there being a higher percentage of individual fibres, which occupy the spaces between the bundles.

The following were found to be related: the index of whiteness and viscosity, specific surface and the mean bundle surface; fibre length and the surface occupied by the pores; viscosity and specific surface; dispersability and apparent density, relation between fibre length and width and bundle surface.

*This paper forms part of Project AMB93-0794 (CICYT) and Group 4065 of the Junta de Andalucía.*

Table 1. Physical and morphological properties of the sepiolites studied

	Vicálvaro	Parla	Yuncillos
Index of brightness (%)	61.4	70	68.2
Apparent density ( $\text{g/cm}^3$ )	0.89	0.90	1.00
Brookfield viscosity (5 rpm)	21600	29800	24000
Dispersability at 72 h (%)	60	63	70
Specific surface ( $\text{m}^2/\text{g}$ )	336	347	345
Mean fibre length ( $\mu\text{m}$ )	1.95	1.80	2.06
Mean fibre width ( $\mu\text{m}$ )	0.140	0.130	0.146
Length / Width	13.93	13.85	14.11
Surface occupied by pores (%)	15.61	27.47	12.80
Mean bundle surface ( $\mu\text{m}^2$ )	19.01	56.68	63.70

## References

- Allard D and Sotin C (1988). Determination of mineral phase percentages in granular rocks by image analysis on a microcomputer. *Computers and Geoscience* **14** (2): 261-269.
- Alvarez A (1984). Sepiolite: properties and uses. In: A Singer y E Galán (Eds). *Palygorskite-Sepiolite. Occurrences, Genesis and Uses*. *Dev. Sedim.* **37**, Elsevier, 253-287
- Dilks A and Graham SC (1985). Quantitative mineralogical characterization of sandstones by back-scattered

- electron image analysis. *Journal of Sedimentary Petrology* **55** (3): 347-355.
- Evans J, Hogg J, Hopkins MS and Howard RJ (1994). Quantification of quartz cements using combined SEM, CL, and image analysis. *Journal of Sedimentary Petrology* **64** (2): 334-338.
- Frykman P (1992). Quantification of pore geometry in carbonates using image analysis; Upper Permian (Zechstein) of Denmark. *Geologie en Mijnbouw* **71**: 23-32.
- Galán E and Castillo A (1984). Sepiolite-palygorskite in Spanish Tertiary basins: genetical patterns in continental environments. In A Singer and E Galán (Eds): *Palygorskite-sepiolite. Occurrences, genesis and uses. Development in Sedimentology* **37**, Elsevier, 87-124.
- Svarovsky L (1990). Characterization of powders. In: *Principles of powder technology*. MJ Rhode (ed.): 40-69.
- Torres-Ruiz J, López-Galindo A, González-López JM and Delgado A (1994). Geochemistry of Spanish sepiolite-palygorskite deposits: genetic considerations based on trace elements and isotopes. *Chem. Geol.*, **112**, 221-245.

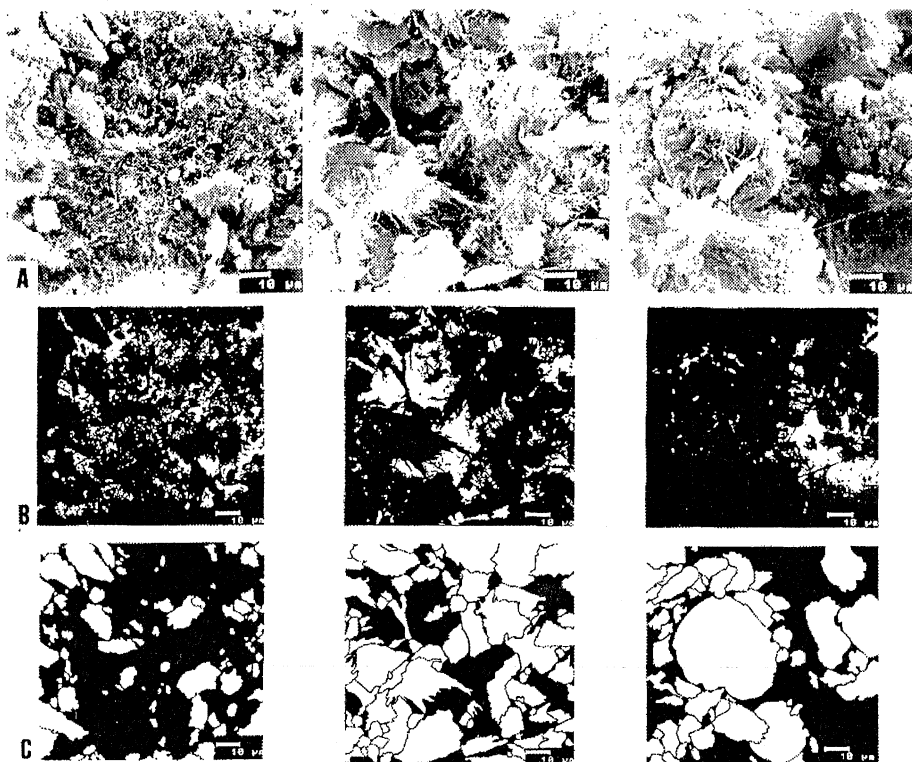


Fig 1. SEM and processed images of studied samples used to calculate the surface occupied by pores and by bundles. (A) From left to right, sepiolite from Vicávaro, Parla and Yuncilllos (B) Segmented images showing pore surfaces (white zone) in the same order. (C) Delimited bundles in white.

Dpto. Mineralogía y  
Petrología. Fac. Ciencias.  
Univ. del País Vasco. Bilbao,  
España

## Clay mineralogy and the organic matter maturity grade of the Gordexola formation (Basque-Cantabrian basin, northern Spain)

Zuluaga M C, Aróstegui J, García Garmilla F and Suárez Ruíz I

The Gordexola Formation (Zuluaga et al., 1996, maximum thickness 2.400 m in the type-section, lower to middle Albian) is widely outcropped at the south limb of the Bilbao anticlinorium, whose structural trend is NW-SE. The lower limit of this formation is marked by the first appearance of carbonate breccias indicating an important sedimentary rupture during the lower Albian. The top of the unit coincides with the earliest deltaic-lobes progradational sequences of the Valmaseda Formation (Upper Albian-Lower Cenomanian). The Gordexola Formation exhibit significant thickness variations along 16 Km in the studied sector. Thus, whereas in Gordexola it reaches to 2.400 m., in Orozko is only about 1.700 m. thick.

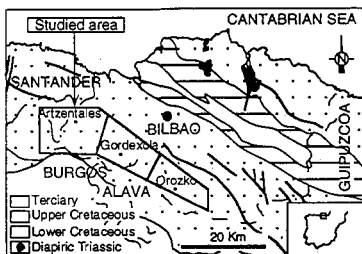


Fig. 1.- Geographic and geologic location of the studied area.

The Gordexola Formation is largely composed by black shales, bearing a relatively high content in organic matter, and interbedded sandstones. This fact suggests that the unit was deposited in a very restricted environment, with strong reducing conditions more emphasized in the central-area. Fossils indicating normal-marine salinity waters are almost absent, with the exception of some echinoderm fragments, orbitolinids and other foraminifers. The unit shows important lateral and vertical facies intertonguings. Although the background sedimentation is clearly lutitic, five different facies has been differentiated (Zuluaga et al, op. cit.).

These facies features lead us to think in a marine, related to reef complexes, restricted depositional environment for the Gordexola Formation. In some places a shallowing tendency is conspicuous towards the upper part of the unit, with development of tidal/subtidal facies associations which anticipate the shallow-deltaic-marine character of the Valmaseda Formation.

The study area has been divided into three sections: western (Artzentales), central (Gordexola) and eastern (Orozko) (fig. 1). A total of 280 pelitic samples, uniformly distributed among the sections, were collected and the whole rock and the <2 µm fraction were analyzed by X-ray diffraction (XRD).

The whole mineralogy is very homogeneous and consists on clay minerals and quartz as major minerals in almost all the samples. Feldspars, pyrite and carbonates have also been detected, and the later ones are more abundant in the Artzentales section, where the proportions in some samples can be more than 25%.

The <2 µm fraction mineralogy is composed by illite, chlorite and I-S mixed-layers. The I-S mixed-layers determined are R1 and R3 types (Reynolds, 1980). The clay mineralogy distribution, and specifically that of the I-S mixed-layers, is not homogenous, showing the total absence of R1 in the Orozko section (fig. 2).

The Kübler index values of the central and western sections are more scattered by the variable proportions of the R1 I-S mixed-layer. In both sections the values are typical of diagenesis. Nevertheless, in the eastern section the Kübler index values are less scattered and lower, and they fall into the anquizon (fig. 3).

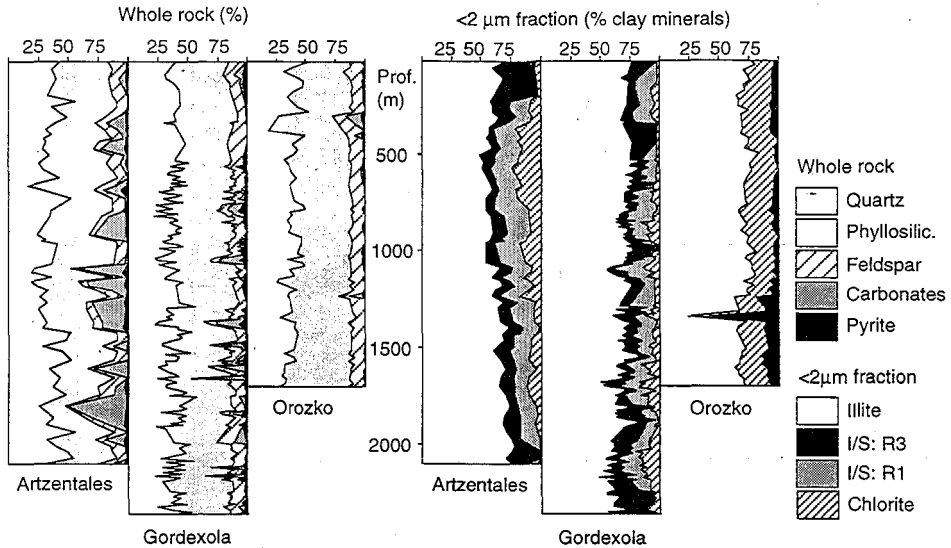


Fig. 2.- Mineralogical distribution of the whole rock and <2 μm fraction along the three sections.

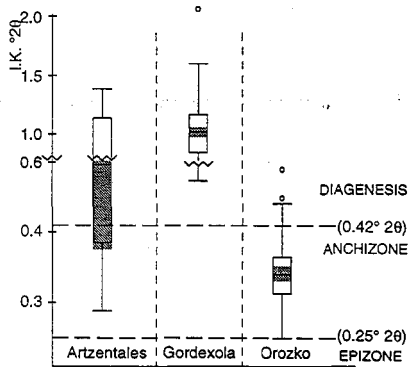


Fig. 3.- "Boxplot" diagrams of the Kübler index for the <2 μm fraction.

Likewise, a petrographic study of the disperse organic matter in pelitic rocks has been made. The mean values of the vitrinite reflectance (%Rr) obtained are: 3.00% for the Artzentailes section, 4.38% for Gordexola and 4.4% for Orozko.

A comparative analysis of both, mineralogical and organic, parameters shows a different maturity grade between the Orozko series and the other ones (fig. 4). Otherwise it has also been observed that both parameters indicate different diagenetic grades of maturity. This difference could be explained on the basis of physical and chemical factors which take part on the evolution of those parameters.

In this way, while clay minerals depend on (i) the diagenetic environment chemical composition (Roberson and Lahan, 1981; Eberl, 1978), (ii) the initial smectite composition (Freed and Peacor, 1992), (iii) the permeability of the rock (Freed and Peacor, 1989) and (iv) the residence time (Ramseyer and Boles 1986), the vitrinita maturity is a function of temperature (Baker and Pawlewicz, 1986) and time (Bostick et al, 1978).

The maximum temperature values that reached the Gordexola Formation were obtained by application of the EASY%Ro model (Sweeney y Burham, 1990). This model was applied to several samples bearing vitrinite layers and located in overlying-to-Gordexola Formation horizons (Arostegui et al., 1996). The measured reflectance values for synchronic horizons have been 2.75% and 3.75% for Artzentailes-Gordexola and Orozko, respectively. The maximum temperatures calculated in this way for the top and bottom, in the central section of the Gordexola Formation, are 280 and 352°C respectively. The observed differences in the organic matter maturity grade, between the Gordexola and the Orozko series, could be explained in three different ways: (i) a local hiperthermal

anomaly, (ii) the presence of convectivity phenomena associated to an important hydrothermal activity or (iii) the influence of shear stress .

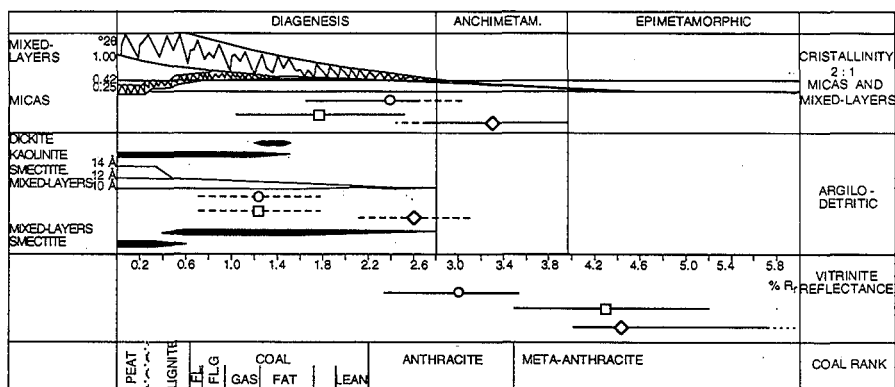


Fig. 4.- Comparison between mineral associations and vitrinite reflectance following the diagrams of Kübler et al. (1979). (□: Gordexola, ○: Artzentales, ◇: Orozko).

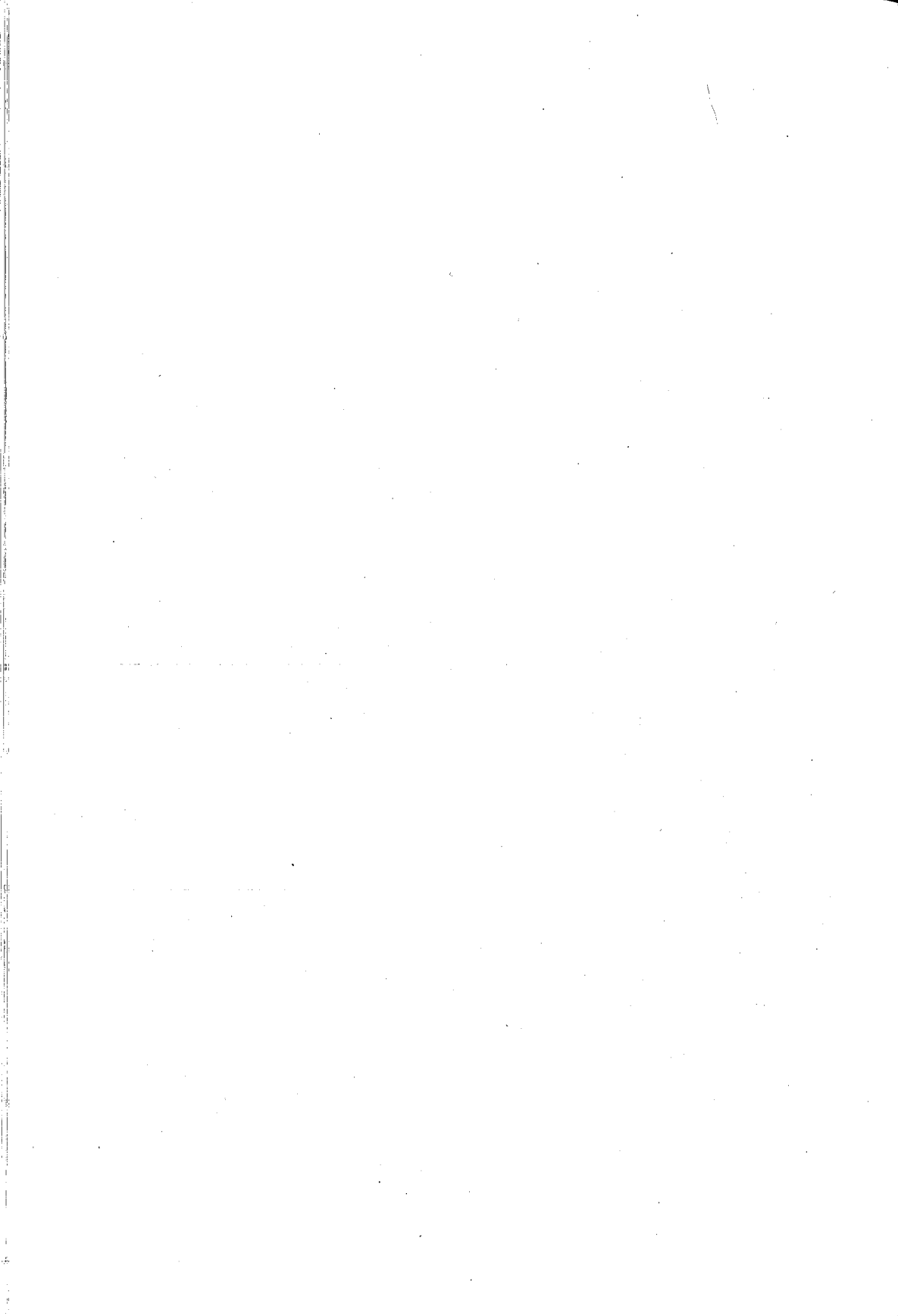
As it has been observed, the obtained temperatures are high enough to complete the illitization process. However, the Orozko section, which presents the more advanced diagenetic trend, only shows the I-S mixed-layer R3, whereas the temperatures at Gordexola were not been able to perform the total transformation from R1 to R3. This fact suggests that in the Gordexola Formation there should be other decisive factors than temperature and time responsible for the illitization process. Among them, the mineral composition should be rejected because of the great homogeneity of petrographic and geochemical data (Zuluaga, 1995). Thus, it would be reasonable to think of another ways to explain the illitization process, as it could be the potassium availability, which, together with the relatively high proportion of organic matter in Orozko (Surdam and Crossey, 1985), could yield a more advanced trend.

#### Acknowledgments

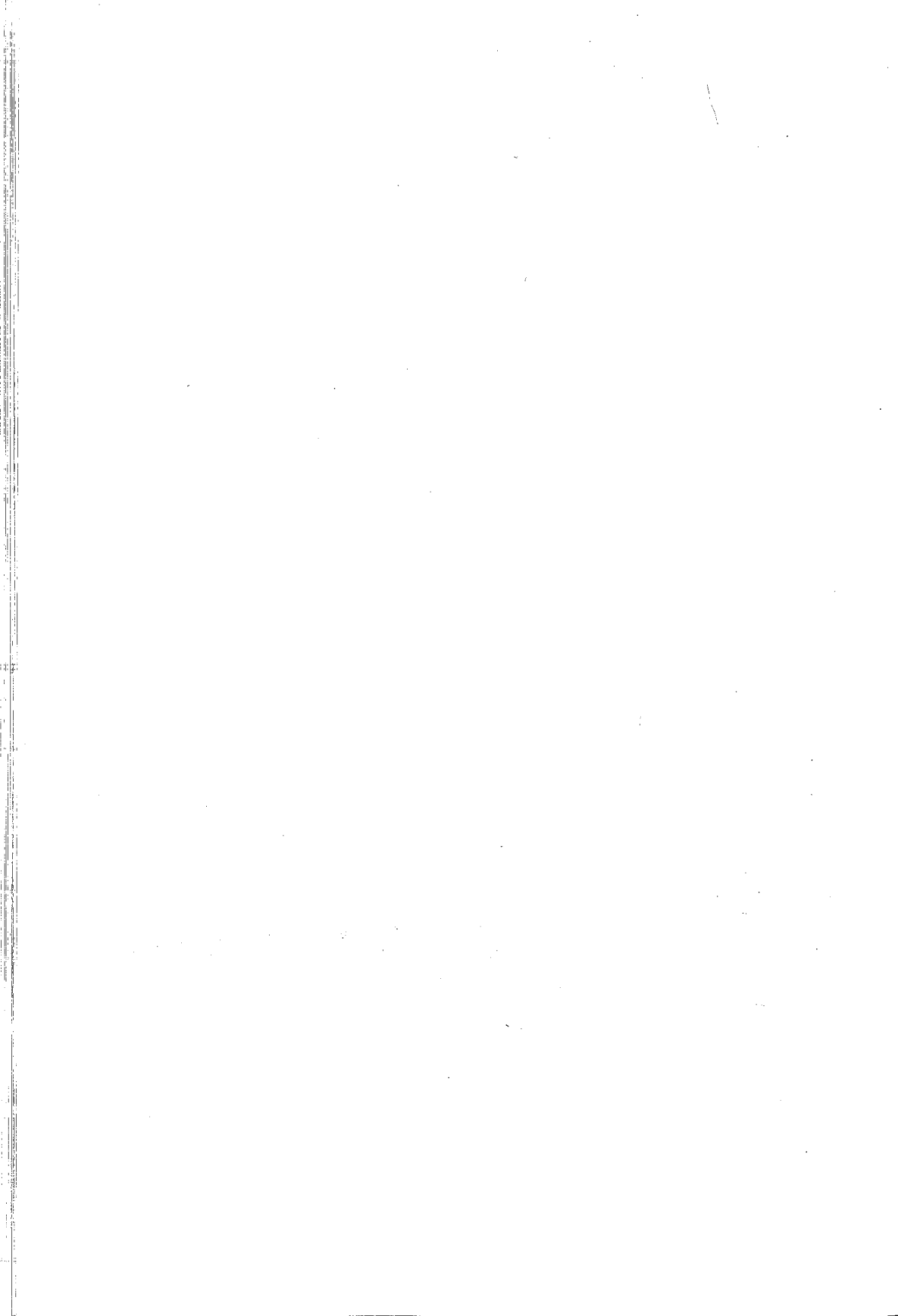
This work was financially supported by the Research Project of the Universidad del País Vasco (UPV/EHU) No. 130.310-EA039/94.

#### References

- Arostegui J, Zuluaga M C, García-Garmilla, Sangüesa F J & Suárez-Ruiz I (1996). 16ème Réunion des Sciences de la Terre. RST.96 Orléans. 121.  
 Baker C E & Pawlewicz M J (1986). *Paleogeothermics, lecture notes in earth sciences*. 5. Ed. G. Buntbarth & L. Stegena. Springer Verlag. 79-228.  
 Bostick N H, Cashman S M, McCulloh T H, & Waddell C T (1978). *Low temperature metamorphism of kerogen and clay minerals*. S.E.P.M. Special Symposium. 65-96.  
 Eberl D (1978). *Geochim. Cosmochim. Acta*. 42, 1-7.  
 Freed R L & Peacor D R (1989). *Clay Miner.* 24, 171-180.  
 Freed R L & Peacor D R (1992). *Jour. Sed. Petrol.* 62, 220-234.  
 Ramseyer K & Boles J R (1986). *Clays Clay Miner.* 34, 115-124.  
 Reynolds R C (1980). *Crystal Structures of Clay Minerals and their X-ray Identification*. (G.W. Brindley & G. Brown, editors). Mineralogical Society, London. 249-304  
 Roberson H E & Lahann R W (1981). *Clays and Clay Minerals*. 29, 129-135.  
 Surdam R C & Crossey L J (1985). *S.E.P.M. Short Course*. 17. Tulsa. 177-232.  
 Sweeney J J & Burnham A K (1990). *A.A.P.G. Bull.* 74, 1559-1570.  
 Zuluaga M C, Arostegui J & García-Garmilla (1996). *Geocaceta*. 20  
 Zuluaga M C (1995). Unpubl. PhD Thesis UPV/EHU (ined.). 340 pp.



# SOIL MINERALOGY



(1) Dpto. Edafología y Química Agrícola. Fac. Farmacia. Univ. de Granada, España

(2) Dpto. Edafología y Química Agrícola. Fac. Ciencias Experimentales. Univ. de Almería, España

(3) Dpto. Geología. Fac. Ciencias Experimentales. Univ. de Jaén, España

(4) Dpto. Óptica. Fac. Ciencias. Univ. de Granada, España

## Kaolinite formation and soil color in Mediterranean red soils

*Delgado G (1), Sánchez Marañón M (2), Martín García J M (3), Melgosa M (4), Pérez M M (4) and Delgado R (1)*

### Introduction

Kaolinite is a stable mineral in Mediterranean red soils (Torrent, 1995). In these soils, argillization (increase in clay content) and rubification (hematite formation and consequent reddening) are simultaneous pedogenetic processes (Bornand, 1978; Delgado et al., 1995) and a quantitative relation has been found between hematite content and soil color, expressed as a redness ratio (Torrent et al., 1980). This paper discusses the quantitative relation between soil color and kaolinite content in the clay fraction in Mediterranean red soils, establishing a pedotransfer function enabling the calculation of this content from soil color, measured instrumentally and expressed in the CIELAB color space.

### Materials and Methods

18 soil profiles, 10 in Italy (Siena and Gorizia) and 8 in Spain (Granada and Málaga) with 36 samples of soil horizon (A/E or Bt). Substrates of hard carbonate rocks; mountainous landscape; xeric or udic soil moisture regime. Classification (Soil Survey Staff, 1994): Haploxeralf, Hapludalf, Rhodoxeralf, Argixeroll, Argiudoll, Palexeralf and Paleudalf. Munsell color (Munsell Co., 1990) between 2.5YR and 5YR; clay content in fine earth between 19% and 88%. Clay mineralogy: illite, smectite, vermiculite, illite-vermiculite and illite-chlorite interstratified phases, kaolinite, quartz, feldspar, goethite and hematite.

Spectroradiometric color measurements were taken in undisturbed (natural peds) and disturbed (ground and pressed) samples under standard conditions (CIE, 1986; Sánchez-Marañón et al., 1995); the CIELAB coordinates  $C_{ab}^*$ ,  $h_{ab}$  and  $L^*$  (CIE, 1978) and color index  $R_{Lab}$  (Barrón and Torrent, 1986) were recorded. Clay was extracted by sedimentation and expressed as % by weight of the fine earth (C). The kaolinite (K) and illite (I) content in the clay fraction was determined by X-ray diffractometry (XRD) using the intensity factor method (Schultz, 1964). Correlation and regression analysis was performed with Statgraphics software.

### Results and Discussion

In Data Set 1 (Table I) the color parameters correlated significantly well with K and to

Table I. Correlation analysis between soil color and mineralogical parameters.

	Disturbed samples				Undisturbed samples				Data Set
	L*	C* <sub>ab</sub>	h <sub>ab</sub>	R <sub>Lab</sub>	L*	C* <sub>ab</sub>	h <sub>ab</sub>	R <sub>Lab</sub>	
K	<u>-.5192</u>	.3879	<u>-.5133</u>	<b>.6394</b>	<b>-.5938</b>		<b>-.6089</b>	<b>.7717</b>	1
K/I	<u>-.4276</u>			<u>.4511</u>	<u>-.4713</u>	-.3458	-.3900	<b>.6325</b>	
K/C	<u>-.4737</u>		-.4178		<u>-.4889</u>		<u>-.4774</u>	<b>.7174</b>	
K			<u>-.6250</u>		-.6164		<u>-.7110</u>	<b>.8863</b>	2
K/I				.5993			<u>.7191</u>		
K/C				<u>.6200</u>			<b>.7496</b>		
K				.8060			-.7476	<b>.9637</b>	3
K/I							<u>.8830</u>		
K/C							<u>.8402</u>		
K							-.7685	.8104	4
K				.7356					5
K/I							.8040		
K				.9312					6
K/C	<u>-.9865</u>								

L\*, C\*<sub>ab</sub>, h<sub>ab</sub>: CIELAB color parameters. R<sub>Lab</sub>: color index (Barrón and Torrent, 1986). K: kaolinite in clay. I: illite in clay. C: Clay content (% wt). Significance level: bold letters < 0.001; underline letters < 0.01; normal letters < 0.05. Data sets: 1) A/E and B horizons from all the soils (n=36); 2) A/E and B horizons from Spanish soils with xeric moisture regime (n=16); 3) A/E horizons from Spanish soils with xeric moisture regime (n=8); 4) B horizons from Spanish soils with xeric moisture regime (n=8); 5) A/E and B horizons from Italian soils with udic moisture regime (n=8); 6) B horizons from Italian soils with udic moisture regime (n=5).

a lesser degree with the K/I and K/C ratios. The correlations indicate that K increases with soil reddening (< h<sub>ab</sub> and > R<sub>Lab</sub>) and darkening (< L\*).

The correlation between K and reddening indicates that the kaolinite and hematites are simultaneously neoformed in these soils. Kaolinite neoformation in Mediterranean red soils is documented in the bibliography (Bornand, 1978 ; Delgado et al., 1995; Torrent, 1995), and the simultaneous formation of kaolinite and hematite has been described by Bornand (1978). However, the relation between K and reddening has not previously been described.

The correlations between reddening and the K/I ratio corroborate the neoformation origin of kaolinite and that of illite by inheritance (Delgado et al., 1995); thus, soil evolution, which intensifies reddening, produces increases in the neoformed mineral phase (kaolinite) with respect to the inherited mineral phase (illite).

The direct correlations between reddening and the K/C ratio may also be interpreted in a genetic sense: clay content increases with soil evolution (Delgado et al., 1995) and the most important argillization process is the neoformation of kaolinite (Bornand, 1978).

The number of correlations with a level of significance >95% (p < 0.05) decreases

when the samples are grouped into smaller, more homogeneous populations, taking into account the soil horizon, the site and the soil moisture regime (Table 1, Data Sets 2, 3, 4, 5 and 6). However, the correlation index increases and, in some cases, so does the level of significance. The results for this data set corroborate the tendencies discussed above:  $R_{Lab}$  has constant high correlation coefficients with K, K/I and K/C. The best correlation ( $r = 0.9637$ ,  $p < 0.001$ ) was observed between  $R_{Lab}$  and K, in A horizons of the Spanish soils with a xeric moisture regime.

Pedotransfer functions have been established enabling the calculation of K from  $R_{Lab}$  (Table 2). Discrimination by soil horizon, site and soil moisture regime improves the forecast results of the pedotransfer functions, in which the  $R^2$  of 0.596 for data set 1 ( $n = 36$ ) rises to 0.928 for data set 3 ( $n = 8$ ).

Table II. Pedo-transfer functions between  $R_{Lab}$  (x) and kaolinite content (y).

DATA SET	PEDO-TRANSFER FUNCTION	n
A/E and B hs. from all the soils	$y = 2.462 + 0.093x$ $R^2 = 0.596$	36
A/E and B hs., Spanish soils with xeric m.r.	$y = 0.766 + 0.091x$ $R^2 = 0.785$	16
A/E hs. from Spanish soils with xeric m.r.	$y = 0.002 + 0.087x$ $R^2 = 0.928$	8
B hs. from Spanish soils with xeric m.r.	$y = 1.206 + 0.098x$ $R^2 = 0.657$	8
B hs. from Italian soils with udic m.r.	$y = -5.085 + 2.329x$ $R^2 = 0.867$	5

\*  $R_{Lab}$  in disturbed samples. hs.: soil horizons. m.r.: soil moisture regime.

## Conclusions

It is shown that the greater evolution of these Mediterranean red soils produces simultaneous kaolinite neoformation and reddening. The  $R_{Lab}$  index is the parameter that best correlates with kaolinite content in the clay fraction; pedotransfer functions were established between these, and prediction rates improved when the population was discriminated by pedogenetic factors.

**Acknowledgements:** We thank Mr. Claudio Mondini for help with field sampling and Mr. Glenn Harding for translating the original manuscript into English.

## References

- Barrón, V. & Torrent, J. (1986). *Soil Sci.* 37, 499-510.
- Bornand, M. (1978). Ph. D. thesis, Univ. Montpellier, 329 pp. Francia.
- CIE. (1978). Supplement No. 2 to Publication CIE No. 15. CIE Central Bureau, Paris. Francia.
- CIE. (1986). Publication 15.2, 2nd Ed. CIE Central Bureau, Vienna, Austria.
- Delgado, R., Aguilar, J. & Delgado, G. (1995). *Catena* 23, 309-325.
- Munsell Color Company. (1990). Munsell soil color charts. Baltimore. USA.
- Sánchez, M., Delgado, G., Delgado, R., Pérez, M.M. & Melgosa, M. (1995). *Soil Sci.* 160, 291-303.
- Sóil Survey Staff. (1994). Tch. Monograph No. 19, 6nd ed., USDA, Washington DC. USA.
- Schultz, L.G. (1964). *Geol. Surv. Prof. Paper* 391, 31 pp., Washington DC. USA.
- Torrent, J. (1995). Publ. Università Degli Studi di Napoli Federico II, 111 pp. Italia.
- Torrent, J. Schwertmann, U., Fechter, H. & Alférez, F. (1980). *Geoderma* 23, 191-208.

(1) Istituto di Ricerca sulle  
Argille. CNR. Area di Ricerca di  
Potenza, Italia

(2) Istituto Sperimentale per lo  
Studio e la Difesa del Suolo.  
Rieti, Italia

(3) Istituto Sperimentale per lo  
Studio e la Difesa del Suolo.  
Firenze, Italia

## A lithological discontinuity in a volcanic soil derived from latite (Mt. Cimini complex, Italy)

*Fiore S (1), Lorenzoni P (2) and Mirabella A (3)*

Several authors have detected different mineralogical compositions in soils derived from weathering of volcanic rocks, with the formation of kaolinite in the higher part of the profile and of halloysite in the deeper horizons. The authigenic formation of halloysite has been accounted for by the reduction of the porosity of the matrix, reducing the drainage and promoting Si enrichment in the lower horizons, whereas kaolinite could have formed in the higher horizons by ageing of halloysite (e.g., Allen & Hajek, 1989; Violante & Wilson, 1983).

The distribution in the 1:1 clay minerals with depth of the profile has therefore been explained in terms of a different pedogenetic process. However, it should bear in mind that volcanic deposits may change suddenly both chemical and mineralogical composition, as well as the grain-size distribution, especially in the case of pyroclastic rocks. Therefore, volcanic soils originated by weathering of a non homogeneous substratum might be much more common than described in literature.

In a recent study dealing with volcanic soils of the Cimino Volcanic Complex (Italy), (Lorenzoni et al., 1995) it was evidenced the influence of pedogenetic substratum in the formation of clay minerals. In detail, leucite tephritic lava was found to produce mainly amorphous short-order phases and lesser amounts of halloysite, while latitic lava yielded mainly crystalline clays .

In the higher part of the Mt. Cimino, Central Italy, it was observed a soil showing a discontinuity between the surface horizons and the lower ones. The site was characterized by the outcropping of latitic lava which, a few meters away from the profile, appeared fractured and overlying a friable pyroclastic layer.

This fortunate circumstance lead to the study of the soil and the pyroclastic layer to ascertain if the discontinuity evidenced within the soil was pedogenetic in origin or produced by differences in lithology of the substratum and the distribution of clay minerals within the profile.

The soil profile, classified as Vitrandic Haplumbrept, was constituted by the following horizons: A2, BA, Bw1, 2Bw2, 2BC1, 2BC2, and 2BC3. Samples from some of these horizons (A2, Bw1 and Bw2) were impregnated with Araldite resine, thin-sectioned and observed by optical microscopy. The clay fraction of soil horizons and two levels of

the pyroclastic layer were analysed by X-ray diffraction, following routine procedure and K-acetate intercalation, and by scanning electron microscopy.

Microscopic observations showed that the coarse fraction in the A2 horizons was mainly composed of phenocrysts of sanidine, with common ortho and clinopyroxenes, few flakes of weathered biotite and rare spherulites with concentric radial microstructure presumably of chalcedony. The Bw1 horizon differentiated itself for the absence of chalcedony and for a greater amount of biotite which was the dominant mineral. The 2Bw2 horizon was also dominated by moderately weathered biotite. Orthopyroxenes appeared almost completely pseudomorphosed into ferruginous products. The textural features were formed of few fragments of non microlaminated clays with strong continuous orientation and diffusion associated to the edges of ferruginous products derived from pyroxenes.

X-ray diffraction analysis carried out on the fractions  $< 2\mu\text{m}$  evidenced difference in clay mineralogy between the upper and the lower part of the profile. The upper three horizons were characterized by the presence of illite, of a mineral having 0.72 nm basal spacing, and of vermiculite, whose degree of hydroxy interstratification was higher in the upper two horizons. The lower part of the profile was composed of illite and of a mineral with a broad peak at about 0.72 nm. The two pyroclastic levels also contained small amounts of illite as well as the mineral with a broad X-ray peak at about 0.7 nm.

K-acetate intercalation procedure allowed the differentiation between kaolinite and halloysite (0.7 nm). Kaolinite is the only clay mineral present in the uppermost A2 horizon and it decreased towards the lower part of the profile, disappearing in the 2BC3 horizon. Halloysite, present in a very low amount in BA and Bw1 horizons, increased with depth until being the only mineral with 0.7 nm basal spacing in the deepest 2BC3 horizon. The two pyroclastic levels contained only halloysite (0.7 nm).

Microscopic analyses confirmed the field observations indicating the presence of a lithological discontinuity within the soil profile; in fact the lower part of the soil appeared as more weathered with a major iron segregation. These evidences are in agreement with the results of a previous study on the same soil profile (Bidini et al., 1995) indicating an increase in the amount of crystalline iron oxides towards the bottom of the profile.

The presence of halloysite and illite in the pyroclastic levels indicates that the minerals were formed before pedogenesis took place and therefore they are inherited by the soil. It is likely that illite is an initial constituent of the parent material whereas halloysite is formed by alteration of glass fragments owing to low temperature volcanic fluids or to percolating meteoric water. Such a mechanism of formation of halloysite seems to be common in volcanic deposits (Fiore et al., 1996).

## References

Allen B L & Hajeck B F (1989). In *Minerals in soil environments*, Dixon & Weed (eds.), SSSA, 198-278.

Bidini D, Lorenzoni P & Mirabella A (1995). Proc. XII Conv. Naz. Soc. Chim. Agr., 41-47.  
Fiore S, Genovese G & Miano TM (1996). This issue  
Lorenzoni P, Mirabella A Bidini D & Lulli L (1995). *Geoderma* **68**, 79-99.  
Violante P & Wilson M J (1983). *Geoderma* **29**, 157-174.

(1) Dpto. Geología. Fac. Ciencias Experimentales. Univ. de Jaén, España

(2) Dpto. Edafología y Química Agrícola. Fac. Farmacia. Univ. de Granada, España

(3) Dpto. Edafología y Química Agrícola. Fac. Ciencias Experimentales. Univ. de Almería, España

## Mineralogical composition and ultramicrofabric of entisols from Sierra Nevada (Granada, Spain)

*Martín García J M (1), Delgado G (2), Párraga J F (2), Sánchez Marañón M (3) and Delgado R (2)*

### Introduction

The formation and degradation of soils comprise essentially two aspects: changes in chemical and mineralogical composition, and the development of a characteristic morphological organization (fabric) at all levels, especially at the microscopical level (plasma) (Pédro, 1987). In this work we established the interrelationship between the mineralogy and the organization of soil particles at the ultramicromorphological level (ultramicrofabric) in poorly-developed soils (Entisols; Soil Survey Staff, 1994) from Sierra Nevada in Granada province, Spain. These soils are abundant in the mountain range, and they are initial phases of pedogenesis as well as erosive phases. The study of these soils can thus provide information on both soil genesis and degradation of the soil cover.

### Material and methods

We selected two soil profiles in Sierra Nevada; a Typic Xerorthent (P1) and a Lithic Xerorthent (P2) (Soil Survey Staff, 1994). The parent materials were micaschist and quartzites from rock slope deposits (P1), and "in situ" micaschists (P2). Mineralogical composition was determined in fine earth fractions ( $< 2$  mm) and clay ( $< 2 \mu\text{m}$ ) by X-ray diffractometry (XRD) with a Philips PW 1730 diffractometer in samples of disoriented crystalline powder (fine earth fraction and clay fractions), and in oriented aggregates (clay fraction). Semiquantitative mineral analysis (XRD) was done with the intensity factors method (Klug & Alexander, 1976). Ultramicrofabric was studied with scanning electron microscopy (SEM) in unaltered samples of horizons, using a Hitachi S-510 equipe.

### Results and discussion

Quartz, feldspar, chlorite, illite (K-mica) and paragonite were inherited from parent materials. Smectite and interstratified minerals were produced by transformation. Kaolinite resulted from neof ormation. Iron minerals originated from inheritance and neof ormation (Martín

García, 1994), and were slightly more abundant in P2, where seasonal iron release was more conspicuous. Kaolinite neoformation was also favored in this profile, from a higher altitude.

Macroscopic structure comprised subangular blocks (10-20 mm) divided into spheroid peds (1-1.5 mm). Ultramicroscopically, the structure hierarchy consisted of the following levels: 1) polyhedral and spheroid clusters (Yong & Warkenting, 1975) ranging in size from 40 to 100  $\mu\text{m}$ ; 2) phyllosilicate domains *s.str.* (Aylmore & Quirk, 1960) as large as 5  $\mu\text{m}$ , the most frequent domains corresponding to the fine silt range (5-2  $\mu\text{m}$ ) and coarse clay (2-1  $\mu\text{m}$ ).

Phyllosilicates (mainly micas) were the main constituent of plasma and the skeleton. Both face to face and face to edge associations of the mica layers were seen. Face to edge were facilitated by soil movements together with cementing agents, while face to face bonds arose through pedologic processes and through inheritance from the parent material: during weathering, the primary mica grains generate domains *s.str.* of laminas that follow the {001} cleavage planes.

Zonation was evident in the clusters. 1) In terms of mineral composition, the content of phyllosilicates and hematites increased toward the exterior of clusters, whereas the interior was relatively rich in quartz grains. 2) In terms of particle size, smaller particles were more frequent in the interior, and larger particles toward the exterior. 3) In terms of aggregation and porosity, the volume of voids is weaker in the exterior zone of the cluster. 4) Anisotropy was greater toward the exterior, where laminar domains were ordered tangentially.

Polygonality of the clusters depended on the arrangement of coarser particles (sands), and roundness was greater in the presence of cementing agents. The main cementing agents were iron minerals (hematite and goethite), organic matter, and fine clay. Hematite is neoformed in soils from Mediterranean areas (Torrent, 1995) and the surfaces of micas favor its epitaxial growth (Boero & Fanchini-Angela, 1992). Consequently, roundness and cluster identification in P2, as a result of the greater iron content in this profile, were greater than in P1 (Table 1). In the Ah horizons biological activity and humic cementing agents were important factors in the development of the ultramicrofabric. The finer clays associated with iron minerals also acted as structuring agents in these soils, accumulating on the surface of clusters and autocatalyzing structure genesis.

Acknowledgements. Project DGCYT PB94-07870 (M.E.C. Spain)

## References

- Aylmore L & Quirk J (1960). *Nature*, **187**, 1046-1048.  
Boero V & Franchini-Angela M (1992). *Eur. J. Mineral*, **4**, 539-546.

- Klug H P & Alexander L E C (1976). *X-ray Diffraction Procedures for Polycrystalline and Amorphous Material*. Wiley, New York.
- Martín-García J M (1994). *La génesis de suelos rojos en el macizo de Sierra Nevada*. PhD thesis, University of Granada, Spain.
- Pédro G (1987). *Cah. ORSTOM, sér. Pédol.*, **XXIII**, 169-186.
- Soil Survey Staff (1951). *Soil Survey Manual*. USDA, Washington, DC.
- Soil Survey Staff (1994). *Keys to Soil Taxonomy*. SMSS Technical Monograph No. 19. Sixth Edition. US Government Printing Office, Washington, DC.
- Torrent J (1995). *Genesis and properties of the soils of the Mediterranean regions*. Publ. Univ. Napoli Federico II, Napoli.
- Yong R N & Warkenting B P (1975). *Soil Properties and Behaviour*. Developments in Geotechnical Engineering 5. Elsevier, Oxford.

Table 1. Main morphological and analytical characteristics of soil horizons from Sierra Nevada, Spain. **P1**.- Altitude: 1460 m; UTM coordinates: 30SVG647116; **P2**.- Altitude: 2000 m; UTM coordinates: 30SVG678111

Prof/Hor	Struc.	Clay (%)	Silt (%)	OC (%)	pH	Mineralogy (%)										
						Fine earth (<2mm)			Clay (<2 µm)							
						Tect	Phyll	IM	Tect	Phyll			IM			
			Chl	Ill	Pa	Ka	Others									
P1	Ah	m1sbk	10.2	27.0	1.90	6.7	39	61	<5	13	8	59	11	9	Sm, Int	<5
	AC	m2sbk	11.2	25.4	1.09	6.7	34	66	<5	10	9	64	7	10	Sm, Int	<5
	C1	msbk	6.6	23.5	0.40	6.8	38	62	<5	14	7	61	7	11	Sm, Int	<5
	C2	msbk	7.1	22.4	0.34	6.6	34	66	<5	10	6	59	12	13	Sm, Int	<5
P2	Ah	m1sbk	14.1	25.1	1.64	6.1	30	64	6	11	12	56	<5	21	Sm, Int	<5
	AC	m1sbk	10.7	22.9	0.67	5.8	29	65	6	11	13	53	<5	23	Sm, Int	<5
	C	sg	8.5	22.3	0.53	5.8	34	60	6	13	13	49	<5	25	Sm, Int	<5

Struc. = soil structure (abbreviated notation, Soil Survey Staff, 1951); OC = organic carbon; Tect = tectosilicates (quartz, potassium feldspar and plagioclases); Phyll = phyllosilicates (Chl = chlorite; Ill = illite; Pa = paragonite; Ka = kaolinite; Sm = smectite; Int = interstratified minerals); IM = iron minerals (hematite and goethite). Data from Martín-García, 1994.



Figure 1. Zonation in a polygonal cluster from horizon AC in profile P1.

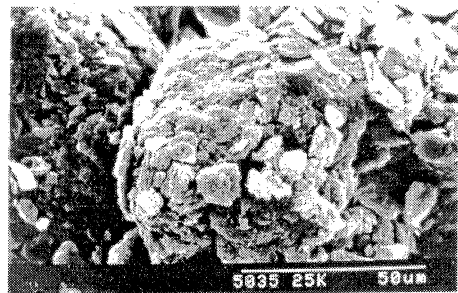


Figure 2. Rounded cluster from horizon AC in profile P2.

(1) Escuela Politécnica  
Superior. Univ. de Huelva,  
España

(2) Instituto de Recursos  
Naturales y Agrobiología.  
CSIC. Sevilla, España

(3) Instituto de Ciencia de  
Materiales. CSIC-  
Universidad. Sevilla, España

## Hydroxy interlayered minerals in soils of Huelva (Spain)

*Rodríguez Rubio P (1), Maqueda C (2) and Pérez Rodríguez J L (3)*

### INTRODUCTION

The weathering of potassium bearing micas has been described in the literature to results in the formation of expandable 2:1 clay minerals. This process is interpreted, as a mica-to vermiculite-to smectite continuous sequence. Smectites weathered from micas are likely to be tetrahedrally substituted and they usually show a behaviour midway between those minerals of normal smectite and vermiculite and have been called high-charge smectite, low charge vermiculite or transformation smectite. This mineral has been reported in many soils as a weathering product of mica (Badraoui et al., 1987, Aragonese and García-González, 1991). Hydroxy-Al interlayered smectite and vermiculite are thought to occur in soils as either weathering products derived from deposition of hydroxy-Al polymeric components within the interlayer spaces of these expandable layer silicates. The alteration of mica and the distribution of hydroxy-Al interlayered clays along the profiles may be uniform or restricted to one horizon. More frequently interlayering is greatest in the surface horizon and decreases with depth.

The aim of the present paper is to report the weathering of potassium bearing micas to intercalation of hydroxy-Al in 2:1 minerals and expandable 2:1 minerals in soils of Huelva and to relate the properties of the 2:1 minerals formed to its genesis in an attempt to increase our knowledge of the process of formation and development of these formations.

### MATERIALS AND METHODS

Three profiles of soils were studied. Profiles 20 and 23 developed on shales and classified as Palexerult and Ultic Palexeralf respectively and profile 22 derived from granites that is a Dystric Xerocept. Chemical analysis, particle size distribution, extraction methods, X-ray diffraction, CEC were used to characterize the samples.

## RESULTS AND DISCUSSIONS

The chemical analysis show that the clay minerals are dioctahedric. The mineralogical composition of different samples studied in this work are shown in table 1.

In the surface horizons of profile 23 the 14A diffraction did not shift to lower angles when the samples were solvated with ethylene glycol. The potassium saturated samples clearly showed the 14A peak that becomes diffuse and shift towards 10A on heating to 300 °C and 550 °C, remaining a shoulder in the 10A peak towards lower angles. According to Robert (1975) and Barnhised and Bertsch (1989) all these features indicate the existence of hydroxy-interlayered 2:1 clay minerals.

A peak at about 12A appears, possible due to the either presence of an interstratified mineral or to fact that  $Mg^{2+}$  was not capable substituting for the interlayered cation in the 14A mineral. The treatment of the sample with Na acetate and Mg chloride, keeping the temperature at 70 °C, confirms the presence of interstratified mineral. At the bottom of the profile a weak 14A reflection appears, shifting to 17.6A after the treatment with ethylene glycol and disappearing after potassium saturation and heating at 110 and 350 °C. This fact is in agreement with the presence of smectite.

The fine silt fraction showed clearly a 12A peak increasing the intensity with depth. At the bottom of the profile this reflection together with others at 24.3A, 8.10, 4.80, 4.01A, etc. appear - disappearing after  $K^+$  saturation - corresponding to a interstratification vermiculite-illite.

The fine silt fraction shows a high proportion of illite in the surface horizon decreasing with depth, whereas kaolinite distribution is the opposite. In the clay fraction kaolinite is the main component increasing with depth whereas illite decreases. The proportion of hydroxyl-Al interlayered clays is greatest in the surface horizon and decrease with depth, disappearing at the bottom.

The oxidazing conditions and frequent wetting and drying cycles are optimal for hydroxy-Al interlayer formation in upper horizons and the kaolinite would form in the portion of the solum where interlayering of vermiculite is not favoured.

The smectite formation, at the bottom of this profile, is difficult to explain, according with its physical and chemical characteristics that favoure kaolinitic formation. In this horizon the aluminium extractables with KOH, citrate-bicarbonate-dithionite or oxalic-oxalate ammonium decreases in agreement with the absence of hydroxy-Al in the 2:1 minerals that appear in very low proportion. It is possible that in the acid condition of this horizon the illite is altered to vermiculite and later to beidellite (showed by the Greene-Kelly test). In this soil

it is suggested the transformation illite - interstratified Illite - vermiculite - vermiculite - hydroxy Al interlayer vermiculite. At the bottom the illite is transformed to beidellite.

The study of profile 20 shows similar results than profile 23 but at the bottom smectite does not appear and the proportion of hydroxy-Al interlayered is similar with depth.

The mineralogical composition Profile 22 is similar along the profile. Hydroxy-Al interlayer in the surface horizon and interstratified vermiculite-illite at the middle and bottom of the profile were found. Transformation illite - interstratified Illite - vermiculite - hydroxy-Al vermiculite is suggested.

Table 1  
Mineralogical composition of the clay fractions

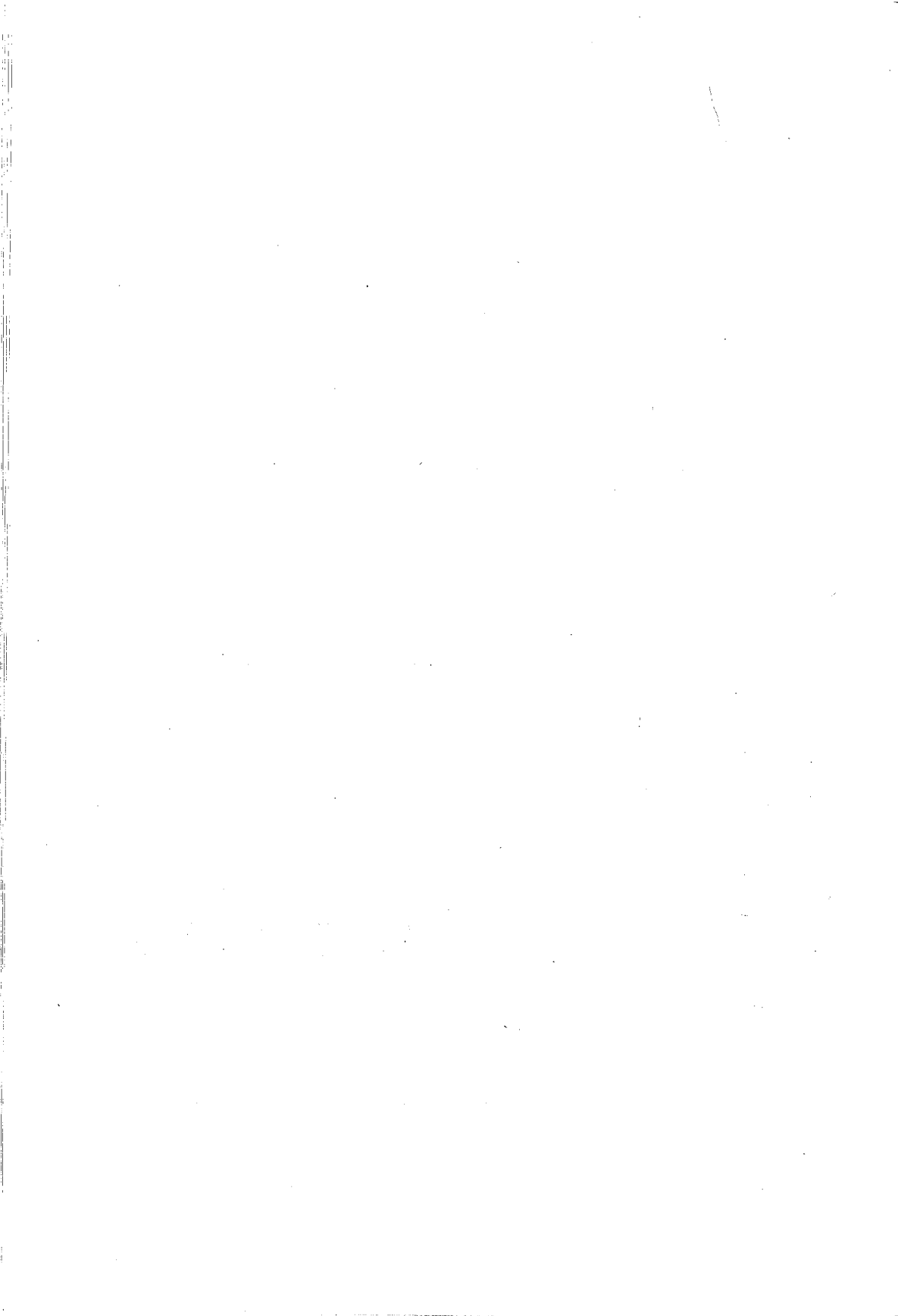
	S	K	I	Q	Hm	Gt	Al*
<b>P-20</b>							
A11	---	35	51	5	3.28	3.02	5
A12	---	55	33	1	3.81	3.29	5
A/B	---	53	35	---	4.13	3.52	5
B	---	72	15	---	5.36	3.34	5
B/C	---	74	10	---	6.62	4.54	5
<b>P-22</b>							
A11	---	29	54	3	1.22	1.52	10
A12	---	27	56	1	1.60	1.72	9
B/C	---	34	50	1	1.44	1.48	9
<b>P-23</b>							
Ao+A11	---	42	25	2	3.78	3.80	16
A/B	---	52	19	4	4.69	3.50	11
IIB1	---	63	15	4	6.05	3.93	4
IIB2	---	74	6	3	5.54	4.04	---
IIB3/C	6	73	5	---	4.60	4.51	---

S: smectite; K: kaolinite; I: illite; Q: quartz; Hm: hematite; Gt: goethite; Al\*: hydroxy interlayer mineral

#### REFERENCES

- Badraoui, M., Boom, P.R. and Rust, R.H. (1989). *Soil Sci. Soc. Amer. J.* 51, 813-818.  
 Aragoneses, F.J. and García-González, M.T. (1991). *Clays and Clay Minerals* 39, 211-218.  
 Barnhisel, R.I. and Bertsch, P.M. (1989). *Minerals in Soil Environments*, Eds. Soil Sci. Soc. American Madison.  
 Egeshira, K. and Tsuda, S. (1983). *Clay Sci.* 6, 67-71.  
 Robert, M. (1975). *Ann. Agrom.* 26, 363-399.

# APPLICATIONS



Dip. di Scienze della Terra.  
Univ. di Roma "La  
Sapienza". Roma, Italia

## Sr isotope ratio in relationship to hydraulic permeability of clayey lacustrine from the Tiber Valley (Central Italy)

*Barbieri Maurizio*

The data discussed in this paper, are related to the area known in literature as the south-west branch of the Tiberin Basin (Central Italy), filled up with Plio-Quaternary continental deposits. Structurally, the Tiberin Basin is a distensive intermountainous type of basin. It was originated on thick continental crust from the indirect effect of the tyrrhenian rifting and is one of the closest basins to the axis of the Apenninic Chain which still undergoes compression (Basilici, 1992).

In this area some boreholes were drilled with the aim of reconstructing the detailed lithostratigraphic and geochemical environment until the calcareous substratum (116.5 meters b.g.l.) (Ambrosetti et al., 1995).

The samples studied in this papers were collected in the borehole S7 at depth ranging from 18.50 to 45 m b.g.l).

Tab. 1 - Samples analyzed and depth of sampling

Sample	Depth (m)
S7 - CR-2	18,55-18,65
S7 - CR-3	19,25-19,35
S7 - CR-4	19,75-19,85
S7 - CR-9	39,15-39,25
S7 - CR-12	41,35-41,45
S7 - CR-13	43,55-43,65
S7 - CR-14	44,95-45,05

The samples represented by clayey-silty laminated strata with frequent sandy levels and rare gravelly horizons; these coarser levels represent the 20% of the drilled sequence.

Samples were prepared for Sr isotope ratio determinations and then the results have been related to the hydraulic conductivity which was measured with oedometric hydraulic tests.

## Methods

0,5 g of powdered sample was dissolved with 1N HCl acid and soluble Sr (Sr related to CaCO<sub>3</sub> content of the samples) was separated from the bulk of other elements by means of ion exchange columns.

The residual insoluble fraction (constituted essentially by clay minerals) was dissolved with HNO<sub>3</sub> and HF acids and the Sr was separated by the same procedure used for the Sr in the soluble fraction.

Isotope ratios were measured and compared with standard SrCO<sub>3</sub> (SRM NBS 987) for which a ratio of 0.71024 has been assumed. Measurements were made using a VG 54E mass spectrometer. <sup>87</sup>Sr/<sup>86</sup>Sr values have been normalized to <sup>87</sup>Sr/<sup>86</sup>Sr = 0.1194.

Accuracy is estimated to be 0.00002 or 0.00003 at the 95% confidence level.

## Results and discussion

The analytical results for the samples from borehole S7 are shown in tab. 2

Tab. 2 - <sup>87</sup>Sr/<sup>86</sup>Sr ratios of the carbonate and silicate fractions and % CaCO<sub>3</sub> of the analyzed samples.

Sample	<sup>87</sup> Sr/ <sup>86</sup> Sr sol. fraction	<sup>87</sup> Sr/ <sup>86</sup> Sr insol. fraction	<sup>87</sup> Sr/ <sup>86</sup> Sr whole rock	CaCO <sub>3</sub> (%)
S-7 CR-2	0,70861±2	0,71235±3		15,1
S-7 CR-3	0,70871±2	0,71347±2	0,71033±2	19,7
S-7 CR-4	0,70851±2	0,71730±2		15
S-7 CR-9	0,70853±2	0,71965±2		13,5
S-7 CR-12	0,70871±2	0,72217±2	0,71093±2	21
S-7 CR-14	0,70833±2	0,71899±2		20,7

$^{87}\text{Sr}/^{86}\text{Sr}$  isotope ratios of the carbonate fraction range from 0.70833 to 0.70871. In general it is possible to observe that these isotopic values are consistent with a provenance of Sr from water circulating in the Mesozoic to Cenozoic carbonate rocks outcropping in the Dunarobba area. It is noteworthy that these values are significantly different from sample to sample, suggesting that each sedimentary horizon behaves as a closed geochemical system, for the Sr isotopes point of view.

In the same table 2 it is possible to observe that the  $^{87}\text{Sr}/^{86}\text{Sr}$  ratios measured in the clayey fraction of the sample are higher than that measured in the carbonate fraction of the same sample.

In addition it is possible to observe that as for the carbonate fraction is concerned, the silicatic fraction of each sample behaves as a closed geochemical system.

## Conclusions

In all the Tiberin sequences, fine grained levels are widespread; based on mineralogical and geotechnical analyses they are composed of clayey minerals. Each pelitic level shows different thicknesses (sometimes up to 10m) and are interbedded within sandy and gravely horizons.

Oedometric hydraulic conductivity of pelitic levels has been assessed both normally and parallel to the stratification; it ranges from  $8 \cdot 10^{-9}$  to  $1 \cdot 10^{-13}$  m/s in relation to the applied stress.

Geochemical analyses confirm the evaluated conductivity attained data. At this regard, both carbonatic and silicatic detrital fractions of each different clay strata have own Sr isotope signature long geochemical identity long the bedding plane and normally to them.

## References

Basilici F (1992). Tesi di Dottorato

Ambrosetti P, Barbieri M, Basilici G, Bozzano F, De Pari P, Di Filippo M, Di Mario R, Duddrige G, Etiope G, Grainger P, Lombardi S, Mottana A, Patella, Pennacchioni L, Ruspandini T, Scarascia Mugnozza G, Tazioli S, Toro B, Valentini G, Zuppi G (1995). CEE - Progetto MIRAGE

(1) Esc. Sup. de Tecnologia de Tomar, Portugal

(2) Depto. Geociencias. Univ. de Aveiro, Portugal

(3) Centro Tecnológico de Ceramica e Vidrio. Coimbra, Portugal

## “Argilas de Aveiro” (Portugal): appraisal of their ceramic properties

Coroado J (1), Rocha F (2), Correia Marques J (3) and Gomes C (2)

### INTRODUCTION

Ceramic raw materials in order to be utilized on structural ceramics require to comply with some technological specifications, depending on parameters, such as: texture, mineral composition and chemical composition.

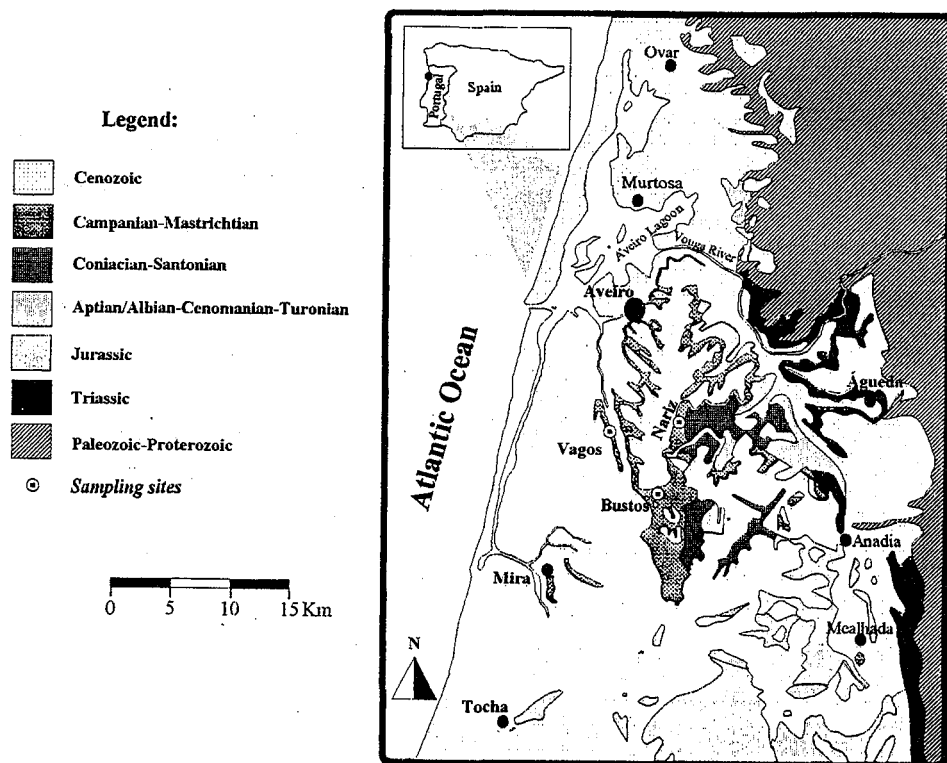


Fig. 1 - Location and geological setting.

The present paper deals with the physical, chemical and technological characterization of the heavy clays representative of the several quarries which occur in the region of Bustos - Vagos - Nariz (Fig. 1), with the aim of, through selective exploitation and lotation, to improve both technological properties and types of products. Identified technological problems caused by hygroscopic expansion, rehydration and loss of mechanical resistance of the ceramic products, require understanding of those problems and adequate processing control.

## GEOLOGICAL SETTING AND CERAMIC USES

Clay quarries are located in a lithostratigraphic formation belonging to the upper Cretaceous named "Argilas de Aveiro" (Moura & Grade, 1983; Barbosa, 1985). Lithologies of this formation comprise: greenish, brownish and reddish silty clay layers, intercalated with layers of marly dolomitic limestone. The strata are tabular, almost horizontal, metric or decimetric.

Raw materials from three quarries: Mano (Vagos), Nariz and Bustos had been studied. In the quarry of Mano (Vagos), the heavy clays are used without any previous treatment and admixture with raw materials from other sources to make structural ceramic products in a nearby plant. In the quarry from Nariz, where extraction is halted, the heavy clays were applied in structural ceramics as well. In the huge quarry from Bustos, clayey raw materials, rich in smectite, are utilized mixed with other raw materials in ceramic formulations for floor-tiles, wall-tiles and roof-tiles.

## MATERIALS AND METHODS

Properties of samples representatives of three quarries from Vagos, Nariz and Bustos were studied through various methods:

- X-ray diffraction (XRD) and X-ray fluorescence (XRF) were used to assess both mineralogical and chemical composition of the raw materials.
- Grain size distribution, using dry sieving (fraction  $>63 \mu\text{m}$ ) and a Sedigraph (fraction less than  $63 \mu\text{m}$ ).
- Plasticity measurements estimated from the Atterberg limits.
- Thermal analyses (differential, gravimetric and dilatometric).
- Technological tests after drying and firing (at three temperatures), such as: extrusion water, green-dry and dry-fired shrinkage, mechanical resistance to bending, water absorption and efflorescences.

## PRELIMINARY RESULTS

From the research carried out the following generic comments could be put forward:

- Clay fraction of the raw materials is composed mainly of smectite, followed by illite and kaolinite. Smectite is more abundant in Bustos quarry than in the other quarries.
- Clays from Bustos contain less SiO<sub>2</sub> (58 ≈ 60%), more Al<sub>2</sub>O<sub>3</sub> (≈ 19%), more Fe<sub>2</sub>O<sub>3</sub> and higher Ignition Loss than the clays from the other quarries.
- Sand fraction (>63 μm) is small in all the clays. Silt fraction (63 μm - 2 μm) is higher in clays from Nariz, whereas clay fraction is about the same (55 ≈ 80%) in clays from Vagos and Bustos.
- Clays from Bustos exhibit higher plasticity than the clays from Vagos and Nariz. Workability for all clay is good.
- Clay from Bustos contain more hygroscopic and zeolitic water than clays from Vagos and Nariz.
- The clays from Bustos show the highest values of extrusion water (19 ≈ 23%).
- Bustos clays exhibit the highest mechanical modulus (150 ≈ 180 Kgf.cm<sup>-2</sup>), comparatively to the other clays (70 ≈ 100 Kgf.cm<sup>-2</sup>).

## CONCLUSIONS

The physical, chemical and technological characterisation of the studied clays allows us to consider them as important structural ceramic raw materials.

The lateral and vertical variations of the analysed parameters require a better understanding of their implications and also an adequate processing control.

The future results of our investigations and a more selective exploitation and lotation may allow the industry to improve both technological properties and types of products.

## REFERENCES

- Barbosa, B. (1985) - Os sedimentos da coluna cretácica de Aveiro-Vagos. Análise da evolução granulométrica, mineralógica, e química aplicada às argilas para fins cerâmicos. Est. Not. e Trab., Serv. Fom. Min., XXV, pp. 99-104.
- Moura, A.C. & Grade, J. (1983) - Argilas da região Aveiro-Ílhavo-Vagos. Considerações sobre os pontos de vista químico, mineralógico e tecnológico. Est. Not. Trab., Serv. Fom. Min., XXV, pp. 135-146.

(1) Dip. di Scienze della  
Terra e Geologico  
Ambientali. Univ. di  
Bologna, Italia

(2) Istituto di Ricerca sulle  
Argille. CNR. Potenza, Italia

## Fine-grained weathering products in a waste disposal from the sulfide mine of Vigonzano (Parma province, Italy)

*Dinelli E (1), Morandi N (1) and Tateo F (2)*

Sulphide waste disposal are an important environmental challenge both in wide mineralised areas, and in spot sites. In those areas, the formation of secondary minerals can cause quite different effects on the distribution of pollutant elements (for example dispersion throughout fluids, concentration in insoluble residues, concentration in weathering products). In order to test the role of fine grained phases on the control of environmental conditions, one waste disposal has been studied. The mine was established in ophiolitic rocks associated to sulphide ores deposits (a very common situation in the northern Apennines). Mineralogical and geochemical data have been collected by XRD, TG, DTG, DTA, XRF, AAS, FAAS, SEM-EDS and by measurements of physic-chemical parameters of stream waters and soils.

The Vigonzano waste (and mine) area lies on various ophiolitic rocks (serpentinite, amphibolite, basalts and gabbros). The tail material is composed of ophiolitic breccias, part of which was heated during manufacturing. The mineralogy is represented by (more or less in decreasing order) phyllosilicates (chlorites, talc, smectite), amphiboles (tremolite-actinolite), plagioclases and quartz. The occurrence of goethite is detectable in many samples, whereas sulphides are below the detection limit (XRD). The geochemical composition of tails shows high Co, Se and S anomalies compared to surrounding soils; other elements (Cr, Mo, Co, Fe, Mg and Sr, in decreasing order) are enriched to a lesser extent (Dinelli, 1993).

Concentrations of weathering phases are detectable within the discharge area and downhill. Based on chemical data they can be classified into two groups: Fe-rich (ochraceous association) and Cu-rich (green-blue association). The compositional characters of these two associations of phases are matched by peculiar appearances (first of all the colour) that enable an easy detection in the field. The chromatic signature underline a different spatial distribution of the two association: the Fe-rich phases are abundant within the waste disposal site, but show also a wide dispersion throughout the stream valley, whereas the Cu phases are concentrated up to about 100m downhill the waste site.

The ochraceous sediments show a fine grain size (finer than silt), so their mineralogy is characterised by clay minerals like talc (40-60%), chlorite (10-20%), smectite s.l. (likely saponite, see Morandi et al., 1982) and goethite (20-30%). The major elements chemistry is compatible with the mineralogical composition, with the addition of few percent sulphate occurrence. Compared to surrounding soils, not involved in anthropic actions, the trace elements composition of ochraceous associations indicate positive anomalies of V, Cr, Co, Cu, and As. Some of these elements (Co, As and Cu) are slightly enriched also compared to the bulk tail materials. Because of the fine grain size of Fe-rich association, they are easily transported along the stream path and locally accumulated in low-energy environments. Other ochraceous sediments developed in similar environment (Libiola waste site, La Spezia province) were considered because of the occurrence of great amounts of ferrihydrite instead of goethite. Also the materials from Libiola are slightly enriched in transition elements, particularly Cr, Co and Cu, and have similar tendency to accumulate in low energy realms.

The green-blue sediments occur as aggregates of very fine grained materials, not detectable with optical microscope. The mineralogy of these Cu sediments is peculiar because of very high quantities of amorphous (or very low-crystalline) Cu phases, associated to detrital minerals (talc, chlorite, amphiboles, vermiculite and accessory phases). The examination of such amorphous component with SEM-EDS (selected samples) shows a rather homogeneous composition with Co, S, and Al allowing to suppose a stoichiometric relationship among these elements. A weak XRD evidence of such a Cu-phase is detectable in very few samples showing only broad bands near 0.9, 0.4 (composite bands) and 0.26 nm. All these reflections are sensitive by heating up to 150°C, whereas over 200°C tenorite (CuO) starts to crystallise without affecting the peaks of other minerals, indicating that the Cu enrichment (at least much of it) is not related to alluvial phases. From a chemical point of view, the green-blue associations are enormously Cu enriched (up to 100-200 times the waste average, already about 5 times the surrounding soils) and shows also high Zn concentration (> 1000 ppm). The green-blue associations in the field are related to the interaction of waters flowing within the mine tailings with surface water. The former are characterized by low pH values (around 4, which justify the mobilization of Al) and by high water soluble fractions of Cu and Zn (Dinelli, 1993) whereas the surface waters have significant higher pH values, a common feature of waters flowing through ophiolitic rocks (Drever, 1982). The stability of such a geochemical barrier, involving the precipitation of low crystalline phases enriched in transition metals, represent a key factor for the control of metal mobility in the mine tails surrounding.

As this situation looks very dangerous, another alteration process is suitable to play the role of regulating, at least for some time, the environmental pollution and to delay the toxic metal dispersion. In fact over the waste a soil is developing with very high smectite content. This mineral shows good exchange capacity (complete expansion after ethylene glycol solution) and no interstratification. The smectite is restricted to the dump area and associated streams, where inevitably - interacts with the acid drainage. The effect of such exchange is under study at the moment.

Dinelli E. (1993) - Ph.D. Thesis, pp. 203, University of Bologna.

Drever J.I. (1982) - The geochemistry of natural waters. Prentice Hall, pp. 437.

Morandi et al. (1982) - Rendiconti SIMP, 38 : 849-855.

## Chemistry of pyroxene and melilite formed during the firing of ceramic clay bodies

Dondi M, Ercolani G, Fabbri B and Marsigli M

Carbonate-bearing ceramic bodies are frequently used to manufacture bricks, roofing tiles, wall and floor tiles, pottery and tableware. During the firing of these bodies, the formation of new calcic crystalline phases occurs over 800°C. Among these phases compounds identifiable as clinopyroxene and melilite by X-ray diffraction are often present. In literature, they are generally referred to as "diopside" and "gehlenite". The crystal size of the new-formed phases is usually very small, 1-5  $\mu\text{m}$  or less, and this circumstance makes the assessment of their crystallochemical characteristics very difficult.

In order to achieve a chemical characterization of melilite and pyroxene formed during firing, an approach was carried out by means of energy dispersive spectrometry (EDS) applied to a scanning electron microscope. To this aim, some industrial products (bricks, wall and floor tiles, earthenware and majolica pottery) were taken into account and their ceramic bodies were analyzed by XRF and XRD (bulk sample) and SEM-EDS (on fracture surface). The quantitative analyses of pyroxene and melilite crystals were performed by means of ZAF method. They showed a certain chemical variability from one sample to another and sometimes within the same sample.

### Clinopyroxene

The main elements vary in the following ranges:  $\text{SiO}_2$  35-50%,  $\text{Al}_2\text{O}_3$  9-20%,  $\text{Fe}_2\text{O}_3$  1-15%,  $\text{MgO}$  3-14%, and  $\text{CaO}$  16-25%. Sodium, potassium and titanium are minor components (<1%), while bivalent iron is always negligible (<0.2%  $\text{FeO}$  in the bulk sample). Overall, clinopyroxenes taken into consideration are basically characterized by:

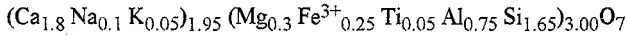
- 1) abundance of both tetrahedral- and octahedral-coordinated aluminium;
- 2) abundance of  $\text{Fe}^{3+}$  and virtual absence of  $\text{Fe}^{2+}$ ;
- 3) abundance of wollastonite molecule (Figure 1).

In conclusion, the chemical composition of "ceramic" pyroxenes seems fundamentally to be consistent with a "fassaite", i.e. a *peraluminous diopside, rich in trivalent iron*.

## Melilite

The most frequent ranges of chemical composition are the following:  $\text{SiO}_2$  35-40%,  $\text{Al}_2\text{O}_3$  12-15%,  $\text{Fe}_2\text{O}_3$  4-10%,  $\text{MgO}$  3-5%, and  $\text{CaO}$  35-38%. Sodium is sometimes in significant amounts (1-2%) while potassium and titanium are always in traces; bivalent iron is negligible.

On the whole, "ceramic" melilite is characterized by the following average composition:



Aluminium, magnesium and trivalent iron are generally in comparable amounts (Figure 2), so that the name *gehlenite* is not fully consistent with the composition of the "ceramic" phases and the general term *melilite* should be preferable.

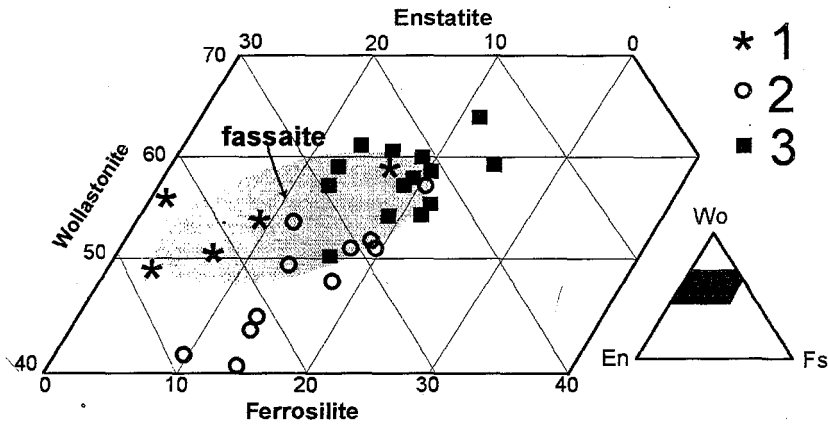
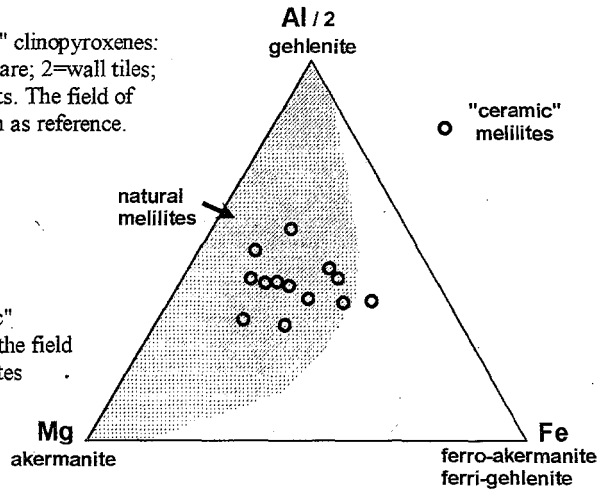


Figure 1  
Composition of "ceramic" clinopyroxenes:  
1=majolica and earthenware; 2=wall tiles;  
3=structural clay products. The field of  
natural fassaite is shown as reference.

Figure 2  
Composition of "ceramic"  
melilites with respect to the field  
defined by natural melilites



CNR-IRTEC, Istituto di  
Ricerche Tecnologiche per la  
Ceramica, Faenza, Italia

## Composition and ceramic properties of Tertiary clays from southern Sardinia (Italy)

*Dondi M, Marsigli M and Strazzeri B*

Ceramic production in Sardinia basically consists of heavy clay materials, particularly hollow bricks, hollow floor blocks, and vertically perforated bricks. Ten brickworks are currently operating with a total annual output of about 650,000 tons.

The clay raw materials used by this brickmaking industry are recovered from Tertiary sedimentary sequences of fluvio-lacustrine environment outcropping in the southern part of the island. In particular, pelitic bodies present in the Cixerri Fm (Eocene-Oligocene), Ussana Fm (Oligocene-Miocene) and Samassi Fm (Pliocene) are exploited.

In order to achieve a compositional and technological characterization of these raw materials, both operating quarries and brickworks were sampled. On the whole 23 clays were analysed from the chemical (XRF), mineralogical (XRD, TG-DTA) and granulometric (X-ray monitoring of gravity sedimentation) viewpoints. Technological tests were performed on a laboratory scale with reference to brick and roofing tile manufacture (extrusion-drying-slow firing) as well as to wall and floor tile production (grinding-pressing-drying-fast firing).

Cixerri Fm is mainly represented by carbonate-bearing (20% on average, both calcite and dolomite) silty clays. The fine fraction is prevalently composed of illite and randomly interstratified I/S, with minor kaolinite, chlorite, and smectite. Quartz-feldspathic component is always significant (30-40%).

Ussana Fm provides silty clays and clayey silts, usually rich in quartz and feldspars (30-50%) as well as in carbonates (10-20%, mainly calcite). Clay minerals are mostly illite, with subordinate kaolinite and chlorite.

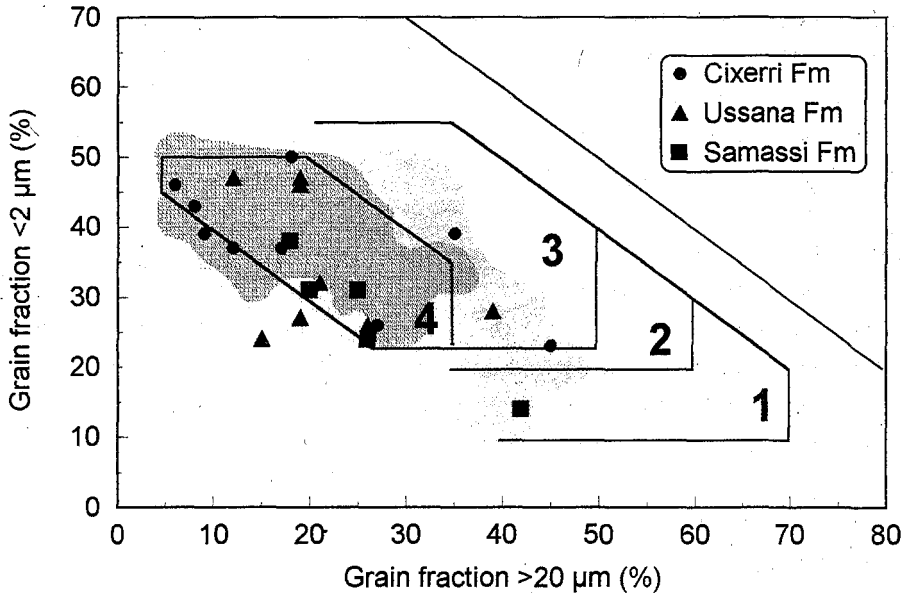
Samassi Fm is characterized by a relatively coarse grain size distribution (clayey silts) and a high carbonate content (generally 30-40%, essentially calcite). Smectite and illite are the main components of the fine fraction, together with scarce chlorite. The quartz-feldspathic portion ranges around 30%.

Technological tests indicate that Cixerri and Ussana raw materials are suitable for brick and roofing tile production. Cixerri clays present acceptable values of plasticity (PL 22-28%, PI 10-11%) and, after firing at 900-1000°C, acceptable values of shrinkage (<1%), water absorption (17-23%) and bending strength (8-20 MPa). Ussana clays are slightly more plastic (PL 22-27%,

PI 14-16%) with satisfactory properties after firing at 900-1000°C: shrinkage <1%, water absorption 16-23%, and bending strength 10-13 MPa.

The high smectite and carbonate contents make Samassi clays generally unsuitable for brick manufacture. Plasticity seems too high (PL 32-38%, PI 23-24%) and samples fired at 900-1000°C resulted to be very porous (water absorption >27%) and poorly resistant (<10 MPa). At any rate, small amounts of these raw materials could be used in mixes together with Cixerri or Ussana clays, especially in order to improve plasticity.

Sardinian tertiary clays appear to be unsuitable for stoneware floor tiles, for their excessive carbonate content. On the other hand, Ussana and Cixerri materials could be used in wall tile manufacture, owing to their satisfactory behaviour in pressing and fast firing. At temperatures ranging from 1000°C to 1120°C, shrinkage is usually <1%, water absorption 17-20% and bending strength 20-30 MPa. In contrast, Samassi clays resulted too porous (water absorption >20%) with values of shrinkage (2-4%) and bending strength (<20 MPa) faraway from the requirements of wall tile manufacturers.



Grain size distribution of Sardinian Tertiary clays in Winkler's diagram. Fields are referred to: 1) solid bricks; 2) vertically perforated bricks; 3) roofing tiles and lightweight blocks; 4) thin-walled hollow bricks and blocks. Frequency distribution of Italian bodies for structural clay products is represented (two levels of grey) as reference.

CNR-IRTEC, Istituto di  
Ricerche Tecnologiche per la  
Ceramica, Faenza, Italia

## Grain size distribution of the Italian raw materials for structural clay products: a reappraisal of Winkler's diagram

Dondi M, Fabbri B and Guarini G

### Objective

In the ambit of a wide research program (Fabbri and Dondi, 1995a, b), the aim of this paper was: a) to determine the grain size distribution of clay raw materials used for brick and tile production in Italy, b) to verify the opportunity of updating the well known Winkler diagram, currently used to assess the suitability of the granulometric features of the clay raw materials for brick and tile production (Kolkmeier, 1991).

### Materials

Approximately 350 clay samples were collected from 240 Italian brickworks, where they were used to manufacture different types of products: solid and vertically perforated bricks = 55; lightweight blocks = 27; facing bricks = 35; paving bricks = 13; hollow bricks = 59; hollow floor blocks = 46; roofing tiles = 30; hollow slabs = 10.

The correspondent bodies were prepared with a different number and type of raw materials: one clay = 40% of cases; 2 or 3 clays = 36%; sand was added in the remaining 24% of cases.

### Investigation methods

Clay samples were analyzed in order to obtain their complete grain size distribution curves. The analyses were performed by wet sieving (fraction  $>63 \mu\text{m}$ ) and by sedimentation with a Micromeritics Sedigraph 5000-ET apparatus. When clays were mixed together with sand to obtain production bodies, the grain size distribution of the mixes was calculated by adding the quantity of sand to the  $>63 \mu\text{m}$  fraction.

### Granulometric features

#### a) general vision

By using the Shepard ternary diagram (Shepard, 1954), the main part of the clay samples can be classified as silty clays, clayey silts and clays *strictu sensu*. When the bodies are considered, the variations of grain size distribution from one sample to another result in a smaller range in comparison with clays. According to the Winkler diagram (Winkler, 1954), the situation is:

>20  $\mu\text{m}$  fraction = 4 - 44% (more frequent values 20-25%)

20  $\div$  2  $\mu\text{m}$  fraction = 19 - 59% (more frequent values 33-47%)

<2  $\mu\text{m}$  fraction = 18 - 57% (more frequent values 33-47%).

b) with reference to the type of product

All the Italian bodies fall into the "thin walled hollow bricks" field in the Winkler diagram (figure 1). The exceptions to this general trend are few and they are relative to facing bricks and paving bricks. In these two cases, a lot of bodies fall into the field of "roofing tiles and lightweight blocks".

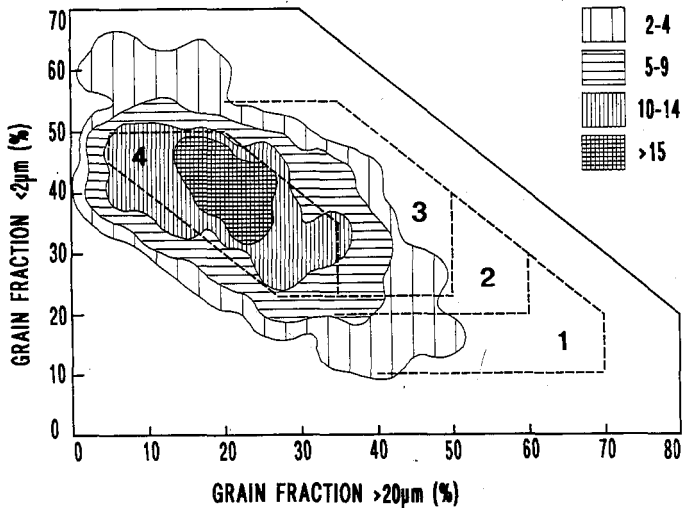


Figure 1 - Italian bodies in the Winkler's diagram

**Proposed classification scheme**

If we consider the two grain size values which subdivide the granulometric curve of each Italian body into three equivalent fractions, we find that 2 and 10  $\mu\text{m}$  are the most frequent values. Therefore, we propose to use a ternary diagram with the quantities of the fractions <2  $\mu\text{m}$ , 2-10  $\mu\text{m}$  and >10  $\mu\text{m}$  at the vertexes (figure 2). In this way, four groups of products can be drawn:

- solid and perforated bricks, hollow bricks and hollow floor blocks; they fall in the same area of the diagram;
- facing bricks; extruded bricks show a grain size distribution thinner than soft mud bricks;
- roofing tiles; the best products (high mechanical strength and frost resistance) are concentrated in a very small and typical area;
- lightweight blocks, paving bricks and hollow slabs; the trend to use thinner bodies for very fine-grained products is evident.

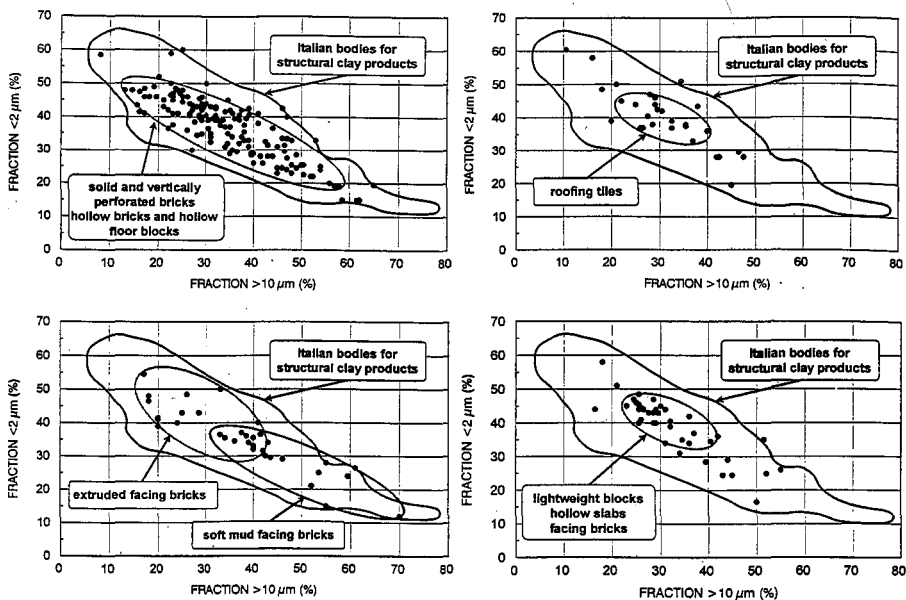


Figure 2 - Reference ternary diagram proposed for Italian bodies

### Conclusions

The Winkler diagram is suitable in the case of German structural clay products (Schmidt-Reinholz Ch., 1993), but it is not useful to differentiate the granulometric features of the bodies for different types of product in the Italian brick and tile industry. Italian raw materials are generally thinner and a ternary diagram with the fractions  $<2 \mu\text{m}$ ,  $2-10 \mu\text{m}$  and  $>10 \mu\text{m}$  at the vertexes should be preferred.

### References

- Fabbri B., Dondi M.: La produzione del laterizio in Italia. Faenza Editrice, Faenza, 1995.
- Fabbri B., Dondi M.: Caratteristiche e difetti del laterizio. Faenza Editrice, Faenza, 1995.
- Kolkmeier H.: Reliable test methods for the evaluation of brickmaking raw materials. Ziegelindustrie International, 6 (1991) 282-290.
- Schmidt-Reinholz Ch.: Influence of preparation on certain quality characteristics of building ceramics. Tile & Brick International, 9/2 (1993) 81-84.
- Shepard F.P.: Nomenclature based on sand-silt-clay ratios. Journal Sedimentary Petrology, 24 (1954) 151-158.
- Winkler H.G.F.: Bedeutung der Korngrößen-verteilung und des Mineral-bestandes von Tonen für die Herstellung grobkeramischer Erzeugnisse. Berichte Deutsche Keramische Gesellschaft, 31/10 (1954) 337-343.

(1) Dip. di Scienze della Terra. Univ. di Pavia, Italia

(2) C.G.S.-Centro Grandi Strumenti. Univ. di Pavia, Italia

## The dynamics of firing process in clays: from "bulk" to "point" analysis

*Duminuco P (1), Messiga B (1), Riccardi M P (2) and Setti M (1)*

Firing test on natural clays of different compositions allows us to investigate a sequence of microtextural and mineral association changes related to different firing temperatures (550 - 850 - 1050° C). Compositionally, samples plot in the ternary diagram  $Al_2O_3$  - CaO -  $SiO_2$  within the quartz - corundum - gehlenite sub-triangle, defining Ca - rich and Ca - poor clays.

The analytical strategy couples micro - textural observations (under optical and scanning electron microscopes), bulk (XR diffraction) and "point" analyses (electron microprobe). This represents a powerful tool to unravel the sequence of events characterizing the firing process in clays. Textural and mineralogical differences are then related to both different firing temperatures and clay compositions. At the same firing temperature the Ca-poor sample show less evident grains and matrix transformations with respect to the Ca-rich one.

In the Ca-poor sample, the firing process produces dehydration of the clay minerals giving Al-richer phases, whereas the growth of new mineral phases only occurs around carbonates. On the contrary, in the Ca-rich sample the transformation of clays minerals is associated to the collapse of the calcite, and produces a widespread occurrence of Ca-Al-silicates.

Mineral phases formed during firing at different temperatures show strong chemical variability with respect to the pure phase compositions, this should be accounted to the fast firing process in which the nucleation and growth is inhibited, owing to short time span. In this case only the XR-diffraction traces allow the mineral phase identification.

In feldspar the variation of shape and intensity of the main peaks with the temperature increasing seems to be related to compositional changes as evidenced by electron microprobe analyses.

In the Ca-rich clay, several lines of evidence indicates that clay mineral and calcite break-down reactions produce a  $H_2O$  and  $CO_2$  rich fluid which could be responsible of the enlargement of reaction domains. On the  $Al_2O_3$  - CaO -  $SiO_2$  triangle the chemographic relationships indicate that during the increasing of temperature the reaction domains evolve, towards a greater compositional homogenization of the system, as testified by the close compositional relationships existing between firing mineral phases and clay composition.

(1) Dpto. Geología, Fac.  
Ciencias, Univ. de Huelva,  
España

(2) Dpto. Ingeniería Minera,  
Univ. de Huelva, España

(3) Dpto. Cristalografía,  
Mineralogía y Química  
Agrícola, Fac. Químicas,  
Univ. de Sevilla, España

## Clay mineralogy and heavy metal content of suspended sediments in an extremely polluted fluvial environment: the Tinto river (SW Spain). Preliminary report

Fernández Caliani J C (1), Requena A (2) and Galán E (3)

The Tinto river, so-called because of its wine-red colour, has its origin in one of the most important metallogenic provinces of Europe -the Iberian Pyrite Belt-, which consists of great massive sulphide orebodies mined since prehistoric times. As a consequence of the large mining and smelting operations occurred in the proximity of the upper river banks, waters are very acidic (pH ranges between 2 and 4) and extremely polluted by toxic metals and suspended particles that are discharged into the Huelva estuary, on the southwest coast of Spain.

Although there are chemical analyses of water and bottom sediments available, particularly from the intertidal sediments of the estuary (e.g. Pérez *et al.* 1991; Cabrera *et al.* 1992), investigations on clays in suspension have not been reported. This work is focused on determining the mineralogical composition and metal concentration of suspended clays, in order to understand the factors controlling the origin and evolution of clay minerals and contamination through the river basin.

Sampling was performed during a rainstorm period, when suspended matter concentrations were high, at different localities distributed along the whole length of the river (Fig 1). The water samples were collected with plastic bottles and filtered in-situ over 0,4  $\mu\text{m}$  pore-size filter for chemical, mineralogical and particle size analyses.

The grain size of the sediments in suspension is commonly less than 20  $\mu\text{m}$ , however sand grains and even heavy mineral, such as pyrite, as well as some organic debris supplied by terrestrial erosion, can be transported in suspension due to strong turbulence.

Phyllosilicates, quartz and feldspars are the basic and omnipresent mineral phases identified from the bulk sample. Poorly crystallized and inorganic amorphous components (allophane and iron oxide gels) have been detected by XRD. Locally, significant amounts of jarosite and hematite are also present in the upper course, and

carbonates occur as suspended particles when going downstream. The silt and clay grain fractions are dominated by micas with minor quantities of kaolinite and chlorite. They are dioctahedral micas (illite/muscovite) with Kubler index values (from 0.23 to  $0.25^\circ \Delta 2\Theta$ ) within the typical range of mica crystallinity from the Iberian Pyrite Belt (Fernández Caliani *et al.* 1994). Smectites are mostly present in the  $<2\mu\text{m}$  fraction of clays collected at the Candón stream, an uncontaminated tributary of the Tinto river.

The clay mineral association found in suspended sediments is in accordance with the composition of the rocks and soils drained and submitted to erosion by the water river, and it does not seem the result of important mineralogical changes. Well-crystallized micas and chlorites have their source area in the Paleozoic basement that contains the large pyritic deposits. Kaolinite, jarosite and hematite are the weathering products of the polymetallic sulphide masses and their host rocks. Calcite and smectites are supplied by limestones and marls-rich sediments of Cenozoic age that outcrop in the lower course of the river. Therefore, the mineralogical assemblage reflects the inherited detrital character of the suspended sediments.

On the other hand, the clays in suspension are extremely contaminated by heavy metals, especially in the upper river, where the total Fe content can reach 22% of the bulk sample, and other toxic metals such as Pb and Cu are present in a concentration as high as 4554 ppm and 1164 ppm, respectively. The pollution by these heavy metals decrease significantly in the downstream direction, however the Mn and Zn contents remain in the same levels along the whole river course. Taking into account the spatial variation in the abundance and nature of the clay minerals, the high variability of the Pb content suggests that this metal is not bonded to clay minerals as an exchange element nor adsorbed onto particle surfaces. Thus, a partitioning of the pollutant metals in different geochemical components of the suspended matter must be considered.

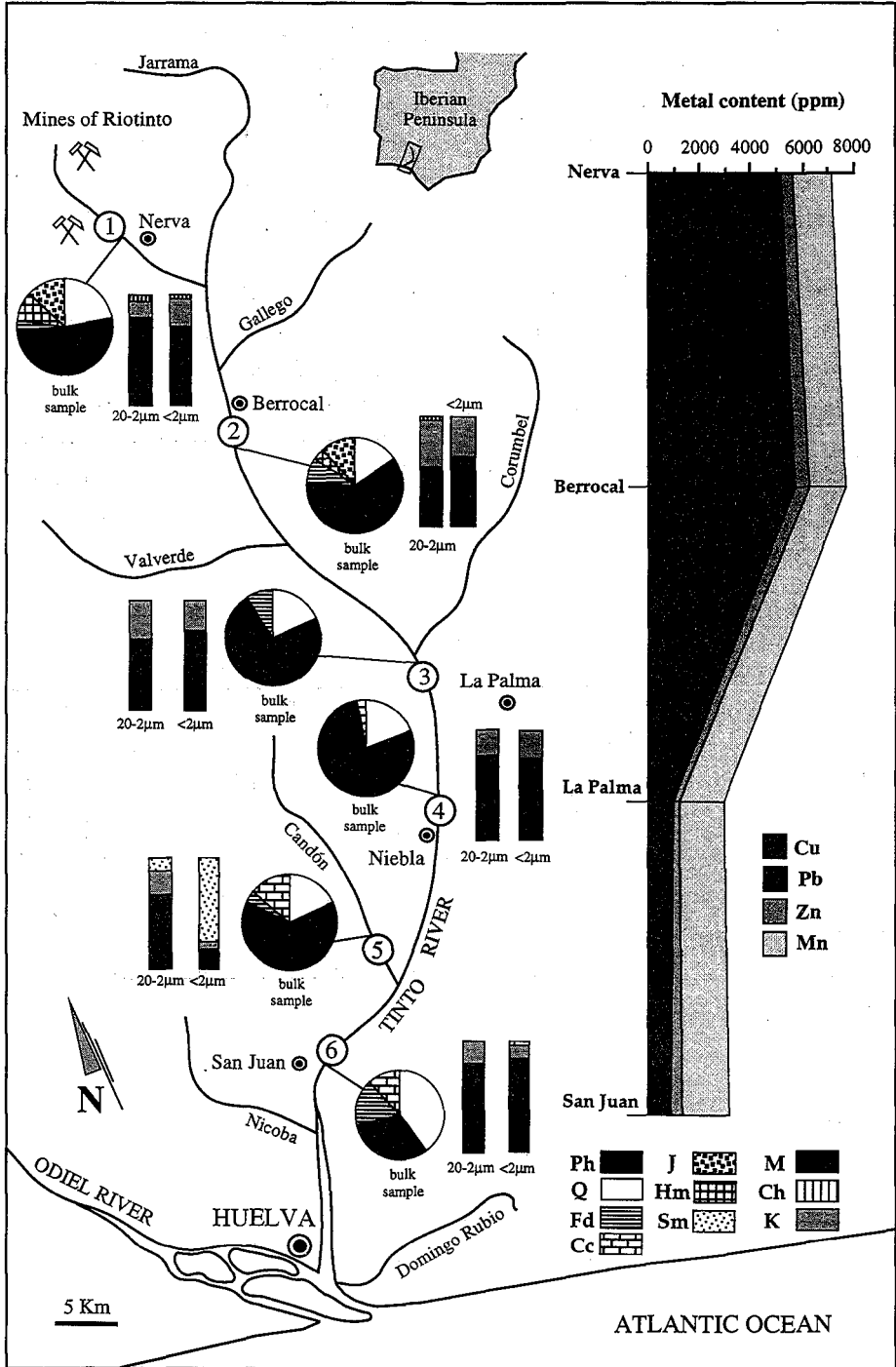
## References

- Cabrera F, Conde B & Flores V (1992). *Fresenius Environ. Bull.* **1**, 400-405  
Fernández Caliani JC, Mesa JM & Galán E (1994). *Bol. Geol. Min.* **105**, 213-220  
Pérez M, Usero J, Gracia I & Cabrera F (1991). *Toxic. Environ. Chem.* **31**, 275-283

---

**Figure 1:** Spatial variation in the clay mineral composition and heavy metal content of the suspended sediments in the Tinto river.

*Mineral abbreviations:* Ph (phyllosilicates); Q (quartz); Fd (feldspars); Cc (calcite); J (jarosite); Hm (hematite); Sm (smectites); M (micas); Ch (chlorites); K (kaolinite).



(1) Instituto de Ciencias de  
Materiales. CSIC-  
Universidad. Sevilla, España

(2) Instituto de Recursos  
Naturales y Agrobiología.  
CSIC. Sevilla, España

## Clay-based cleaning methods. Absorption/adsorption of magnesium-sulphate

*Franquelo M (1), Maqueda C (2) and Pérez-Rodríguez J L*

### INTRODUCTION

Clay materials are very good adsorbents/absorbents of contaminants in many scientific fields. They are natural products, abundant, cheap, easy to get and to use, and with some properties such as large surface area, adsorbent property and easily adhered to the substrate to be cleaned, that make them very adequate for cleaning and desalination of the materials, moreover the properties of the system may be enhanced by incorporating to the clay suspension other additives in order to improve the reologic properties, speed of drying, etc.

Clay based poultice materials for cleaning the external part of different monuments have been used by some research groups (Trujillano et al., 1995). The R&D Laboratory of Tolsa prepare clay materials for this purpose.

We investigate on the mechanism of ion transfer and soiling removal in the most widely used types of rocks in building and ornamentation of the Historical Heritage of Andalusia using clay-based poultice materials. In the present work we study the feature of clays in order to remove some salts being contaminants in the surface of monuments.

### MATERIALS AND METHODS

Supermold® (Alvarez et al. 1994) and Bentonite supplied by Tolsa and Gador mines respectively were used.

The physical and chemical processes at the soiling-clay interfaces were carried out by a dialysis method. The different samples were introduced into dialysis bags and tied with double knots at both ends. The bags were introduced into glass bottles and 120 ml of magnesium

sulfate solutions of 0 to 5 g/l were added.

The cations concentration in solution were measured using atomic absorption spectrometry. The pHs evolution were measured.

The salts at the monuments were characterized by XRD, SEM and chemical analysis by dispersive energies.

## RESULTS AND DISCUSSION

The salts characterized on Almeria Cathedral were mainly constituted by magnesium sulphate with different hydration degrees, potassium sulphate and sodium chloride also appear. Dolomite is present as residual part of the rock. Due mainly to the fact that magnesium sulphate hydrated is the most important pollutant in that monument the adsorption/absorption of different concentration of such salt by bentonite and supermold were investigated.

Three main parameters are determined: magnesium and calcium cations in solution and pH evolution during the experiments.

### Bentonite experiments

Once the salt solution has been put in contact with the clay mineral, the following phenomena were observed. The  $Mg^{++}$  concentration in solution sharply decrease after three days, the higher decreases correspond with the more concentrated solution, and latter remaining almost constant with the time. The  $Ca^{++}$  concentration - ion that was not initially present in solution - increases with the time, the variation more remarkable occurs at higher concentration and short period of time. The pH of the solution change with the time, the initial pH, lightly acid (6.5 at 7) move to basic pH (8.2 at 8.8).

These data are mainly in agreement with a cation exchange process but other mechanisms are involved. Equilibrium concentration of magnesium ion and cation liberated depend of initial concentration of salt solution used.

### Supermold® experiments

The  $Mg^{++}$  concentration solution decreases between 0 and 6 days and later remain constant with the time. The  $Ca^{++}$  concentration, ion that was not initially present in solution - increase with the time, decreasing after 16 days. The proportion of  $Ca^{++}$  desorbed (180 mg/L) is higher than  $Mg^{++}$  adsorbed/absorbed (75 mg/L) by the supermold.

The  $Mg^{++}$  absorption is attributed to absorción/adsorción processes. The  $Ca^{++}$  in solution comes from the supermold components, probably, carbonates. The decrease of  $Ca^{++}$  concentration in solution after 16 days is due to the calcium sulphate precipitation.

#### Supermold® plus FDTA experiments

The experiments carried out with supermold plus EDTA show some differences in comparison with supermold without EDTA. A higher proportion of  $Mg^{++}$  is released and a lower proportion of  $Ca^{++}$  are found in solution. This variation is attributed to the effect of EDTA forming complexes.

The pH of the solution changes with the time, the initial pH lightly acid (6.2 at 7) move to basic pH, reaching values between 8.4 at 8.8. After 9 days the pH slowly decrease. This last variation is attributed to the calcium sulphate precipitation.

#### **REFERENCES**

- Alvarez, A.; Duch, I.; Del Valle, B. (1994). Composición a base de sepiolite sincronizada, procedimiento para su preparación y su aplicación en la limpieza y restauración de edificios y monumentos. Pat. Española 9400075.
- Trujillano, R.; García-Talegón, J.; Iñigo, A.C.; Vicente, M.A.; Rives, V. And Molina, E. (1995). Removal of salts from granite by sepiolite. Applied Clay Science, 9, 459-464.

#### **ACKNOWLEDGMENTS**

This work was supported by project SEC95-0793.

Dpto. Geociencias, Univ. de Aveiro, Portugal

## Influence of the clay mineralogy and geochemistry on the geotechnical behaviour of the "Argilas de Aveiro" formation (Portugal)

*Galhano C, Rocha F and Gomes C*

### INTRODUCTION

The Aveiro region (Fig. 1) corresponds to the northern sector of the Portuguese Occidental Meso-Cenozoic sedimentary basin. At the Aveiro region the upper Cretaceous is represented by the "Argilas de Aveiro" formation (Campanian-Maastrichtian), which are composed of greenish clays and marls intercalated with thin dolomitic layers. In the region, the outcrops of this formation are relatively extensive, with a maximum length (oriented N-S) of about 20 Km and a maximum width of about 5 Km, partially covered by quaternary old beach and alluvial deposits.

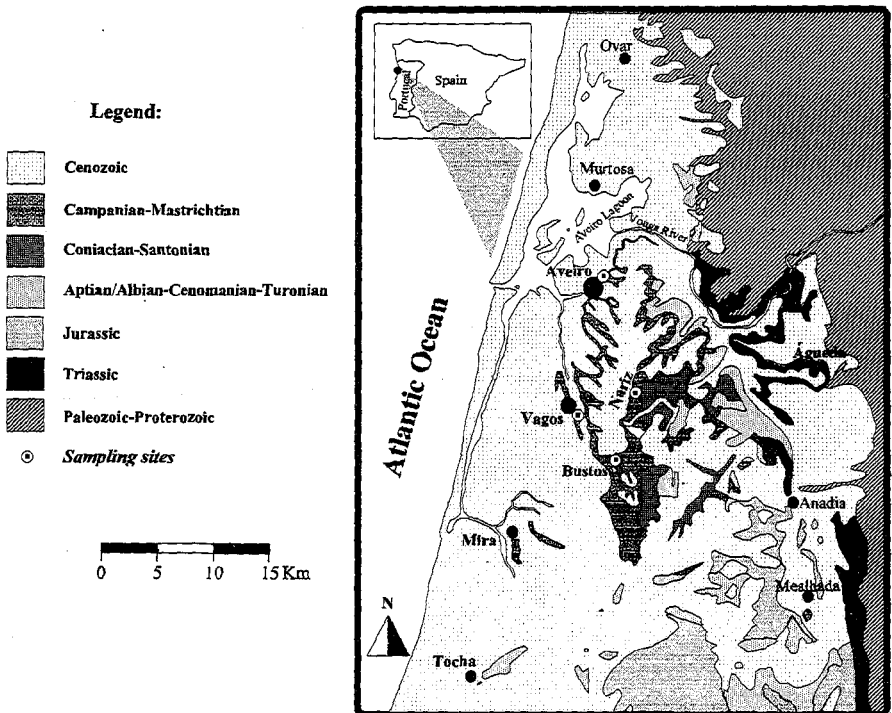


Fig. 1 - Location and geological setting.

The thickness of the "Argilas de Aveiro" formation varies from a few meters in the North (Cacia sector) to a maximum of more than 150 meters South of Aveiro (Vagos sector). In the studied region, "Argilas de Aveiro" are overlain by Plio-Pleistocene sands and gravels.

Therefore, as regards to the main urban settlements in the Aveiro region, foundations for buildings, roads and other infrastructures are built on clays, sands or gravels. The particular geotechnical behaviour of the "Argilas de Aveiro" clays, namely in what concerns expandability and "softning", are responsible for some problems in some works, expressed by damaging collapses followed by settlements and expansions followed by intumescences.

This paper deals with the influence of clay mineralogy and geochemistry on geotechnical behaviour of clays from the "Argilas de Aveiro" formation. The knowledge of these clays in what concerns their texture, mineralogy and chemistry could be very usefull to prevent future problems.

## MATERIALS AND METHODS

We have studied about twenty samples, located in different sites (Fig. 1), considered to be representative of the heterogeneity of the "Argilas de Aveiro" formation.

The mineralogical study of the clays from the "Argilas de Aveiro" formation, particularly of their clay components, has been based mainly on X-ray/diffraction (XRD). Qualitative and semi-quantitative determination of clay and non-clay minerals has been done both in natural sample and in the clay fraction. The clay mineral composition was determined both in oriented and non-oriented specimens. For semiquantitative determinations of clay and non-clay minerals, criteria recommended by Schultz (1964) and Thorez (1976) had been followed.

Chemical analyses of both major elements (MgO, Al<sub>2</sub>O<sub>3</sub>, SiO<sub>2</sub>, CaO, TiO<sub>2</sub>, Fe<sub>2</sub>O<sub>3</sub>, MnO, Na<sub>2</sub>O and K<sub>2</sub>O) and minor elements (Zn, Cu, Ni, Sr, Cr, Ba, Nb, Zr, Y, Th and V), had been carried out using X-ray fluorescence (XRF) and flame-spectroscopy methods.

Several geotechnical tests were carried out. Particular consideration was deserved to the expandibility test (according to LNEC E200-1967 norm), carried out on fraction less than 0.420 mm, as well as to the Atterberg limits test (according to the portuguese norm NP 143-1969), following the Casagrande test.

The experimental data obtained was complemented with other data available (Gomes, 1992 and Rocha, 1993).

## RESULTS AND DISCUSSION

Clays from the "Argilas de Aveiro" formation present a mineral composition characterized by a predominance of very simple mineral assemblages in regards with both clay minerals (essentially illite+smectite, with a subsidiary presence of kaolinite) and the associated non-clay minerals (essentially quartz+K-feldspar, with a episodic presence of dolomite). Results achieved by the mineralogical studies point out, in what concerns the clay minerals, to a gradual evolution from an illitic-smectitic-kaolinitic composition in the northern sectors of the "Argilas de Aveiro" outcrops to, firstly, an illitic-smectitic assemblage in the central sectors and, finally, a more smectitic one in the southern sectors, where we can also find some distinctive aspects of the geochemical data, characterized by higher contents in  $Al_2O_3$ ,  $Fe_2O_3$  and Ignition Loss and lower contents in  $SiO_2$ .

In what concerns the textural data, we can assume that the samples collected at Nariz are richer in silt fraction whereas the samples collected at Vagos and Bustos are richer in clay fraction.

The geotechnical data available so far allowed the following considerations:

- The expandibility varies from a minimum of 10% (Vagos samples) to a maximum of 35% (Bustos samples).
- The plasticity index varies from 20% (Nariz and Vagos samples) to 30% (Bustos samples)

These two parameters present a very good correlation not only between themselves but also with the lateral variation of the clay minerals assemblages for the studied formation. In fact, the higher values of these two geotechnical parameters are related to the higher contents in smectite, whereas their decrease northwards reflects the decrease in smectite, counterbalanced by the increase, firstly, in illite and, finally, in kaolinite.

### References:

Rocha, F.Tavares (1993)- Argilas aplicadas ao estudo Litoestratigráfico e Paleoambiental na Bacia Sedimentar de Aveiro. Tese, Universidade de Aveiro.

Gomes, L.F. (1992)- Zonamento geotécnico da área urbana e sub-urbana de Aveiro. Tese, Universidade de Aveiro.

(1) Dpto. Química  
Inorgánica. Fac. Ciencias.  
Univ. de Salamanca, España

(2) Instituto de Recursos  
Naturales y Agrobiología.  
CSIC. Salamanca, España

## Adsorption of phenyl salicylate on sepiolite and its use as UV radiation protectors

*Hoyo del C (1), Rives V (1) and Vicente M A (2)*

The increasing development of skin cancer in recent years has led to numerous studies on protecting agents. We have reported several studies on the interaction of different drugs with clays, and their use for these purposes, and, in the present study, our report concerns the system formed by phenyl salicylate and sepiolite.

Although widely used to produce polymers and plastics, and also adhesives, phenyl salicylate (also known by its commercial name "salol") is a current component of creams for solar radiation protectors. Its molecular weight is 214 mol<sup>-1</sup> and its melting point is 41-43°C, boiling at 173°C (Merck Index, 1989). It is almost insoluble in water (1 g in 6670 g water, only).

In previous papers (Vicente et al., 1989; del Hoyo et al., 1993a) we have reported on drug/clay systems prepared by conventional methods, i.e., adsorption from solutions. A study on the interaction between salol and montmorillonite has been also reported (del Hoyo et al., 1993b). In the present study we want to report on two alternative, and very efficient, methods, as alternatives to the common one, consisting in melting of the drug onto the surface of the clay, or grinding both together. The study reported has been carried out on sepiolite, a fibrous silicate less sensitive to grinding than the layered ones (Cornejo and Hermosín, 1986; Cicel and Kranz, 1981).

Optimum grinding time was determined by grinding from 1 to 15 min (del Hoyo, 1995), and checking by Vis-UV/Diffuse Reflectance spectroscopy the adsorption process, using a constant ratio of drug to clay (10/100 g/g). A maximum absorption was reached after 10 min grinding. In a second step, but using a constant grinding time, the effect of different drug/clay ratios, was studied, by using ratios of 1, 2, 3, 5, 10, 25, 50, 75, and 90 g drug in 100 g clay.

For the samples prepared *via* the melting method, mixtures of drug and clay were kept at 43°C during 24 h; in all cases, the drug/clay ratios were the same as for the samples prepared by grinding.

Results obtained indicate that both methods, grinding and melting, improve the absorption of the solids in the 290-190 nm range, the so-called "C" ultraviolet radiation, that are though to be more effective to induce skin cancer. The spectrum of the samples prepared by melting shows a broad absorption band with maxima at 212, 255, and 312 nm. However, for the samples prepared by grinding the maxima of the broad band are recorded at 220 and 284 nm. On montmorillonite both spectra were identical (del Hoyo et al., 1996).

Plots similar to "adsorption isotherms" for these samples correspond to type-L in Giles classification (Giles et al., 1960), indicating saturation of adsorption sites as the amount of drug increases.

The drug/clay systems have been characterized by X-ray diffraction, differential thermal analysis, thermogravimetric analysis and FT-IR spectroscopy.

The X-ray diffraction diagrams are identical to that of the pure support, without any change in the position nor the relative intensities of the diffraction peaks, indicating that the support is unaltered by the adsorption process. Thermal studies indicate an almost complete removal of free and bonded water molecules, and their substitution by the drug molecules.

On the other hand, phenyl salicylate does not undergo any sort of chemical change, and the FT-IR spectra of the samples are identical to that obtained upon superimposition of the spectrum of the drug and that of the clay.

Finally, the stability of the drug/clay complex has been studied. This is one of the most outstanding aspects of this sort of studies, as a protective cream needs not only to be very effective in absorbing the UV radiation, but also to be very stable to be effective during a prolonged period of time. So, the desorption of phenyl salicylate from the surface of sepiolite under conditions as close to those of real use was studied.

A portion of 100 mg of the drug/clay complex was suspended in 50 ml of an aqueous solution containing 2.925 g NaCl/l and 0.745 g KCl/l at pH=5.5, in order to reproduce the composition of human sweat (del Hoyo, 1995). The suspension was immersed in a water bath at 40°C and was continuously stirred; after 15 min it was centrifuged and half of the supernatant liquid was removed and its Vis-UV spectrum recorded, adding an identical volume of solution. The process was repeated six times. The amount of drug desorbed was measured from the Vis-UV spectra of the sample before and after desorption at a maximum wavelength. Results indicate that 19% of drug is removed in samples obtained by grinding, but only 4% in those samples prepared by melting.

The desorbed percentages are very low, indicating that most of the drug remains adsorbed on the surface of the clay. So, we conclude that systems obtained by melting or grinding phenyl salicylate on sepiolite may constitute good alternatives for sun radiation protectors.

#### REFERENCES

- Cicel B & Kranz Z G (1981). *Clay Min.* **16**, 151-162.
- Cornejo J & Hermosín M C (1986). *Clay Min.* **23**, 391-398.
- Del Hoyo C (1995). Ph. D. Thesis, University of Salamanca (Spain).
- Del Hoyo C, Rives V & Vicente M A (1993 a). *Appl. Clay Sci.* **8**, 37-51.
- Del Hoyo C, Rives V & Vicente M A (1993 b). "Adsorption of Phenyl Salicylate on Montmorillonite". XVIII Iberian Meeting of Adsorption.
- Del Hoyo C, Rives V & Vicente M A (1996). *Clays and Clay Min.* In press.
- Giles C H, MacEwans T H, Nakhwa S N & Smith D (1960). *J. Chem. Soc.* **786**, 3973-3985.
- The Merck Index (1989). 11th ed. Centennial Edition. Merck and CO., Inc. Boca Ratón, Florida.
- Vicente M A, Sánchez Camazano M, Sánchez Martín M J, Del Arco M. Martín C, Rives V & Vicente Hernández J (1989). *Clays and Clay Min.* **37**, 157-163.

## Mineralogical and sedimentological characterization of clay raw materials and firing transformations in the brick-making industry from the Bailén area (southern Spain)

*Jiménez Millán J, Molina J M and Ruíz Ortíz P*

A major problem facing brick manufacturers of the Bailén area lies in selecting the appropriate raw materials and its proportion to make pastes yielding high quality fired ware. This work aimed to characterize the clay raw materials from the area as well as the fired bricks to suggest the best mixtures and modify the inappropriate steps.

### **Geological setting and raw materials**

Clay raw materials occur in the Miocene marine sediments of the Guadalquivir Basin (Fig. 1a and b). Three formations can be distinguished in the stratigraphic section of the area: 1) Lower Formation (Lower-Middle Tortonian) is 20-40 m thick and consists of breccias, conglomerates, and sandstones; 2) Intermediate Formation (Upper Tortonian-Messinian) 200 m thick as average is made by blue or yellow marls with interbedded sands. 3) Upper Formation (Messinian) composed by carbonate sandstones, with interbedded marls. The raw materials are obtained from the Intermediate Formation, in which the following materials can be distinguished (Fig. 1c): 1) Dark-gray marly limestones more than 2 m thick. 2) Clayey marls and marly clays 12 m thick with interbedded fine-sized sand levels, locally known as "negro". Its average mineralogical composition consists of phyllosilicates (45 %), quartz (35 %), calcite (15 %) (Table 1). Illite is the most abundant phyllosilicate, and lower quantities of smectite and chlorite are present. 3) Yellow marly clays with interbedded fine-size sands levels, locally known as "rubio", lower than 2 m thick. It is richer in quartz (until 50 %) and poorer in calcite (10 %) than the "negro" but its clay mineralogy is similar. It is very common the presence of veins of gypsum. 4) White clayey marls 2,5 m thick (locally known as "blanco") consisting of carbonates and phyllosilicates (smectite proportion >75%) in similar proportions and traces of quartz and feldspar. 5) Diatomitic marls. This materials are composed by calcite (40 %) and an important content in amorphous and microcrystalline silica ranging between 20 and 30 %. 6) White clayey marls, 3 m thick. This material is similar to that described as "blanco". 7) The upper part of the sequence is characterized by the presence of a level 2,5-3 m thick of meterorized marls and soils in which calcretes are very abundant.

Apart from these materials, red raw clays are imported from Triassic units of the Iberian Massif. These materials consist of illite, quartz and Fe-oxides and are known as "rojo".

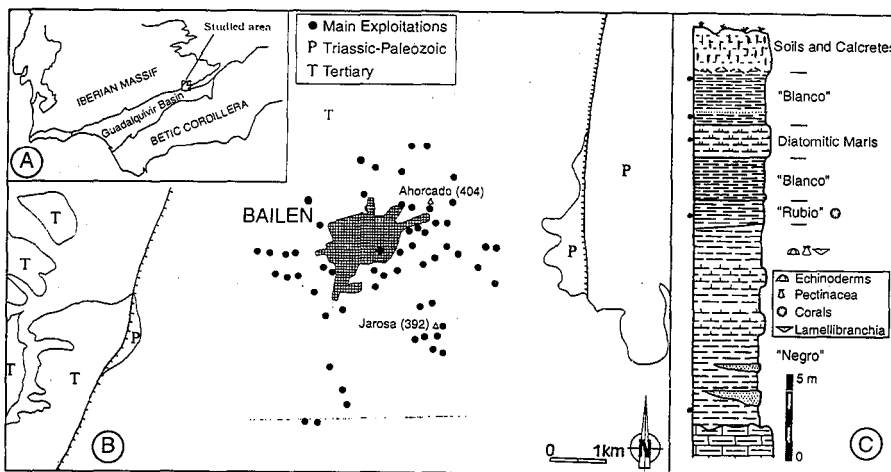


Fig.1.- Geological context and stratigraphic section

### Mixtures of raw clays materials and firing transformations

The most extended mixture of clay raw materials to make pastes is very rich in "negro" (about 70 %). "Rubio" is an usual component and some manufacturers add to the mixture variable proportions of "rojo". Three types of pastes are prepared according the ingredients and the milling process: a) Paste of milled local raw materials. b) Paste of unmilled local raw materials. c) Paste of unmilled raw materials with addition of imported "rojo" component.

XRD data reveals that the mineralogy of pastes is very similar to that of "negro". The influence of the "rojo" component is poorly appreciated in the XRD bulk mineralogy. Fired bricks are very rich in quartz and are characterized by the absence of calcite and the presence of Ca-silicates such as wollastonite ( $\beta\text{CaSiO}_3$ ), gehlenite ( $\text{Ca}_2\text{Al}_2\text{SiO}_7$ ), and anorthite ( $\text{CaAl}_2\text{Si}_2\text{O}_8$ ) which are commonly found in fired mixtures of clays and  $\text{CaCO}_3$  (González-García et al. 1990).

Petrographically, the pastes present abundant phenocrysts and the fired bricks show porphyritic texture. Pastes have a yellowish matrix while, in the bricks, the matrix is reddish. The matrix/phenocrysts proportion is around 80 % when pastes have been elaborated with milled raw materials, while in pastes consisting of unmilled raw materials, the matrix proportion is around

Table 1.- Mineralogical composition of the raw materials in the brick industry of Bailén.

		Quartz	Calcite	Dolom.	Fds.	Clays	Illite	Chlorite	Smec.
"Negro"	Average	35	15	<5	<5	45	55	10	35
	Range	30-45	10-20	<5	<5	35-55	50-60	10-15	30-40
"Rubio"	Average	40	10	<5	<5	45	60	<5	40
	Range	35-50	10-15	<5	<5	35-50	55-60	<5	35-40
Diatom Marls	Average	10	40	<5	<5	15	20	<5	75
	Range	5-10	40-45	<5	<5	15-20	15-20	<5	70-75
"Blanco"	Average	10	40	<5	<5	40	15	<5	75
	Range	5-10	40-45	<5	<5	40-45	15-20	<5	75-80

60 %. In unmilled pastes and bricks the most common phenocryst size is around 75  $\mu\text{m}$  and the greatest crystals are until 800  $\mu\text{m}$ . However, in milled materials, phenocrysts are lesser in size, showing 50  $\mu\text{m}$  as the more common size and 200  $\mu\text{m}$  as maximum. Phenocrysts of quartz and plagioclase are present in all the studied materials, while phenoclasts of calcitic rounded planktonic foraminifera and prismatic phyllosilicates are restricted to the unfired pastes. In the fired bricks, it can be recognized the shape of the foraminifera microfossils but calcite is not present inside and its boundaries are characterized by the presence of gehlenite. Prismatic muscovite in the pastes is replaced in the bricks by phenocrysts of gehlenite and Fe-oxides. "Rojo" phenoclasts raw material, ranging in size between 1 and 3 mm, are observed in bricks and pastes of type c. Inside these clasts, rounded crystals of quartz and prismatic muscovites are present in a red matrix rich in Fe-oxides. In the fired bricks, an empty rim is present between the "rojo" clasts and the matrix. Also, contraction cracks restricted to the clasts of "rojo" are very common.

### Conclusions

The mineralogical composition of the materials currently used in the Bailén brickmaking industry shows a balanced mixture of quartz, that provides mechanical resistance and permanence, and clay minerals. The mixture of clays and calcite favours the crystallization of Ca-(Al)-silicates on heating above 800 °C which according to González García et al. (1990) can yield fired ware with excellent physical properties in this industry. Ceramic tests performed on diatomitic marls of similar mineralogical composition (Galán et al., 1993) indicate that these materials could be used to manufacture lightweight bricks, but manufacturers from the Bailén area do not employ these materials in the paste elaboration.

On the other hand, the milling process lead to the decrease of phenocryst size and the increase of the matrix proportion in bricks that apparently improves the quality of fired ware. The mixture of the autochthonous materials with the allochthonous sandier and illitic "rojo" could increase the compactness and hardness of bricks, but when this material is added unmilled, phenoclasts with internal contraction cracks appear which could negatively affect the resistance, permeability and permanence of the fired ware. A similar effect is yielded by the volatilization of the calcitic phenoclasts during the firing process of the bricks.

**Acknowledgment:** Project "Caracterización mineralógica y textural de la materia prima y productos elaborados en la industria cerámica de Bailén" (Univ. Jaén, ACEBA, J. Andalucía).

### References

- Galán E, González I, Mayoral E & Miras A (1993) *Applied Clay Sci.* **8**, 1-18.  
González-García F, Romero-Acosta V, García-Ramos G, González-Rodríguez M (1990) *Applied Clay Sci.* **5**, 361-375.

(1) Dpto. Ingeniería Geológica y  
Minera. EUPA. Univ. de Castilla-  
La Mancha. Almadén, España

(2) Lab. Mineralogía Aplicada.  
Fac. Químicas. Univ. de Castilla-  
La Mancha. Ciudad Real, España

(3) Dpto. Cristalografía y  
Mineralogía. Fac. Geológicas.  
Univ. Complutense de Madrid,  
España

(4) Dpto. Estratigrafía. Fac.  
Geológicas. Univ. Complutense  
de Madrid, España

## Clay materials from Cameros basin (NE Spain) and their possible ceramic uses

*Parras J (1), Sánchez C (2), Barrenechea J F (3), Luque F J (3),  
Rodas M (3) and Mas J R (4)*

### INTRODUCTION

The Cameros Basin presents an extremely thick sequence (up to 5000 m) of sediments, with a high proportion of lutitic beds. Since these clays are predominantly illitic in composition, they are likely to present appropriate ceramic properties. However, up to date, no specific work has been carried out regarding the potential industrial applications of these materials. The aim of this paper is to present the first data concerning their ceramic uses.

### MATERIALS AND METHODS

A set of violet to green lutitic samples from different areas of the Cameros basin have been selected for this study, following a criteria based on their varying mineralogical composition and degree of diagenesis and metamorphism.

The mineralogical characterization of these samples has been achieved by means of X-ray diffraction analyses and afterwards, their behaviour upon firing has been observed, including the determination of the following parameters: linear shrinkage (L.S.), water absorption (W.A.), open porosity and bulk density.

In addition, the changes in firing colours and the evolution of the different mineral phases at increasing temperatures have been estimated as well. Colours have been determined by means of a colorimeter DR. LANGE Microcolor LMC on the raw materials and on fired samples. All the data were registered under the chromaticity system CIE  $L^*$ ,  $a^*$  and  $b^*$ .

The parameters were determined on slabs obtained by pressing the raw materials at 300 Kg/cm<sup>2</sup> and fired from 900 to 1175°C, under a firing speed of 200°C/h.

## RESULTS AND DISCUSSION

The raw materials studied in this work are formed by phyllosilicates (illite + chlorite ± kaolinite ± pyrophyllite ± rectorite ± paragonite ± mixed-layer muscovite/paragonite), quartz and minor amounts of feldspar and hematite, except for sample YAN-22, where the latter phase is absent. Samples PSA-25 and PSA-30 were collected in the area affected by deep-diagenetic conditions. Sample SPM-33 corresponds to very-low grade metamorphism (anchizone), and sample YAN-22 belongs to the epizone (Barrenechea et al., 1995).

According to the analytical results, in the temperature range between 900-1000°C, all the samples present L.S. values lower than 1%, with W.A. over 9.5%. At maximum firing temperatures (1150-1175°C) there is a significative decrease in the W.A. (<1%), while the L.S. data increase up to 6% (for samples PSA-25 and PSA-30) and reach even slightly higher values for samples YAN-22 and SPM-33. Therefore, the conditions of linear shrinkage, water absorption and open porosity observed at low temperatures (900-1000°C) are adequated for the use of these raw materials in the porous tiles industry. On the other hand, the estimation of these parameters together with the bulk density values determined at high temperatures (over 1100°C) indicate their potential usefulness in the stoneware tiles industry.

An increase in the  $a^*$  and  $b^*$  values has been detected in every sample upon firing. This feature is closely related with an increase in the proportion of hematite in samples PSA-25, PSA-30 and SPM-33, whereas the lack of this mineral in the original composition of sample YAN-22 indicate that hematite in this case is a neoformed phase. The iron supply generated by the destruction of Fe-chlorite and chloritoid would be responsible for both the increasing proportion of hematite and the neoformed phase (in sample YAN-22), through a mechanism similar to that proposed by Murad and Wagner (1996) for clays rich in Fe-illite.

There is a progressive increase in the  $L^*$  values up to 1000°C, but a decrease in such parameter has been observed at higher temperatures. In sample YAN-22 there is a constant decrease in the  $L^*$  values for the whole temperature range considered. Thus, samples PSA-25,

PSA-30 and SPM-33 present a red colour after firing and could be used for manufacturing? coloured products, while sample YAN-22 shows a pale pink colour. At high temperatures, all the samples present dark red colours.

The clay minerals recognized within the firing temperature range include: illite (stable up to 975°C) and pyrophyllite (up to 1000°C). Quartz has been recognized in the fired samples within the whole firing temperature range. Hematite is present in sample YAN-22 only after firing at 1000°C and it is related to an increase in the  $a^*$  and  $b^*$  parameters. Mullite coming from the transformation of previous illites appears at 1000-1050°C. At slightly lower temperatures (900-1000°C) mullite coexists with an intermediate  $\gamma$ -Al<sub>2</sub>O<sub>3</sub> phase, in good agreement with the data obtained by Parras et al. (1996).

#### CONCLUDING REMARKS.

Considering the low shrinkage and water absorption values, together with an adequate open porosity and the firing colours determined, we may conclude that samples PSA-25, PSA-30 and SPM-33 could be used in the manufacturing of red-coloured porous tiles and coatings, with firing temperatures around 1000°C. At higher firing temperatures (1125°C), these samples might be used in the production of red stoneware tiles, since water absorption is negligible and linear shrinkage values are lower than 6%.

On the other hand, sample YAN-22 could be used in a similar way, although its use as coloured porous tiles would require the presence of an additive to enhance the red colour at low firing temperatures.

#### REFERENCES

- Barrenechea, J.F.; Rodas, M.; Mas, J.R. (1995) *Clay Miner.*, **30**, 119-133.  
Murad, E.; Wagner, U. (1996) *Clay Miner.*, **31**, 45-52.  
Parras, J.; Sánchez, C.J.; Rodas, M.; Luque, F.J. (in press) *Appl. Clay Science*.

(1) Dpto. Ingeniería Civil de  
Materiales y Fabricación.  
ETS Ingenieros Industriales.  
Univ. de Málaga, España

(2) Instituto de Ciencia de  
Materiales. CSIC-  
Universidad. Sevilla, España

## Processing and properties of mullite-based composites from kaolinite

*Pascual J (1), Zapatero J (1), Ramos J R (1), Ramiro A (1), Sánchez  
Soto P J (2), Justo A (2) and Pérez Rodríguez J L (2)*

---

Mullite (nominal composition  $3\text{Al}_2\text{O}_3 \cdot 2\text{SiO}_2$ ) is the only stable crystalline phase, at normal pressure, in the  $\text{SiO}_2\text{-Al}_2\text{O}_3$  system and produced after the thermal decomposition of kaolinite and clay-based minerals [1-5]. Although it is one of the most commonly found phases in industrial ceramics, the importance of mullite as a ceramic phase was only recognized during this century when the first binary phase diagram was proposed [6]. This late recognition can be attributed to two factors: (a) the occurrence of mullite as a mineral is very rare in nature, and (b) although it is very common reaction product of most aluminium silicates at high temperatures ( $> 1000^\circ\text{C}$ ), mullite was mistakenly identified as a sillimanite mineral in earlier studies. Sillimanite and its two polymorphs (kyanite and andalusite) have orthorhombic crystal structures very similar to that of mullite, but at atmospheric pressure the sillimanite minerals always convert to mullite at elevated temperatures [7]. Its excellent properties such as high-temperature strength and creep resistance, good chemical and thermal stability, low thermal expansion coefficient, and good dielectric properties make this ceramic and its composites important candidates for electronic, optical and high-temperature structural applications as advanced materials [8,9].

Different combinations of precursors for silicon and aluminium have been used for mullite preparation, including aluminium and silicon sols from inorganic salts or alkoxydes, but the experimental conditions have to be carefully controlled [5,10]. The reaction series of kaolinite or metakaolinite [1,5] is similar to that of silica-alumina diphasic precursors (with a scale of homogeneity from 1 to 100 nm). Initially, a transient

alumina or alumina-type spinel forms at 980°C with an exothermic thermal effect, and mullite crystallization follows at higher temperatures, often with a distinct second exotherm at *ca.* 1200°C. Although kaolinite is an atomically layered structure of  $(\text{Si}_2\text{O}_5)^{2-}$  and  $[\text{Al}_2(\text{OH})_4]^{2+}$  molecular sheets, the level of mixing of Si and Al is not sufficient to prevent the segregation of alumina and amorphous silica. Mullitization will be produced after mixing of kaolinite and alumina attaining an overall composition  $3\text{Al}_2\text{O}_3 \cdot 2\text{SiO}_2$  and treating the reactive precursors to high temperature.

The present investigation deals with a preliminar study on the processing conditions and properties of mullite and mullite-based composites. These were obtained by thermal reaction of a precursor prepared using a suspension of kaolinite mixed with precipitated aluminium hydroxide. The hydroxide was precipitated, using ammonia or amines, from aluminium salts or aluminium metallic powder from recycled wastes. Different thermal treatments were performed. The precursors and the thermal reaction products have been mainly investigated using X-ray diffraction (XRD), Infrared Spectroscopy (TFIR), thermal analysis (DTA-TG), optical and electron microscopy and microanalysis (SEM-EDX).

The effect of some processing variables has been examined and evaluated, such as the influence of precipitation and reaction conditions, particle size, temperature of thermal treatment, and firing atmosphere, principally. The effect of the processing variables on the ceramic (sintering and densification, porosity, shrinkage), mechanical (flexural strenght and thermal coefficient) and electrical properties (conductivity) has been also studied. The densification was followed according to standard ceramic methods, and the porosity using mercury porosimetry (Fisons). The flexural strength at room-temperature was measured after firing using an Instron machine (model 8501), and the thermal coefficient by dilatometry (Bähr GmbH). The electrical conductivity was measured by impedance spectroscopy using a Solartron 1260 analyzer.

It is concluded that the processing variables strongly influence the behaviour of the mullite and mullite-based composites prepared from kaolinite using the proposed

chemical synthetic pathway, and the processing-structure-properties relationships are discussed on the basis of the present results. For instance, the electrical conductivity (frequency range 10-1 MHz and temperature 200-600°C) as described by the Bode plots showed two relaxations. The deconvolution analysis suggests an equivalent circuit with an element of constant phase. The activation energies were found dependent of the nature of chemical used in the processing step of aluminium precipitation. Thus, mullite samples obtained from kaolinite using amines showed higher activation energies in the process intra-granular and lower values in the inter-granular. This behaviour was observed inverse when the composites are processed using ammonia for aluminium hydroxide precipitation in the presence of kaolinite.

#### ACKNOWLEDGMENT

This work was supported by DGICYT through research project PB92-0014.

#### REFERENCES

1. W.D. Johns, *Mineral. Mag.* **30** (1953) 186; G.W. Brindley and M. Nakahira, *J. Am. Ceram. Soc.* **42** (1959) 311; *ibid.* 319.
2. J. Lemaitre, M. Bulens and B. Delmon, pp. 539-44 in: *Proc. Int. Clay Conference 1975* (ed. S.W. Bailey), Applied Publishing, Wilmette, IL, USA.
3. B. Sonuparlak, M. Sarikaya and I.A. Aksay, *J. Am. Ceram. Soc.* **70** (1987) 837.
4. J. Sanz, A. Madani, J.M. Serratos, J.S. Moya and S. de Aza, *J. Am. Ceram. Soc.* **71** (1988) C418.
5. J.A. Pask and A.P. Tomsia, *J. Am. Ceram. Soc.* **74** (1991) 2367.
6. F.H. Norton, pp. 1-91 in: *Fine Ceramics, Technology and Applications*, McGraw-Hill, NY, USA, 1970.
7. J.L. Holm and O.J. Kleppa, *Am. Mineral.* **51** (1966) 1608.
8. S. Somiya, R.F. Davis and J.A. Pask, *Mullite and Mullite Matrix Composites*, Vol.6 Ceramics Transactions, The American Ceramic Society, Ohio, USA, 1990.
9. I.A. Aksay, D.M. Dabbs, M. Sarikaya, *J. Am. Ceram. Soc.* **74** (1991) 2343.
10. M.D. Sacks, H.W. Lee and J.A. Pask, pp. 167-207 in reference 8.

Instituto de Ciencia de  
Materiales. CSIC-  
Universidad. Sevilla, España

## Mechanochemical effects on kaolinite- pyrophyllite-illite natural mixtures

*Sánchez Soto P J, Justo A, Avilés M A, Ruíz Conde A, Jiménez de  
Haro M C and Pérez Rodríguez J L*

Particle size reduction of clay samples is produced by grinding (wet or dry), the nature of which plays an important role in determining the physico-chemical properties of the powdered material and further processing steps in the laboratory and industry [1]. Grinding of clay minerals produces various effects on their structure and properties, often accompanied by polymorphic transformations and chemical reactions. The significant grinding processes involved in the preparation of ceramic raw materials have been studied. However, little is known about the effects of grinding on natural mixtures of layer silicates. In previous papers [2,3], the authors have studied the effects of dry grinding on pyrophyllite. In the present work, the mechanochemical effects caused by dry grinding in a ball mill on a natural mixture composed by kaolinite-pyrophyllite-illite have been studied. The results are of great interest in a broader systematic work on processing of silicates, especially their applications as raw materials in synthesis of advanced ceramics (mullite and mullite-based composites).

### EXPERIMENTAL

**Samples.** The kaolinite-pyrophyllite-illite (30-40-30 wt%) natural mixture (ZS clay, fraction under 63  $\mu\text{m}$ ) was selected from a clay deposit near Badajoz (Spain) [4]. Pyrophyllite (~ 90 wt%, Hillsboro NC, USA) was also used in this study, lightly ground and sieved to pass 50  $\mu\text{m}$ . Purified pyrophyllite was also used [4]. Well-crystallized kaolinite (KGa-1 standard sample from Georgia, USA) was supplied by Source Clay Repository (Clay Minerals Society, USA). Illite (> 95 wt %) was extracted by wet sedimentation and separation of the 2-0.2  $\mu\text{m}$  fraction after adequate dispersion from a raw material [5], and subsequently purified.

**Methods.** Dry grinding of the samples was conducted in a ball mill (Model S-1 Retsch) as described previously [2]. DTA and TGA diagrams were obtained simultaneously in static air with a thermal analyzer (PTC-10A, Rigaku), at a heating rate of 12 °C/min. XRD powder patterns were obtained using a diffractometer (D-500 Siemens). Specific surface areas (BET) were obtained with an automatic system (Model 2200 A, Micromeritics) with nitrogen gas as adsorbate at liquid nitrogen temperature. Original and ground samples dispersed in acetone were examined by SEM using a ISI microscope model SS-40.

## RESULTS AND DISCUSSION

Grinding of this natural mixture produces an increase in surface area with grinding time, associated to particle size reduction, and a structural alteration in the silicates that constitute the mixture, producing broadening of diffraction peaks and decreasing of X-ray intensities, originated mainly by domain size reduction, with total degradation of the crystal structure of kaolinite after 60 minutes of grinding; pyrophyllite and illite X-ray reflections disappear after 90 minutes, yielding finally a more amorphous material. At higher grinding times, only weak reflections corresponding to rutile in an amorphous matrix are detected. Grinding is also influencing the thermal behaviour because the decrease in particle size causes the elimination of structural OH groups at lower temperatures in ground than in unground material, where a more defective or stressed structure is being also produced by mechanical treatment.

The endothermic DTA effect in the unground mixture centered at ~ 700 °C, associated to dehydroxylation of pyrophyllite, is shifted to lower temperatures, reaching the endothermal effect of kaolinite dehydroxylation centered at 530 °C in this sample. After 32 minutes of grinding, a single broader endothermic DTA effect centered at ca. 530 °C is detected, and decreases in intensity as grinding time proceeds, disappearing after 90 minutes of grinding. The exothermic DTA effect at 985 °C increases markedly in sharpness and height as grinding proceeds, especially from 32 minutes to longer grinding times when structural breakdown is very important. After 240 and 325 minutes, the intensities of the exothermic effects are remained practically constant. This treatment also produces the detection of weight losses (water dehydration and dehydroxylation) at lower temperature than in unground samples. Further grinding produces a breakdown of the

crystal structure of the silicates, and also an agglomeration process of the amorphous and activated material, accompanied by a decrease in surface area and a strong increase of the exothermic DTA. As a consequence of the enhanced surface energy of the comminuted and activated particles provided by the grinding treatment, the particles become more agglomerated, and the surface area begins to decrease. The gradual size reduction and associated morphological changes which occur during grinding the natural mixture were also revealed by SEM. All these effects are due to the mechanochemical activation of the ground powder.

It has been concluded that the main contribution to the increased exothermic DTA peak in the mixture after grinding is due to pyrophyllite, irrespective of the other aluminium silicates present in the sample. Mullite was always detected after heating. The intensities of the X-ray peaks of this phase increase as increasing grinding time, with subsequent destruction of dehydroxylated pyrophyllite X-ray patterns detected in the unground mixture. The presence of pyrophyllite in the mixture contributes strongly to the detection and increasing in intensity of mullite in the XRD patterns, in accordance with DTA results and those obtained after grinding the pure silicates kaolinite, pyrophyllite and illite. The formation of the DTA exothermic peak is most likely due to the release of energy associated with a change in coordination of the Al ions transforming to a more stable sixfold coordination, thus facilitating the formation of mullite [6].

#### ACKNOWLEDGMENTS

This work was supported by DGICYT through research project PB92-0014.

#### REFERENCES

1. J. Lin and S. Nadiv, *Mater. Sci. Eng.* **39** (1979) 193.
2. J.L. Pérez-Rodríguez, L. Madrid and P.J. Sánchez-Soto, *Clay Miner.* **23** (1988) 399.
3. P.J. Sánchez-Soto and J.L. Pérez-Rodríguez, *J. Am. Ceram. Soc.* **72** (1989) 154.
4. J.L. Pérez-Rodríguez, C. Maqueda and A. Justo, *Clays Clay Miner.* **33** (1985) 563.
5. A. Bernal, G. García, F. González, A. Justo and J.L. Pérez-Rodríguez, *Bol. Soc. Esp. Ceram. Vidr.* **17** (1978) 17.
6. J. Sanz, A. Madani, J.M. Serratosa, J.S. Moya and S. de Aza, *J. Am. Ceram. Soc.* **71** (1988) C418.

(1) Instituto de Ciencia de Materiales. CSIC-Universidad. Sevilla, España

(2) Refractarios Alfrán S.A. Alcalá de Guadaíra, Sevilla, España

(3) Dpto. Ingeniería Civil de Materiales y Fabricación. ETS Ingenieros Industriales. Univ. de Málaga, España

(4) Instituto de Bachillerato "Mariana Pineda". Granada, España

## Sintering of a clay containing pyrophyllite and industrial evaluation of its ceramic properties

*Sánchez Soto P J (1), Raigón M (2), Jiménez de Haro M C (1), Justo A (1), Pascual J (3), Pérez Rodríguez J L (1) and Béjar M (4)*

During past years, the development and investigation of ceramics from raw clay materials has been increasing [1-4]. They contain mainly kaolinite and other clay minerals, such as pyrophyllite, which decompose by thermal treatment producing mullite [5-7]. The formation of mullite after firing the clay bodies leads to interesting technological properties, in particular for high-temperature structural applications [8]. On the other hand, clays and clay-based materials are basic for low-cost production in the ceramic industry, in particular refractories after adequate processing [6]. According to this, it is valuable to know new ceramic raw materials, to study the sintering behaviour or vitrification process, to determine its technological properties, and to assess the industrial applications. Vitrification is the result of heat treatment during which a glassy or non-crystalline phase is produced [9-10]. The vitrification range is then defined as the temperature interval between the temperature at which it begins to deform by melting. Thus, semiempirical attempts to analyze the vitrification rates have been proposed, calculating heat treatment conditions using experimental observations of density and apparent porosity and an Arrhenius analysis involving the temperature dependence of the vitrification rate [9].

The objective of the present investigation is to study a ceramic raw material mined in the province of Badajoz (Extremadura, Spain) from a bed of great potential, its sintering behaviour and main industrial applications of interest.

## EXPERIMENTAL

A preliminary characterization of the raw sample has been carried out by several instrumental techniques, such as XRD (Siemens D-5000 equipment), DTA-TG (Setaram 1600, model 92.16,18), Particle size by sedimentation, Chemical analysis (Atomic Absorption), Dilatometry (Bähr Thermoanalyse) and SEM-EDX (ISI SS-20). The ceramic properties have been determined using standard methods. The porosity has been also studied using mercury porosimetry (Fisons). The flexural strength at room-temperature was measured after firing the specimens (Instron), and the thermal coefficient by dilatometry. The sintering behaviour has been analyzed according to a model taking into account the experimental observations. Finally, an industrial evaluation of its applications has been made, in particular for the refractories industry.

## RESULTS AND DISCUSSION

Chemical, mineralogical and textural studies indicated that the raw material is composed of the layered silicates pyrophyllite, mica and kaolinite. Minor components are quartz and feldspar. It shows an average alumina content of 30 wt% and low  $\text{Na}_2\text{O} + \text{K}_2\text{O}$  content (1.64 wt%). The texture is silt-clayey, with more than 80 wt% of particle size less than 50 micrometers.

The ceramic properties were determined in pressed bodies (prismatic bars) fired from 800°C to 1500 °C for 1-4 hours of soaking time. It was found that after firing at 1200°C-1300°C the material is sintered. Water absorption of the test samples decreases from 12 % at 800°C to 3.2 % at 1200°C for 4 hours. Water absorption decreases from 2.5 % at 1200°C to 0.94 % at 1300°C for 1 hour, being the open porosity 2.2 % after firing at this temperature. The porosity evolution was also investigated by mercury porosimetry and the pore size distributions are reported. The degree of vitrification and the activation energy of the process have been also evaluated from these results using Arrhenius analysis. It has been obtained a low coefficient of thermal expansion after firing at 1200°C, maximum mechanical strength and homogeneous microstructure as studied by electron microscopy. The phase evolution have been also examined by X-ray diffraction, showing the formation of mullite after heating the raw material. All these data were useful to discuss the microstructure-properties relationships.

The results have shown the good ceramic capabilities of this raw material and allowed an assessment of its potential applications of interest. This clay containing pyrophyllite is suitable for manufacturing porous ceramic facing tiles and gres products in which the mineralogy and original fine particle size are valuable. The materials obtained after firing at 1300 °C and higher could be applied as calcined products or chamotes with high mullite content, with interest for the preparation of clay-based refractory and fireproofing materials. In this sense, further experiments were also carried out using this clay and calcined alumina of adequate particle size, and firing at 1450°C-1500°C to find the requirements of high-alumina refractories and fireproofs products. The results were compared using both laboratory and industrial tests, obtaining refractory bricks with good properties similar to other commercial products, but at relatively lower cost.

#### ACKNOWLEDGMENTS

The authors are grateful to Mr. Eduardo Garcés for provide samples used in this study and the partial financial support of research project PB92-0014.

#### REFERENCES

1. E. Galán, *Bol. Soc. Esp. Ceram. Vid.* **20** (1981) 33.
2. B. Ulrich and L. Lesh, *Silikattechnik* **8** (1987) 274.
3. V. Zaykov and V.N. Udachin, *Appl. Clay Sci.* **8** (1994) 417.
4. Annual Minerals Review, *Am. Ceram. Soc. Bull.* (1995).
5. G.W. Brindley and J. Lemaitre, pp. 319-370 in: *Chemistry of Clays and Clay Minerals*, Ed. A.C.D. Newman, Longman, Essex, 1987.
6. J. Sanz, A. Madani, J.M. Serratos, J.S. Moya and S. de Aza, *J. Am. Ceram. Soc.* **71** (1988) C418; J.A. Pask and A.P. Tomsia, *J. Am. Ceram. Soc.* **74** (1991) 2367.
7. P.J. Sánchez-Soto, I. Sobrados, J. Sanz and J.L. Pérez-Rodríguez, *J. Am. Ceram. Soc.* **76** (1993) 3024.
8. I. Aksay, D.M. Dabbs, M. Sarikaya, *J. Am. Ceram. Soc.* **74** (1991) 2343.
9. V.T.L. Bogahawatta and A.B. Poole, *Br. Ceram. Trans. J.* **90** (1991) 52.
10. S.M. Faieta-Boada and I.J. McColm, *Appl. Clay Sci.* (1993).

Dpto. Geociencias. Univ. de Aveiro, Portugal

## Clays for waste disposal liners: comparative appraisal of the relevant properties of smectitic clays from Aveiro and Taveiro (Portugal)

Santos H, Rocha F and Gomes C

### INTRODUCTION

In recent years there has been in Portugal a deep political and social concern on waste disposal and treatment. After an initial stage for people sensibilization, field work and research is being carried out in order to select the most favourable sites to install incineration units and waste land-fills.

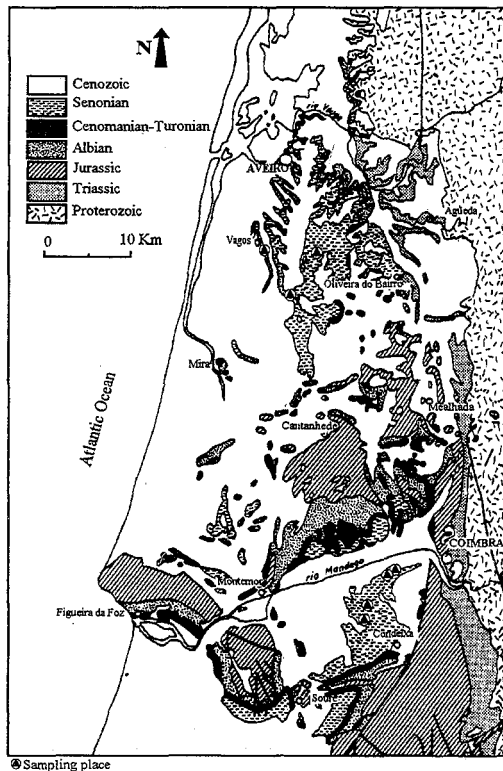


Fig. 1 - Location and geological setting

Clays are fundamental materials to be used as impermeable liners in the waste land-fills. Taveiro (Coimbra) and Vagos (Aveiro) were two of the selected areas to install those infrastructures. Both selected sites are related to disactivated clay quarries, located in upper Cretaceous (Campanian-Maastrichtian) terrains (Fig. 1). In Taveiro and Vagos regions, heavy clays utilized for structural ceramics are quite common. These clays contain smectite-illite-kaolinite assemblages and quantitative variation of these clay minerals occur locally.

This paper deals with the comparative appraisal, in terms of mineral composition, chemical composition and other relevant properties required for clay liners, of representative samples from both Taveiro and Aveiro/Vagos clay deposits.

## MATERIALS AND METHODS

Sampling was carried out in clay quarries, either with works or disactivated, found both in Aveiro and Taveiro regions.

For each sample mineralogical composition was estimated on total assemblage,  $<63 \mu\text{m}$  and  $<2 \mu\text{m}$  fractions, by X-ray diffraction (XRD). The less than  $63 \mu\text{m}$  fraction was separated by wet sieving whereas the less than  $<2 \mu\text{m}$  fraction was separated by sedimentation in water according to Stokes law. For clay minerals characterization oriented specimens either in natural state or saturated with Mg and glycerol were analysed by XRD. Oriented specimens heated up to  $300^\circ\text{C}$  and  $500^\circ\text{C}$  were X-rayed too. For semiquantitative determinations of clay and non-clay minerals, criteria recommended by Schultz (1964) and Thorez (1976) had been followed.

Clays chemical composition was assessed by X-ray fluorescence (XRF) and flame-spectroscopy (FC) methods.

Grain size distribution was assessed using a laser grain size analyser. Specific surface area was estimated by the methylene blue method, whereas cation exchange capacity was estimated by the ammonium acetate method. Expandability was measured according to LNEC E200-1967 norm.

## RESULTS AND DISCUSSION

In terms of mineral composition, both Taveiro and Aveiro clays are essentially smectitic-illitic (Lauverjat, 1982; Pena dos Reis, 1983; Rocha, 1993). In comparative terms Aveiro clays have mineral and chemical compositions similar to those shown by Taveiro clays. However, differences could be detected on the clays found in various areas of both Aveiro/Vagos and Taveiro regions. Besides this lateral variations, vertical changes could be

found also in the clay strata of the quarries. For instance, relatively to the clays from the Taveiro region, clays from Taveiro quarry show layers richer in phyllosilicates than the clays from Ribeira de Frades quarry, nevertheless these clays show some layers richer in smectite (50~60%). In regards to the clays from the Aveiro/Vagos region, clays from Bustos quarry are richer in smectite comparatively to the clays from Vagos and Nariz quarries, where illite is more abundant.

In terms of the average chemical composition, clays from Aveiro/Vagos region contain lower SiO<sub>2</sub> (58~60%, against 60~70) but higher Al<sub>2</sub>O<sub>3</sub> (19~20%, against 15~19%), Fe<sub>2</sub>O<sub>3</sub> and Ignition Loss.

## CONCLUSIONS

In general terms, the studied clays from the "Argilas de Aveiro" and "Argilas de Taveiro" formations are good materials to be used as impermeable liners in the waste land-fills.

In terms of the comparative appraisal between the different studied clay deposits we can consider, from our first results, that the clays showing better characteristics are those from the "Argilas de Taveiro" formation, in particular those from the western/south-western quarries. In regards to the clays from the Aveiro region, those from the southern sector (Bustos) are the most favourable.

## REFERENCES

- Lauverjat, J. (1982) - *Le Crétacé supérieur dans le Nord du Bassin Occidental Portugais*. Unpublished PhD thesis, Université Pierre et Marie Curie, Paris VI, 717 pp.
- Pena dos Reis, R. (1983) - *A sedimentologia de depósitos continentais. Dois exemplos do Cretácico superior - Miocénico de Portugal*. Unpublished PhD thesis, Universidade de Coimbra, 404 pp.
- Rocha, F.J.F.T. (1993) - *Argilas aplicadas a estudos litoestratigráficos e paleoambientais na Bacia Sedimentar de Aveiro*. Unpublished PhD thesis, Universidade de Aveiro, 399 pp.
- Schultz, L. G. (1964) - Quantitative interpretation of mineralogical composition from X-ray and chemical data for the Pierre Shale. *U.S. Geol. Surv. Prof. Paper*, 391-C, p. 1-31.
- Thorez, J. (1976) - *Practical identification of clay minerals*. Ed. G. Lelotte (Belgique).

Dip. di Scienze della Terra.  
Univ. di Pavia, Italia

## Role of clay components in soil stability. Case-histories in the Italian territory

*Veniale F, Setti M and Soggetti F*

---

Characteristics and features of clay components (particle dimension, specific surfaces area, kinds of clay minerals, interaction with water, nature and concentration of electrolytes in pore solutions, spatial arrangement of solid particles and size-shape of interstitial voids, coating-cementig substances, etc.) are influencing the soil behaviour.

Several case-histories occurred in the Italian territory are showing various aspects:

- (i) landslide bodies along the Apennines stripe and treatments applied for their consolidation-stabilization (electro-osmosis and salt diffusion);
- (ii) Vajont dam out-flow as a consequence of rock-mass sliding into the water reservoir caused by water lubrication of smectite strata;
- (iii) (in)stability of clayey ground-soil of the ancient town of Orvieto due to damage by seepage of urban fluid discharge;
- (iv) subsidence in the area of Venice and Po-delta as a consequence of ground water and gas-oil exploitation;
- (v) last but not least, the behaviour of the clay levels in the subsoil of the "leaning" Tower of Pisa: in-situ and laboratory tests for selecting suitable interventions (deep anchors and/or underexcavation = controlled subsidence) to prevent further leaning risk, and to reduce the inclination.

(1) Dip. di Scienze della  
Terra. Univ. di Pavia, Italia

(2) The Getty Conservation  
Institute. Marina del Rey,  
California, USA

## Swelling-shrinking behaviour of clay levels in marly rocks and its influence on planar sliding events

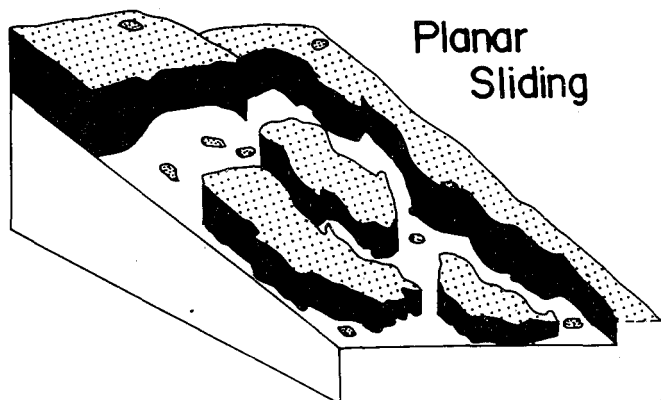
Veniale F (1), Rodríguez Navarro C (2) and Setti M (1)

Planar sliding phenomena (strata inclination 8-14°) are typical of Piedmont's Langhe region (northern Italy). They occur periodically (correlated with rain events) and are characterized by the sliding of rock blocks along limited dip planes, often coinciding with the joints between marl and sand strata (see figure).

Marl samples taken in the proximity of sliding surfaces were submerged in water and after few hours, exfoliation-like fissures parallel to the sedimentation planes were formed. X-ray diffraction analyses performed on clay materials constituting the exfoliation (micro) levels (1-2 mm thick) revealed amounts of swelling clay (smectite) significantly higher than those detected within the unexfoliated portions of the marl.

SEM observations, of clay materials present on the sliding surfaces showed that the clay particles re-arrange in a sub-parallel way after water intake (and consequently, decrease of the electrolyte concentration within the interstitial pore solutions). Such isorientation causes a repulsion between the negative charged bases of adjacent clay particles, thus priming the sliding movements.

Further experiments are in progress using the ESEM (Environmental Scanning Electron Microscope) to dynamically evidenciate on video-tape movie the fabric modifications caused by water flux.



Dpto. Geociencias. Univ. de Aveiro, Portugal

## Emission and fixation of F and S in clay based ceramics

*Vieira A I, Gomes C, Rocha F and Bobos I*

### INTRODUCTION

Clays are fundamental raw materials for structural ceramics. They might contain chemicals which are volatiles, such as: H<sub>2</sub>O, F, S, Cl and P. These volatiles are located in mineral structures, either of clay minerals or of non-clay minerals.

Aveiro is a region where huge clay and sand deposits do occur. From them large volumes of clay and sand are extracted in order to be used in the numerous ceramics plants dispersed throughout the region. These ceramic plants produce bricks, roof tiles, wall tiles and floor tiles.

### MATERIALS AND METHODS

Sampling had been carried out both on those ceramic raw materials and on their ceramic products. In regards with their chemical composition particular attention was paid to F and S taking into account their environmental impacts. Volatiles nature and content were determined using spectrophotometric and selective electrode methods.

The herein disclosed data is concerned with a local ceramics plant producing both brick and roof tile, whose mean overall production is estimated at 15,000 tons /month, 5,000 tons of roof tile and 10,000 tons of brick. Brick is fired at 910°C whereas roof tile is fired at 985°C. Raw materials formulation is the same for both products: 40% Bustos clay +60% Aguada clay. To this mixture is added 13% of Sosa sand. F and S contents in the final mixture were estimated at 0.34% and 0.05%, respectively.

### RESULTS AND DISCUSSION

F is hosted in clay minerals, replacing (OH) structural groups. Bustos clay, an illitic/smectitic clay, contains more F (0.65%) than Aguada clay (0.30%), an illitic/kaolinitic clay. F average content for roof tiles was estimated at 0.022%, whereas F average content for bricks was estimated at 0.030%.

It is evident the large quantity, estimated at 45 tons/month of fluor emitted to the atmosphere.

S average content for roof tiles was estimated at 0.12%, whereas S average content for bricks was estimated at 0.30%.

S is hosted either in sulfates (gypsum, anhydrite and melanterite) or in sulphides (pyrite and marcassite) which have been identified in the clays.

Roof tiles and bricks fix a significative amount of S from the fuel (thick fuel oil containing 3.5% S + gas propano) utilized in the ceramic plant.

Interpretation of the analytical results referred to is put forward, taking into account raw materials, ceramic products and fuel compositions as well as firing temperature, regime and residence time.

Experimental data related with the fixation of F in the ceramic products using the addition of carbonates to raw materials mixture are disclosed also.

(1) Dpto. Farmacia y Tecnología  
Farmacéutica. Fac. Farmacia.  
Univ. de Granada, España

(2) Sclumberger Cambridge  
Research. Cambridge, United  
Kingdom

(3) Instituto Andaluz de Ciencias  
de la Tierra. CSIC-Universidad.  
Granada, España

## Effect of mixing conditions on the rheological properties of some clay suspensions

Viseras C (1), Meeten G H (2), López Galindo A (3), Cerezo A (1)  
and Rodríguez I C (1)

Clays can be defined as materials with particle sizes of below 2  $\mu\text{m}$ . The dispersion of particles having colloidal dimensions (at least one dimension of the particle between 1 nm and 1  $\mu\text{m}$ ) involves a number of different stages including incorporation, wetting, breakdown of particle clusters (aggregates and agglomerates) and flocculation of the disperse particles. The properties of the final product depend on both particle characteristics, such as shape and size, layer charge, exchangeable cations, etc., and elaboration conditions such as mixer shear rate and time, kind of mixer used, heat, pH, ionic strength, etc.

It is generally difficult to explain marked differences in the rheological properties of suspensions elaborated with apparently similar clays. Two categories of factors are capable of affecting the rheological properties of suspensions: hydrodynamic and non-hydrodynamic factors. All the interactions between the dispersion medium and the particles are usually referred to hydrodynamic effects. These kind of forces are predominant in suspensions of particles greater than 10  $\mu\text{m}$  (Mewis, 1985; Kamal and Mutel, 1985), and are determined by the concentration of the particles (Everett, 1988), their shape (Weinberger and Goddard, 1974), size and size distribution (Henderson *et al.*, 1982) and the rheology of the suspending medium (Metzner, 1985).

The second category refers to the non-hydrodynamic effects and includes the colloidal properties of dispersions, where the attractive interactions between solid particles are so strong that a rigid network is obtained. Several authors have treated the formation and stability of clay gels and the effect of pH and salt concentration on the properties of the resultant product. Permien and Lagaly (1994a,b, 1995) explained the effect of the presence of different substances on the rheology of montmorillonite suspensions on the basis of non-hydrodynamic interactions. Similar studies were made with fibrous clays by Chang *et al.* (1993). The rheological properties of both sepiolite and montmorillonite suspensions were studied by Thomas *et al.* (1988). However, few investigations have been focused on the effects of hydrodynamic factors, such as size and shape of the particles, on the final product properties. There are also few studies of the effect of mixing conditions on the rheology behaviour of clay dispersions.

The objective of this work was to investigate the effect of mixing conditions (mixing power and time) on the rheology of suspensions elaborated with fibrous (sepiolite and palygorskite) and laminar (montmorillonite) clays. Finally, the effect of changes in the pH of the suspensions was studied, and the gel stability measured. Stability is explained on the

basis of both hydrodynamic and non-hydrodynamic factors.

### Materials and methods

Bentopharm, a bentonite obtained from Bromhead & Denison Ltd, UK, was used as received. It contains a certain amount of  $\text{Ca}^{2+}$  and  $\text{Zn}^{2+}$ . The quantitative analysis showed some quartz and mica as impurities. Spanish sepiolite from Vallecas (Madrid) and palygorskite from Turón (Ciudad Real) were supplied by Tolsa SA, Spain. They were also used as received. Analysis showed the samples to have a purity of between 80% and 95%. The pH level was adjusted by adding various amounts of HCl or NaOH, the ionic strength being adjusted by adding KCl.

Dispersions of 2% and 10% in distilled water were elaborated using a high shear rate rotor-stator mixer (Silverson L4RT, Silverson Machines Ltd. UK). 1000 rpm and 8000 rpm for 1 and 10 minutes were used. Samples were then shaken for 24 hours.

The rheological properties of the dispersions were measured just after mixing and after the 24 h homogenization process. The viscometer used was a couette type (Chand 35, Chandler Ltd., USA) working at 20°C. The pH was monitored until an equilibrium value was reached, and then the flow curves were obtained.

### Results

All the flow curves presented have a continuous part corresponding to the increase in shear rate and a discontinuous part corresponding to the decrease. Bentonite showed a pseudoplastic flow in all the samples. Viscosity depended greatly on the concentration, only being significant for the 10% suspensions. As can be observed in Fig. 1, viscosity increased greatly after the 24 hour homogenization period. Fig. 2 shows the effect of mixing energy on the rheology of bentonite suspensions. Both mixing time and mixing power seem to affect the viscosity of the suspensions. The pH affects the structure of gels in a different magnitude depending on the previous conditions of elaboration. Viscosity of suspensions elaborated using 1000 rpm for 1 minute showed a high dependency on the pH, whereas those corresponding to 8000 rpm for 1 or 10 minutes did not.

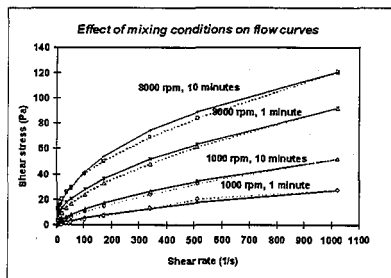
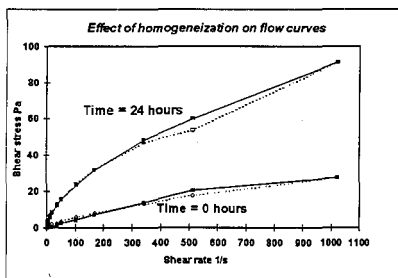


Fig.1. Shear stress vs. shear rate for 10% aqueous bentonite gels elaborated at 1000 rpm for 1 minute, and two periods of homogenization.

Fig.2. Shear stress vs. shear rate for 10% aqueous bentonite gels elaborated using different mixing energies.

Sepiolite and palygorskite gels were more viscous than the montmorillonite gels, forming good pseudoplastic gels in water at 2% and 10% concentrations. Fig. 3 shows the flow curves of 10% gels (Vicálvaro sepiolite) produced at different mixing energies; mixing power seems to affect viscosity more than mixing time. Fig. 4 illustrates the effect of pH on the rheology of 10% sepiolite suspensions elaborated at 8000 rpm for 10 minutes. Changes in the pH of the suspensions produced some decrease in the stability of gels elaborated at 8000 rpm, while those elaborated at 1000 rpm showed a significant decrease.

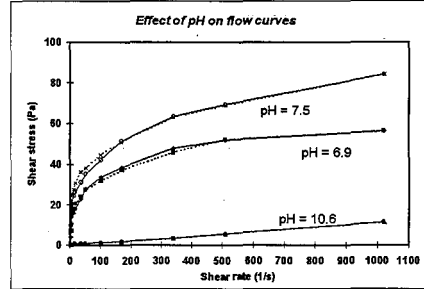
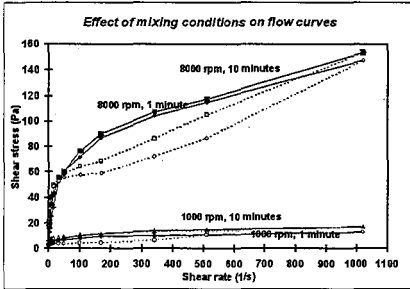


Fig.3. Shear stress vs. shear rate for 10% aqueous sepiolite gels elaborated using different mixing energies.

Fig.4. Shear stress vs. shear rate for 10% aqueous bentonite gels as a function of the pH.

This research has been financed by project AMB93-0794 (CICYT).

## References

- Chang SH, Ryan ME and Gupta RK (1993). The effect of pH, ionic strength, and temperature on the rheology and stability of aqueous clay suspensions *Rheologica Acta* 32:263-269
- Everett DH (1988). Basic principles of colloid science *Royal Society of Chemistry*, London
- Henderson CB, Scheffee RS and McHale ET (1982). Coal water slurries: A low-cost liquid fuel for boilers *Aiche meeting* 1982, Cleveland
- Kamal MK and Mutel A (1985). Rheological properties of suspensions in newtonian and non-newtonian fluids *J. Polym. Eng.* 5:293-382
- Mewis J (1985). Flow and microstructure of concentrated suspensions" *Powtech 85: Particle Technology, I. Chem. E.*, Rugby, 83-93
- Metzner AB (1985). Rheology of suspensions in polymeric liquids *J. Rheol.* 29: 739-775
- Permien T and Lagaly G (1994a). The rheological and colloidal properties of bentonite dispersions in the presence of organic compounds:I. Flow behaviour of sodium-bentonite in water-alcohol. *Clay Minerals* 29: 751-760
- Permien T and Lagaly G (1994b). The rheological and colloidal properties of bentonite dispersions in the presence of organic compounds:II. Flow behaviour of wyoming bentonite in water-alcohol. *Clay minerals* 29:761-766
- Permien T and Lagaly G (1995). The rheological and colloidal properties of bentonite dispersions in the presence of organic compounds:V. Bentonite and montmorillonite and surfactants *Clays and clay minerals* 43:229-236
- Thomas CS, Sidhar K and Rustum R (1988). Gelling properties of sepiolite versus montmorillonite *Applied Clay Sci.* 3: 165-176
- Weinberger CB and Goddard JD (1974). Extensional flow behaviour of polymer solutions and particle suspensions in a spinning motion *Intern. J. Multiphase Flow* 1: 465-486

TOLSA, S.A. Crta. Vallecas  
a Mejorada del Campo. Km.  
1,6. 28031 Madrid, España

## Technical properties of a magnesium smectite from Yuncillos

*Santarén J, Alvarez A, Gutiérrez E and Casas J*

The deposit of magnesium smectite of Yuncillos is located in the so called Madrid basin, within a strip of land parallel to the highway Madrid-Toledo, between the villages of Yuncos and Cabaña de la Sagra. The magnesium smectite is found in a lacustrine zone with a variable thickness (from 5 to 15 meters), intercalated between arkosic sands. Usually, the magnesium smectite appears at the lower part of the lacustrine episode, forming a layer with uniform thickness of 2 meters. In some places, the magnesium smectite also appears at the upper part of the lacustrine episode, although in an irregular way both in thickness as well as in continuity.

This clay material was characterized by X-ray diffraction, chemical analysis and  $^{27}\text{Al}$ -NMR.

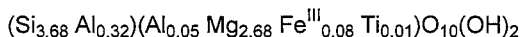
The X-ray diffraction pattern of this clay material shows that it is mostly composed by smectite (up to 95%), with minor quantities of quartz, feldspars and carbonates. The chemical composition was determined by atomic absorption spectroscopy (Table 1). The cation exchange and the BET surface area of the clay are also shown in Table 1.

Table 1. Chemical composition of the magnesium smectite

	Composition (%)
SiO <sub>2</sub>	58.00
Al <sub>2</sub> O <sub>3</sub>	4.83
Fe <sub>2</sub> O <sub>3</sub>	1.45
MgO	24.92
CaO	0.75
TiO <sub>2</sub>	0.23
Na <sub>2</sub> O	0.14
K <sub>2</sub> O	0.67
Mn <sub>2</sub> O <sub>3</sub>	0.04
Ignition loss	9.06
Total	100.07
C.E.C. (meq/100g)	78
BET surface area (m <sup>2</sup> /g)	163

The  $^{27}\text{Al}$ -NMR analysis confirms the high ratio of tetrahedral aluminum to octahedral aluminum that is about 6.

Based on the chemical composition, cation exchange capacity and NMR analysis, the following structural formula is proposed:



The technical properties of this clay material have been determined in order to evaluate its potential industrial applications. The material was studied as rheological additive for drilling muds, raw material to produce "clumping" pet litter. The catalytic activity of the magnesium smectite, the smectite exchanged with Al as well as the activity of pillared clays prepared with this magnesium smectite were also studied.

The rheological properties and absorbent characteristics as pet litter were determined on the natural clay material as well as on the clay activated with 3% and 4%  $\text{Na}_2\text{CO}_3$ . The results (Table 2) show that the optimum activation percentage is 3%, obtaining very good properties as rheological additive for drilling muds.

Table 2. Rheological properties of the magnesium smectite

	Natural magnesium smectite	Activated with 3% $\text{Na}_2\text{CO}_3$	Activated with 4% $\text{Na}_2\text{CO}_3$
Swelling volume ( $\text{cm}^3/2 \text{ g}$ )	17	45	39
Plastic viscosity (cP)	8.5	31.0	20.5
Yield at 15 cP ( $\text{m}^3/\text{ton}$ )	13.1	29.8	25.4
Mud yield (bbls/US sh. ton.)	74.6	169.4	144.3
Liquid limit	< 300	630	-

The characteristics of the magnesium smectite as an absorbent product for pet litter are summarized in Table 3. The results also show that the optimum activation percentage with  $\text{Na}_2\text{CO}_3$  is 3%.

A pillared clay was prepared using this magnesium smectite and clorhidrol commercial solutions. The chemical analysis of the pillared clay shows an increase in the aluminum oxide content to 9.79% which means an incorporation of about 5% aluminum oxide. As a consequence, the BET surface area of the clay material increased to  $250 \text{ m}^2/\text{g}$  before calcination, and to  $197 \text{ m}^2/\text{g}$  after calcination at  $350 \text{ }^\circ\text{C}$  for 3 hours. The X-ray diffraction pattern of the pillared clay shows a shift of the 001 reflection from about  $14.5 \text{ \AA}$  to  $17.54 \text{ \AA}$ .

The catalytic activity of the magnesium smectite, the smectite exchanged with Al and the pillared clay obtained from the smectite was studied using a MicroActivity Test (MAT). This MAT is a typical reaction to characterize FCC catalysts, which consists in

the cracking of gas-oil in lighter fractions as gases and gasoline, heavier fractions as heavy gas-oil, and coke as a by-product. The results are shown in Table 4.

The best conversion yield and gasoline conversion were obtained with the magnesium smectite exchanged with aluminum.

Table 3. Characteristics of the magnesium smectite as pet litter

	Natural magnesium smectite	Activated with 3% Na <sub>2</sub> CO <sub>3</sub>	Activated with 4% Na <sub>2</sub> CO <sub>3</sub>
Moisture (%)	7.5	14.7	12.7
Bulk density (g/l)	771	808	802
pH at 10%, 24 hr	9.4	10.4	10.5
Westinghouse water absorption (%) <sup>(1)</sup>	160	309	295
Westinghouse oil absorption (%) <sup>(1)</sup>	56	53	54
Clumping test <sup>(2)</sup>			
Yield in water absorption (%)	75	89	97
Consistency <sup>(3)</sup>	2	4	4
Strength test (inches) <sup>(4)</sup>	< 6	24	24

(1) Determined on a product with a standard particle distribution between 6 and 30 ASTM mesh

(2) Determined on a product with a standard particle distribution between 20 and 50 ASTM mesh

(3) Rated from 1 (minimum) to 5 (maximum)

(4) Maximum height the clumping is let to fall without breaking

Table 4. Results of the MicroActivity Test

	Natural magnesium smectite	Smectite exchanged with Al	Pillared clay
Conversion yield (%)	49.14	57.48	57.02
Gas (C <sub>1</sub> -C <sub>4</sub> )	9.59	15.32	21.80
Gasoline (C <sub>5</sub> -C <sub>12</sub> )	39.56	42.15	35.22
Gas-oil (C <sub>13</sub> -C <sub>34</sub> )	43.19	35.18	34.07
Coke	6.62	7.34	8.91
Heavy fraction	1.04	-	-

(1) Dip. di Geofisica e  
Vulcanologia. Univ. Degli  
Studi di Napoli Federico II.  
Italia

(2) Dip. di Fisica Teorica e  
Applicata. Univ di Salerno a  
Benevento, Italia

## Swelling behaviour of compacted clayey soils

*Esposito L (1) and Guadagno F M (2)*

Some of the factors affecting the swelling behaviour of clayey compacted soils are the molding water content, the compaction method and energy and, the soil type (e.g. the type of clay minerals, the base cation exchange, the specific surface, etc). In particular soil type has a significant influence because of the physical - chemical behaviour and the interparticle forces strictly depend on soil type (Sridaran et al., 1986).

When the properties of the soil and those of the electrolytes contained in pore water are kept constant, swelling pressure depends primarily on dry density and time (Sridaran et al., 1986). The aim of this work is to discuss the way in which these factors affect the swelling behaviour of four clayey soils of various areas of Southern Italy. The studied soils indicated as A, B, C and D, have similar grain - size distribution, in term of the finer fraction of the soil, but the mineralogical composition differs substantially (table 1).

Soil	Sand %	Silt %	Clay %	Montmorillonite %	Illite %	Kaolinite %
A	50	27	23	79	12	9
B	10	63	27	10	60	30
C	30	43	27	13	27	60
D	30	47	23	16	55	29

Table 1 - Granulometric and mineralogical composition of the soil tested

The difference in the larger fraction greater than 75  $\mu\text{m}$ , are not believed to affect significantly the swelling behaviour. Nagaraj (1983) showed that, if the percentage of the clayey is more than 15%, the behaviour of clay matrix is not significantly modified by the presence of a coarser fraction.

The specimens, after dynamic compaction (A.A.S.H.O. T 180), were tested both under saturated condition, defined as "standard", and unsaturated condition, that is "as compacted conditions".

This procedure consists of two stages. In the first stage, care is taken to avoid that the specimen should come into contact with water. Therefore, any existing pressure develops in presence of the molding water content as stated by Barden et al. (1970). In the second stage, the specimen is brought into contact with water. This test procedure simulates field conditions when the soil is used as construction material. In the earthworks for an earth dam construction the soil comes into contact with water only after the end of the works. Consequently, in the first period, the material which constitutes the impervious core of the dam, can exert its swelling pressure due to its molding water content.

Swelling pressures were measured using constant volume test. With this method, the specimen is placed in an odometer and its volume is kept constant throughout the test. The

maximum pressure corresponding to the equilibrium condition is assumed as swelling pressure. The equilibrium condition is reached when the measured increase of swelling pressure can be considered negligible.

In the used method, swelling pressure develops in a time interval which can be considerable and, the relationship in function of the time is non linear, as can be seen in the figura 1.

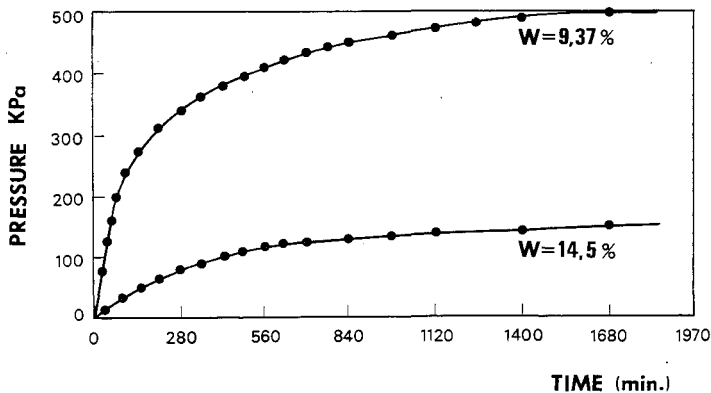


Fig. 1 - Pressure versus time for two standard specimens of soil A

The asymptotic value of the swelling pressure, can be defined by the interpolation with the rectangular hyperbole as suggested by Sridaran et al. (1986).

They stated that the relationship of swelling pressure versus time can be represented by an equation which has the form:

$$\rho_s = \frac{t}{\alpha} + \beta t \quad (1)$$

where:

- $\rho_s$  is the swelling pressure
- $t$  is the time
- $\alpha, \beta$  are the appropriate constants.

The validity of this relationship is defined if a linear interpolation is allowed between the experimental points, reported in the diagram with axes of  $t/\rho_s$  and  $t$ . Consequently the maximum value of swelling pressure can be determined by evaluating the limit of equation (1) for  $t \rightarrow \infty$ .

For the soils examined in this study, the swelling pressure is essentially function of initial dry density of samples,  $\gamma_{di}$ , while the influence of the initial water content is negligible. This dependence of  $\rho_s$  on  $\gamma_{di}$  is perfectly consistent with the double - layer theory in which pressure depends essentially on the osmotic pressure that develops between the median plane lying between two clay particles, or structural units, and bulk solution.

The differences found between the soils, with regard to the amplitude and the form of the variation of the law  $\rho_s - Y_{dl}$  are attributed to the soil characteristics (specific surface and exchangeable cations), and therefore, to the mineralogical compositions.

Barden L. and Sides G.R. (1970). *Jour. of the Soil Mech. And Found Div., A.S.C.E.*, **96** (S.M.4), 1171-1200.

Nagaraj, T. S. (1983). *Proc. Conf. On recent Devel. In Lab. And Field Test.* Bangkok

Sridaran A., Rao A.S. and Sivapullaiah (1986). *Geotec. Testing Jour.* **9**, 24-33

Dpto. Cristalografía,  
Mineralogía y Química  
Agrícola. Fac. Química,  
Univ. de Sevilla, España

## New applications for the brickmaking materials from the Bailén area, Spain

*González-Díez I, Galán E, Miras A and Aparicio P*

---

### Introduction

Tertiary clays from Bailen area have traditionally been used for manufacturing bricks and other ceramic building materials (González, et al., 1985) and their reserves are virtually unlimited, except for some clays. More than 90% of the industrial products are perforated bricks, and only two factories manufacture products of high-grade (clinker, wall tile, roofing tile and floor tile).

The aim of this work was thus to assess the most suitable potential uses of these materials on the basis of their mineralogical, chemical, and drying and forming properties. Also we propose to blend them with other minerals or rocks (kaolin, feldspar, diatomite) for making high-grade products. The quality of the new products were also studied determining the ceramic properties over the temperature range of 750-1200° C.

### Materials and Methods

Thirteen representative samples were selected from the clays used at the factories, which include raw clays and mixtures. Samples were labeled: a) 1, 2, 3, 6, 7, 9 for the raw clays, and ECG, LAG, SRG, MPG1, MPG2, MPG3, TRG for the mixtures. In order to correct the chemical and mineralogical composition of these materials a Spanish washed kaolin, commercial feldspars from Otavi, and a diatomite from Porcuna (Jaén, Spain) were used.

Samples were mineralogically characterized by XRD (bulk and < 2µm fraction), and chemically analyzed by atomic absorption spectrometry and gravimetry. Ceramic properties including grain-size distribution, plasticity, and firing properties in the range from 750 to 1200° C (linear shrinkage, water absorption capacity, bulk density, and open porosity determined according to the Spanish Normative, UNE, 61-033-75) were determined. SEM was also used to study the mineral phases formed and microstructures.

## Results and Discussion

Materials used in the factories consist of a maximum of 35% of carbonates (mainly calcite), quartz (10-45%), and some feldspars (<7%) in all the samples. Phyllosilicates accounted for 30-60 % of the overall sample weight. The clay minerals consisted essentially of illite and smectite with kaolinite in small proportions.

According to the diagrams proposed by Schmith-Reinolz and Essen-Kray (1986) and Fiori et al. (1989) chemical data indicated that such samples are appropriate for making red stoneware by pressing or by extrusion except for sample 7, which is not suitable for ceramic uses because of its high lime percentage. The composition of some samples allow the manufacturing of high-grade products (clinker, light coloured wall tile, vitrified red floor tile ) if some alumina is added. The bulk mineralogy endorses the assesment obtained from the chemistry. Clay mineralogy indicates that samples 3 and 7 are out from the theoretical composition field for bricks because of their high smectite content.

The particle-size distribution plotted on the Winkler diagram, shows that samples 6 and 7 are not appropriate for making ceramic products due to their high percentage of < 2 $\mu$ m fraction. The others fall into the field of roofing tiles ( LAG, SRG, TRG, MPG1, MPG2, MPG3) or hollow blocks (1,2,3,9, and ECG)

Concerning the plasticity, these loams are suitable for the manufacturing of ceramic bodies, except in the case of the white and red loams (samples 7 and 6).

According to these results the most suitable uses for the materials studied are suggested and in order to improve the quality (and price) of products some mixtures are proposed using regional minerals and rocks, such as diatomite, feldspar (available in Córdoba and Jaén), or any Spanish kaolin of medium-grade.

Most suitable uses for the Bailén clay materials and a proposal for new formulations are as follows:

a) Stoneware by pressing:

1) **Porous red wall tiles** : Raw materials and mixtures presently used in Bailen are suitable for making porous red wall tiles ( SRG, LAG, 1, 3, MPG3).

2) **Porous light-coloured wall tiles**: Ideal composition could be obtained by blending samples 2, ECG, LAG with kaolin in 75% / 25% ratio. These high lime bodies should show almost no firing shrinkage in the temperature range used and an open pore volume remarkably high. So, to obtain the desired properties they must be fired in a low interval of temperature (850 -900° C) because shrinkage could increase with higher firing temperatures. Samples TRG, 6 and

3) **Vitrified red floor tiles.** The most suitable mixture would be poor in carbonates ( i.e. 9 with feldspar, 80%-20%). In this case, the vitrification process is accompanied by firing shrinkage externally and by reduction of the open pore volume internally. The interval 1000-1100 °C would be the most appropriate to obtaine low porosity products and low shrinkage.

b) Stoneware by extrusion.

1) **Clinker.** Samples 1, 6 ,9, MPG2 are the most suitable because of their low carbonate content. In order to increase the firing temperature for getting a high mechanical resistance product, these samples were blended with 20% of kaolin. The best firing temperatures for these mixtures were 1050-1100° C, and porosity of the products was as low as 5%.

2) **Facing bricks and roofing tiles.** Most appropriate samples for making these products are MPG1, MPG3, and TRG, and the temperature range for firing was 850-1000° C.

3) **Lightweight bricks.** Samples 2 and 3 are appropriate clays for these products because of their particle-size distribution and lime content. Their properties can be improved by blending with diatomite (30%) and the product obtained is a low refractory insulating material.

#### REFERENCES

Fiori, C., Fabbri, B., Donati, G., and Venturi, I. 1989. Mineralogical composition of the clays bodies used in the Italian tile industry. *Applied Clay Science*, 4, 461-474.

González, I., Renedo, E., and Galán, E. 1985. Clay materials for structural clay products from the Bailen area, Southern Spain. *Symposium Clay Minerals in the Modern Society*, 77-90. Uppsala.

Schmith-Reinolz, Ch. & Essen-Kray, F. 1986. Typical raw materials for the manufacture of heavy clay products. *Interbrick*, 2, 11-15.

Instituto de Ciencias de  
Materiales. CSIC. Madrid,  
España

## Sepiolite based materials for ecological control of pesticides

*Merino J, Casal B, Ruiz-Hitzky E and Serratos J M*

---

### Introduction and Objectives

World agriculture encounters an environmental problem caused by the increasing use of agrochemical. In many cases, pesticides can act as serious contaminants with undesirable environmental and health effects. Chemical movements of organic pesticides and their ability to contaminate ground water are mainly determined by the type and strength of interaction between the pesticide molecules and the organic matter of the soils, as well as the nature of the adsorbent substrate. In this sense, the thermal and photochemical stability of the pesticides are important factors affecting the pesticide amount for use in the soils, avoiding higher rates and/or repeated applications.

This work deals with the interaction of porous clays, as sepiolite, and several herbicides which has been selected by its extensive application in sunny and warm regions. The main goal is to provide the surface character of the raw solid or their organo derivatives to control thermal and/or photolability behaviours of the adsorbed herbicides.

Previous work has been successfully developed in this sense by using 2:1 phyllosilicates, as montmorillonite (REFs), in which the organic molecules can penetrate into the interlayer space of the solid. In our case, the adsorption of the organic matter must be mainly on the external surface of the sepiolite; the study of the interaction in the proposed system (sepiolite-organic matter-herbicide) represent a new alternative in order to avoid the effect that the excess of the pesticide molecules causes in our environment.

Finally, we want to remark that the choice of sepiolite as clay substrate in this study has been considered adequate by both, its particular physico-chemical properties widely studied by our research groups and, because its abundance in our Country, which can imply at the future a new rational use to apply this mineral substrate in ecological fields.

#### **REFERENCES:**

**Brauner K. & Presinger A.**, "Structure and origin of sepiolite"(1946). *Miner. Petr. Mitt.*, **6**, 120-140 .

**Serna C., Rautureau M., Prost R., Tchoubar C., Serratosa J.M.**,(1975). "Etude de la sépiolite a l'aide des donnés de la microscopie électronique, de l'analyse thermoponderale et de la spectroscopie infrarouge", *Bull. Groupe Franç. Argiles*, **26**, 153-163

**Giles C.H., Mc Evan T.H., Nakhma S.N, Smith D.**(1960) "Studies in adsorption. Part XI. A system of classification of solution adsorption isotherms, and its use in diagnosis of adsorption mechanisms and in measurements of specific surface areas of solids.", *J. Chem. Soc.*, 3973 .

**Margulies L., Rozen H., Nir S.**,(1988) " Model for competitive adsorption of organic cations on clays", *Clays and Clay Minerals*, **36**, 270 .

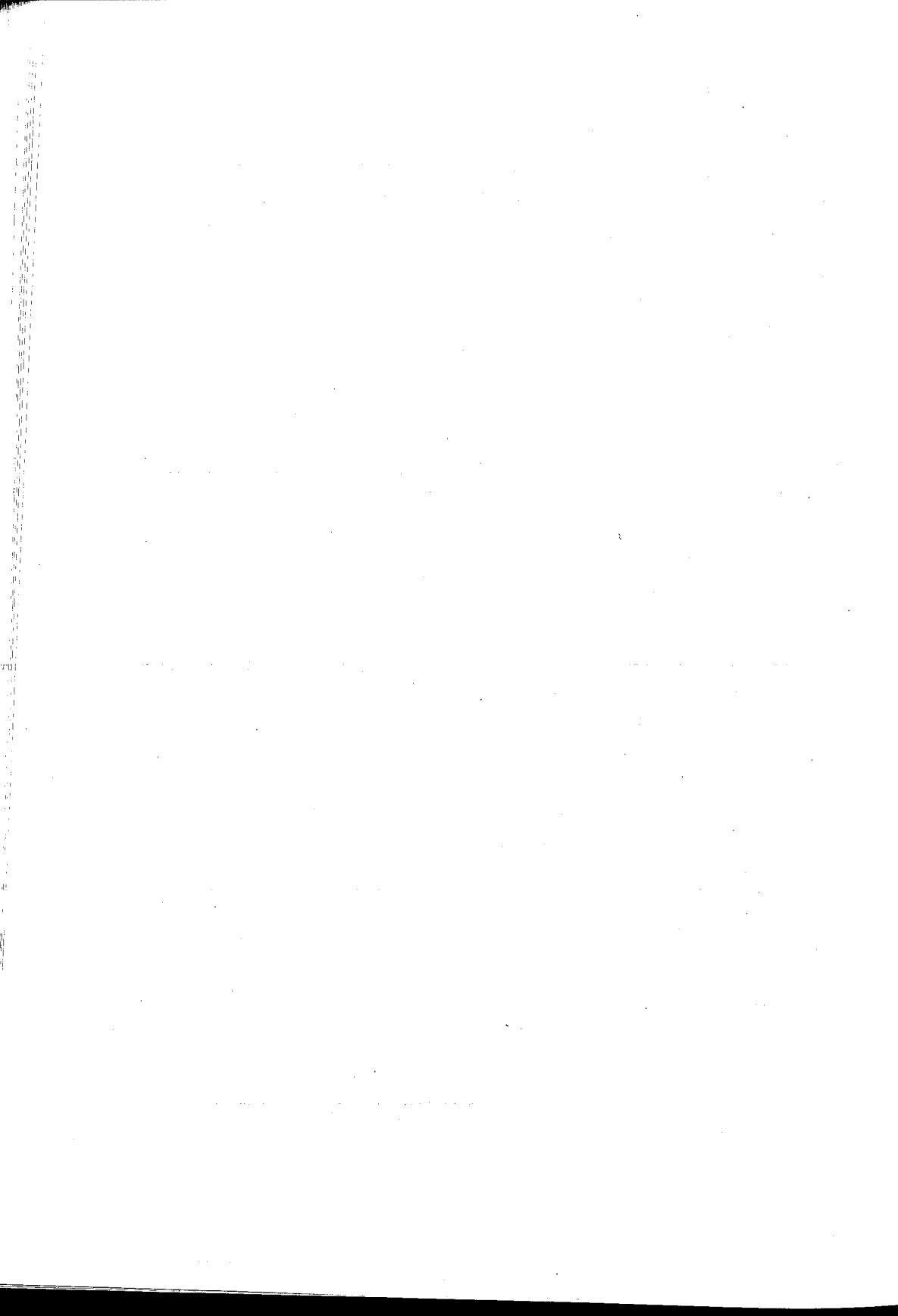
**Ahlich J.L., Serna C., Serratosa J.M.**(1975). "Structural hydroxyl in sepiolites", *Clays and Clays Minerals*, **23**, 119-124

**Aznar J.A., Casal B., Ruiz-Hitzky E., Lopez-Arbeloa I., Lopez-Arbeloa F., Santaren J., Alvarez A.**,(1992) "Adsorption of methylene blue on sepiolite gels:spectroscopic and rheological studies.", *Clay Minerals*, **27**, 101 .

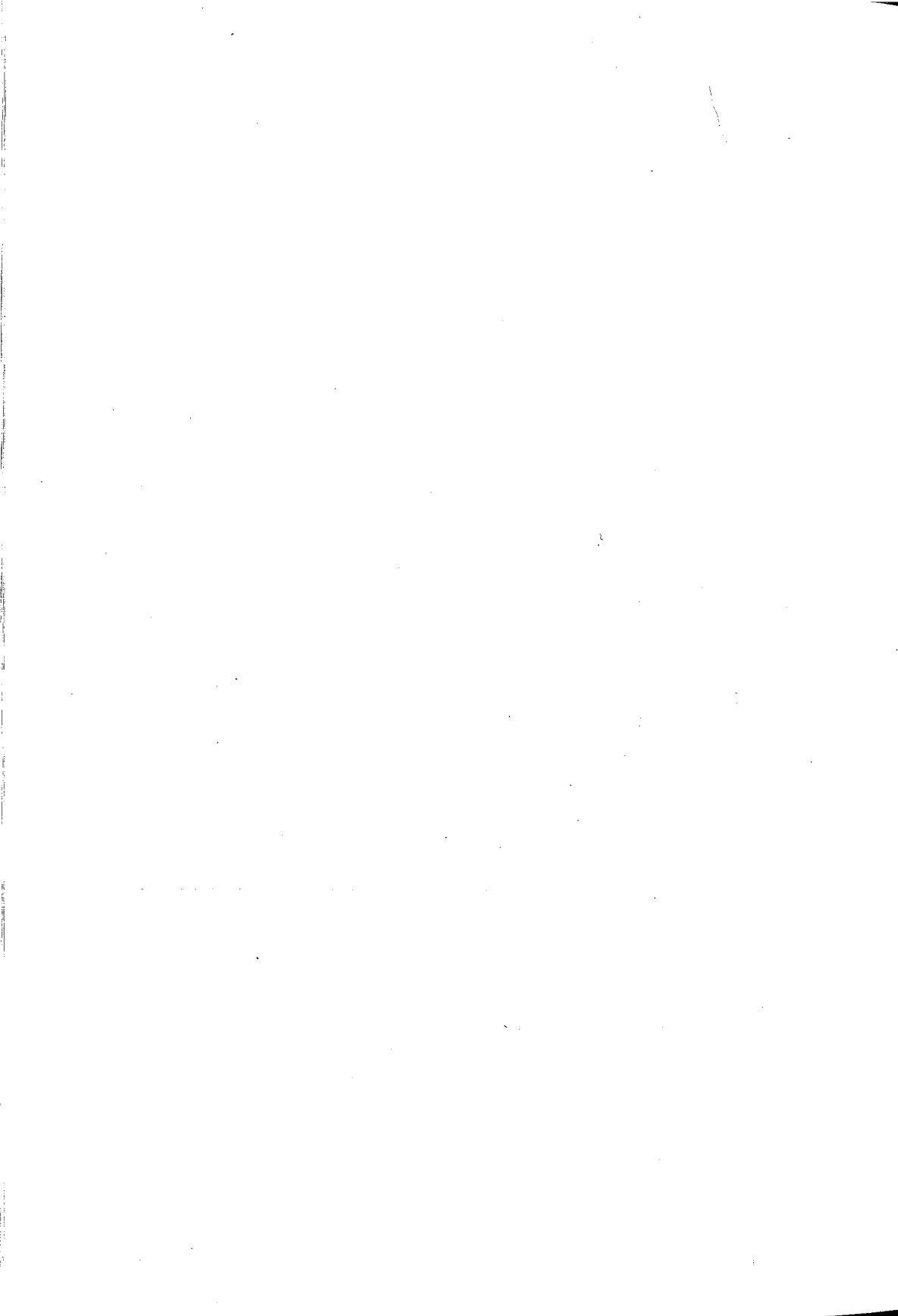
**Cenens J., Schoonheydt R.A.**,(1988) "Visible Spectra of Methylene blue on Hectorite, Laponite B and Barasym in aqueous suspension", *Clays and Clay Miner.*, **36**, 214-224 .

**Margulies L.; Rozen H.; Cohen E.** ( 1985) " Energy transfer at the surface of clays and protection of pesticides for photodegradation" *Nature*, **315**, 658-659 N.

**Nir, S.; Rytwo,G.; Yermiyahu,U.; Margulies,L.**, (1994), "A model for cation adsorption to clays and membranes" , *Colloid Polym.Sci.*, **272**, 619-632.



ANCIENT CERAMIC  
AND ARCHEOMETRY



## Proposal of a non destructive analytical method by SEM-EDS to discriminate Mediterranean obsidian sources

Acquafredda P, Andriani T, Lorenzoni S and Zanettin E

### INTRODUCTION

The identification of the source areas of obsidians used for ancient artefacts gives information about cultural and social relationships of people as well as trade routes. Several physical and chemical methods have been proposed to solve the problem of the source area of obsidians (e.g. Aspinall *et al.*, 1972; Bigazzi & Bonadonna, 1973; Game, 1945; Stevenson *et al.*, 1971). Most of these methods, however, are destructive.

In this work we propose to discriminate obsidians from different source areas by non destructive analyses. We set up a method using an Energy Dispersive Spectrometer linked to a Scanning Electron Microscope, which produces precise data and, in addition, it's non-destructive, quick, and can be used for samples in a very wide range of size: from few micrometers to 15 centimeters.

Using this method we were able to discriminate obsidians from the six major Mediterranean obsidian sources, that are: Gyalì, Melos, Pantelleria, Lipari, Mt. Arci (Sardinia), Palmarola.

### ANALYTICAL METHODS

Obsidian is a volcanic rock which consists of glass and microphenocrysts. SEM-EDS method represents a powerful tool to analyse both glass and phenocrysts.

As glass has quite homogeneous composition in the same sample, the analysis (major and minor elements), performed in several points of the glass, gives its average composition. Glass mean composition varies in obsidians of different provenance allowing different obsidian samples to be discriminated (Fig.1).

Samples were analyzed, after cleaning by absolute alcohol in an ultrasonic bath and after coating natural surface with carbon. The carbon film is removable by ultrasonic treatment, washing the specimen in absolute alcohol or acetone: this is particularly important when artefacts are analysed.

The microanalyses were performed with a S 360 Cambridge SEM coupled with a Link AN 10000 ED Specrometer (Dipartimento Geomineralogico - CNR Chimica dei Plasmi, Bari). The X-ray intensities were converted in wt.% of oxides using a ZAF4/FLS Link Analytical software support.

The analyses were carried out on the same rock either on polished thin sections or on raw surfaces. In the latter case analyses were performed on very small and flat surfaces thus, the errors related to different geometry between the standardization of the spectrometer and the microanalyses of the obsidians are negligible: the data obtained on the polished thin section (open markers) and on the raw surface (closed markers) are comparable (Fig. 1).

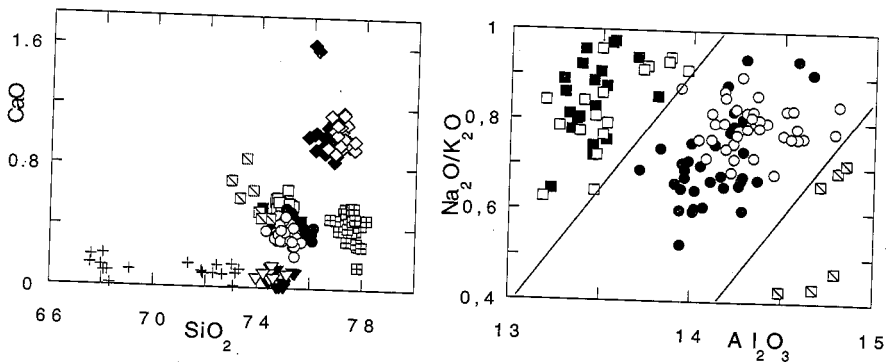


Fig. 1: Diagrams of major chemical elements of the obsidian glass (open symbols: polished thin sections; closed symbols: raw surfaces). Square with cross: Gyali samples; Cross: Pantelleria samples; Square: Lipari samples; Circle: Archi Western side samples; Square with diagonal: Archi Eastern side samples; Triangle: Palmarola samples.

Tab. 1: SEM-EDS microanalyses, on thin sections and on raw surfaces, of obsidian glass.

	Gyali (n=38)		Melos 1 (n=42)		Melos 2 (n=2)	Pant. (B.A.) (n=8)		Pant.(S.V.) (n=11)	
	$\bar{x}$	$\sigma$	$\bar{x}$	$\sigma$	$\bar{x}$	$\bar{x}$	$\sigma$	$\bar{x}$	$\sigma$
SiO <sub>2</sub>	77.50	0.28	76.90	0.41	76.13	68.10	0.47	72.45	0.66
TiO <sub>2</sub>	0.17	0.06	0.16	0.07	0.16	0.69	0.09	0.23	0.06
Al <sub>2</sub> O <sub>3</sub>	12.55	0.15	13.67	0.22	13.41	0.89	0.80	8.20	0.20
FeO	0.82	0.14	0.59	0.13	1.28	8.35	1.19	7.67	0.36
CaO	0.43	0.08	1.00	0.08	1.60	0.13	0.06	0.10	0.04
Na <sub>2</sub> O	3.79	0.63	4.37	0.48	4.05	6.48	1.02	6.85	0.77
K <sub>2</sub> O	4.73	0.53	3.33	0.13	3.37	4.98	0.40	4.20	0.04

	Lipari (n=40)		M.te Archi (W) (n=73)		M.te Archi (E) (n=7)		Palmarola (n=18)	
	$\bar{x}$	$\sigma$	$\bar{x}$	$\sigma$	$\bar{x}$	$\sigma$	$\bar{x}$	$\sigma$
SiO <sub>2</sub>	75.00	0.26	75.26	0.36	73.76	0.52	74.77	0.39
TiO <sub>2</sub>	0.07	0.06	0.10	0.06	0.32	0.07	0.11	0.07
Al <sub>2</sub> O <sub>3</sub>	13.49	0.20	14.23	0.22	14.78	0.21	13.95	0.23
FeO	1.41	0.15	1.11	0.11	0.99	0.24	0.89	0.10
CaO	0.51	0.06	0.38	0.06	0.60	0.14	0.06	0.04
Na <sub>2</sub> O	4.36	0.35	3.83	0.34	3.50	0.54	5.27	0.39
K <sub>2</sub> O	5.15	0.29	5.01	0.16	6.05	0.60	4.95	0.19

## RESULTS AND CONCLUSIONS

SEM-EDS analysis points out a different chemical mean composition of the glass in each of the analyzed populations (Tab.1). In fact, glass composition is also related with the amount and species of microphenocrysts.

In particular Lipari obsidian is characterized by pyroxene (diopside) in synneusis with magnetite microphenocrysts; M.te Arci's samples are so rich in K-feldspars and biotite microphenocrysts that they cannot be considered obsidians s.s. but glassy rhyolites; Gyalì obsidians, instead, present few or no microphenocrysts.

Among various diagrams CaO vs. SiO<sub>2</sub>, and Na<sub>2</sub>O/K<sub>2</sub>O vs. Al<sub>2</sub>O<sub>3</sub> diagrams (Fig.1) discriminate the obsidians of these six islands. Furthermore two different populations can be identified among obsidians of Melos (Melos 1 and 2), Pantelleria (Bagno dell'Acqua - Salto la Vecchia), and Mt.Arci (Western and Eastern side of the mountain).

The main results of our work are as follows. SEM-EDS analyses show different chemical composition for obsidian from Gyalì, Melos, Pantelleria, Lipari, Mt.Arci, Palmarola. The discrimination of obsidian from the six islands is possible on the basis of major elements (e.g. Fig. 1). Analyses performed on obsidian microphenocrysts also demonstrate their different nature and stress the discrimination.

The SEM-EDS analytical method proposed is an important tool for archaeometrical purposes because it reliably allows to recognize non destructively the provenance of the raw material used in obsidian artefacts.

## SELECTED REFERENCES

- Aspinall A, Feather S W & Renfrew C (1972). *Nature* **237**, 333-334.  
Bigazzi G & Bonadonna F (1973). *Nature* **242**, 322-323.  
Game P M (1945). *Trans R. Soc. Afric.* **30**, 271-409.  
Stevenson D P , Stross F H & Heizer R F (1971). *Archaeometry* **13**, 17-25.

(1) Dip. di Scienze della  
Terra. Univ. "La Sapienza"  
di Roma, Italia

(2) Dpto. Prehistoria,  
Historia Antigua i  
Arqueologia. Univ. Central  
de Barcelona, España

## Magnetometric investigation of the archaeological site of Arva (Seville, Spain)

*Burrigato F (1), Di Filippo M (1), Grubessi O (1), Remesal J (2) and  
Toro B (1)*

### Introduction

A program of magnetic measurement was conducted near the archaeological site of the Roman city of Arva (Sevilla, Spain). The program was expected to identify kilns anciently used for baking of olive oil amphorae. A total of 1750 differential magnetic measurements were carried out in the area which extends from the Roman city of Arva to the banks of the Guadalquivir river.

### Magnetometric investigation

The magnetic method was selected because of its sensitivity to bricks and ware. The magnetometer, used in differential mode, can detect magneto-sensitive objects in the more superficial of the subsoil. The prospecting program was targeted to: i) monitor and adjust the performance of the method in the proximity of two already-known kilns for amphorae baking; and ii) identify archaeological objects not yet exposed by excavations.

In archaeology, determination of the geomagnetic field has a paramount importance, as ware, ceramics and kilns are capable of recording the geomagnetic field of upon cooling. During this process, ceramics and their fragments are generally removed from their original position. By contrast, the bricks of the kilns remain in their original position, thereby recording the geomagnetic field at the time of the last baking cycle.

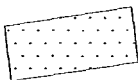
Magnetometric prospecting relied on a Scintrex Geometric G856 proton magnetometer, capable of measuring and storing the total intensity value of the magnetic field via two sensors, which were spaced about 0.5 m from each other. The other sensor was kept 1.3 m below ground level. The measurements were made with a 1 m pitch, along N 245° azimuth profiles, and spaced 1 m from each other.

As a result, the differential magnetic field map shows at least 5 areas with similar gradients, which are likely to reflect as many buried kilns.

JUNTA DE ANDALUCIA  
 CONSEJERIA DE CULTURA  
 DELEGACION PROVINCIAL DE SEVILLA  
 ZONA ARQUEOLOGICA DE ARVA

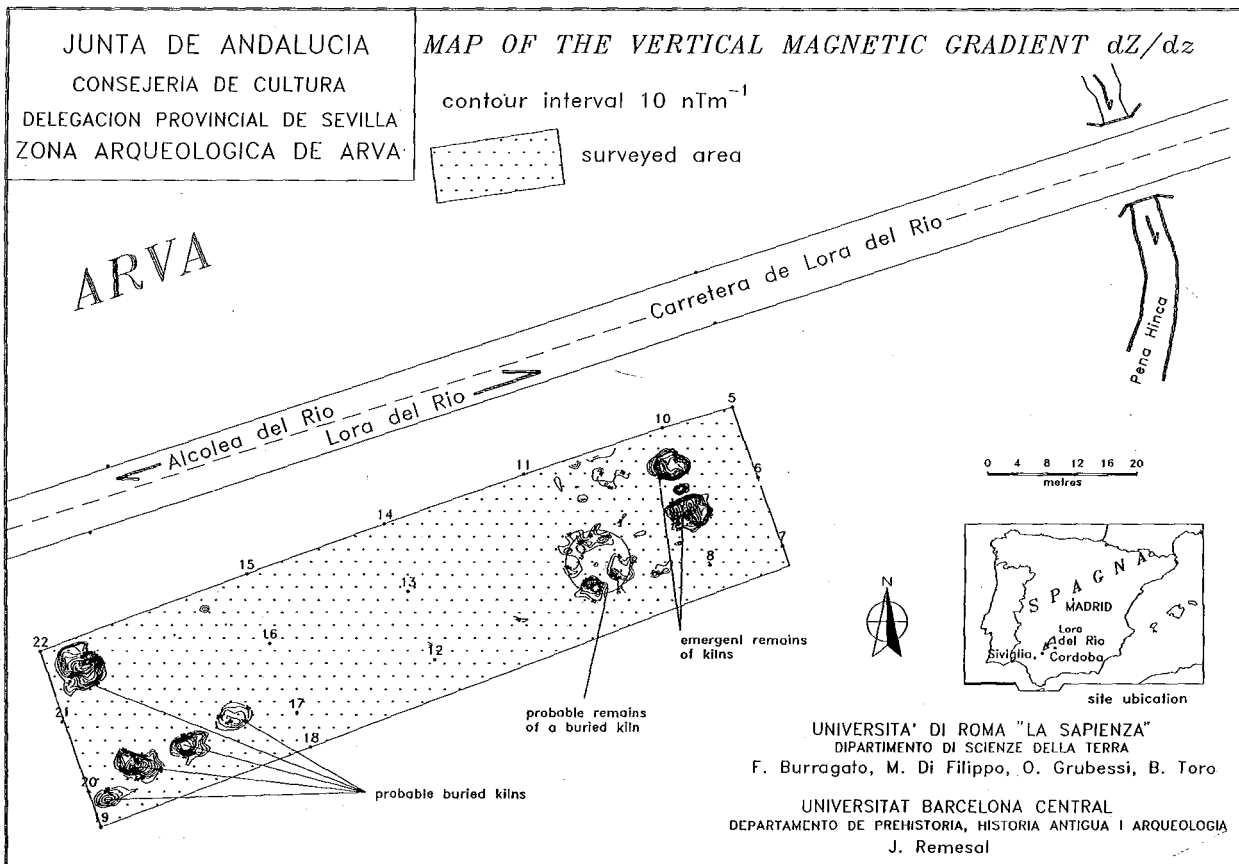
MAP OF THE VERTICAL MAGNETIC GRADIENT  $dZ/dz$

contour interval  $10 \text{ nTm}^{-1}$



surveyed area

ARVA



UNIVERSITA' DI ROMA "LA SAPIENZA"  
 DIPARTIMENTO DI SCIENZE DELLA TERRA  
 F. Burrigato, M. Di Filippo, O. Grubessi, B. Toro

UNIVERSITAT BARCELONA CENTRAL  
 DEPARTAMENTO DE PREHISTORIA, HISTORIA ANTIGUA I ARQUEOLOGIA  
 J. Remesal

(1) Dip. di Scienze della  
Terra. Univ. di Pavia, Italia

(2) C.G.S.-Centro Grandi  
Strumenti Univ. di Pavia,  
Italia

## The "Cotto Variegato": a case-study of XVII century tiles. Some archeometric implications

Cairo A (1), Duminuco P (1), Riccardi M P (2), Setti M (1), Soggetti F (1) and Messiga B (1)

The aim of this study is to establish bulk composition and firing temperature of tiles (Cotto Variegato), constituting the floor of "Chiesa del Cristo", in order to get information on ancient technologies to obtain similar potter-tiles for restoration purposes. The tiles display folded bands of whitish (thicker) and reddish (thinner) potters, this has suggested a correlation between the production techniques and the criteria used in structural geology to explain the rock ductile deformation (Ramsay & Huber, 1987).

Besides the colour differences, the two parts have also different mineralogical composition when analysed under optical microscope, by X-ray diffraction (XRD), X-ray fluorescence (XRF) and scanning electron microscope (SEM) coupled with WDS system. The results show that different raw-materials were used to manufacture the tiles: whitish and reddish portions developed distinct mineral assemblages during firing. The kiln temperatures have been estimated integrating "in situ" microstructural and microanalytical "bulk" data.

The reddish assemblages (Fig. 1) is composed of quartz + K-feldspars + Na, Ca - feldspars + diopside + hematite; the whitish portion is composed of quartz + K-feldspars + Na, Ca - feldspars + diopside + hematite (tr) + calcite. XRF analysis shows that the chemical composition (Tab. 1) of different parts can be plotted in two different fields of the ternary ceramic phase diagram ACS ( $\text{SiO}_2\text{-CaO-Al}_2\text{O}_3$ ). Remarkable differences between raw materials are evidenced by "bulk" chemical composition and mineral assemblages. Reddish portion (Ca-poor clay) plots within the quartz-anorthite-mullite area, whereas the whitish one (Ca-rich clay) is in the quartz-anorthite-wollastonite sub triangles (Fig. 2). In the Ca-rich portion, the firing temperature was higher than 800°C, as indicated by the growth of plagioclase-diopside associations, in presence of quartz. On the other hand the absence of mullite in the reddish portion indicates that the temperature does not exceed 1100°C according to Letsch & Noll (1983), Heimann (1989). Owing to the presence of hematite indicates an oxidizing kiln atmosphere. This prevents a more precise kiln temperature estimation, since

the stability field of wollastonite resulus enlarged towards lower temperature. Firing also induced some textural changes. Firing related microtexture, observed under Electronic Microscope indicate that sintering phenomena are dominated by the presence of reaction rims (coronas) along the melt-temper boundaries. Microprobe analysis of corona-forming minerals evidence that firing mineral and temper clast compositions are closely related. Feldspars display a wide miscibility between K, Na and Ca end members.

## References

- Ramsay JG & Huber MI (1987): The techniques of Modern Structural Geology, vol. 2. Academic Press, London.
- Letsch J & Noll W (1983): N. Jb. Mineral. Abh., 147: 109.
- Heimann RB (1989): Archeomaterials 3: 123.

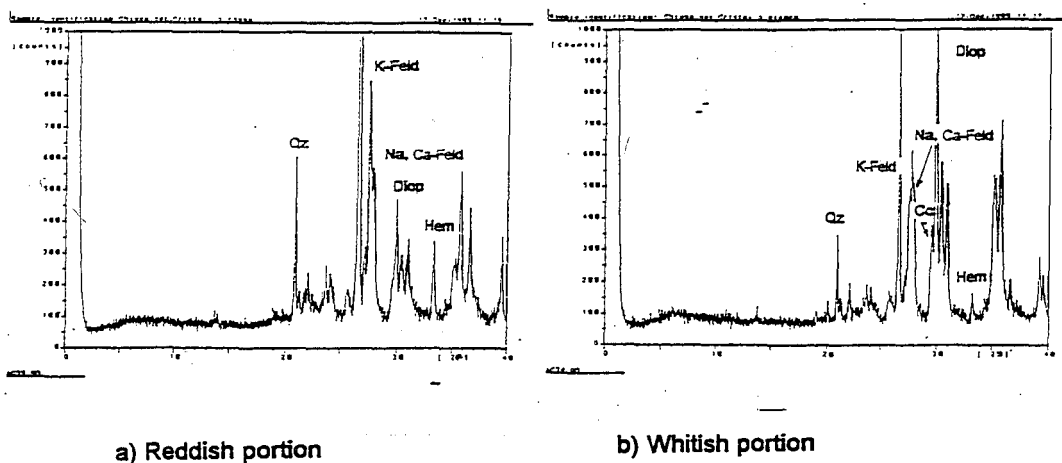


Fig. 1 - Mineral assemblages

WT%	T.V.C.	P.B.C.	P.R.C.
SiO <sub>2</sub>	47.56	47.56	53.03
TiO <sub>2</sub>	0.56	0.51	0.66
Al <sub>2</sub> O <sub>3</sub>	12.81	12.12	14.34
Fe <sub>2</sub> O <sub>3</sub>	5.68	5.39	6.31
MnO	0.20	0.21	0.19
MgO	11.74	12.95	11.25
CaO	11.78	13.20	5.97
Na <sub>2</sub> O	1.07	1.08	1.20
K <sub>2</sub> O	1.86	1.53	2.00
P <sub>2</sub> O <sub>5</sub>	0.11	0.11	0.10
LOI	6.63	7.15	4.95

Tab. 1 - Oxides distribution: T.V.C.: tout venant; P.B.C. and P.R.C.: whitish and reddish portion

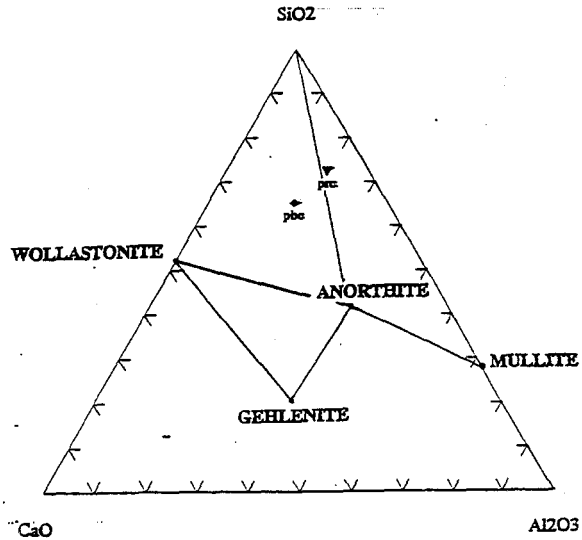


Fig. 2 - Diagram ACS of different portions: P.R.C.) Reddish; P.B.C.) Whitish

(1) Dip. di Scienze della  
Terra. Univ. di Pavia, Italia

(2) Dip. di Chimica  
Generale. Univ. di Pavia,  
Italia

## Mineralogical and geochemical characterization of clay deposits (Pavia area, northern Italy): inferences of provenance on restoring ancient artifacts

*Cairo A (1), Genova N (2), Meloni S (2), Oddone M (2) and Setti M (1)*

The study of ceramics and bricks can give a substantial contribute to the characterization of mixtures, technologies, kiln conditions and firing temperature, but a great open problem is the individuation of the provenance of raw materials. The aim of this work is to establish some mineralogical, geochemical and physical parameters, that allow to solve such problem. The archeological area "Villa Maria" at Lomello (Pavia) in which has been sampled for clays, sands and artifacts. The artifacts bricks, roofing tiles, etc.), of roman origin were employed during Middle Ages in the building of town-walls, courts and many other constructions. All samples were subjected to bulk and "in situ" analysis to obtain a model for compare the actual soil deposits to the ancient ceramics. There are some geochemical anomalies (REE and trace elements) and mineralogical variations (firing minerals as diopside, gehlenite, hematite) connected to the firing temperature and to the mineralogical-chemical Characteristics of sampled clays.

The methodologies of study are essentially based on mineralogical analysis by X-ray diffraction (XRD), petrographic microscopy, Scanning Electron Microscopy (SEM) with system coupled WDS (Wavelength dispersive system), and chemical analysis by X-ray fluorescence (XRF) and Instrumental Neutron Activation Analysis INAA).

Clays and sands have been sampled around the archaeological excavation sites and further trasformed in small bricks, dried at 75 °C and then fired AT 950 °C with the aim to obtain data representing end members of geochemical and mineralogical behaviour of green and fired materials. The NEXT step was the detection with SEM-WDS and XRD of the variations induced by firing on raw materials, and the connection beetwen mineral assemblages and chemical composition of clays. Ca-rich and Ca-poor clays rise to different minerals (Cairo et al. in this Meeting). Data obtained on raw materials were compared with the ancient roman artifacts to verify possible correlation between mineral assemblages and chemical composition of clays. Ca-rich and Ca-poor clays rise to different minerals (Cairo et al. in this Meeting). Data obtained on raw materials were compared with the ancient roman artifacts to verify possible correlation between actual raw material and ancient artifacts in the individuation of provenance areas of original materials employed in the manufacture of the moderm and ancient artifacts.

(1) Museo Archeologico Nazionale "D. Ridola", Matera, Italia

(2) Dip. Geomineralogico. Univ. di Bari, Italia

## Archaeometric investigations of the "ceramiche a figure rosse" of Dario's painter (IV cent. b.C) coming from Timmari

*Canosa M (1), Lacarbonara F (2), Laviano R (2), Lorenzoni S (2) and Acquafredda P (2)*

Timmari is a wide hill, on the left slope of the Bradano river of which dominates the middle valley. It is been frequented by the man for a long period that goes from the Neolithic age up to Middle Ages.

During the IV cent. B.C. the built up area achieved the maximum expansion and his greatest economic prosperity, attested by the discovery of funeral kits of great quantity and value.

Particularly, the only tomb of the IV cent. B.C., that was discovered intact, gave back a grave kit of exceptional affluence and importance which many vessels, attributed to the Dario painter, were present in. Conventional name of this painter comes from a big crater (discovered in Canosa and safeguarded in the National Museum of Naples), on which it has represented Dario Persian's King. Dario's painter is biggest ceramist in Apulia in the 2nd half of the IV cent. B.C..

In the present work seven fragments of ceramic coming from four different vessels with imagery redheads decorations have been studied. The petrographic, mineralogical and chemical investigations demonstrate an accentuated homogeneity of all the finds.

The matrix is abundant (average = 85%) and not resolvable to the microscope; the tempering is constituted by grain, with 0,025 mm of diameter, of quartz, feldspars, micas and ore minerals. The rock fragments are rare and lightly bigger, all of them of likely metamorphic and magmatic origin. The pores are of isooriented and lengthened shape in the walls of the vessels samples, roundish in those which constitute the bottom of vessels. The calcite is secondary and it crusts or obstructs pores.

The textural characteristics are the uniformity of the grain size, the homogeneity of the distribution of the grain, the micas and pores isoorientation.

The diffrattometric analysis has emphasized that the mineralogical association is constituted by quartz (Q) + feldspars (Feld) + pyroxenes (Px) + calcite (Ca) + gehlenite (Geh) + hematite (He) + clay minerals (CM) (Tab. 1). The pottery samples have been heated to 1000°C for 12 hours to evidence other phase transformations. Tab. 1 shows only the disappear of calcite, clay mineral and gehlenite while there is an increase of plagioclases, as regards to K-feldspars (due to gehlenite-anorthite transformation), and of hematite. It is in accordance with a oxidizing heating temperatures among 900° and 1000°C (Maggetti, 1981; Letsch & Noll, 1983).

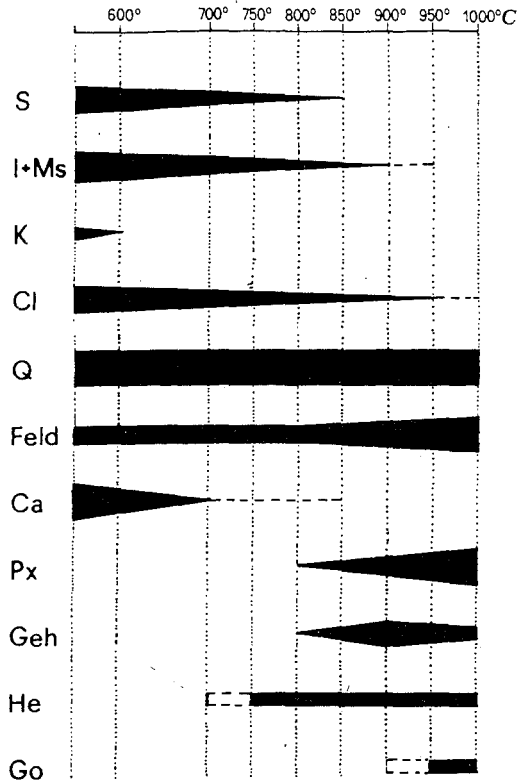


Fig. 1: phase transformation during heating temperature.

These Subappennine clays have been heated from 600°C to 1000°C, with step of 50°C; results, synthesised in Fig. 1 (S = smectite; I+Ms = illite+muscovite; K = kaolinite; Cl = chlorite; Go = goethite; other symbols as in Tab.1), are in accordance with those suggested from Maggetti (1981), while they are lightly at variance with those of Letsch & Noll (1983).

#### REFERENCES

- Letsch J & Noll W (1983). *Ber. Dt. Keram. Ges.*, 7, 259-267.  
 Maggetti M (1981). *British Museum, Occ. Papers*, 19, 33-49.

Tab. 1: mineralogical composition of normal and heat treated sherds

	Q	Feld	Px	Ca	Geh	He	CM
TM3A	xxxx	xxx	xxx	x	x	x	x
1.000°C	xxxx	xxxx	xxx	-	-	xxx	-
TM3B	xxxx	xxx	xxx	x	xxx	xx	x
1000°C	xxxx	xxxx	xxx	-	-	xxx	-
TM5	xxxx	xxx	xxx	x	x	xx	x
1000°C	xxxx	xxxx	xxx	-	-	xxx	-
TM6A	xxxx	xxx	xxx	xx	x	x	x
1000°C	xxxx	xxxx	xxx	-	x	xxx	-
TM6B	xxxx	xxx	xx	x	x	x	x
1000°C	xxxx	xxxx	xxx	-	-	xx	-
TM7A	xxxx	xxx	xxx	x	x	xx	x
1000°C	xxxx	xxxx	xxx	-	-	xx	-
TM7B	xxxx	xxx	xxx	x	x	x	x
1000°C	xxxx	xxxx	xxx	-	-	xxx	-

The chemical data are extraordinarily uniform for both major oxide and trace elements (Tab. 2) and point out a composition of rich ceramics of Ca to the limit of poor ceramics of Ca.

The results show same raw materials for all the ceramics in evidence, a very refined purification that has brought uniform temper, a very long processing and of excellent execution modelling and, finally, a cooking to temperatures between 900° and 1000°C in surrounding oxidiser.

Tab. 2: average chemical composition of the examined sherds (n=7)

(wt.%)	SiO <sub>2</sub>	TiO <sub>2</sub>	Al <sub>2</sub> O <sub>3</sub>	Fe <sub>2</sub> O <sub>3</sub>	MnO	MgO	CaO	Na <sub>2</sub> O	K <sub>2</sub> O	P <sub>2</sub> O <sub>5</sub>	LOI
Average	55.66	0.92	17.87	8.12	0.12	2.86	9.85	0.71	2.44	0.18	1.26
σ	0.24	0.01	0.10	0.06	0.01	0.05	0.39	0.02	0.07	0.02	0.35
(ppm)	Ba	Rb	Sr	Y	Zr	Nb	V	Cr	Ni	La	Ce
Average	324	134	300	28	163	22	135	140	68	50	88
σ	19	2	11	2	8	1	6	1	1	2	3

Some clays belonging to the "Formation of the Argille subappennine" (Plio-Pleistocene age), cropping out in the Bradanic trough, have been analysed to reconstruct the raw materials used for manufacturing pottery. The mineralogical and chemical data of the clayey, silty and sandy fractions are consistent with the hypothesis that "Argille subappennine" are the raw materials and after a strong purification they were used to realize the studied vessels.

(1) Dpto. Prehistoria y  
Arqueología, Univ. de  
Granada, España.

(2) Estación Experimental del  
Zaidín. CSIC. Granada,  
España

## Influence of the medium of deposit in the alteration of ceramic materials

*Capel J (1), Linares J (2), Huertas F (2), Nájera T (1) and Molina F (1)*

---

### Introduction

One of the problems encountered in the study of ceramic materials of archaeological origin is to identify the degree to which the sedimentary medium in which they are buried contributes to the alteration of the original characteristics possessed by the ceramic when it was made. Difficult in identifying these alteration processes results in research on this subject being relatively limited and with inconclusive results.

For the purposes of the present research, a set of ceramic vessels from Motilla de los Palacios was selected. This site belongs culturally to the Bronze Age with a chronology between 1650-1300 BC. (Nájera, 1984). Geographically, Motilla de los Palacios is located in the municipality of Almagro, Province of Ciudad Real, Central Spain.

The Motilla of los Palacios is a conical, almost table-like, mound 11 metres in height and some 100 metres in diameter. Excavation of the site (Nájera, 1977) has confirmed the existence of a fortification which constitutes the central monticule of the Motilla. A Bronze Age settlement, linked to the Motilla, has been identified nearby. The stratigraphic sequence obtained has confirmed the existence of thirteen superimposed building levels of which the lower eleven belong to the Bronze Age whereas the upper two are associated with Ibero-Roman settlement. These Ibero-Roman phases have prevented the sedimentary context in which the ceramic materials were deposited in the prehistoric era from being altered by subsequent soil movements produced either by human or climatic agency.

These characteristics converted this site into an ideal one for determining whether the medium of deposit in which the sets of ceramic vessels were found influenced the sherds by altering the characteristics they possessed at the time of manufacture.

## Material and Methods

The material selected consisted of 26 ceramic fragments belonging to the Main Bronze Age ( Complexes I, II and III ) and three coming from Iberian levels.

Given the research aim of identifying possible changes that burial had conferred on the ceramic materials, a sample with the following variables was chosen :

- Differing manufacturing techniques.
- Different depths of location.
- Ceramic shapes whose formal characteristics implied that they were not employed as cooking vessels, the aim being clearly to determine the influence of the sediment on the materials.

Method employed was : R-X diffraction (Mineralogical study of the whole sample and the 2 micron minor fraction). Physio-chemical tests : Hygroscopicity ;  $H_2O^+$  and  $H_2O^-$  ; pH ; Microscopic petrography : Thin Section study of the selected sample.

## Results and Discussion

The bulk mineralogical study enabled the presence of high-temperature phases, diopside, wollastonite and gehlenite to be confirmed in the ceramic samples, though the calcite content was very low ( between 1% and 6% ). For a group of samples whose quantities vary between 15% and 24% it was possible to confirm the secondary character of the same by Thin Section study. The presence of high temperature phases and the virtual absence of primary calcite enabled firing temperatures of between 800 and 900 degrees Celsius to be established ( Capel, 1985). These values are consistent with the highest oven temperatures employed for ceramics during the Iberian period. The Bronze Age ceramic samples show values consistently around 800-850 degrees Celsius. The presence of mixed-layers, whose content ranged from 2% to 19% , was

established for all the samples as were variations in the crystal-size of the illite, between 88 Å and 382 Å. The absence of Smectite should be stressed.

The values established for  $H_2O^+$  and  $H_2O^-$  were between 0.06 - 8.36 for structural water and between 0.91 - 3.32 for hydration water.

The Thin Section petrographic demonstrated the existence of different degrees of iron-loss from the clay matrix, as well as the homogeneous nature of the material employed for fabrication of the ceramic vessels.

It is observed that the samples which present a higher structural water content or Illite crystal-size correspond to those found close to the surface, or at greater depth near the water table. The same goes for those samples with a higher mixed-layer content.

Therefore, the analytical results of the ceramic materials studied favour the conclusion that the transformations detected in the clay matrix are due to conditions in the medium of deposit since the samples which manifest greater alteration are those which were exposed to greater contact either with water from precipitation or with-logged layers.

The Thin Layer study corroborates these data, since the degree of iron-loss manifest by the samples studied is homogeneous to the whole matrix, being more intense in samples found close to the surface or in the zone of contact with the freatic levels upon which the site is located. The form of presentation of iron oxides in these samples contrasts with that found in previous work carried out to study the functionality of ceramic vessels, and in which standard ceramic types were produced and then modified in the laboratory so as compare them with ceramics of archaeological origin. That research concluded that Fe-oxides associated with functionality did not display a homogeneous distribution but formed bands which were more intense in zones close to the interior wall of the ceramic vessel concerned.

## References

- Capel, J., Huertas, F. & Linares, J. (1985). Clays and Clay Minerals. XXIX - A, 563-575  
Nájera, T. & Molina, F. (1977). CPUGR. 2, 251-301  
Nájera Colino, T. (1984). Thesis Dissertation, 458

CNR-IRTEC, Istituto di  
Ricerche Tecnologiche per la  
Ceramica, Faenza, Italia

## Application of SEM/EDS analysis for studying ceramic materials of archaeological interest

Fabbri B

### Objective

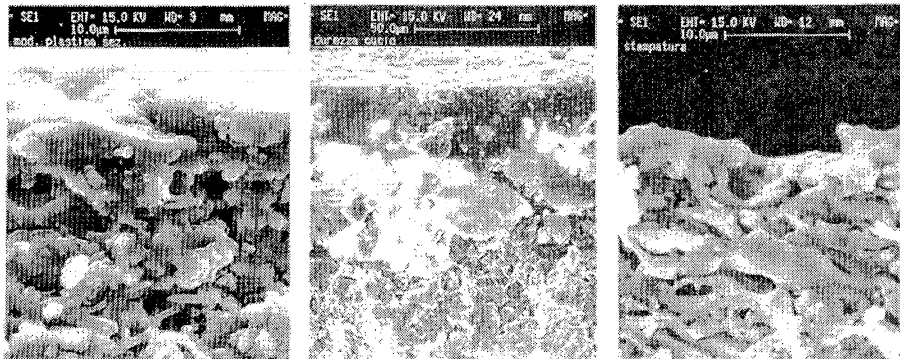
The aim of this paper is to describe some special examples of how to use SEM/EDS analysis for studying archaeological ceramics.

Classical ceramics can be defined as "inorganic non metallic materials, obtained from mineral substances, cold shaped and irreversibly hardened by firing". In case of archaeological ceramics, however, a lot of different alteration and degradation states could occur. As a consequence, SEM/EDS analysis can be applied to ancient ceramic materials for the definition of technological aspects and alteration phenomena as well.

### Technological characteristics

#### Inclusions

The chemical and dimensional characteristics of inclusions in coarse bodies can be analysed by elemental distribution maps. In such a way, the correlation among the distribution of the different chemical elements will result evident and the grain size range as well.



A

B

C

Figure 1 - SEM micrographs of different shaping or surface finishing techniques

### Shaping technique

SEM observations can help us to distinguish surfaces obtained with different technique, because of the presence and thickness of a surface layer of compact structure (figure 1):

- a) manual shaping and finishing of the object at plastic state = presence of a very thin layer;
- b) manual shaping at plastic state with finishing at leather-like state = presence of a big layer;
- c) moulding at plastic state = no presence of a surface layer.

### Defects in the coating layer

It is usual to recognize air bubbles and undissolved quartz crystals (figure 2); these marks can be used as provenance tracers together with chemical compositions determined by SEM/EDS.

### Firing temperature

A relative evaluation of the firing temperature can be obtained by comparing the vitrification state, for example in the case of slip decoration layers (figure 3): the higher the vitrification state the higher the firing temperature.

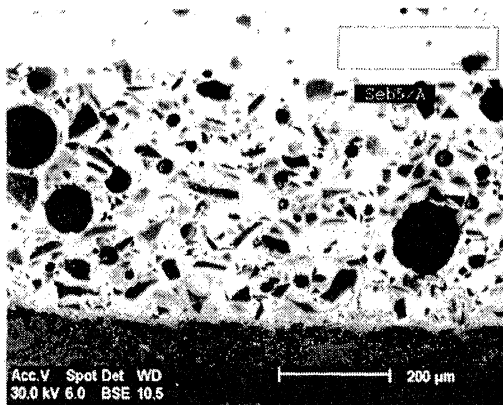


Figure 2 - SEM observation (in backscattering) of bubbles and undissolved quartz crystals in a majolica glaze layer

### **Alteration states**

In general, the investigations by SEM/EDS are very efficaceous if the alteration compounds can be individuated and the deep of alteration evaluated. Alteration due to phosphorus deposition is one of the most frequent.

### Phosphorus deposition

A lot of ancient ceramics show a very high content of phosphorus. It deals with an elemental deposition from aqueous solutions in the soil during burial. SEM/EDS analyses reveal that phosphorus is very diffused in the body in case of not coated ceramics, while it is highly concentrated on the surface in case of glazed ceramics.

### Finishing layers on terracotta

Architectural terracotta was frequently finished with the application of surface treatments with different materials, both inorganic and organic. Treatments with organic materials often gave rise to alteration products, among which calcium oxalate probably are the most frequently recognized (figure 4).

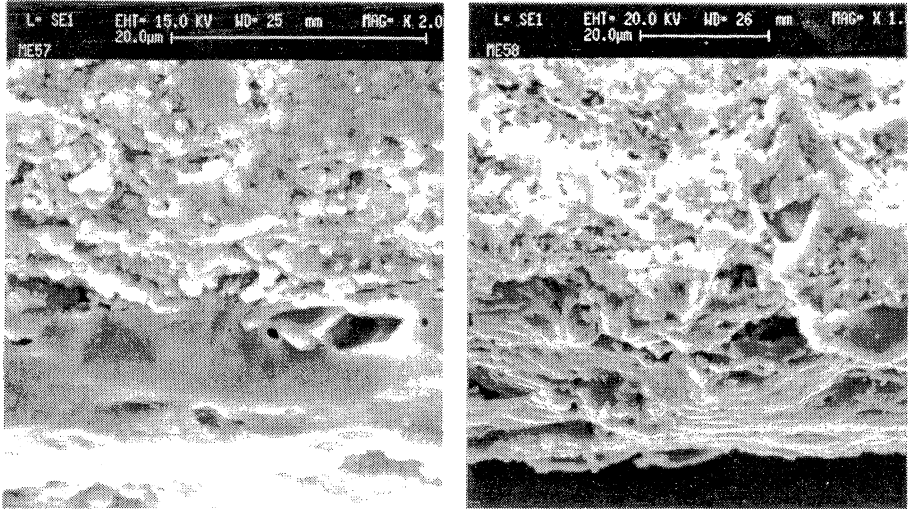


Figure 3 - Different vitrification grade of slip decoration layers in ceramics from Mesopotamia dated IV millennium b.C.

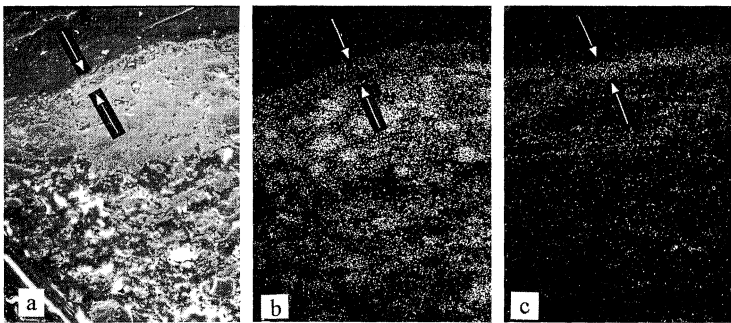


Figure 4 - The arrows indicate an oxalate layer (about 50 μm thick) on architectural terracotta: a) examined area; b) Si EDX map; c) Ca EDX map

(1) Dpto. Química Analítica.  
Univ. de Sevilla, España

(2) Dpto. Construcciones  
Arquitectónicas. Univ. Sevilla,  
España

## Study of ceramic materials from the settlement of Italica (Seville)

*Flores Alés V (1), Barrios Sevilla J (2) and Guiraúm Pérez A (1)*

### INTRODUCTION

The aim of this work is the study of two groups of ceramic pieces from the roman archeological site of Italica, in the town of Santiponce in the province of Seville.

The first group consist of ten broken pottery pieces, they are fragments of wine or oil amphoraes. The second one is composed of five construction bricks.

Four analytical methods were adopted: physical tries, water suction and absortion, according to the UNE standards methods; chemical analysis by atomic absortion/emission spectrophotometry; mineralogical analysis performed by X-ray diffraction; and Differential Thermal Analysis (DTA) and Thermogravimetric in high thermal termic apparatus.

### RESULTS AND DICUSSION.

Two of the bricks were irregular and broken, so they were tested only by water absortion, the other three were also tested by water suction.

Results obtained for suction were correct. Absortion values are low in some cases, but they show an important dispersion, with a standar deviation of 4.4 for bricks and 3.8 for pottery pieces. The sample I4 reach a 23.41%, it also show many small holes in the paste. The pottery samples values are lower than bricks results, they have a carefull and good massed, and also a good firing.

samples	min.	max.	med.	std.dev.
I (suct.)	0.03	0.09	0.06	0.25
I (abs.)	14.8	23.4	17.1	4.4
IA (abs.)	4.7	17.9	11.7	3.8

Chemical analyses do not show significant differences between the two groups. It is important to point that CaO and lost of ignition results are directly relateded.

Sample IA7 analysis is quite different than the other pieces, it shows a  $\text{SiO}_2$  high percentage and low for CaO. Also it may be seen that samples IA6s and IA6i were taken from the surface and the inner part of the brick, due to the differences that the piece showed; in this way, there are no deviations in the results, this texture difference may be due to an irregular firing process.

For bricks, results obtained are similar for all mineral phases present, only the sample I3 is significantly different, that differences have been also detected in chemical analysis.

Diopside was detected and quantified in a maximum value of 22%. Gehlenite and kilchoanite were also detected with lower percentages. With these values it may be supposed a firing temperature around  $800^\circ\text{C}$  and  $850^\circ\text{C}$ .

Pottery samples show a similar behaviour with some logical deviations due to their different provenience.

It should be noticed that bricks show a lower values for calcite and higher for diopside than pottery pieces. According to their mineralogical composition, samples IA4, IA8, IA9 and IA10 may have reached the highest firing temperatures, above  $850^\circ\text{C}$ .

(1) Dpto. Geología. Area de Cristalografía y Mineralogía. Fac. Ciencias. Univ. de Zaragoza, España

(2) Dpto. Cristalografía, Mineralogía, Estratigrafía, Geodinámica, Petrología y Geoquímica. Fac. Ciencias del Mar. Univ. de Cádiz, España

## Elimination of the temperature effect in the variation of the quantitative mineralogical composition of prehistoric pottery: a new method

*Gallart Martí M D (1), Mata Campo M P (1) and López Aguayo F (2)*

A new method of eliminating the effect of temperature in the variation of the quantitative mineralogical composition of prehistoric pottery, consisting of analyzing the behaviour of several natural and artificial samples during heating, is developed.

The mineralogical composition of the natural samples selected is summarized in table 1. On the other hand, several mixtures of calcite and illite were made, including different proportions of these two minerals (table 2). The semiquantitative analysis by XRD (powder method) was made using the "reflecting power" technique (Schultz, 1964; Barahona, 1974).

sample	Il	Sm	Ka	Chl	Ca	Dol	Q	Fd	Gyp
SE-A-14	33	-	9	13	18	<5	20	<5	-
TU-4	63	<5	-	<5	20	<5	10	<5	-
VI-22	77	5	<5	-	<5	-	13	-	<5

Il= illite, Sm= Smectite, Ka= Kaolinite, Chl= Chlorite, Ca= Calcite, Dol.= Dolomite, Q= Quartz, Fd= Feldspars, Gyp= Gypsum

sample:	Ca (%)	Il. (%)
Ca(75)-Il(25)	75	25
Ca(50)-Il(50)	50	50
Ca(25)-Il(75)	25	75

Natural samples were heated in an electric furnace at 300, 400, 500, 600, 700 and 800°C respectively, for one hour, starting in each case from room temperature. Mixtures were also heated at 500, 600, 700 and 800°C. The equipment used was a Philips

PW-1150 with microprocessor PW-1710 and graphite monochromator. All diffractograms were made in the same experimental conditions.

Experience shows that several minerals present structural modifications during heating before their breakdown, which are reflected in changes in intensity of the characteristic X-ray reflections of these phases. It could be related with the researches carried out by Heller-Kallai *et al* (1987) and Shoval *et al* (1993). For this reason, it can be supposed there are several variations in the apparent percentages of crystalline phases as a function of temperature when the quantification method is applied, using intensities. Consequently, a classification of pottery from the same

settlement based on the mineralogical composition must eliminate this effect. The results of the semiquantitative analysis by XRD are summarized in table 3

Table 3. Calcite (Ca) and clay minerals (CM) percentages at different temperatures

T °C	VI-22		SE-A-4		TU-4		Ca(75)-II(25)		Ca(50)-II(50)		Ca(25)-II(75)	
	Ca	CM	Ca	CM	Ca	CM	Ca	CM	Ca	CM	Ca	CM
300 °	<5	86	10	72	25	64	-	-	-	-	-	-
400 °	<5	88	10	74	23	64	-	-	-	-	-	-
500 °	-	89	7	78	19	70	59	41	47	53	19	81
600 °	-	89	5	83	13	78	58	42	39	61	12	88
700 °	-	88	<5	83	7	83	46	54	<5	97	<5	99
800 °	-	87	<5	83	-	-	12	88	10	90	<5	99

The changes observed correspond to an apparent increase in the relative percentage of clay minerals and a decrease in calcite with the rise in temperature, except sample VI-22 due to the scarcity of calcite.

The generalization of results obtained in the quantification of these samples, in relation to calcite and clay minerals, was made applying least-squares fits to several function types. Optimal results were obtained when a second order polynomial function,  $y=a+bx+cx^2$ , was applied, being y the dependent variable, percentage, and x the independent variable, temperature. The correlation coefficients, significance levels and standard error are summarized in tables 4 and 5.

Table 4. Natural samples. R<sup>2</sup> correlation coefficient. P. significance level. S<sub>vv</sub> standard error of the estimate of the regression curves.

	SE-A-14		TU-4	
	Ca	CM	Ca	CM
R <sup>2</sup>	0.981	0.945	0.997	0.980
P	0.01	0.03	0.002	0.01
S <sub>vv</sub>	0.49	1.05	0.30	1.02

Table 5. Mixtures R<sup>2</sup> correlation coefficient. P. significance level. S<sub>vv</sub> standard error of the estimate of the regression curves.

	Ca(75)-II(25)		Ca(50)-II(50)		Ca(25)-II(75)	
	Ca	II	Ca	II	Ca	II
R <sup>2</sup>	0.995	0.995	0.818	0.818	0.952	0.952
P	0.008	0.008	0.27	0.27	0.08	0.08
S <sub>vv</sub>	1.22	1.22	7.93	7.93	1.68	1.68

Figures 1 and 2 include calculated curves fitted to the observed percentages of calcite and clay minerals versus temperature for natural samples and mixtures respectively. This experimental method makes possible to adjust the mineralogical composition of pottery for classification. However, it is necessary to know the firing temperature. On the other hand, experimental curves must be built for each diffraction apparatus.

The determination of the firing temperature in pottery may be made from different existing crystalline phases and other methods. A generalization of Maggetti's method of estimating firing temperatures lower than 800°C in pottery with clay minerals such as illite, using the Fischer's variance analysis, was made (Maggetti, *et al* 1981, Maggetti, 1982).

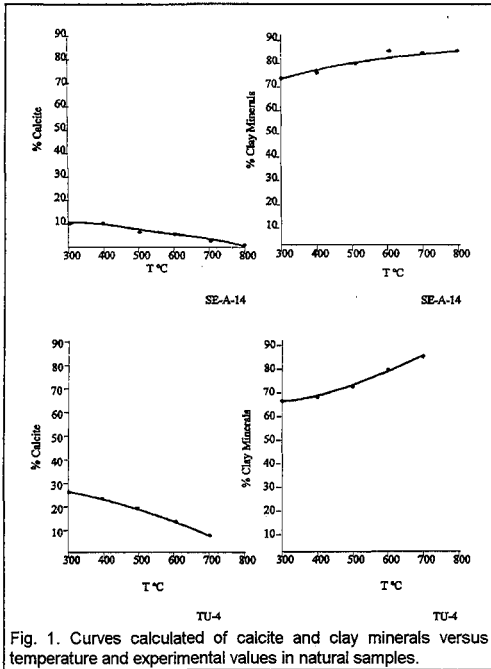


Fig. 1. Curves calculated of calcite and clay minerals versus temperature and experimental values in natural samples.

### References

- Barahona, E. (1974). Tesis doctoral. Univ. Granada. 398. pp.
- Heller-Kallai, L.; Miloslawski, I and Aizenshtat, Z. (1987). Clay minerals, **22**, 339-348.
- Maggetti, M. (1982). In: Archaeologic Ceramics. Smithsonian Inst. Press. 121-133.
- Magetti, M. and Schwab, H. (1982) *Révue d'Archéométrie*, III, Sup. 185-194.
- Schultz, L.G. (1964). Geol. Surv. Prof. Papers, **391**,c. 1-31.
- Shoval, S.; Gaft, M.; Beck, P and Kirsh, Y (1993). *Journal of thermal analysis*, **40**, 263-273.

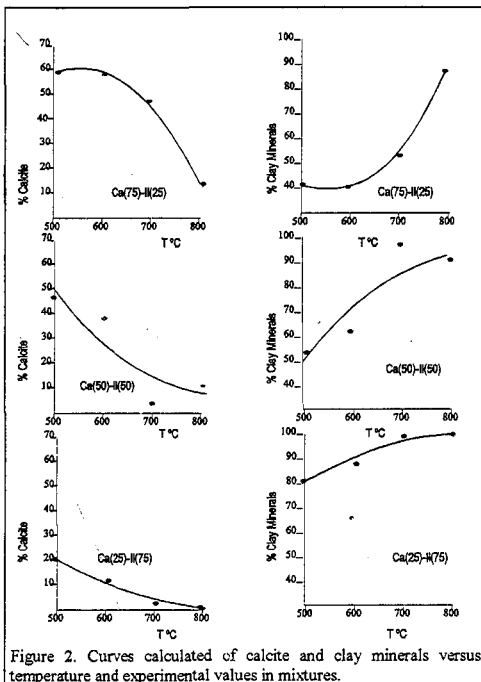


Figure 2. Curves calculated of calcite and clay minerals versus temperature and experimental values in mixtures.

(1) Dip. di Scienze della  
Terra e Geologico-  
Ambientali. Univ. di  
Bologna, Italia

(2) Dip. di Archeologia.  
Univ. di Bologna, Italia

(3) Dip. di Matematica. Univ.  
di Bologna, Italia

## **Ceramics from the etruscan city of Marzabotto: geochemical-mineralogical approach for identification of the origin and treatment techniques of the raw material**

*Morandi N (1), Nannetti M C (1), Minguzzi V (1), Monti S (1), Marchesi  
M (2), Mattioli C (2) and Desalvo F (3)*

The results are reported of the statistical treatment of the mineralogical and geochemical analysis data, carried out on a vast collection of ceramic artefacts coming from the excavations, still in progress, involving the end house (House 1) of *Insula II* in *Regio IV*, situated in the western central sector of the Etruscan city of Marzabotto. From more than 25,000 pieces found so far, the chosen samples include: 21 fragments of purified ceramics, 4 of which showing traces of painting, 9 fragments of rough paste, 8 fragments of bucchero, 3 examples of imported ceramics, (Atticus, Magna-Grecia and Volterra) and a sample of "raw" clay. The aim was to ascertain a single, local or multiple origin of the raw material used for the ceramic mixtures and to reconstruct the treatment methods of the mixtures used for the different types of ceramics.

The samples, previously surface-scraped to remove pollutant substances and/or colorants, were subjected to: i) optical analysis of a thin section of the samples made from not too fine mixture; ii) diffractometric analysis on pulverized samples or on parts of them, enriched or separated or subjected to heat treatment; iii) chemical analysis of the main and trace elements; iv) thermal analysis (TG, DTG and DTA); v) statistical analysis of all the numerical data available.

Mineralogical analysis showed the presence of quartz and feldspars in ratios ranging from 4:1 and 2:1 with the exception of G-B3-26, where the ratio was 1:1, justified by the presence of numerous fragments of granitic rock within the very coarse body. Four samples of "coarse-paste" ceramics and eight samples of "refined" ceramics had large quantities of calcite. All the other samples examined either contained no calcite or very little, barely detectable by X-ray diffractometry. In thin sections of coarse-paste fragments it was noted that the high calcite content coincided with the presence of large granules of non-decarbonated limestone. If this observation is extended to the entire population examined, it can be deduced that the absence of calcite or its presence in negligible quantities can be attributed to the absence of carbonates in the unfired raw materials or a firing temperature above that corresponding to the CO<sub>2</sub> loss process (600 to 700°C). In the latter case the CaO content measured by chemical analysis should nevertheless be high. Diffractometric analysis revealed a sporadic and limited presence of micaceous minerals, clino- or orthopyroxenes, gehlenite and hematite throughout the entire population. More specifically, it was observed that hematite was normally absent from fragments of bucchero and became progressively more abundant in other samples of ceramics characterised by a generally reddish colour becoming gradually darker. It was also observed that in general the quantity of clinopyroxene was inversely proportional to that of calcite, showing that the former had been formed by reaction following the liberation of CaO by the decarbonating process during firing. Where diffractometry failed to detect either clinopyroxenes or calcite, it seems obvious that carbonate-free clay was used. Gehlenite and orthopyroxenes were found regularly in samples either completely or almost completely free of calcite. Their presence could therefore

demonstrate either firing temperatures well above the decarbonating temperature (where gehlenite is present) or the use of clay with a low carbonate content (where orthopyroxenes are present).

The composition of the "raw" clay includes not less than 15% of carbonates, a component of framework in which quartz predominates over feldspar and an argillaceous matrix consisting of illite, smectite and chlorite in order of decreasing quantity. Firing tests carried out on this sample of clay showed the following: 1) heating to 950°C did not modify the quantitative ratio of quartz and feldspar; 2) complete CO<sub>2</sub> loss takes place when the clay is heated to a temperature of between 600 and 700°C; the detection of calcite reflections during X-ray diffractometry on test samples heated to temperatures of more than 800°C can be attributed to a recarbonating process by part of the CaO unused by the production of new clinopyroxene; 3) the gehlenite appears at lower temperatures (800°C) than the clinopyroxene; 4) calcium silicates appear only at very high temperatures and in very small quantities as a result of the short length (two hours) of the ceramic synthesis experiments.

The results of analyses of the main oxides carried out on the entire population of samples examined are strongly consistent with those relating to mineralogical composition. The trace elements data are not capable to characterise one individual group of samples with respect to the others. There were however anomalies regarding trace elements (V, Cr, Ni, Zn, Co) in the three samples of imported ceramics and an exceptionally high Cu content in sample DAI-11, probably linked to sulphur impurities in the clay or post-firing contamination. Sr and Ba values varied considerably, either because (in the case of Sr) the nature of the calcium carbonate added to clay raw material or present as a primary component in the unfired clay changes from sample to sample or because (in the case of Ba), the barite in the fine clastic sediments is not regularly and evenly distributed.

The chemical data were statistically processed by calculating the cluster analysis of the samples and the factor analysis, discarding a number of variables for the reasons mentioned above. The dendrogram in Fig. 1 was obtained by calculating the cluster using the squared Euclidean distance and the mean bonding method. SiO<sub>2</sub> and CaO were excluded as they are mainly linked to the minerals which each ceramics producer chose to use as addition. Also excluded were P<sub>2</sub>O<sub>5</sub>, as it was held to be correlated to contamination resulting from burial in agricultural land, and Cu because of the above mentioned anomalous value. The Fig. 1, through the groups of samples with the lower RDCC (rescaled distance cluster combine) value, shows that there are marked similarities in the composition of samples belonging to the same group of ceramics and also between samples from different groups attributable to the same area of production. From observation of the comparison extended to the entire population examined, it can be noted that RDCC values of not more than 5 group together a large number of samples (group 1) including all the buccero (letter B), some coarse ceramics (letter G), the "raw" clay (Ter 1A) and numerous examples of refined ceramics (letter D). There were also marked chemical similarities within a further two groups of samples (2 and 3) containing either refined ceramics only or predominantly coarse ceramics. These first three groups appear to be closely linked. This type of relationship should be attributable to the fact that all these ceramic objects have been made with clay from the same geographic area and from sediments with the same origin and petrographic nature. The fourth group is isolated from the other three and includes samples with no significant relationships. The only samples which show similarities are the pair of samples from ceramics imported from Attica and Magna Grecia and the samples from Volterra and the refined D-A1-07. This group therefore includes six samples where the particular composition of the raw materials distinguishes them from all others, characterising them as "imported products" in the Marzabotto region.

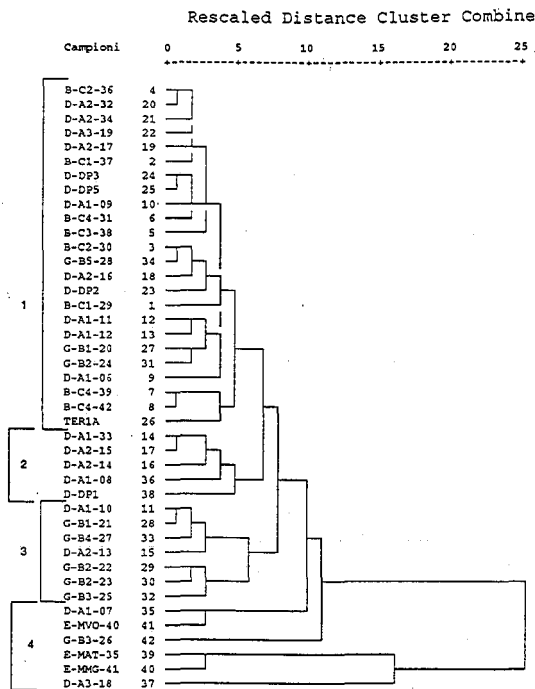


Fig. 1

Examining the results of the factor analysis using the varimax rotation method on the same variables as used for the cluster analysis, it can be noted that the first three factors explain 62.8% of the variance and group the variables together in an extremely interesting way. Factor 1 groups together the components  $TiO_2$ ,  $Al_2O_3$ ,  $Fe_2O_3$ , Co, Ce, Ga, V and La; factor 2 groups together Rb, Zr,  $Na_2O$  and  $K_2O$  and factor 3 groups together Ni, Cr and MgO (all variables are indicated in order of decreasing coefficient value). The grouping of variables is not noticeably modified by changing the type of rotation. Factor 1 variables are mainly linked to kaolinite type of clay minerals accompanied by hydroxides of Al, Fe and Ti and bound to a common origin which should involve the hydrolysis of silicates in well-drained environments. Clays in the Marzabotto region do not have these characteristics and it can therefore be supposed that factor 1 variables are characteristic of the raw materials used to make imported ceramics (group 4 of the cluster). This hypothesis is confirmed by noting that the chemical elements grouped together in factor 1 are generally found in higher quantities in group 4 samples. In the context of the mineralogical components of the raw materials used to make the ceramics, the variables grouped together in factor 2 are dominated by feldspars. Feldspars are sometimes added to the clay to obtain a change for the better and it cannot be excluded that such additions were made in the case of imported ceramics. The variables grouped together in factor 3 are dominated by serpentine/chlorite type mineralogical components coming from the decomposition of ophiolitic rocks. All clays in the Marzabotto area suitable as a raw material for ceramics contain both serpentine and chlorite in very variable degrees. The results relating to factor 3 of the factor analysis probably represent the stamp of the raw material used to make local ceramics.

(1) Estación Experimental del Zaidín. CSIC. Granada, España

(2) Dpto. Prehistoria y Arqueología. Univ. de Granada, España

## Hydrolysis of ceramic materials: neoformation or rehydroxylation of clay minerals. Stable isotope analysis

*Núñez R (1), Capel J (2), Reyes E (1) and Delgado A (1)*

### Introduction

The heating and high-temperature firing processes of clay materials lead to the destruction or collapse of clay minerals (Brindley & Lemaitre, 1987). In old ceramic materials which may have been exposed to meteorization processes, the presence of clay minerals is frequent. Different hypotheses have been put forward to explain the origin of these minerals: neoformation or inherited characteristics. Knowledge of these processes is important for the study of alterations undergone by archaeological ceramic materials.

The aim of this paper is to obtain complementary information about the nature of these mechanisms, for which the isotopic composition of the oxygen in ceramic pieces fired at different temperatures—and subsequently subjected to hydrothermal treatments of differing duration—has been determined.

### Material and methods

Various ceramic bricks were made (by means of oxidizing firing at 700 and 800°C) from illite-rich clay sediments, which were then placed with water in reactors at a temperature of 150°C, for periods of 300, 600 and 1200 h.  $\delta^{18}\text{O}$  isotope analyses were carried out both on the <2  $\mu\text{m}$  fraction of the fired and hydrolysed pieces and on the water introduced into the reactors, using the routine methodology used at the stable isotope geochemistry laboratory of the Estación Experimental del Zaidín, Granada (Spain).

### Results and discussion

Figure 1 shows the values obtained from the isotope analyses. The non-hydrolysed fired pieces present isotope values of approximately 13.5‰ (V-SMOW). However, the hydrolysed pieces tended towards values of 11.3‰. In general, there was a decrease in  $^{18}\text{O}$ , which became more

acute as the duration of the hydrolysis period increased, although the most pronounced variation occurred after 300 h, and in the case of I800 also after 600 h (see Figure 1). The isotopic composition of the water in the reactors was -9‰.

Three hypotheses may be put forward in order to explain this behaviour:

**(a) Neof ormation of phyllosilicates from glass and amorphous material.**

Smectite or illite formed in equilibrium with water with an isotopic composition of -9‰ and at a temperature of 150°C, would have a  $\delta^{18}\text{O}$  value around -0.3‰ (Eslinger & Savin, 1973). Thus, the value of 11.3‰, i.e. radically different from -0.3‰, indicates that phyllosilicates neof ormation could not have been the main cause of this variation in the isotopic composition.

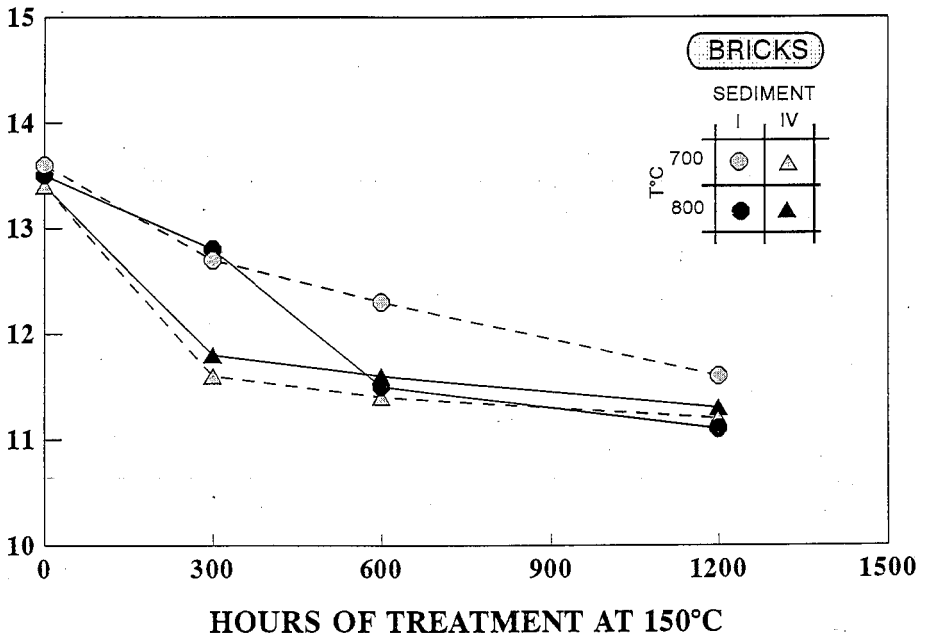


Fig.1 Variation in the  $\delta^{18}\text{O}$  of pieces I and IV fired at 700°C and 800°C, and subsequently hydrolysed (clay fraction).

### (b) Isotope exchange

It could be during hydrolysis part of the oxygen in the tetrahedral layers of the collapsed phyllosilicates (the main component of the <2- $\mu\text{m}$  fraction in the fired pieces) might have been replaced by oxygen from the water. In order to obtain an isotopic composition such as that found in the pieces after 1200 h, a theoretical exchange of 8.4% would be required. However, this percentage conflicts sharply with the data obtained by various authors (O'Neil & Kharaka, 1976) under similar conditions, especially if we consider that in the present experiment exchange did not occur with the OH groups (which virtually disappeared during the firing) but rather with the tetrahedral oxygen strongly bonded to the  $\text{Si}^{4+}$ .

### (c) Rehydration of the collapsed phyllosilicates, by means of the supply of oxygen to the octahedral layer.

During hydrolysis the dehydroxylized phyllosilicate structures (mostly illite) are rearranged and rehydroxylized, capturing OH groups from the water in the reactors. Totally dehydroxylized illite or smectite which is then rehydroxylized would take one oxygen from the environment for every 11 in its cell unit, i.e. 8.4%. This may be expressed as:

$$91.6\delta^{18}\text{O}_{\text{fired}} + 8.4\delta^{18}\text{O}_{\text{water}} = 100\delta^{18}\text{O}_{\text{rehydroxylized}}, \text{ producing } \delta^{18}\text{O}_{\text{rehydroxylized}} = 11.6\text{‰}.$$

This assumes a rapid oxygen-assimilation process from the water with negligible isotope fractionation. At the opposite extreme, if we consider the fractionation of the octahedral oxygen with water given by Bechtel and Hoernes (1990) at 150°C, the octahedral oxygen would tend towards values of -19‰, thus giving  $\delta^{18}\text{O}_{\text{rehydroxylized}} = 10.7\text{‰}$ .

The value of around 11.3‰ obtained for the hydrolysed phases, which falls between the two values, suggests the rehydroxylation process as the main cause of the variation in the isotopic composition.

### References

- Bechtel A & Hoernes S (1990) *Contrib. Mineral. Petrol.* 104:463-470.
- Brindley G W & Lemaitre J (1987) In: *Chemistry of Clays and Clay Minerals* (Newman ed.) 319-370.
- Eslinger E V & Savin S M (1973) *Am. J. Scien.* 273:240-267
- Núñez R (1993) Ph.D. Thesis Dissertation, 269
- O'Neil J R & Kharaka Y K (1976) *Geochim. Cosmochim. Acta.* 40:241-246

Dpto. Cristalografía,  
Mineralogía y Química  
Agrícola. Fac. Química.  
Univ. de Sevilla, España

## Replicate of archaeological ceramics from Carmona (Seville, Spain)

*Polvorinos del Río A and Gómez Morón A*

Most archaeometric studies of ancient ceramics are mainly concerned with the identification of their origin and other aspects related with manufacture technology. Archaeological knowledge of trade, exchange routes and evolution of ceramic production methods can be approached integrating analytical data on ceramic fragments. Even if the origin of such ceramic remains can be assessed as local or foreign, their classification is difficulted because the high variability of the determined parameters and the reduction of their discriminating power. The main sources of such variability are linked to the local diversity of raw clay materials joined to technological artifacts of production as sieving, mixing, temperature and conditions of firing ceramics. The objective of this work is to evaluate such conditions by ceramic experimentation on well characterized local clay resources. For the experimental replication of ancient ceramics a test area was selected in Carmona (Seville) where previous archaeometric studies have been carried out. Four samples have been characterized by whole sample and clay fraction X-ray diffraction, grain size distribution (Fig. 1) and chemical analysis (Table 1).

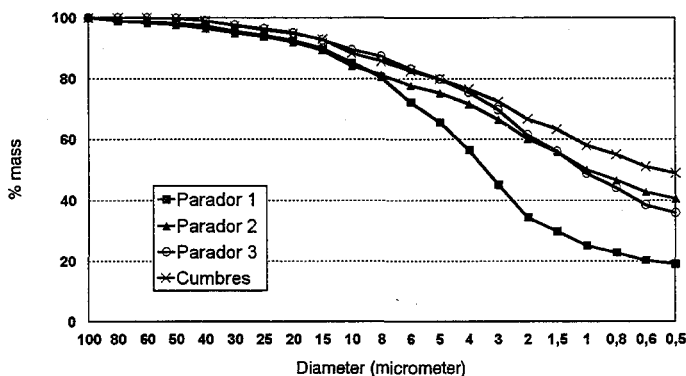


Fig. 1. Grain size distribution.

In the four studied samples accumulation of limestone and clay fractions exceeds 90% of the whole sample. The lowest clay fraction 35% has been found in Parador1 while more than 60% of clay is characteristic in the other cases.

SAMPLES	SiO <sub>2</sub>	Al <sub>2</sub> O <sub>3</sub>	Fe <sub>2</sub> O <sub>3</sub>	MgO	CaO	Na <sub>2</sub> O	K <sub>2</sub> O	TiO <sub>2</sub>	MnO <sub>2</sub>
Parador1	55.34	10.93	5.65	1.44	19.96	4.94	1.39	.32	.035
Parador2	50.41	12.55	5.42	1.73	20.57	7.67	1.60	.38	.49
Parador3	48.59	12.04	4.68	2.11	23.93	6.62	1.64	.36	.033
Cumbres	42.88	10.48	25.63	1.84	9.95	7.47	1.33	.37	.048

Table 1.

Mineralogy composition of the clay samples have been studied including oriented samples of fined-grained clay fraction, by using the standard procedure (2-30° 2θ, air dried, etilenglycol 60°C for 24 h., DMSO 80°C for 48 h., fired 550°C for 2 h.) and are mainly of illite, smectite and kaolinite (Table 2).

SAMPLES	Quartz	Calcite	Kaolinite	Illite	Montmorillonite	Gypsum
Parador1	++++	+++	+	++	+	+
Parador2	++++	++++	++	++	+	+
Parador3	++++	+++	++	+	+	++
Cumbres	++++	+++	++	+	++	-

Table 2. (Very abundant: +++++; Abundant: ++++; Medium: ++; Trace: +; Non existant: -)

Firing experiments on whole clay samples or previously sieved to the maximum size of grains previously measured in ancient fragments have been carried out in air atmosphere from 600 to 1000°C at 100°C steps. In all cases the heating rate was 5°C/min, and fired during 4 hours when maximum temperature was reached.

Induced colour changes by thermal treatment has been measured in the tre-estimulus space and shows a general trend of red component increase with firing temperature.

Results on X-ray diffraction of sample Parador 1 submitted to thermal treatment (Fig. 2) shows the transformation of gypsum to anhydrite and progresive thermal decomposition of phyllosilicates and calcite. The last remain of calcite observed at 700°C and in the same temperature beging the formation of portlandite and at 800°C of gehlenite. In the 900-1000°C range can be observed the formation of diopside and plagioclase.

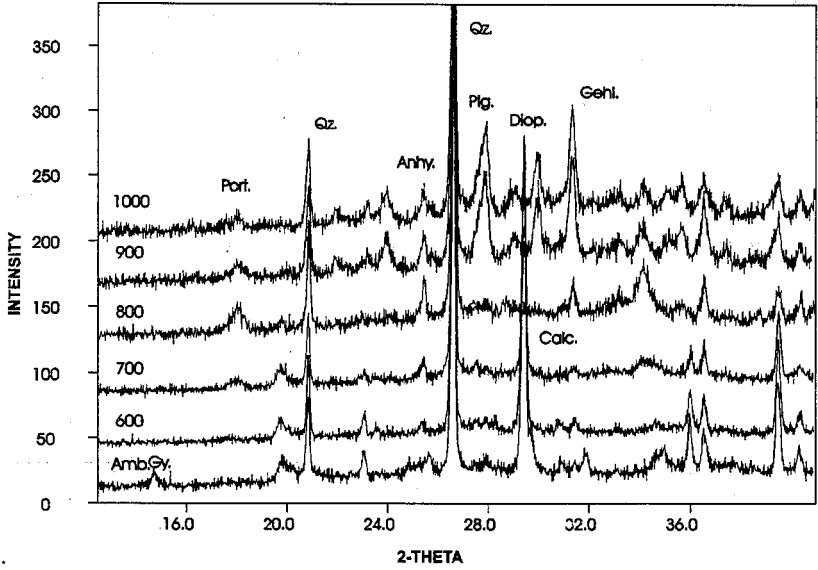


Fig. 2. Mineralogy phases of fired clay sample Parador 1 (Qz=Quartz; Port=Portlandite; Anh=Anhydrite; Gy=Gypsum; Plg=Plagioclase; Diop=Diopside; Gehl=Gehlenite).

(1) The Getty Conservation Institute, Marina del Rey, California, USA

(2) Depto. Mineralogía y Petrología. Fac. Ciencias. Univ. de Granada, España

## ESEM analysis of the swelling process in sepiolite-bearing Egyptian limestone sculptures

Rodríguez Navarro C (1), Sebastián Pardo E (2) and Ginell W S (1)

### Introduction

One type of Egyptian limestone from Naga-el-Deir (Abydos/Thebes region) exhibits an on-going problem of deterioration that is evidenced by continued delamination of the surface of a stela acquired from archaeological investigations carried out in the early 20th century. Various types of Egyptian limestone sculptures in the collection of the British Museum that exhibit similar deterioration have been studied by Bradley & Middleton (1988). In this study, it was believed that damage was due to the presence of small quantities of salt (sodium chloride and sodium nitrate). In fact, such sculptures had been treated and desalinated by aqueous poulticing, but the decay process was not stopped, as evidenced by major loss of surface stone after storage for a period of years. Nevertheless, Bradley & Middleton (1988) pointed out that the mineralogy, and especially the clay content, should play a role in the susceptibility of this stone to decay.

Having determined that the amount of salt in this limestone was very small, other modes of deterioration were considered. Mineralogical and petrographic data showed this stone to have a high proportion of clay. The results of laboratory tests confirmed that the clay, which is concentrated along bedding planes, may be largely responsible for the type of deterioration noted. The role of clay minerals in the decay of this type of limestone was demonstrated by experiments involving in situ, high magnification, environmental scanning electron microscopy (ESEM) of clay swelling behavior in the presence of water.

### Material and methods

Samples from a II to IV Dynasty (2720-2150 BC) Egyptian limestone Stela from the Phoebe Hearst Museum (California) were studied by means of optical microscopy, x-ray diffraction and scanning electron microscopy. The clay fraction was extracted using the following experimental protocol: Fifty grams of crushed limestone were treated with 1 M acetic acid and the acid-insoluble residue was washed repeatedly with distilled water and the clay fraction was separated by centrifugation. Oriented clay aggregates (air-dried, ethylene glycol [EG] and dimethyl sulfoxide [DMSO] solvated, and after heating to 550°C) were prepared. XRD analysis of the oriented clay aggregates was performed with a Philips PW-1710 diffractometer, equipped with graphite monochromator and automatic slit, using CuK $\alpha$  radiation. Elemental Si was used as an internal standard. The clay content was calculated from the weight of the clay fraction following drying at 90°C for 24 hours. The high magnification study of in situ dynamics of the clay swelling was performed using an environmental scanning electron microscope (ESEM, ElectroScan, Model E-3) by treating limestone samples (3x6x4mm) with distilled water (using a syringe) after they were placed in the ESEM chamber at low vacuum (3 torr). Condensation over the sample surface was subsequently reached by increasing the chamber pressure to 15 torr. Numerous images were recorded on video-tape before, during and after water treatment.

## Results and discussion

The Egyptian limestones studied belong to the upper member of the early Eocene Thebes formation (Said, 1990) and were quarried at Naga-el-Deir (Abydos/Thebes region, Egypt). Optical microscopy revealed these stones to be limestones containing mostly micritic calcite with a small amount of dispersed bioclasts (mostly foraminifera). A few dolomite rhombohedra were also seen dispersed within the matrix. Bedding planes appear clearly marked by parallel fractures and bands of dark color, probably due to the high concentration of clays and iron oxides deposited along these planes. Powder XRD analyses of the bulk samples showed that calcite was the major phase (70 %), with dolomite (< 20 %), clay minerals (< 10 %) and quartz (< 5 %) as minor phases. Also minor amounts of NaCl and NaNO<sub>3</sub> (< 1% in weight) were detected. The acid

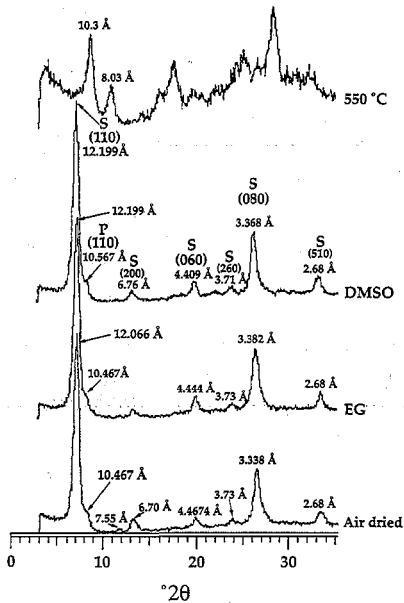
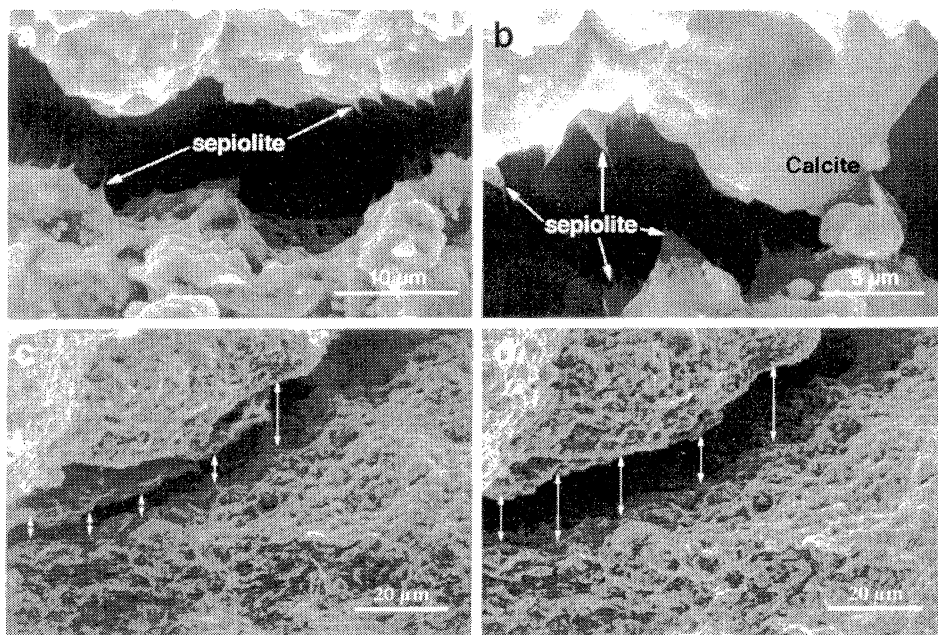


Fig. 1 XRD patterns of clay fraction oriented aggregates.

insoluble fraction of the limestone was 15.89 % in weight. The fraction with particle size < 2  $\mu\text{m}$  was separated by centrifugation (3.49 % in weight), and oriented clay aggregates were prepared and analyzed by means of XRD (Fig. 1). An intense peak appears at 12.066 Å, which changes to 12.199 Å after treatment with either EG or with DMSO, disappears after heating to 550°C and is transformed into a broad peak at 10.3 Å. This peak was assigned to the (110) reflection of sepiolite (S). The sepiolite peak at 3.338 Å (080) shifts, after glycolation, to 3.382 Å, and the (060) peak at 4.467 Å, shifts to 4.444 Å. A minor peak at 10.467 Å, corresponding to the palygorskite (110) reflection, shifts to 10.567 Å after DMSO solvation, and collapses after heating to 550 °C. It is worth mentioning, that intracrystalline swelling of sepiolite has been reported by Fleischer (1972), Guven & Carney (1979), and Jones & Galán (1988). The ESEM analyses (Fig.2) demonstrated that when wetted, the fibrous clay minerals accumulated along bedding planes within the stone, swell and produce tensile stresses perpendicular to the bedding planes that leads to fissure development, resulting in stone delamination. The results of this same process can be observed by the naked eye when this stone is immersed in water. Complete disintegration of the stone occurs within a few hours.

However, the small intracrystalline swelling of sepiolite can not explain the large expansion suffered by the limestone when in contact with water. In this case, another type of swelling process takes place. Osmotic swelling, resulting from electrostatic forces and differences in concentration between the pore water and the water existing between two clay particles, should be the major factor responsible for the decay of these sepiolite-bearing limestones. According to the double layer theory (van Olphen, 1977), the negatively charged surface of the sepiolite can adsorb positively charged ions. The presence of Na<sup>+</sup> (from NaCl and NaNO<sub>3</sub>), which can be strongly hydrated (Marshall, 1949; van Olphen, 1977), can contribute to the electric double layer formation, and act as counterions. Electrostatic repulsion forces between sepiolite particles can produce high

enough swelling pressures to overcome the wet strength of the limestone. The close-packed arrangement of the sepiolite particles along the bedding planes of the stone, facilitates the formation of cracks and fissures along these weak planes when swelling take place. In a storage environment (museum) where relative humidities can become high, water condensation and penetration into the limestone pore system occurs, which leads to clay swelling and the delaminating degradation that is characteristic of this type of Egyptian limestone. This decay process was also reproduced and observed in situ, at high magnification, using the ESEM. Thus, close environmental control in the museum display and storage areas to avoid water condensation due to changes in temperature and relative humidity, seems to be the least invasive conservation procedure for the preservation of this type of historic limestone.



**Fig. 2** ESEM micrographs of : a) sepiolite fibers concentrated along bedding planes; b) detail of sepiolite fibers covering calcite crystals; c) crack before wetting, and d) after wetting

#### Acknowledgment

This work was supported by a postdoctoral fellowship (MEC, Spain) no. PF94 24232705. Financial support was also provided by the DGICYCT project no. PB93/1090 and the Research Group 4065 (Junta de Andalucía) We are indebted to Ms. Madelaine W. Fang of the Phoebe Hearst Museum of Anthropology (Berkeley, California) who supplied the Naga el-Deir stela samples.

#### References

- Bradley, S.M. & Middleton, A.P. (1988) *Jour Amer Institute Conservation* **27**, 64-68.  
 Fleischer, P. (1972) *Amer Miner*, **57**, 903-913.  
 Guven, N. & Carney, L.L. (1979) *Clays and Clay Miner*, **27**, 253-260.  
 Jones, B.F. & Galán, E. (1988) *Review in Mineralogy, Min Soc Amer*, **18**, 631-674.  
 Marshall, C.E. (1949) *The colloid chemistry of the silicate minerals*. Acad Press, New York, 195 p.  
 Said, R. (1990) *The Geology of Egypt*. Rushdi Said Ed., Balkema Publishers, Rotterdam, 734 p.  
 van Olphen, H (1977) *An introduction to clay colloid chemistry*. J. Wiley & Sons, New York, 31 p.

(1) Dpto. Geología. E.U.P.  
Linares. Univ. de Jaén,  
España

(2) Dpto. Mineralogía y  
Petrología. Fac. Ciencias.  
Univ. de Granada, España

(3) Dip. di Scienze della  
Terra. Univ. di Pavia, Italia

## Decorated terracotta from the province of Pavia, Italy: a mineralogical and petrographic study

Torre López de la M J (1), Sebastián Pardo E (2) and Zezza U (3)

### Introduction

A preliminary study has been made of terracotta decorating the late Gothic windows of a Renaissance palace in Sartirana Lomellina (province of Pavia, North Italy). These ceramics, of varying design, outline the window frames. In spite of their great artistic value they are in an unfortunate state of deterioration. It should be noted that these pieces are not in a highly polluted urban environment (which would affect their weathering), but in a small town. Terracotta decorations are relatively frequent in this part of Italy, where carving stone is relatively scarce. There are magnificent examples in the cloisters of the Certosa of Pavia (Abrate-Zohar et al., 1985; Duminuco et al., 1992), the Carmine Church, and others. The results of this study can be applied to other similar cases of this material weathering.

### Materials and Methods

Our aim was to study the composition and texture of these terracotta to determine whether the causes of the deterioration were related to the manufacturing process or to external factors. Permission was obtained to take a sample from an apparently unweathered piece that had fallen off (metal staples are used to affix the pieces). Seen straight on, the piece was 19 x 7.5 cm and 8 cm deep, with the decoration reaching 4 cm deep. Several microbore samples were taken from this piece and examined mineralogically and petrographically to ascertain the origin of the material used, the technology used in the manufacture of the pieces and some of the causes of the deterioration. X-ray diffraction (XRD), petrographic microscopy, and scanning electron microscopy (SEM) were employed.

### Results

XRD results reveal that the samples are composed of 50 to 70% quartz, 15 to 30% feldspars (mainly plagioclase, but also potassium feldspar), 10 to 18% phyllosilicates (biotite, muscovite and slightly degraded illite, all with a first reflection at 10 Å), and accessory hematites (<5%). High-temperature mineral phases and carbonates are both lacking.

Under the petrographic microscope it can be seen that the matrix has an intense unvitrified

reddish colour. The temper is abundant (>50%) and varies from grains that are nearly indistinguishable from the matrix to others 1-2 mm in diameter. These fragments are subangular and most of them are mono- or poly-crystalline quartz, usually with undulose extinction. Plagioclase and potassium feldspar grains are also seen. There are also minor amounts of biotite, amphibole, garnet and rock fragments (schist with graphite and quartzschists with biotite). There are large pores but no significant fissures and no growth of alteration minerals in the empty spaces.

SEM shows the degree of vitrification in the paste to be scarce, as the minerals have a sediment-like appearance (Tite & Maniatis, 1975; Freestone & Middleton, 1987). This fact is particularly noteworthy in the case of the clay minerals, which, as may be seen in Photo 1, are very little affected by the firing, preserving the original edges with no signs of vitrification. The samples are also seen to be heavily colonised by fungi, with details of the micelium visible in Photo 2.



**Figure 1.** SEM microphotograph showing the morphology of the matrix phyllosilicates.

### **Discussion**

The results indicate that these terracotta pieces were manufactured with a paste low in calcite, as is the case for other such examples from Lombardia (Abrate-Zohar et al., 1985; Duminuco et al., 1992). The temperature necessary for sintering is therefore higher than for calcareous pastes (Tite & Maniatis, 1975), resulting in the scarce development of high-temperature mineral phases and glass apparent here. Another contributing factor to this lack may be relatively low firing temperatures, as can be deduced from the phyllosilicate morphology observed with the SEM. The kiln atmosphere must have been oxidizing, judging from the presence of hematites (Maggetti & Schwab, 1982).

Another aspect worth mentioning is the colonisation by fungi. Fungi growth can cause a certain amount of chemical-mechanical deterioration in the ceramic pieces due to filament adherence to the mineral particles.

Preliminary data on total porosity and pore size distribution indicate the terracotta are highly

porous, similarly to those from Certosa.

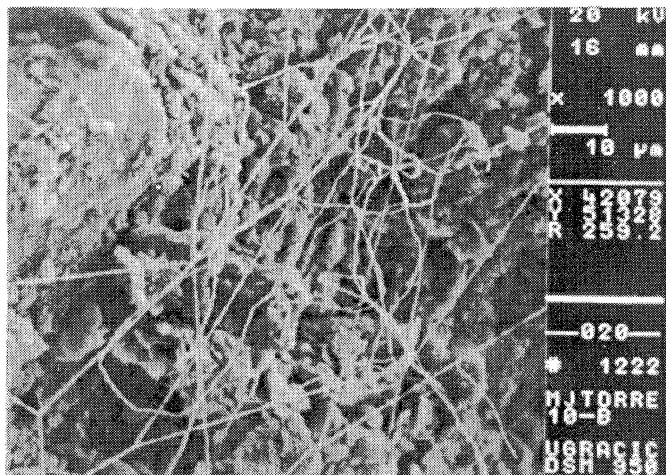


**Figure 2.** SEM microphotograph in which the growth of fungi inside the sample can be seen.

### Conclusions

These terracotta were manufactured with an illitic non-calcareous paste and fired at temperatures under 900° C (Tite & Maniatis, 1975), probably even lower than 850°C since the reflection (001) was not affected (Maggetti, 1982). These factors result in scarce durability given that neither high-temperature mineral phases nor glass formed and so the clay particles in the matrix and the temper have a low degree of adhesion. We can therefore conclude that the main factor causing the deterioration of the terracota is their own nature and the manufacturing technology employed, aided by secondary factors such as exposure to high environmental humidity, which favours microbiological attack.

### Acknowledgments

This project has been financed by Investigation Project PB-93-1090 (DGICYT) and by Research Group 4065 of the Regional Government of Andalusia

### References

- Abrate-Zohar, M.A., Zezza, U., Veniale, F., Setti, M. (1985) Vth Int. Congress on Deterioration and Conservation of Stone, 1, 443-451.
- Duminuco, P., Setti, M., Tortelli, M., Veniale, F., Zezza, U. (1992) In: *Le Superfici dell'Architettura: il cotto. Caratterizzazione e trattamenti*, Bressanone, 445-449.
- Freestone, I.C., Middleton, A.P. (1987) *Min. Magazine*, 51, 21-31.
- Maggetti, M. (1982) In: *Archaeological Ceramics*, Smithsonian Institution, 121-133.
- Maggetti, M., Schwab, H. (1982) *Archaeometry*, 24, 1, 21-36.
- Tite, M.S, Maniatis, Y. (1975) *Nature*, 257, 122-123.

## Provenance and technology of Galloroman terra Sigillata imitations from western Switzerland: preliminary results

Zanco A

In this work about one hundred sherds of Galloroman Terra Sigillata Imitations (TSI) (1<sup>st</sup> - 3<sup>rd</sup> C. AD) from three different sites of Western Switzerland (Lausanne, Yverdon, Avenches) have been analyzed to investigate their provenance and technology. Preliminary results are presented here.

The material is being studied with the collaboration of the Archeologists interested to solve the question if the TSI-potters, which names are stamped under the base of the sherds, produced each one in his own, distinct pottery workshop or if the potters worked at different places, using different clays. Another purpose of this work is to know if there is any chemical and technological time-depending evolution of the pottery manufacturing at different sites.

The sherds have been studied by Optical Microscopy, X-Ray Diffraction (XRD) and Chemical Analysis (XRF) of major and trace elements.

Petrographical observations on the Lausanne samples allow to distinguish the use of two kinds of clays, the first one rich in coarse-grained temper with a siliceous matrix and the second poor in fine-grained temper with a carbonatic-siliceous matrix. XRD show the presence of primary minerals such as Quartz, Illite and of firing ones such as K-feldspar, Gehlenite, Pyroxene and Hematite. Wairakite and Calcite are secondary phases. The firing temperatures are estimated between 850°-950° resp. >950° C.

Samples from Yverdon are chemically very homogeneous with high CaO (mean 12 wt%), and a fine-grained temper-poor matrix. Abundant secondary Calcite is present in pores. The firing temperatures, deduced from the phase analyses, were probably for one group about 850°C, for the second between 850-950° C, and for the third > 950°C.

Ceramics excavated at Avenches are chemically homogeneous, and the sherd matrix is fine-grained, with few temper fragments, and a lot of clay pellets and secondary calcite. Five sherds show a siliceous and temper rich matrix. Their CaO content is lower (< 5% wt) than the major group, and the firing temperature is estimated to > 950°C. In addition other two samples of this group show an abnormal behaviour in their chemical and petrographical composition, indicating therefore a probable foreign origin.

## REFERENCES

- Joumet A (1982). *Unpublished PhD Thesis*.
- Maggetti M (1980). *Cahier d'archéologie romande* 20, 81-95.
- Maggetti M (1981). *British Museum Occasional Paper* 19, 33-49.
- Maggetti M (1982). *Archaeological Ceramics*, 121-133.
- Maggetti M, Westley H & Olin J (1984). *ACS Advances in Chemistry Series* 205, 151-191.
- Maggetti M (1994). *1st European Workshop on arch. ceramics*, 23-35.

**LAST ABSTRACTS**



(1) Centro de Investigaciones  
Energéticas, Medio  
Ambientales y Tecnológicas.  
Instituto de Medio Ambiente.  
Madrid, España

(2) Estación Experimental del  
Zaidín. CSIC. Granada,  
España

## Clay minerals of the fracture fillings from the "El Berrocal" site: characterization and genesis

*Pelayo M (1), Pérez del Villar L (1), Cózar J S (1), Reyes E (2),  
Caballero E (2), Delgado A (2) and Núñez R (2)*

El Berrocal site is situated in the El Berrocal granitic pluton, which is in the central part of the Central Iberian Zone (Julivert et al., 1972). The dominant facies is an alkali feldspar granite, with two micas, that has an uranium-rich, sulphide-bearing quartz vein (Pérez del Villar and De la Cruz, 1989; Pérez del Villar et al., 1992).

The clay minerals studied in this work belong to the fracture fillings present in deep zones of the El Berrocal site. The sampling was carried out from five cored boreholes. These fracture fillings are the result of the differential alteration of the granite minerals, precipitation of other minerals and the dissolution of some of them, since the formation of the fractures till now. They are essentially composed of quartz, K-feldspar, albite, phyllosilicates and carbonates.

Clay minerals are fundamentally constituted by illite, smectite, kaolinite, and minor palygorskite and chlorite, the latter generally inherited from the granite. The transformation of muscovite into illite or smectite was observed by SEM (Fig.1A). Smectite, identified as beidellite (Pérez del Villar et al., 1993b), presents the typical webby pore-lining morphology (Fig.1B). It has been observed albite being transformed into smectite. Kaolinite is idiomorphic, with the face-to-face stack-type texture (Fig.1C). Palygorskite is very rare and presents the typical fibrous habit (Fig.1D).

The  $\delta^{18}\text{O}$  values have been determined in samples rich in illite, smectite, kaolinite and palygorskite. These values indicate that illite and kaolinite were formed at a minimum temperature of 100°C. Smectite was formed between 16° and 30°C and palygorskite was formed at 39°C (Reyes et al., 1995).

According to the textural, mineralogical and geothermometric features, a relative sequence can be established for the clay mineral neoformation processes. Illite and

kaolinite were formed by hydrothermal process at 100°C. The fault granitic gouges were altered, and feldspars, mainly albite, and muscovite were transformed to sericite-illite. Kaolinite has been found in only 32% of the samples studied. Consequently, the formation of this clay mineral might be related to the variations of pH in the hydrothermal solutions.

Smectite is produced by weathering of illite and residual albite, according to the textures observed by SEM, at a temperature between 16 and 30°C, according to the  $\delta^{18}\text{O}$  values. Consequently, smectite can be considered as a recent mineral.

Palygorskite was probably formed under ambient conditions, by a previous dissolution of dolomite and a subsequent generation of hypersaline conditions in certain fractures.

## REFERENCES

- Julivert, M., Fontboté, J.M., Ribero, D. y Conde, L. *Inst. Geol. Min. de España* (1972).
- Pérez del Villar, L. and De la Cruz, B. *Stud. Geol. Salmant.*, 26, 47-80 (1989).
- Pérez del Villar, L., De la Cruz, B., Pardillo, J. y Cózar, J.S. *Bol. Soc. Esp. Min.*, 15, 123-136 (1992).
- Pérez del Villar, L., De la Cruz, B., Cózar, J.S., Pardillo, J., Gómez, P., Turrero, M.J., Rivas, P., Reyes, E., Delgado, A. and Caballero, E. *Stud. Geol.*, 49(3-4), 199-222 (1993b).
- Reyes, E., Caballero, E., Cortecchi, G. y Delgado, A. 2<sup>as</sup> Jornadas I+D, Madrid 1995.

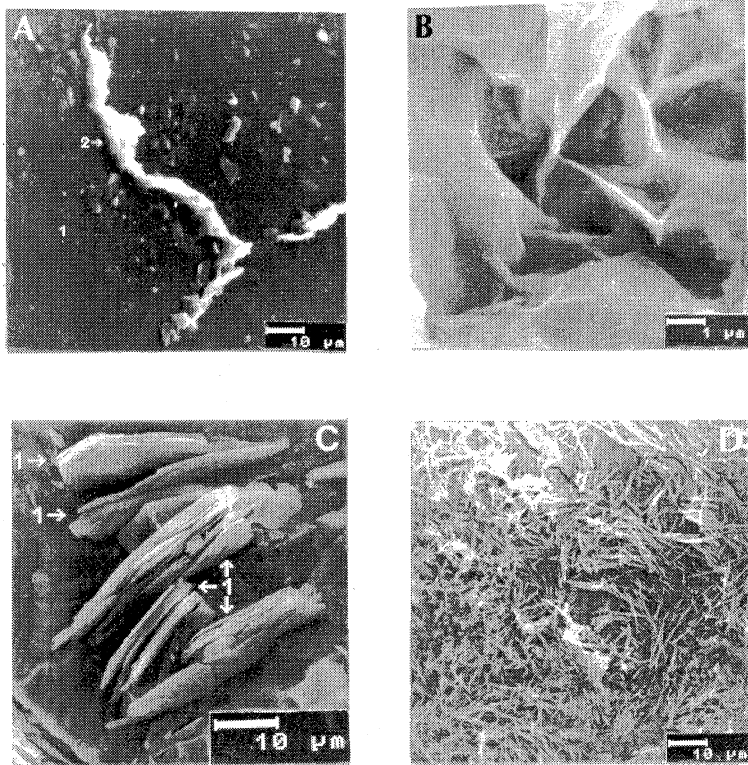


**Fig.1.-A)** Huge plate of muscovite (1) being transformed into illite (2). **B)** Beidellitic-type smectite showing the typical webby pore-lining morphology. **C)** Kaolinite (1) with typical face-to-face stacked-type structure. **D)** Palygorskite overlying the other minerals of the fracture filling. Notice its fibrous habit.

Dpt. Geology and Mineral  
Resources Engineering,  
Norwegian University of  
Science and Technology,  
Trondheim, Norway

## Smectite to illite transformation. Experimental simulation and natural observations

*Wei H, Roaldset E and Grimstad S*

The illitization of smectite has caused great discussion in terms of the factors that control this diagenetic reaction. A laboratory simulation of the diagenetic change from smectite into illite has been undertaken in order to reveal the importance of reaction temperature and concentration of active cations (K).

The simulation has been successful, using the starting material of a Lower Tertiary claystone, rich in smectite from the Oseberg field, North Sea. The fraction of <2 microns was subjected to hydrous pyrolysis with KCl solutions at concentrations of 1.0 N, 0.01 N and 0.001 N, temperatures from 150 °C to 350 °C and a constant reaction time of 24 hours. Qualitative and semi-quantitative XRD analysis were run to examine the products of the pyrolysis and the reaction of smectite into illite and the mixed-layer smectite-illite (S/I). The [K<sup>+</sup>] is a major factor influencing the reaction rates. Under the experimental conditions applied, the conversion from smectite to illite starts at a temperature of about 180 °C and is completed at temperatures around 255 °C for the 1.0 N KCl solution. For the 0.01 N KCl reaction fluid the temperature range of the reaction is about 215 °C - 300 °C. By applying Arrhenius reaction rate equation, a frequency factor of  $A=2.17 \times 10^{10} \text{ s}^{-1}$  and an activation energy of  $E=35.17 \text{ kcal/mol}$  has been calculated for 1.0 N KCl reaction fluid used. With reaction fluid of 0.01 N KCl, a frequency factor of  $A=7.78 \times 10^8 \text{ s}^{-1}$ , and an activation energy of  $E=34.87 \text{ kcal/mol}$  has been found. The experimental runs with 0.001 N KCl reaction fluid are in progress and will be completed by July 1996.

The experiments demonstrate that the availability of K<sup>+</sup> is an important parameter in the illitization of smectite. The importance of time has been considered subordinate to the importance of the potassium concentration and the pyrolysis temperature. For the potassium concentrations, however, it is reasonable to believe that, the 0.01 N KCl reaction fluid used is fairly well corresponding to natural conditions in potassium rich shales. The results show that the conversion of smectite into illite can very well be simulated in the laboratory using temperatures that are below 350 °C. Extrapolation of the reaction rates to the geological conditions for buried shales, using the activation energy and frequency factor, obtained for the 0.01 N KCl solution, give reaction rates of  $6.2 \times 10^{-8} \text{ years}^{-1}$  at 50 °C,  $6.2 \times 10^{-6} \text{ years}^{-1}$  at 80 °C and  $9.1 \times 10^{-5} \text{ years}^{-1}$  at 100 °C for the transformation of smectite to illite.

The experimental results will be discussed in relation to observations on the smectite to illite transformation in North Sea claystones buried to various depths and temperatures.

## AUTHOR INDEX



## AUTHOR INDEX

### A

Acquafredda P 149, 269, 278  
 Achab M 121  
 Adamo P 27  
 Aguer JP 21  
 Alonso-Azcárate J 81  
 Altaner SP 68  
 Alvarez A 159, 255  
 Andriani T 269  
 Aparicio P 261  
 Arana R 119  
 Aróstegui J 181  
 Avilés MA 239

### B

Bañares MA 54, 57  
 Barbieri M 201  
 Barrenechea JF 81, 233  
 Barriga C 30  
 Barrios-Neira J 150  
 Barrios-Sevilla J 287  
 Bauluz B 84, 140, 143  
 Béjar M 242  
 Ben About A 87  
 Bobos I 65, 90, 98, 250  
 Bombin M 94  
 Burrigato F 272

### C

Caballero E 36, 128, 311  
 Caetano PS 97  
 Cairo A 274, 277  
 Canosa M 278  
 Capel J 281, 295  
 Casal B 264  
 Casas J 134, 153, 156  
 Casas-Ruiz J 159, 255  
 Celis R 24  
 Cerezo A 252  
 Cinquegrani G 27  
 Colombo C 60  
 Cornejo J 9, 21, 24, 30,  
 33, 42, 48  
 204  
 Corroado J 204  
 Correia Marques J 204  
 Cózar JS 311  
 Cuadros J 68  
 Cuevas J 110, 159  
 Chellai EH 87

### D

Daoudi L 87  
 Delgado A 295, 311  
 Delgado G 187, 193

Delgado R 187, 193  
 Desalvo F 292  
 Di Filippo M 272  
 Dinelli E 149, 207  
 Domínguez-Díaz 168  
 Domínguez-Díaz MC 100  
 Dondi M 210, 212, 214  
 Doval M 168  
 Duminuco P 217, 274

### E

Ercolani G 210  
 Esposito L 258

### F

Fabbri B 210, 214, 284  
 Fenoll P 87  
 Fernández-Caliani JC 218  
 Fernández-Nieto C 84  
 Fernández-Tapia MT 119  
 Ferraz E 103  
 Fiore S 106, 108, 190  
 Flores V 287  
 Franco E 113  
 Franquelo M 221

### G

Gaitán M 30  
 Galán E 3, 218, 261  
 Galhano C 224  
 Gallart MD 289  
 García-Garmilla F 181  
 García-Romero E 100, 168  
 Garralón A 110, 159  
 Genova N 277  
 Genovese G 108  
 Ghiara MR 113  
 Ginell WS 301  
 Giorgietti G 116  
 Gnazzo L 113  
 Gomes C 65, 90, 93, 97,  
 103, 125, 131,  
 165, 171, 174,  
 204, 224, 245,  
 250  
 Gómez-Morón A 298  
 González-Díez I 261  
 González-López JM 84, 140, 143  
 Grimstad S 314  
 Grubessi O 272  
 Guadagno FM 258  
 Guarini G 214  
 Guillén F 119  
 Guiraúm A 287

Gutiérrez E	255	Meloni S	277
Gutiérrez-Más JM	121	Memmi I	116
<b>H</b>		Merino J	264
Hermosín MC	21, 24, 30, 33, 42, 48	Messiga B	217, 274
Hoyo del C	227	Miano TM	108
Huertas F	36, 128, 281	Minguzzi V	292
<b>I</b>		Mirabella A	190
Iñigo AC	70	Miranda A	93
<b>J</b>		Miras A	261
Jiménez de Cisneros C	36, 128	Molina F	281
Jiménez de Haro MC	45, 239, 242	Molina JM	230
Jiménez-López A	54	Mongelli G	124, 146, 149
Jiménez-Millán J	230	Montealegre L	150
Justo A	45, 236, 239, 242	Montenegro J	125
<b>K</b>		Monti S	292
Krishnamurti GSR	60	Moral J	121
<b>L</b>		Morandi N	207, 292
La Iglesia A	100	Moreno A	153, 156
Lacarbonara F	278	Morillo E	39
Laviano R	124, 278	<b>N</b>	
Leguey S	110, 159	Nájera T	281
Leite S	125	Nannetti MC	292
Linares J	36, 128, 281	Navarro-Gascón JV	100
Lonis R	113	Nicolopoulos S	76
López-Aguayo F	121, 289	Nieto F	116
López-Galindo A	87, 143, 178, 252	Núñez R	295, 311
López-González JD	54, 57	<b>O</b>	
Lorenzoni S	269, 278	Oddone M	277
Lorenzoni P	190	Ortega-Huertas M	137
Luque FJ	233	<b>P</b>	
Luxoro S	113	Palomo I	137
<b>M</b>		Párraga JF	193
Machado A	131	Parras J	233
Maqueda C	39, 196, 221	Pascual J	236, 242
Marchesi M	292	Pavlovic I	30, 42
Marsigli M	210, 212	Pelayo M	311
Martin de Vidales JL	134	Pérez MM	187
Martin-García JM	187, 193	Pérez-Maqueda LA	45
Martin-Pozas JM	51, 94	Pérez-Rodríguez JL	45, 73, 196, 221, 236, 239, 242
Martin-Rubí JA	156, 159	Pérez del Villar L	311
Martínez-Ruiz F	137	Petti C	113
Mas JR	233	Polvorinos del Río A	298
Mata MP	289	Pozo M	134, 153, 156
Matías M	103	<b>R</b>	
Mattioli C	292	Raigón M	242
Mayayo MJ	84, 140, 143	Ramírez S	110, 159
Meeten GH	252	Ramiro A	236
Melgosa M	187	Ramos JR	236
		Remesal J	272
		Requena A	218
		Reyes E	162, 295, 311

Riccardi MP	217, 274	Velho J	93
Rives V	227	Veniale F	177, 248, 249
Roadset E	314	Vicente MA	51, 54, 57
Rocha FJ	97, 103, 125, 131, 165, 171, 174, 204, 224, 245, 250	Vicente MA	227
Rodas M	81, 233	Viedma C	100
Rodriguez I	252	Vieira AI	250
Rodriguez-Navarro C	249, 301	Violante A	27, 60
Rodriguez-Rubio P	196	Violante P	27
Rottura A	149	Viseras C	252
Ruiz-Amil A	73	<b>W</b>	
Ruiz-Conde A	73, 239	Wei H	314
Ruiz-Cruz MD	162	<b>Y</b>	
Ruiz-Hitzky E	264	Yebra A	178
Ruiz-Ortiz P	230	<b>Z</b>	
<b>S</b>		Zanco A	307
Saavedra J	94	Zanettin E	269
Sánchez C	233	Zapatero J	236
Sánchez-Bellón A	121	Zezza U	304
Sánchez-Marañón M	187, 193	Zuluaga MC	181
Sánchez-Soto PJ	45, 73, 236, 239, 242		
Santaloia F	106		
Santamaría J	54		
Santarcangelo R	106		
Santarén J	178, 255		
Santiago de C	76, 168		
Santos A	100, 171, 245		
Sebastián-Pardo E	301, 304		
Serratos J M	264		
Setti M	177, 217, 248, 249, 274, 277		
Silva AP	174		
Socias-Viciana MM	48		
Sogetti F	248, 274		
Strazzera B	212		
Suárez M.	51, 54, 57, 94, 168		
Suárez-Ruiz I	181		
<b>T</b>			
Tateo F	106, 149, 207		
Tessier D	70		
Tomadin L	5		
Toro B	272		
Torre-López de la MJ	304		
Torres-Ruiz J	143		
<b>U</b>			
Ulibarri MA	30, 42		
Undabeytia T	39		
<b>V</b>			

